



McAllister, Mairi I. (2020) *Aromatic nitrile hydrogenation: a journey from a single batch process to sustained primary amine production*. PhD thesis.

<https://theses.gla.ac.uk/81503/>

Copyright and moral rights for this work are retained by the author

A copy can be downloaded for personal non-commercial research or study, without prior permission or charge

This work cannot be reproduced or quoted extensively from without first obtaining permission from the author

The content must not be changed in any way or sold commercially in any format or medium without the formal permission of the author

When referring to this work, full bibliographic details including the author, title, awarding institution and date of the thesis must be given

Enlighten: Theses

<https://theses.gla.ac.uk/>
research-enlighten@glasgow.ac.uk



UNIVERSITY
of
GLASGOW

***Aromatic Nitrile Hydrogenation: A
Journey from a Single Batch Process
to Sustained Primary Amine
Production***

Mairi I. McAllister

*Submitted in fulfilment of the requirements of the Degree of Doctor of
Philosophy*

March 2020

School of Chemistry
College of Science and Engineering
University of Glasgow

Authors Declaration

The work contained within this thesis, submitted for the degree of Doctor of Philosophy, is the result of my own original work, except where explicit reference is made to the contribution of others, and has not been submitted for a degree at the University of Glasgow or any other institution.

Printed Name: Mairi I. McAllister

Signature:

Abstract

Primary amines are industrially valuable intermediate species which are recurrently used in the synthesis of many products, including plastics, pharmaceuticals, and agrichemicals. Whilst various synthetic methods to afford primary amines are available, it is the heterogeneously catalysed hydrogenation of nitriles which is the methodology of choice in an industrial setting. Thus, the liquid phase hydrogenation reactions of various aromatic nitriles are used to probe the reactions progress from nitrile to primary amine. In the first instance, the substrate 4-hydroxybenzyl cyanide was examined before efforts were moved to the cyanohydrin mandelonitrile. It is here that the majority of the investigation was focused. Finally, preliminary studies into the hydrogenation reaction of 1,2-dicyanobenzene were also undertaken. Detailed analysis of the reaction systems, principally by HPLC, provides the basis for this study.

Efforts were focused on understanding the interconnectivity of the reactions which typically accompany a nitrile hydrogenation reaction. Whilst no hydrogenolysis was observed in the 4-hydroxybenzyl cyanide hydrogenation reaction, coupling reactions were detected. Moreover, it was shown that the careful tuning of reaction parameters effectively removed unwanted products, affording the desired primary amine with complete selectivity.

The mandelonitrile hydrogenation reaction system was found to be significantly more complex. Despite this, analysis of the product distribution from the corresponding deuteration reaction allowed some of the finer mechanistic details to be elucidated. The single batch reaction conditions, employed for the mechanistic studies, were found not to be suitable in the assessment of catalyst longevity and durability. The reaction protocol was modified from a single batch regime, to a repeat batch regime, thus allowing the more industrially relevant fed batch protocol to be mimicked.

Utilising the insight gleaned from the mandelonitrile hydrogenation reaction studies, a dinitrile substrate system was preliminarily explored. No prior work had been conducted within the Lennon group on the hydrogenation reaction of 1,2-dicyanobenzene. Hence, suitable methodology and an appropriate analytical protocol were not in place. Whilst aspects of this reaction system were found to be somewhat problematic, an enhanced understanding has been achieved. This minor sub-section of the project is presented as an appendix and is now ready for additional investigation.

Acknowledgements

Well, my time on the mothership has finally come to a close. It has been a varied 4 years, with many ups and downs that certainly hasn't made me any less crazy.

In the first instance, thanks must go to my academic supervisor. Dave, despite, at times, a complete lack of organisation, your many eccentricities meant there was never a dull moment in the Lennon Lab. Thanks for letting me be me.

Without the support of Syngenta my project would not exist. Therefore, thanks go to my industrial supervisor Colin for trusting us and allowing us to essentially "just to get on with it" without much interference. I'm very appreciative of the freedom I was granted and how chilled you always were. Thanks for putting in the time to meet with me about my work – you always gave me something to think about. Hazmi, thanks for looking after me during my visits to Jealott's Hill – I'm very glad you didn't let me starve. I'd also like to acknowledge Philip Sidebottom for his help with ^{13}C NMR spectroscopy. You manage to explain complex things in such an understandable way, an incredibly undervalued skill.

Particular thanks in the Lennon group go to Cédric, without whom I'd still be trying to figure out how my reactor worked. Also, your ability to fix absolutely anything, especially the very temperamental Rancillio! Things really did go downhill when you left and I had to rely on my own sparrer work. To Annelouise and JamCam, obviously you both had the privilege of sitting next to me. Sadly, we were separated by real life and disease. I always appreciated the random chat that each of you provided. Also, Alisha, thanks for not being too traumatised that time I vomited for 3 hours next to you on the plane to Boston I whole-heartedly blame the sneaky mushrooms. Emma – even though you're not really a Lennon group member anymore, you still kind of count. Despite your academic status you are extremely easy to work with, especially when Dave gives us seemingly impossible tasks. That wretched ATR paper may have scarred me for life.

I'd like to thank my project students Ben and Katy. Ben, I'm sorry I worked you so hard. Katy, admittedly knowing nothing about IR, I probably wasn't much help. You definitely experienced the decline in my sanity as the writing progressed, but your acceptance and endless cups of tea eased the pain.

P. Jess, it's a long time since we met in undergrad labs. I'm genuinely amazed we've got this far in life never mind in academia. You've always been on hand to provide me with

a quick slap to keep me on track. Admittedly, in true swan fashion, I did sometimes want you to fail. But, if it came to it, I'd probably still help you hide a body.

IT Stuart, and Arlene – thanks for your eternal calm during my embarrassingly frequent trips to your office to beg for help. I never did realise that I could simply phone you and so am sorry for bursting through your door panting after having run up two flights of stairs in my panic.

Thanks go to Karen and Finlay in stores for being super speedy and organised. Karen your knowledge of all things Joseph Black is truly remarkable. Finlay, somehow you would always overhear the most incriminating things, so thank you for not reporting me to the Police.

Hallam, Glen, Papa Stew (and Jake that one time), thanks for being my climbing buddies. I may still be terrified by heights but at least I now have a real hobby. Also, Alex, Tom and Mike, it was always good to have a general moan about life over coffee on the wall outside the JB. Well, before the builders commandeered the building and ruined the sanctity of the spot.

Thanks go to my Parental Force (Jane and Charlie) for looking after precious Rusty in my absence.

Kirstinator – top job on the proof reading. I know you grumbled about having to trawl through the first draft of the tome but, as you still speak to me, I guess it didn't do too much damage.

And, last but not least, I should probably thank you, Dan. Thanks for allowing me to get pet rats. Splinter and Skelf, you really are my favourite chubby little creatures.

Corner desk next to the printer, B3-16, despite being branded a fire hazard, I will miss you.

Contents

Authors Declaration.....	i
Abstract.....	ii
Acknowledgements	iii
Contents	v
Glossary of Molecule Abbreviations	x
Proem	xiii
CHAPTER 1	1
1.1 The Hydrogenation of Nitriles to Afford Primary Amines is an Industrially Valuable Reaction	2
1.2 Hydrogenolysis is Often Found to Accompany Nitrile Hydrogenation Reactions	5
1.3 Condensation Reactions can cause Catalyst Deactivation	6
1.4 Reaction Conditions and Environment are Critical to a Selective Process	7
1.4.1 Metal Selection is Pivotal to the Observed Product Distribution	8
1.4.2 The Application of Additives to Enhance Primary Amine Selectivity	11
1.4.3 The Role of the Catalyst Support	13
1.4.4 The Effect of Reaction Conditions on Selectivity	14
1.5 The Cyanohydrin Hydrogenation Literature is Somewhat Sparse	15
1.6 Characterisation and Analytical Techniques	17
1.6.1 Atomic Absorption Spectroscopy	17
1.6.2 Inductively Coupled Plasma-Optical Emission Spectroscopy	19
1.6.3 Scanning Electron Microscopy and Energy Dispersive X-Ray Spectroscopy	20
1.6.4 Transmission Electron Microscopy	22
1.6.5 CO Chemisorption	22
1.6.6 Powder X-Ray Diffraction.....	23
1.6.7 Raman Spectroscopy	24
1.6.8 Nitrogen Physisorption	25
1.6.9 Thermogravimetric Analysis	28
1.6.10 High Performance Liquid Chromatography	29
1.6.11 Nuclear Magnetic Resonance Spectroscopy	30
1.6.12 Mass Spectrometry	31
1.7 Project Background	32
1.8 Project Aims	34
CHAPTER 2	36
2.1 Materials	37
2.1.1 Cyanohydrin Safety Considerations.....	38

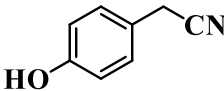
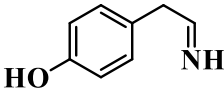
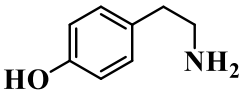
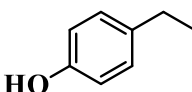
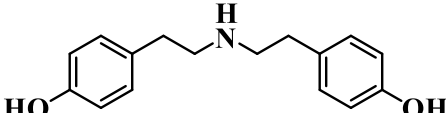
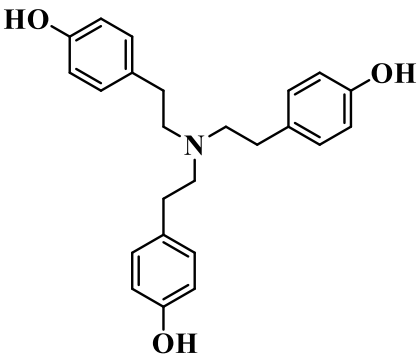
2.2 Hydrogenation/Deuteration Reaction Procedure (University of Glasgow)	38
2.2.1 The Büchi Stirred Autoclave	38
2.2.2 Single Batch Operation	41
2.2.3 Repeat Batch Operation	42
2.2.4 The Determination of Gas-Liquid Mass Transfer Coefficients (K_{La})	43
2.3 Syngenta Hydrogenation Reaction Studies	43
2.3.1 Single Batch Hydrogenation Reactions	44
2.3.2 Continuous Stirred Tank Reactor (CSTR) Reactions	45
2.4 Analytical Techniques	48
2.4.1 High Performance Liquid Chromatography (HPLC)	48
2.4.2 Multinuclear Nuclear Magnetic Resonance (NMR) Spectroscopy	49
2.4.3 Mass Spectrometry	50
2.5 Catalyst Characterisation	50
2.5.1 CO Chemisorption	50
2.5.2 Temperature Programmed Infrared (TPIR) Spectroscopy	52
CHAPTER 3	53
3.1 Introduction	54
3.2 Atomic Adsorption Spectroscopy	54
3.3 Inductively Coupled Plasma Optical Emission Spectroscopy	56
3.4 Scanning Electron Microscopy and Energy Dispersive X-Ray Spectroscopy	57
3.5 Transmission Electron Microscopy	59
3.6 CO Chemisorption	61
3.7 Powder X-Ray Diffraction	62
3.8 Raman Spectroscopy	65
3.9 Nitrogen Physisorption	67
3.10 CO Temperature Programmed Infrared Spectroscopy	70
3.11 Thermogravimetric Analysis	73
CHAPTER 4	75
4.1 Introduction	76
4.2 Hydrogenation of 4-Hydroxybenzyl Cyanide in the Absence of Chemical Modifiers Affords an Unfavourable Product Mixture	78
4.4 Mass Transport Restrictions Limit the Achievable Selectivity Towards Tyramine	85
4.5 Increased Agitation Speed Affords Increased Selectivity Towards Tyramine	89
4.6 Pressure Alterations	93
4.7 Temperature Alterations	96
4.8 The Selective Production of Tyramine is Achieved Through Fine Tuning of the Reaction Parameters	98

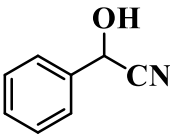
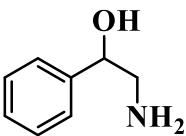
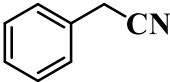
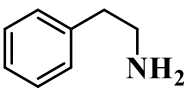
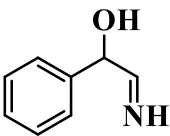
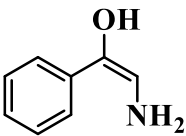
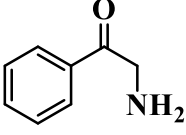
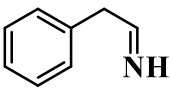
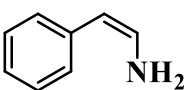
4.9 Quantification of the Imine Intermediate was Attempted using the Mass Balance Relationship	100
4.10 Selective Tyramine Production is Confirmed by ¹ H NMR Spectroscopy	103
4.11 Positioning of the α -Carbon Relative to the Aromatic Ring System Dictates the Accessibility of the Hydrogenolysis Process	109
CHAPTER 5	112
5.1 Introduction.....	113
5.2 Understanding the Mandelonitrile Hydrogenation Reaction Profile	114
5.3 Exploration of the Analytical Protocol Allowed Further Chromatographic Details to be Revealed	118
5.4 Neutral Conditions are Found not to be Conducive for Phenethylamine Production	121
5.5 2-Aminoacetophenone is Identified as a Reaction Intermediate	124
5.6 Development of the Reaction Scheme	127
5.7 The Hydrogenolysis of 2-Amino-1-phenylethanol.....	128
5.8 The Hydrogenation of 2-Aminoacetophenone.....	131
5.9 Full Elucidation of the Reaction Pathway is not Possible by HPLC	136
5.10 Conclusions	140
CHAPTER 6	142
6.2 NMR Spectroscopy Analysis Defines the Location of Deuterium Incorporation within Phenethylamine	147
6.3 Isotopologue Distribution for the Deuteration Reaction of Mandelonitrile is Defined by Mass Spectroscopy	157
6.4 To Rationalise the Increased Hydrogen Content the ‘Reverse’ Tautomeric Reactions must be Considered.....	160
6.6 Quantitative ¹³ C NMR Spectroscopy Confirms the Mass Spectrometry Findings	170
6.7 The Observed Deuterated Phenethylamine Isotopologue Distribution Allows Refinement of the Reaction Mechanism	172
6.8 Isotopologue Analysis is used to Further Enhance the Reaction Mechanism	180
6.9 Density Functional Theory Proposal Relating to the Hydrogenolysis Reaction in the Hydrogenation Reaction of Mandelonitrile to Afford Phenethylamine.....	184
6.10 Conclusions	185
CHAPTER 7	187
7.1 Introduction.....	188
7.2 The Reaction Scheme is used to Rationalise the Product Distribution	189
7.3 Consideration of an Alternative Catalyst	193
7.4 Temperature Alterations.....	196
7.5 Solvent Alterations.....	201
7.5.1 Addition of Water to the Reaction Mixture is Reported to Improve Selectivity..	202
7.5.2 Increasing Alcohol Chain Length is Reported to Increase Hydrogen Solubility .	209

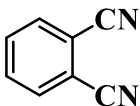
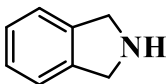
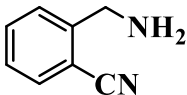
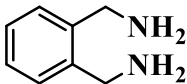
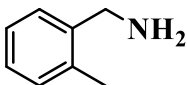
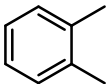
7.5.3 The Consideration of Tetrahydrofuran as an Alternative Reaction Solvent	211
7.6 Acid Alteration Considerations	213
7.6.1 Hydrochloric Acid.....	214
7.6.2 Acetic Acid.....	216
7.6.3 Phosphoric Acid	217
7.6.4 The Acid Additive Function is Compared	220
7.6.5 Variations to the Concentration of the Sulphuric Acid Additive	221
7.6.5.1 Acid Lean Conditions	221
7.6.5.2 Acid Rich Conditions	223
7.7 Conclusions.....	225
CHAPTER 8.....	227
8.1 Introduction.....	228
8.2 A Repeat Batch Protocol was Implemented to Replicate the Industrial Process	228
8.3 Early Investigations into the Repeat Batch Protocol for the Hydrogenation Reaction of Mandelonitrile.....	229
8.4 Improving Hydrogen Availability Improves Catalyst Durability	231
8.5 Examination of the Hydrodynamics of the Reaction System within the Improved Experimental Domain Described in Section 8.4	235
8.6 Methods of Improving the Catalyst Lifetime (Acid Considerations)	238
8.7 The Repeat Batch Experiments were Revisited to Test the Concentration Dependence Theory	243
8.8 Hydrogen Line Pressure, Relating to Reactor Charging Time, was Identified as a Key Contributor to Sustained Product Formation.....	247
8.9 The Optimised Repeat Batch Reaction Profile: Towards an Improved Understanding	251
8.9.1 The Role of the Acid Additive in the Optimised Regime.....	251
8.9.3 The Role of Catalyst Mass in the Optimised Regime.....	254
8.10 A Continuously Stirred Tank Reactor Arrangement was Proposed as a Means of Extending Catalyst Lifetime (Syngenta)	259
8.11 Conclusions.....	264
CHAPTER 9	267
CHAPTER 10	271
CHAPTER 11	273
<i>Appendix</i>	286
12.1 Introduction.....	287
12.2 Analytical Method Development	289
12.3 The Hydrogenation Reaction of 1,2-Dicyanobenzene: Neutral Conditions.....	292
12.4 Inclusion of an Acid Additive Afforded a Drastically Different Reaction Profile	295

12.5 Significant Sample Discolouration After Catalyst Removal in the Presence of Acid Suggests the Occurrence of Homogeneous Chemistry	298
12.6 Consideration of the Effect of Reduced Hydrogen Availability on Product Distribution.....	299
12.7 Consideration of the Effect of Temperature on the Product Distribution.....	302
12.8 The Durability of the Catalyst was Tested with a Repeat Batch Experiment	306
12.9 A Systematic Mass Balance was Detected for all Reaction Conditions.....	309
12.10 Syngenta Mettler Toledo Batch Reactor Studies	310
12.11 Conclusions and Future Directions	313
12.12 References.....	316

Glossary of Molecule Abbreviations

- [1]  **4-Hydroxybenzyl Cyanide (HBC)**
- [2]  **4-Hydroxybenzyl Imine (HBI)**
- [3]  **Tyramine (TYR)**
- [4]  **4-Hydroxyethylbenzene (HEB)**
- [5]  **Di-hydroxyphenethylamine
(2° Amine)**
- [6]  **Tri-hydroxyphenethylamine
(3° Amine)**

- | | | |
|------|---|---|
| [7] |  | Mandelonitrile (MN) |
| [8] |  | 2-Amino-1-phenylethanol
(2-APE) |
| [9] |  | Benzyl Cyanide (BC) |
| [10] |  | Phenethylamine (PEA) |
| [11] |  | 2-Imino-1-phenylethan-1-ol
(Hydroxy-Imine) |
| [12] |  | (E)-2-Amino-1-phenylethen-1-ol
(Hydroxy-Enamine) |
| [13] |  | 2-Aminoacetophenone (2-AAP) |
| [14] |  | 2-Phenylethan-1-imine
(Imine) |
| [15] |  | (Z)-2-Phenylene-1-amine
(Enamine) |

- [16]  **1,2-Dicyanobenzene (DCB)**
- [17]  **Isoindoline (II)**
- [18]  **2-Cyanobenzylamine (CBA)**
- [19]  **Xylene Diamine (XDA)**
- [20]  **2-Methylbenzylamine (MBA)**
- [21]  **1,2-Dimethylbenzene (DMB)**

Proem

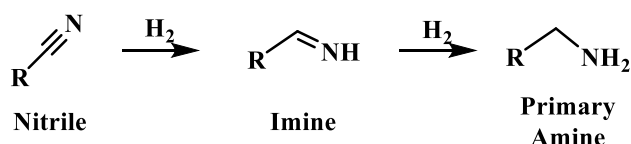
This body of work has been sponsored by Syngenta and thus is not overly typical of traditional academic research. As will be detailed in Section 1.7, this is the third phase of the collaboration between Syngenta and the University of Glasgow. As such, the thesis is focused towards understanding a particular industrial process. Namely, the desire to deliver enhanced, but sustained, yields of a primary amine product *via* the selective hydrogenation of aromatic nitriles. As a consequence of this, certain parameters, for example catalyst choice and substrates, are somewhat limited so that the outcomes are suitably relevant to the industrial counterpart.

CHAPTER 1

Introduction

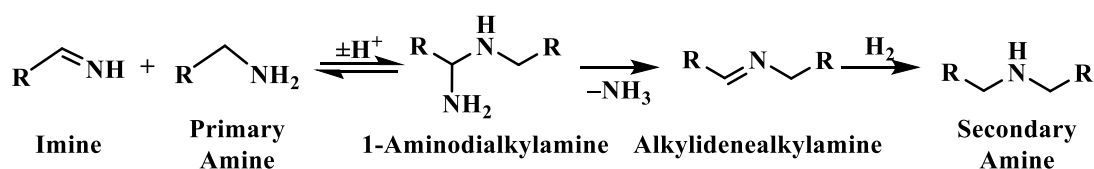
1.1 The Hydrogenation of Nitriles to Afford Primary Amines is an Industrially Valuable Reaction

Primary amines are widely recognised within various industries as exceptionally versatile intermediates. This includes, but is not limited to, the production of intermediates and precursors in the synthesis of natural products, agrichemicals, plastics, pharmaceuticals, dyes, and polymers.^[1–6] As a consequence of their value, several methods are reported to afford primary amines.^[7–11] Examples of such methodology include, the reduction of nitro groups, the reduction of amides, and the reductive amination of oxo compounds.^[12–14] Nevertheless, it is the heterogeneously catalysed hydrogenation reaction of nitriles which is frequently employed for this purpose in an industrial setting.^[3, 7, 11, 15–16] This method will also be employed in this study. Conversion of the nitrile functionality is well reported to be facile, making this reaction attractive for use in large scale industrial processes.^[6, 11, 15] Nevertheless, in contrast to other hydrogenation or hydrogenolytic reactions, which usually proceed relatively simply, the hydrogenation of nitriles typically yields a mixture of products. As such, achieving a high selectivity towards the desired product is identified as the major issue associated with this chemistry.^[17–18] The reason for the prevalence of by-product formation in nitrile hydrogenation reactions is due to the formation of a highly reactive imine intermediate.^[19]



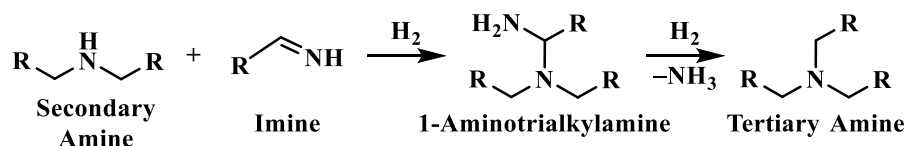
Scheme 1.1. Two-step nitrile hydrogenation reaction to afford the primary amine proposed by Sabatier et al..^[20]

Early mechanistic work on the hydrogenation of nitriles was undertaken by Sabatier and Senders in 1905.^[20] Here, it was proposed that the nitrile was hydrogenated to the primary amine in a two-step process *via* a primary imine intermediate (Scheme 1.1).^[20] The extremely reactive nature of the intermediate species in the hydrogenation of nitriles, however, meant the identification of the intermediate species proved problematic.^[21] Nonetheless, the presence of imines and enamines as intermediate species is now firmly established.^[22–23]



Scheme 1.2. Reaction scheme proposed by von Braun showing formation of the secondary amine.^[24]

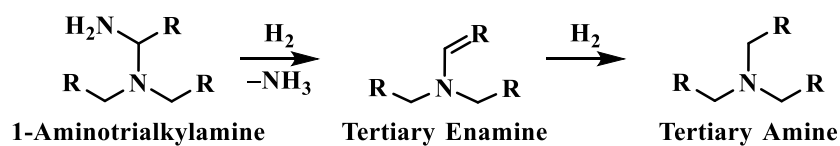
Through his work on aromatic nitriles, Mignonac discovered, in 1920, that Schiff base formation was key in the production of secondary amines.^[25] It was then proposed by von Braun *et al.*, in 1923, that the formation of a 1-aminodialkylamine *via* reaction of the imine intermediate and the primary amine was the first step in the synthesis of the secondary amine. This 1-aminodialkylamine can then undergo hydrogenolysis, releasing ammonia as a by-product and yielding an alkylidenealkylamine, which can then be hydrogenated to the secondary amine (Scheme 1.2).^[24] In two separate occasions, reports from Windans and Adkins (1932), and Juday and Adkins (1955) support von Braun's mechanism.^[26-17] Consequently, the mechanism reported by von Braun is the most widely quoted for the formation of higher amines.^[16, 28]



Scheme 1.3. Reaction scheme showing formation of tertiary amine from an imine intermediate.

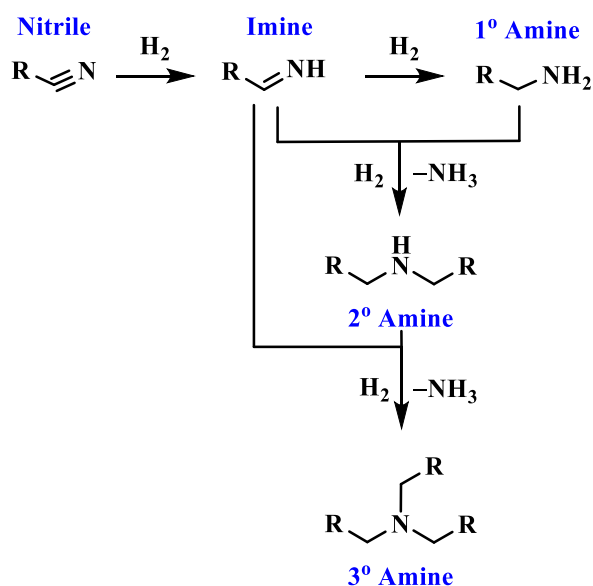
The mechanism for the formation of the tertiary amine was proposed by Kindler and Hesse. Here it was indicated that the addition of a secondary amine to an imine, with subsequent hydrogenolysis of the resultant 1-aminotrialkylamine, yields the tertiary amine with ammonia as a by-product (Scheme 1.3).^[29] In 1967, Greenfield noted that the tertiary amine could also be formed *via* intermediate enamines, again by elimination of ammonia from the 1-aminotrialkylamine (Scheme 1.4). It was, however, noted that enamine formation was not possible in all cases. For example, due to the requirement for an H-atom in the β -position with respect to the N-atom, enamine formation is impossible

for benzonitrile.^[30] The idea to use molecular structure as a means of achieving a selective reaction is thus introduced.



Scheme 1.4. Reaction scheme showing formation of tertiary amine from an enamine intermediate.

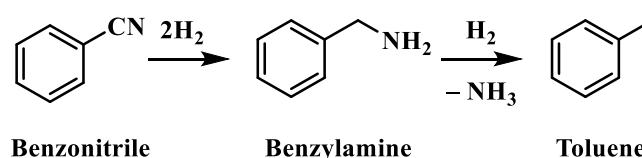
Therefore, it is surmised that the hydrogenation of nitriles can lead to a set of consecutive and parallel reactions, resulting in the production of a mixture of primary, secondary, and tertiary amines, collectively shown in Scheme 1.5. Unfortunately, the formation of these by-products can be challenging in a reaction system if they are retained on the catalyst surface, as they can act as a poison and cause deactivation.^[31] The formation of secondary and tertiary amines is therefore undesirable when considering nitrile hydrogenation as a route to the formation of primary amines.



Scheme 1.5. Proposed reaction pathway for the hydrogenation of a nitrile. [*R* = alkyl; aryl; aralkyl].

1.2 Hydrogenolysis is Often Found to Accompany Nitrile Hydrogenation Reactions

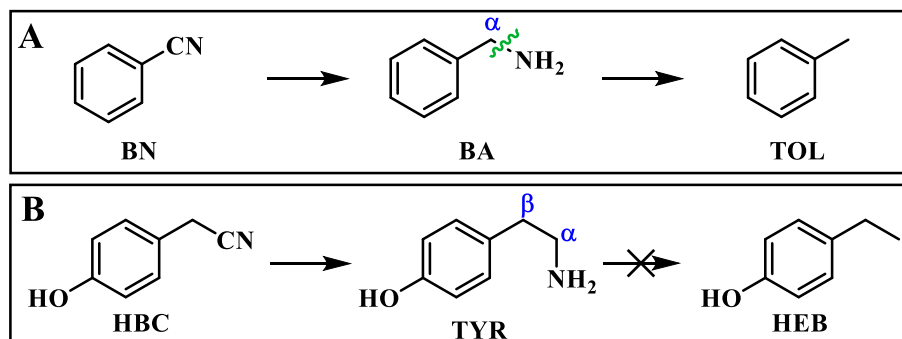
Coupling reactions have been well recognised in the nitrile hydrogenation literature, often to the detriment of primary amine selectivity. Another reaction, commonly seen alongside the hydrogenation of the nitrile species, is the hydrogenolysis of the primary amine product.^[32–33] Historically, this heteroatom cleavage has not been a predominant feature of the heterogeneous catalysis literature, due to the phenomenon typically only occurring under harsh reaction conditions.^[33–34] Despite this, production of the hydrogenolysis product under mild conditions has been reported, for example, by Maschmeyer *et al.*,^[33] through the study of benzonitrile over a Pd/C catalyst. The formation of toluene from the hydrogenolytic cleavage of benzylamine is shown in Scheme 1.6.



Scheme 1.6. Reaction scheme for the hydrogenation reaction of benzonitrile showing the accompanying hydrogenolysis reaction to afford toluene.

Further, previous studies within the Lennon group have utilised the same substrate and catalyst, showing exclusive formation of the hydrogenolysis product toluene.^[35–36] Given the industrial importance of primary amines, the occurrence of a concurrent or consecutive hydrogenolysis reaction which removes the valuable amine functionality can be problematical. Alternatively, the hydrogenolysis of an unwanted functional group may prove to be useful synthetically. Whilst it was only the hydrogenolysis product which was observed at reaction completion for the hydrogenation reaction of benzonitrile, further studies conducted by the Lennon group, focusing on the hydrogenation of 4-hydroxybenzyl cyanide, revealed that no such hydrogenolysis step was observed for this substrate.^[37] This outcome was rationalised by work undertaken, again by Maschmeyer *et al.*,^[32] which suggested that the positioning of the aromatic group, with respect to the heteroatom, dictates the viability of hydrogenolysis. If the heteroatom is not attached to the α -carbon, then stabilisation, as a consequence of conjugation, is not possible, making the cleavage under mild conditions unfavourable. This concept is illustrated in Scheme

1.7 where benzonitrile and 4-hydroxybenzyl cyanide have been used as examples. The hydrogenation reaction of 4-hydroxybenzyl cyanide is examined in more detail in Chapter 4.



Scheme 1.7. The hydrogenation reaction of **A**, benzonitrile and **B**, 4-hydroxybenzylcyanide. The position of the α and β carbons, relative to the heteroatom, specified. [BN = benzonitrile; BA = benzylamine; TOL = toluene; HBC = 4-hydroxybenzylcyanide; TYR = tyramine; HEB = 4-hydroxyethylbenzene].

1.3 Condensation Reactions can cause Catalyst Deactivation

Not only are the condensation reactions described in Section 1.1 inconvenient when striving to achieve a completely selective process, but they can also cause deactivation of the catalyst. Specifically, this is attributed to amine condensation reactions which result in the formation of insoluble oligomeric products. These oligomeric products then adsorb onto the active sites of the catalyst, thereby preventing further reaction.^[38] In some instances, the occurrence of these reactions prevents the complete conversion of the starting nitrile.^[21]

Heterogeneous catalysts claim to offer the advantage of recyclability.^[39] Therefore, it is noted that a prevalence of condensation reactions can be problematic with regard to complying with this statement. Despite catalyst deactivation being of significant importance for an industrial scale process, the successful regeneration and reuse of the associated catalysts is not well documented. Nonetheless, nitrile hydrogenation catalysts are known to rapidly deactivate.

It was reported by Chatterjee *et al.* that Pd/C catalysts deactivate easily.^[40] This particular example applies to the hydrogenation of benzonitrile in the presence of supercritical carbon dioxide. Interestingly, the same level of deactivation for a Pd/MCM-41 catalyst was not reported by the authors.^[40] A more extensive examination into the deactivation mechanism for nitrile hydrogenation catalyst was conducted by Duch and Allgeier in a study where nylon-6 and nylon-6,6 fibres and polymers were recycled to produce predominantly hexamethylenediamine.^[41] In this instance, it was proposed that the deactivation process incurred an induction period, where the production of amine dimers/oligomers proceeded uninhibited until a critical molecular weight growth in condensation polymerisation was reached. From this point, deactivation was observed.^[41] Isotopic labelling studies revealed that the production of oligomeric products, from condensation reactions, resulted in the formation of a reservoir of activated hydrogen which enhanced the rate of nitrile reduction in the early stages of the reaction. It is then rather ironic that the occurrence of these condensation reactions eventually takes on a parasitic role at the catalyst surface, ultimately preventing further reaction through blockage of active sites.^[38]

1.4 Reaction Conditions and Environment are Critical to a Selective Process

It is thus surmised that the hydrogenation of a nitrile group to form the corresponding primary amine is not often a solitary process, with both condensation and hydrogenolysis reactions often occurring alongside the desired pathway. To add insult to injury, these unwanted side reactions not only compromise primary amine selectivity but can often cause catalyst deactivation. In this particular study, the primary amine is sought in high selectivity under reaction conditions that preserve the functionality of the catalyst on cycling. It is therefore essential that a suitable reaction environment is found. A number of reaction parameters are reported to have an influence on the abovementioned criteria. The nitrile hydrogenation literature has been reviewed extensively,^[16–17, 21] but most recently by Lévy and Hegedűs.^[15] The reaction parameters which have the most influential role on selectivity will be discussed in the following sections.

1.4.1 Metal Selection is Pivotal to the Observed Product Distribution

It is recurrently reported that catalyst selection for a reaction is the dominating factor in the determination of product distribution.^[1, 42] In the hydrogenation reactions of nitriles, the use of multiple metals, resulting in varying outcomes, are reported. Historically, it has been skeletal metal catalysts, such as Raney nickel and Raney cobalt which have shown proclivity for the selective hydrogenation of nitriles within an industrial setting.^[43] In addition to its Raney form,^[6, 16, 23, 43–49] nickel is reported to be active for nitrile hydrogenation when supported on silica,^[30, 34, 50–53] alumina,^[54–57] and sepolite.^[58] Nickel nanoparticles have also been reported for these reactions.^[58–61]

Attention is now brought to a few examples of nickel catalysed nitrile hydrogenation reactions. Hofffer and Moulijin^[49] investigated the hydrogenation of aliphatic dinitriles at 77 °C and 50 bar over Raney nickel catalysts in 2009. This study revealed that the reactivity of the substrate was influenced by the hydrocarbon chain length. Short dinitriles, such as succinonitrile, were found to exhibit stronger adsorption on the surface of the catalyst than longer nitriles, such as adiponitrile. Moreover, it was found that, in addition to a decreased adsorption strength, by increasing the hydrocarbon chain length, the reaction rate is also decreased.^[49] In another example, an attempt to reduce by-product formation by conducting a reaction condition optimisation process was performed by Apestegía *et al.* for the hydrogenation reaction of butyronitrile over a Ni/SiO₂ catalyst.^[34] It was found that the highest selectivity towards primary amine butylamine was achieved in ethanol. The results suggest that the use of a protic solvent influences the strength of the solvent-butylamine interaction in the liquid phase and, that it is this interaction which positively affects the selectivity towards the primary amine. It is proposed that as a H-bond donor, ethanol strongly interacts with H-bond acceptor butylamine, thus solvating it in the liquid phase. The butylamine molecules are then surrounded by alcohol molecules, which inhibit the adsorption of the butylamine to the surface of the catalyst. Thereby, by-product formation is decreased.^[34]

Cobalt is also frequently employed for this class of reaction, in either Raney^[23, 48] or supported form.^[30, 34, 52, 54, 62–64] In 2004, Ansmann and Benisch developed an industrially viable process for the production of primary amines, such that the important pharmaceutical intermediate homoverathylamine could be selectively obtained. This was achieved over a 70% Co/SiO₂ catalyst in the presence of ammonia at 80 °C and 80 bar.^[62] In the hydrogenation of butyronitrile, investigated by Apesteguía *et al.*, it was a 9.8%

Co/SiO₂ catalyst which afforded butylamine in the best selectivity (97%).^[34] Some more exotic cobalt catalysts were also shown to be fruitful. Shen and co-workers developed a metal-organic framework derived N-doped Co/C catalyst for the transfer hydrogenation of nitriles in the absence of a base.^[63] Continuing this theme, work conducted in the Beller group examined the preparation of a heterogeneous nanostructured cobalt catalyst from the pyrolysis of a cobalt complex [Co(OAc)₂·4H₂O] containing the nitrogen based ligand 1,10-phenanthroline onto an alumina support.^[64]

Despite the positive reports for the use of nickel and cobalt, particularly of the Raney variety (skeletal metal), catalysts of this nature are known to be pyrophoric, thus causing less than desirable handling difficulties. Further, the high hydrogenation activity of Raney metal catalysts often becomes problematic when more complex molecules, with additional functionality requiring preservation, are considered.^[30] As such, the use of milder, palladium based catalysts have recently come to dominate the literature.^[2, 21, 30, 32, 38] Indeed, among the precious metals, palladium is the most frequently used heterogeneous catalyst for the hydrogenation of nitriles.

Palladium is employed for nitrile reactions exclusively in supported form. Activated carbon,^[3, 32, 35, 37, 66, 68, 77] alumina,^[2, 35, 40, 68–77] MCM-41,^[40] and silica^[77] have all been reported as supports for palladium based catalysts. In 2005, Hegedűs and co-workers hydrogenated benzonitrile to yield benzylamine in high selectivity (95%) under mild conditions (30 °C, 6 bar) over a 10% Pd/C catalyst. This reaction was conducted in a mixture of two immiscible solvents (water/dichloromethane) in the presence of an acid additive (NaH₂PO₄).^[3] Again using a 10% Pd/C catalyst, Beller *et al.* reported the catalytic transfer hydrogenation of aromatic nitriles to the corresponding primary amines. In this instance ammonium formate was employed as a hydrogen donor.^[66] Gas-phase nitrile hydrogenation studies are reported less frequently than their liquid phase counterparts.^[19, 68, 78] One such study, conducted by Marella *et al.*, notes that residence time plays a key role in achieving a high selectivity towards the desired product.^[78] It is further reported that a shorter contact time in a continuous gas-phase operation can prevent condensation of the imine with the primary amine.^[68, 78] Regarding the occurrence of hydrogenolysis, Keane and co-workers document that while toluene was the predominant product of the hydrogenation reaction of benzonitrile over Pd/C, it was benzylamine which was favoured over Pd/Al₂O₃.^[68]

Platinum catalysed nitrile hydrogenation reactions almost exclusively result in secondary [17–18, 79–81] or tertiary amines [82–83] and are significantly less reported than palladium catalysed reactions. There are, however, a few instances where moderate selectivity towards the primary amine was achieved.^[82–83] For example, the gas-phase hydrogenation of acetonitrile over a CeO₂ supported 1% platinum catalyst yielded ethylamine in 56% selectivity.^[83]

The majority of the heterogeneous nitrile hydrogenation literature documents the application of the previously described metals as catalysts. Despite this, there are a few instances where other metals have been employed. As such, a brief description of the use of copper, ruthenium, rhodium, and iridium has been provided.

Copper is seldom used as a nitrile hydrogenation catalyst, largely due to its propensity to form secondary amines. Typically, copper is used in supported form.^[52, 78, 84] Using a magnesium oxide supported copper catalyst Burri and co-workers report the gas-phase hydrogenation of benzonitrile in the absence of additives. A high selectivity towards benzylamine was achieved despite the poor conversion (50–60%). Formed alongside the desired primary amine was secondary amine, dibenzylamine. Further, at temperatures between 200 °C and 220 °C, the dibenzylimine intermediate was also observed.^[78] The high metal loading required (12%) is countered by copper being a relatively inexpensive metal. Also investigated, by Segobia *et al.*, was the copper catalysed hydrogenation of cinnamionitrile in toluene at 40 bar and 100 °C. In this particular case, a 11% Cu/SiO₂ catalyst yielded cinnamylamine in 74% selectivity.^[52, 78] Whilst copper is shown to have activity for the reduction of the nitrile group, this metal possesses a low activity for the hydrogenation of the C=C bond. This property is utilised by Armour and co-workers to afford the selective hydrogenation of unsaturated nitriles to form unsaturated secondary amines.^[85]

Ruthenium can be applied to the hydrogenation of nitriles in supported form^[86–88] or as nanoparticles.^[89] An ionic-liquid based multiphase reaction system was investigated by Wasserscheid and co-workers for the hydrogenation reaction of propionitrile over a Ru/C catalyst at 100 bar and 100 °C. The use of a Brønsted acid ionic liquid, to form a protonated primary amine, and an aprotic ionic liquid which allowed the primary amine to be extracted into the organic solvent, resulted in a high selectivity towards the desired product in both instances.^[86] Another example is reported by Muratsugu *et al.*. Here, decarbonylation-promoted ruthenium nanoparticles, formed from a Ru₃(CO)₁₂ precursor,

were dispersed on a potassium doped Al_2O_3 support. In the hydrogenation of valeronitrile, the primary amine pentylamine was formed in high selectivity (97%) after a period of 90 minutes, which corresponded to a 31% conversion.^[88]

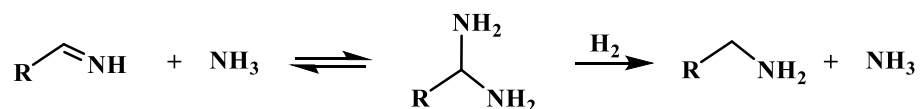
Again, rhodium is rarely used in the heterogeneously catalysed reduction of nitriles.^[90–91] Chatterjee *et al.* examined the hydrogenation of adiponitrile over a 5% $\text{Rh}/\text{Al}_2\text{O}_3$ catalyst with the aim of forming 6-aminocapronitrile.^[91] Indeed, the desired product was synthesised with complete selectivity, at 80 °C, in supercritical carbon dioxide, and in the absence of any additives or organic solvent. A maximum conversion of 97% was achieved after a period of 360 minutes. When the reaction time was extended in an attempt to facilitate complete conversion, this was found not to be possible. Nonetheless, this process was found to be suitable for the selective formation of other aminonitriles from the corresponding aromatic dinitriles. In the hydrogenation of 1,2-dicyanobenzene, steric effects were found to hinder catalyst activity.^[91]

Finally, the use of iridium is considered. A 0.9% $\text{Ir}/\gamma\text{-Al}_2\text{O}_3$ catalyst was employed by López-de Jesus for the hydrogenation reaction of benzonitrile in ethanol at 21 bar and 100 °C. After a period of 240 minutes 50% conversion was achieved, affording the desired benzylamine in 15% selectivity. Unfortunately, coupling reactions and hydrogenolysis, to afford dibenzylamine and toluene respectively, were encountered. It is the occurrence of these side reactions which accounts for the low selectivity.^[92]

1.4.2 The Application of Additives to Enhance Primary Amine Selectivity

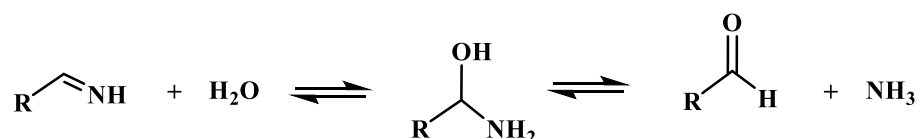
Once metal selection has been made, there are a number of actions which may be taken to enhance selectivity towards the desired primary amine. To this end, both acidic and basic additives have been successfully reported. The addition of ammonia^[6, 30, 44–46] or an appropriate base^[16, 23, 30, 47] has been shown to suppress undesirable by-product formation. The ammonia additive reacts with the imine intermediate, as shown in Scheme 1.8, and hence prevents it from reacting with the primary amine in a condensation reaction.^[21] The use of ammonia, however, has only been reported to be efficacious with Raney nickel^[44, 48] or rhodium catalysts.^[90] In contrast, the use of ammonia with supported palladium and platinum catalysts did not suppress the formation of secondary and tertiary amines, despite increasing the presence of ammonia up to five equivalents.^[6, 30] Moreover, the

benefits gleaned from the use of a base additive, such as NaOH or K₂CO₃, have only been observed for nickel and cobalt catalysts.^[16, 23, 30, 47]



Scheme 1.8. Proposed reaction scheme for the reaction of an ammonia additive with the imine intermediate to form a primary amine and regenerate the ammonia.

An alternative method of improving the selectivity towards the primary amine is to prevent the reaction between this species and the highly reactive imine intermediate. This not only maximises primary amine yield, but also thwarts the formation of secondary and tertiary amines which would otherwise be the products of this reaction. This may be achieved by the application of either water or an acid additive.



Scheme 1.9. Proposed reaction scheme for the reaction of a water additive with the imine intermediate to form an aldehyde and ammonia.

It is documented in the patent literature that, in the presence of nickel or cobalt catalysts, nitrile hydrogenation rate and consequently primary amine yield increases if water is added to the reaction mixture.^[93–94] The water functions much like the ammonia additive (Scheme 1.8) by reacting with the imine intermediate, in this instance forming an aldehyde and ammonia (Scheme 1.9).^[21] It is, however, the combined action of water and ammonia which is usually described to promote high primary amine yields.^[30, 95] This positive influence is associated with the solvation of the amine products by the water additive, leading to weaker adsorption on the surface of the catalyst. This may then suppress their retarding effect on the catalyst.^[21] The interaction between the amine group and the water will take place by means of hydrogen bonding. This interaction competes with the condensation reaction between the primary amine and the imine resulting in a

reduced rate of secondary amine formation. This is particularly useful for catalysts which show favourable production of secondary and tertiary amines. This relates particularly to supported palladium and platinum catalysts. The water functions by hydrating the catalyst meaning that it is predominantly dispersed in the aqueous phase. As the condensation products are only partially water soluble, the concentration of the secondary and tertiary amines in the aqueous phase is low. Hence, these molecules are prevented from acting as catalyst poisons.^[21, 95]

In the presence of acid, the amine products are protonated to form ammonium salts.^[96–98] In 1928, Hartung discovered that it was possible to selectively obtain the primary amine by using an alcoholic HCl solution. Under these conditions, benzonitrile was gently reduced to benzylamine over Pd/C.^[60] Alternatively, a similar outcome can be obtained by acylating the amino group with acetic anhydride.^[48, 99–100] Whilst generally reported to be beneficial, care must be taken to ensure the additive is compatible with the catalyst and other reaction components.

1.4.3 The Role of the Catalyst Support

In a heterogeneous catalyst the active sites are located on its surface. The most efficient catalysts typically have a large catalytically active surface. For most catalytically active metal powders sintering can be observed at temperatures as low as 100 °C. The consequent loss of active surface area as the result of sintering is less than ideal. However, if the catalytically active particulates can be kept separate from each other, thermal agglomeration can be minimised. The most effective way of achieving this is to adhere the active metal to a support. A catalyst support is a material, usually possessing both high thermal stability and an extensive surface area, to which a catalyst is affixed.^[39]

For the hydrogenation of nitriles, the use of various supports has been reported. This includes activated carbon,^[2–3, 32, 35, 37, 63, 65–70, 79, 86] alumina,^[2–3, 19, 35, 54–57, 64, 68–76, 90–92, 101] silica,^[19, 30–31, 34, 50–53, 62, 77, 80–81, 83, 87, 101] titania,^[3, 19, 81] sepolite,^[58] MCM-41,^[40] hydrotalcite,^[102] ceria,^[83] and magnesia.^[78, 82, 83, 101] The nature of the support was reported to have a considerable influence on the activity of the catalyst. Nonetheless, the effect of the support on selectivity is not well documented.^[19, 83, 101–102]

1.4.4 The Effect of Reaction Conditions on Selectivity

In conjunction with the previously discussed factors a number of other parameters, relating directly to operational conditions, are shown to have an effect on the selectivity outcome of a reaction. Examples of such parameters include temperature, hydrogen pressure, and agitation.^[21, 39] In the vast majority of studies where the effects of temperature on nitrile hydrogenation reactions are considered, it is the production of higher amines which is enhanced as temperature is elevated.^[103–106] In the cobalt catalysed hydrogenation reaction of laurionitrile, the enhanced formation of the secondary amines at elevated temperatures is found to be due to the activation energy of the amine and imine condensation reaction ($E_a = 132 \text{ kJ mol}^{-1}$) being higher in energy than the activation energy for the hydrogenation reaction ($E_a = 52 \text{ kJ mol}^{-1}$).^[21] There are, however, exceptions to this trend.^[107] That said, it is important to note that the product distribution observed for a particular reaction is often determined by multiple parameters and not just temperature. It is therefore essential that it is not only trends specific to one parameter which are acknowledged.^[21]

For the nitrile hydrogenation reaction, a supply of hydrogen is arguably the most important parameter. With increasing hydrogen pressure comes an increase in hydrogenation rate.^[39] Moreover, whilst an increase in hydrogen pressure accelerates the hydrogenation rate, the condensation reactions, leading to secondary and tertiary amines, will be independent of this parameter. This observation is found to be imperative to the selectivity outcome of a reaction. Accordingly, the selectivity of primary amines is documented to increase with increasing hydrogen pressure.^[21, 108] Experimental results for the hydrogenation of valeronitrile over a rhodium catalyst, reported by Rylander, were in accord with this statement.^[108] Nevertheless, there is a degree of complexity to the role of hydrogen pressure, with the overall outcome of the reaction dependent on a number of other reaction parameters. Again, the intricacy of the *whole* reaction system cannot be disregarded. Another reaction parameter which has an influence on hydrogen availability, and hence selectivity, in a three-phase reaction system is agitation speed. Less intensive agitation of the reaction mixture decreases the concentration of hydrogen in the liquid phase.^[21]

It is thus apparent that the reaction conditions have an influential role on the rates of the competing hydrogenation and condensation reactions. Accordingly, the product distribution is affected. This clearly illustrates that the fine tuning of various experimental parameters is essential if the desired product is to be yielded in high selectivity.^[21]

1.5 The Cyanohydrin Hydrogenation Literature is Somewhat Sparse

As described in the preceding sections (Sections 1.4.1–1.4.4), simple aliphatic nitriles and more recently aromatic nitriles, have been extensively studied. There is, however, significantly less literature relating to nitrile hydrogenation systems of greater complexity.^[2–3, 32, 68, 72–74] In the agrichemical sector, where this study finds application, the presence of additional functionality is frequently required.^[17] Thus, in a move towards more complex nitrile compounds, the cyanohydrin mandelonitrile was considered an ideal candidate for investigation.

Cyanohydrins are defined as organic compounds which contain a carbon atom, linked to both a cyanide group and a hydroxyl group.^[109] These molecules are found commonly in nature and offer significant synthetic potential in the production of useful pharmaceuticals, agrichemicals and other biologically active compounds.^[110–111] Moreover, cyanohydrins can be used as protecting groups. One such example relates to the protection of aldehydes and ketones as *O*-trimethylsilyl cyanohydrins, which are very stable to multiple conditions, making them attractive for use in multi-step syntheses.^[112] Against this abundance of applications, their synthesis is recurrently reported.^[113–115]

Interestingly, however, the literature available on the hydrogenation of these compounds is rather scarce, featuring significantly less frequently than aromatic or aliphatic nitriles. Despite an earlier, but unsuccessful attempt reported by Kindler,^[116] Hartung successfully hydrogenated mandelonitrile over a palladinised charcoal catalyst in an alcoholic hydrogen chloride solvent in 1928.^[96] Rather to the surprise of the author, no 2-amino-1-phenylethanol was detected. Instead, it was phenethylamine which was produced alongside significant quantities of an unknown by-product.^[96] In 1933, Buck attempted to simplify the preparation of phenethylamines from the catalytic reduction of mandelonitriles.^[117] Similar conditions to those used by Hartung were employed. However, in this instance, it was a mixture of 2-amino-1-phenylethanol and

phenethylamines which were produced. In this instance product selectivity was found to be determined by the nature of the substituent attached to the starting cyanohydrin.

A more recent example is reported by Tinapp.^[118] Here, the catalytic hydrogenation reactions of various substituted mandelonitriles over Raney Ni in the presence of sulphuric acid are documented. Cyanohydrin formation is readily reversible, even under mildly basic conditions, to give the corresponding benzaldehyde and hydrogen cyanide. It is reported by Tinapp that the presence of acid is essential to prevent the equilibrium reverting back to the corresponding carbonyl compound. As shown in Scheme 1.10, the reaction proceeded *via* a hydroxy-imine intermediate to form 2-amino-1-phenylethanol and mandelaldehyde. However, as this paper is written in German, some of the finer details may have been lost in translation.^[118]

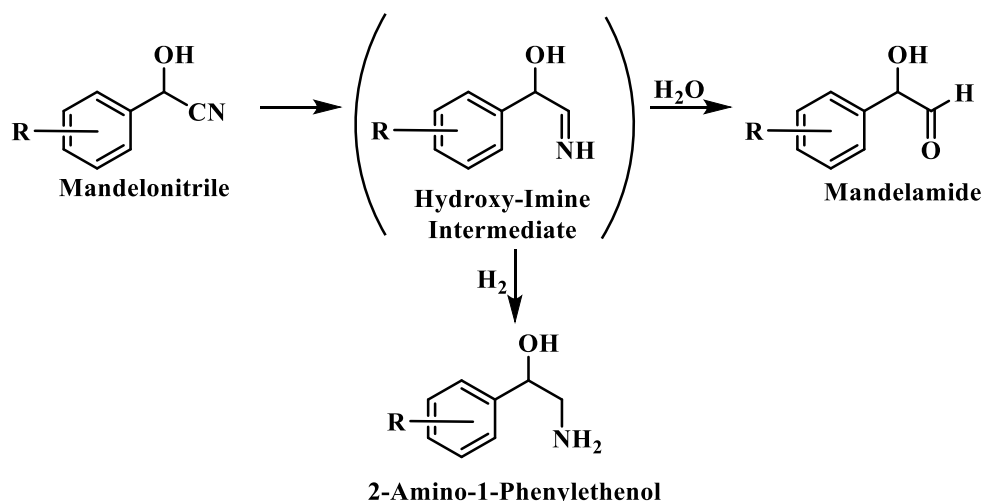
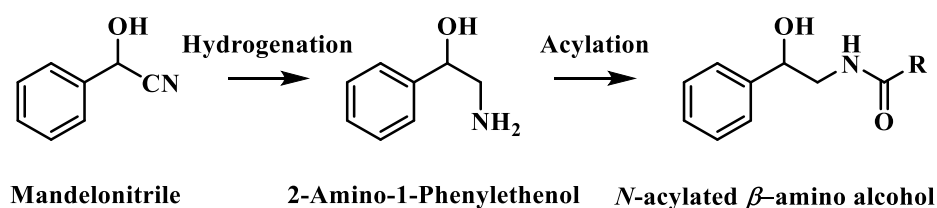


Figure 1.10. Experimental findings reported by Tinapp for the hydrogenation reaction of mandelonitrile. Figure adapted from reference 118.

Another class of compound with application in the pharmaceutical and agrichemical industries are *N*-acylated β -amino alcohols. These can be formed by the reduction of mandelonitriles, followed by acylation of the amino group (Scheme 1.11).^[119] Typically, the reduction is performed using LiAlH_4 , but can also be achieved by catalytic hydrogenation over Pd/C and PtO_2 under strongly acidic conditions.^[96, 120–121] Owing to the facile hydrogenolytic cleavage of C-O bonds over palladium and platinum catalysts, removal of the alcohol functionality was incurred. The amine group, however, was

preserved.^[96] Whilst this was an undesirable outcome for this particular application,^[122] the observations mirror the findings of previous studies in the Lennon group.



Scheme 1.11. Formation of N-acylated β -amino alcohols from mandelonitriles via hydrogenation of the nitrile group followed by acylation of the amino group.

1.6 Characterisation and Analytical Techniques

Whilst selection of an appropriate reaction system is essential, it is also crucial that both the catalyst and product output can be analysed and well understood. As such, both catalyst characterisation and analytical techniques employed in this study are described.

1.6.1 Atomic Absorption Spectroscopy

Atomic absorption spectroscopy (AAS) is an analytical technique which is used to determine the concentration of elements in a sample. Each element has its own distinct set of wavelengths at which it will absorb energy. As such, qualitative and quantitative analysis of a sample is possible using this technique. Upon absorption of light, the atoms undergo an electronic transition where electrons are promoted from one energy level to a higher energy level. The wavelength of light absorbed corresponds to the energy required for this transition to occur.

The sample is first atomised to produce gaseous atoms. A hollow cathode lamp is then used to produce light of the desired wavelength. Following this, the resultant beam of electromagnetic radiation is passed through the vaporised sample. At this point, the absorption intensity is identified by a detector.^[123] Figure 1.1 provides a graphic representation of an atomic absorption spectrometer.

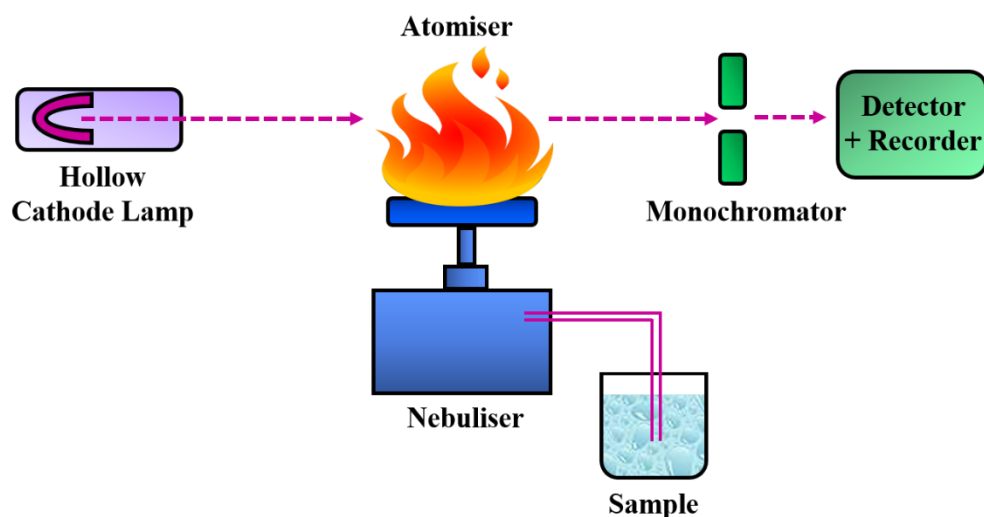


Figure 1.1. *Instrumentation of an atomic absorption spectrometer.*

The amount of adsorbed radiation is proportional to the amount of element present, hence providing the basis of quantification. A calibration curve can be constructed by running several samples of known concentration. From this, the concentration of the unknown substance may be extrapolated from its absorbance (A). As the initial intensity, I_0 , of the radiation used is known and the intensity remaining, I , is measured at the detector, quantitative detection follows the Beer-Lambert Law (Equation 1.1).^[124]

$$A = \log \frac{I_0}{I} = \epsilon cl \quad \text{Equation 1.1.}$$

In which ϵ denotes the molar extinction coefficient whilst c is the molar concentration and l is the path length.

1.6.2 Inductively Coupled Plasma-Optical Emission Spectroscopy

Inductively coupled plasma-optical emission spectroscopy (ICP-OES) is an analytical technique used in the detection of elements. It is a type of emission spectroscopy that uses inductively coupled plasma to produce excited atoms and ions that emit electromagnetic radiation. The wavelength of the emitted radiation is characteristic of the elements present. The intensity of the emissions from the various wavelengths of light are proportional to the concentrations of the elements within the sample, thus providing a means for quantification.

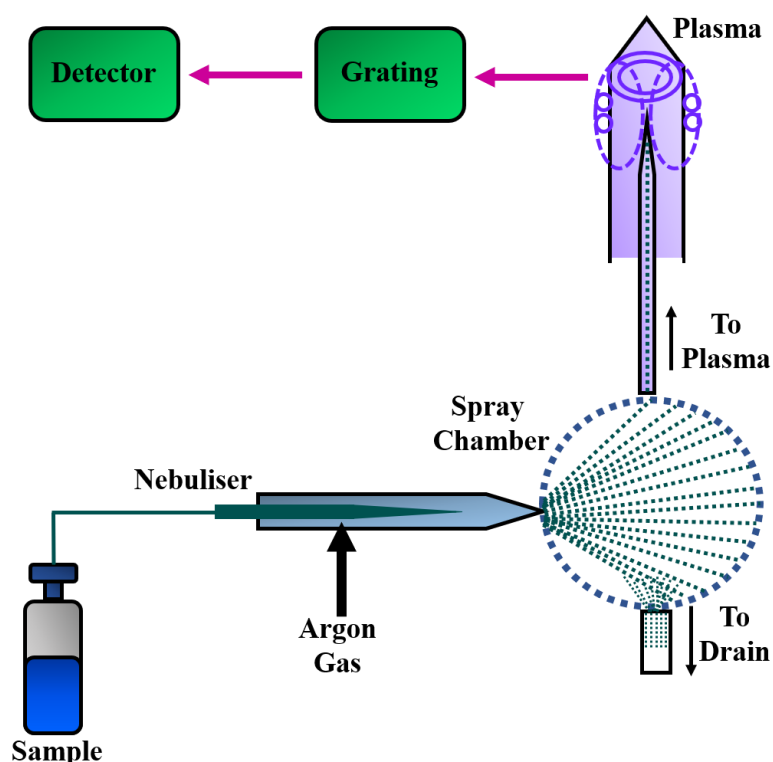


Figure 1.2. Schematic diagram of sample introduction into ICP-OES.

Typically, it is argon gas which is used to generate the plasma. The ICP-OES torch consists of three concentric quartz glass tubes. The output coil of the radio frequency generator surrounds part of this quartz torch. The argon gas flowing through the torch is ignited with a tesla unit that creates a brief discharge arc through the argon flow to initiate the ionization process. The argon gas is ionised in the electromagnetic field and flows in a rotationally symmetrical pattern towards the magnetic field of the radio frequency coil. A stable, high temperature plasma of about 7000 K is then generated as the result of the

inelastic collisions between the neutral argon atoms and the charged particles. The plasma is sustained and maintained by inductive coupling from cooled electrical coils. Solution samples are introduced into the plasma in an atomised state, created *via* nebulisation. The sample collides with the electrons and charged ions in the plasma and is broken down. The high temperature plasma excites the atoms, leading to the emission of radiation.^[123] The ICP-OES set-up is shown schematically in Figure 1.2.

1.6.3 Scanning Electron Microscopy and Energy Dispersive X-Ray Spectroscopy

A scanning electron microscope (SEM) is a type of electron microscope which produces images of a sample by scanning it with a focused beam of electrons. The electrons interact with atoms in the sample and produce various detectable signals which can be used to assess the surface morphology of a substance.^[125] The hardware associated with a scanning electron microscope is shown in Figure 1.3 A.

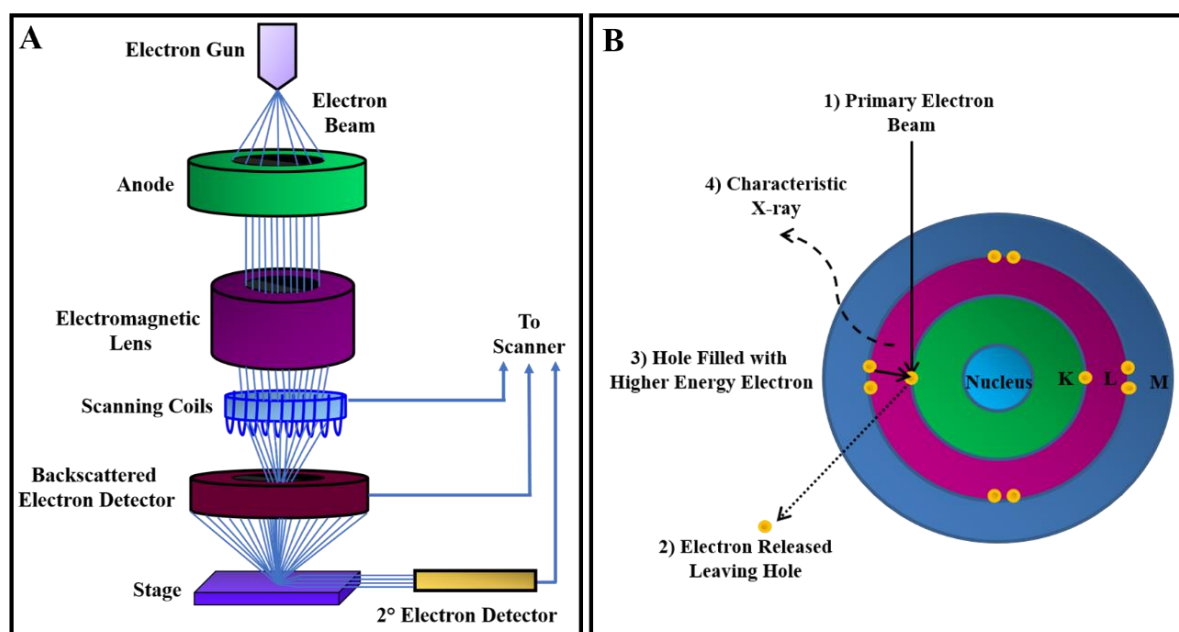


Figure 1.3. *A, hardware associated with a SEM and, B, the X-ray generation process.*

Incoming electrons (primary electrons) provide the atomic electrons present in the sample with energy, resulting in their release as secondary or Auger electrons. These electrons are then emitted with a range of energies.^[126] The primary electrons are focused into a

small diameter electron probe, which is scanned across the sample. Electrostatic or magnetic fields applied at right angles to the beam can be used to change its direction of travel. By scanning simultaneously in two perpendicular directions, a square area of the sample, known as a raster, can be covered. An image of this area can be formed by collecting secondary electrons from each point in the sample.^[126]

Energy Dispersive X-ray (EDX) spectroscopy is a technique used to identify the presence and estimate the quantities of elements in a sample. This is done through the detection of the characteristic X-rays, which are irradiated from a high energy electron beam. Whilst it is backscattered and secondary electrons which are used to make a SEM image, there are many other signals produced as a result of the interaction of the electron beam and the material. One such example are X-rays. These can then be used to provide additional information about the sample.

Every atom has a unique number of electrons that reside in specific locations. These positions belong to certain shells which have different discrete energies. As such, the generation of X-rays in a scanning electron microscope can be described in a two-step process. With reference to Figure 1.3 **B**, in step one, the electron beam hits the sample and, in doing so, transfers energy to the atoms of the samples. This can either excite the electron in the atom to a higher energy level or cause it to be knocked-out of the atom, leaving behind a positively charged hole. In the second step, the resultant hole attracts a negatively charged electron from a higher energy shell. When the higher energy shell electron fills the hole, the energy difference associated with the transition is released in the form of an X-ray. The energy difference between the two shells is dependent upon atomic number and is hence unique to every element. Consequently, the emitted X-rays are characteristic to a particular element, and thus, can be used to ascertain whether or not an element is present in a sample.^[127]

1.6.4 Transmission Electron Microscopy

A transmission electron microscope (TEM) is operated using the same basic principles as a light microscope. However, instead of using light, electrons are used. It is the significantly lower wavelength of electrons, when compared to light, which makes it possible to overcome the limitations experienced with light microscopy and results in an improved resolution.^[128]

A source, located at the top of the microscope, emits electrons which then travel through a vacuum in the column of the microscope. The TEM uses electromagnetic lenses to focus the electrons into a very thin beam. Following this, the electron beam passes through the sample. Upon impact, some of the electrons are scattered and are thus removed from the beam. The remaining unscattered electrons hit a fluorescent screen, giving rise to an image. Varying darkness in the resultant images relates to the density of the sample.^[128]

1.6.5 CO Chemisorption

The chemical adsorption isotherm reveals information about the active surface of a material and has been used for many years as a tool to evaluate catalysts. Chemisorption is a single layer process and is more selective than physisorption, only occurring between certain adsorbate and adsorbent species. Moreover, the process of chemisorption will only occur if the surface has been pre-cleaned of any previously existing surface molecules.^[129]

Chemisorption can be used to determine the quantity of gas required to form a monolayer of chemisorbate on an active surface. The quantity of molecules taken up by a surface depends on several variables. The probe molecule is pulsed in small known volumes over the active surface. The probe molecule will then adsorb onto the surface of the catalyst. Any unabsorbed gas is swept, with a carrier gas, through to the detector where it is quantified. As the monolayer forms on the active surface, increasingly less of the adsorptive gas is taken up by the sample. For a pulse-flow mode of operation, adsorptive gas is repeatedly pulsed over the sample until it is saturated, indicated by the detector when multiple consecutive detector readings are the same.^[129]

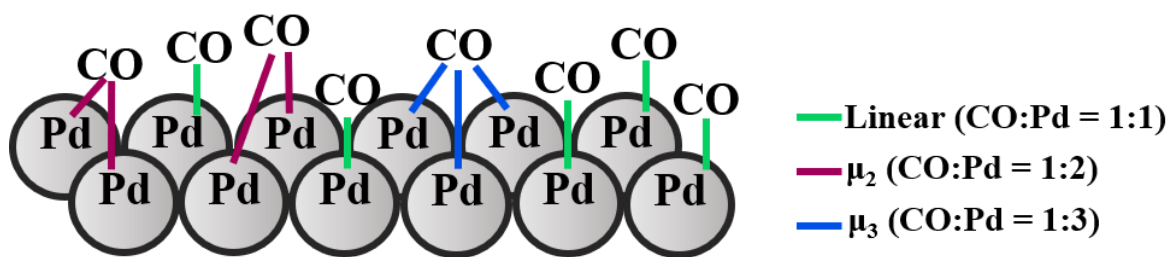


Figure 1.4. Schematic representation of the different binding modes available to CO on a palladium surface.

Chemisorption experiments, where CO is used as the probe molecule, are widely used to determine metal particle size and dispersion for supported palladium catalysts.^[130–131] Despite the simplicity of the technique, the variability of the surface CO:Pd stoichiometry means that it is an *average* chemisorption geometry which is used. The different binding geometries available to a CO probe molecule on a palladium surface are presented in Figure 1.4. Another commonly used chemisorption probe molecule is hydrogen. The use of hydrogen chemisorption to probe the active sites of a palladium catalyst can, nevertheless, lead to difficulties due to the presence of sub-surface hydrogen and the formation of palladium hydride.^[130–131]

1.6.6 Powder X-Ray Diffraction

X-rays are generated in an X-ray tube, produced by a tungsten filament, and are accelerated at high voltage (40–60 kV) towards a metal target. The majority of the kinetic energy, produced by the electron hitting the target, is lost as heat, with only a small proportion of electrons capable of generating X-rays. For electrons that possess sufficient energy for X-ray production, their collision with the metal target results in the ejection of electrons from the atomic orbitals of the metal, resulting in formation of a vacancy. It is then possible for an electron from a higher energy level to fill the vacancy, giving rise to the release of energy in the form of an X-ray.^[132]

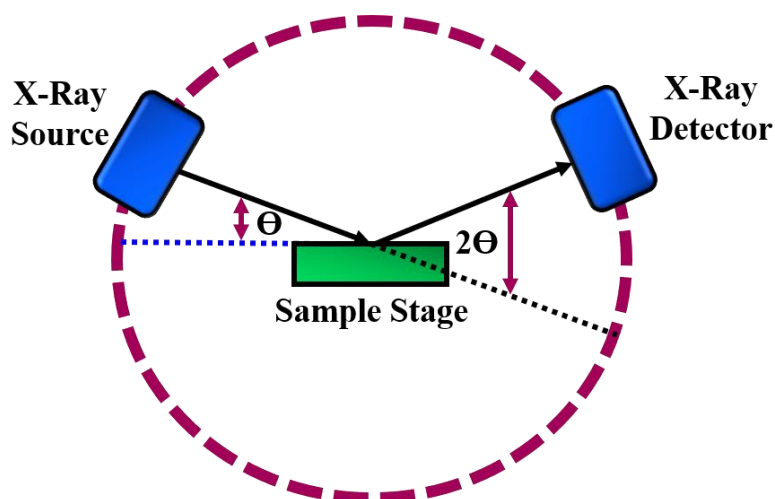


Figure 1.5. Schematic representation of PXRD diffraction geometry.

The resultant X-ray is focused on the sample at an angle, θ , while the detector, opposite the source, reads the intensity of the X-ray it receives at an angle of 2θ from the source path. The incident angle is increased over time. The detector angle, however, always remains at 2θ from the source path (Figure 1.5). When the X-rays reach the sample, the incoming beam is either reflected off the surface or enters the lattice, where it is diffracted by the atoms present in the sample. Each spot in the diffraction pattern comes from the constructive interference of X-rays, reflected from the atoms lying in the planes of the crystal lattice.^[133–134]

1.6.7 Raman Spectroscopy

In Raman spectroscopy the molecules in the sample inelastically scatter monochromatic laser light. The scattered light can subsequently be used to provide information on molecular structure. Energy from the laser is exchanged with the molecules in such a way that the scattered light photons have either a higher or lower energy than the incident photons. This difference in energy is due to a change in the vibrational energy of the molecule.^[135]

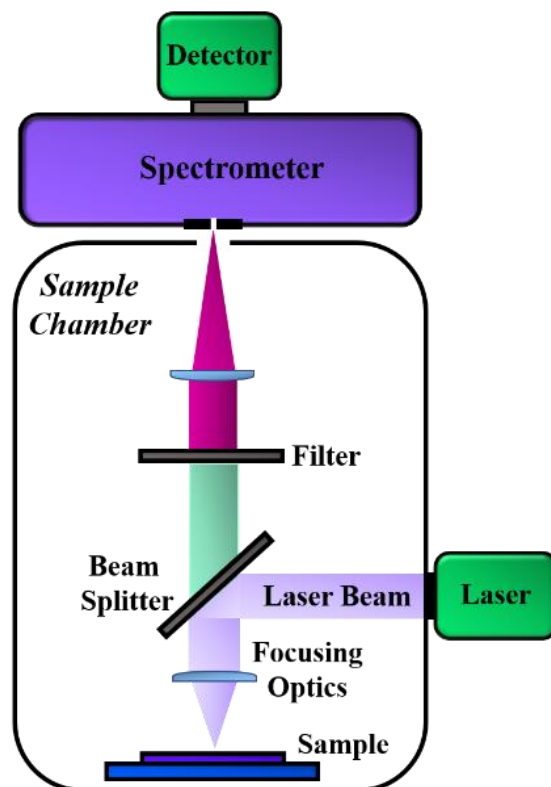


Figure 1.6. *Schematic of a Raman Spectroscopy set-up.*

A representative schematic of a Raman spectroscopy set-up is shown in Figure 1.6. The sample is first illuminated by a source of monochromatic light from a laser. Electromagnetic radiation from the illuminated spot is then collected with a lens and passed through a filter. The majority of the elastically scattered radiation will be of the same energy of the incident beam, defined as Rayleigh scattering and subsequently filtered out. The remainder of the scattered light, resulting from excited electrons which have not relaxed back to their original energy levels, is dispersed onto a detector.^[135]

1.6.8 Nitrogen Physisorption

Physisorption refers to the adhesion of gas molecules to a surface. The adsorbate adheres to the surface solely through weak intermolecular van der Waals interactions. This is a non-specific interaction and a reversible process. Physisorption techniques can be used to provide information on surface area, pore size, and pore architecture; all of which are important factors in catalysis. Indeed, these properties relate directly to catalyst activity and selectivity.^[136]

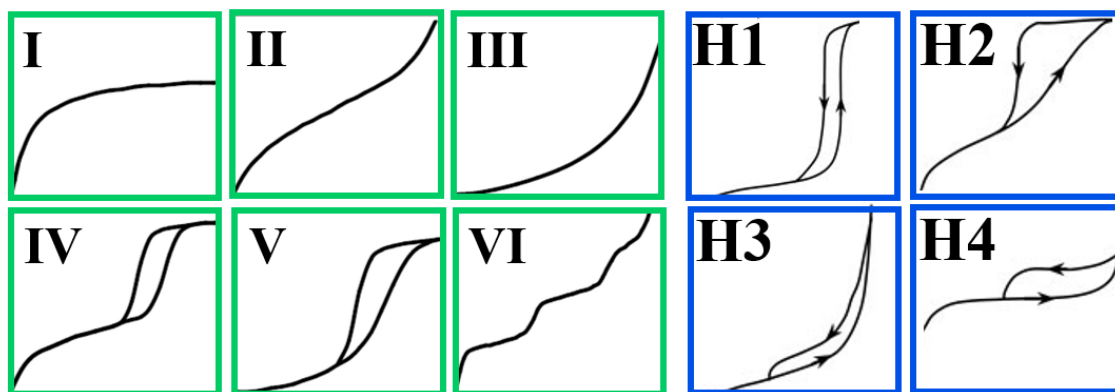


Figure 1.7. International Union of Pure and Applied Chemistry (IUPAC) classification of gas adsorption isotherms (green boxes), and hysteresis loops (blue boxes).^[137–138]

The adsorption isotherm represents the relationship between the pressure and volume of gas adsorbed at a constant temperature. Isotherms, first defined by Brunauer, each possess a characteristic shape, as shown in Figure 1.7 (green boxes).^[139] It is pore size and surface character which determines the type of adsorption which is observed.^[137] Each of the six isotherm types are defined as follows:^[140–141]

- **Type I:** Monolayer adsorption, characteristic of microporous solids.
- **Type II:** Poly-molecular adsorption, present in non-porous or microporous adsorbents.
- **Type III:** An isotherm characteristic of non-porous sorbents.
- **Type IV:** Materials which possess a strong adsorbate-surface interaction.
- **Type V:** Materials which possess a weak adsorbate-surface interaction.
- **Type VI:** A step-wise isotherm, associated with the adsorption onto uniform, non-porous solid surfaces. Each step corresponds to the formation of a complete monomolecular adsorption layer.

For isotherm types IV and V, capillary condensation is observed and is identified by the presence of hysteresis. Capillary condensation is the process by which multilayer adsorption, from the vapour phase into a porous medium, proceeds to the point where pore spaces become filled from the vapour phase. There is a correlation between the shape of the resultant hysteresis loop and the texture of a mesoporous adsorbent. Here, texture refers to pore size, pore distribution, pore geometry and connectivity. Analysis of hysteresis loop shape can hence provide information on the nature of the porosity in the

sample. An empirical classification of hysteresis loops is given by IUPAC (Figure 1.7, blue boxes) which finds its basis on an earlier classification by de Boer.

Hysteresis loops are associated with the filling and emptying of mesopores and, as such, they describe the difference between the adsorption and desorption curves. According to the classifications proposed by IUPAC, hysteresis loops can be categorised into four major groups.

Type H1 exhibits a narrow loop with steep, nearly parallel adsorption and desorption, and is associated with a narrow distribution of relatively uniform cylindrical pores. Materials that give rise to H2 hysteresis contain a more complex and disordered pore structure. Typically, there are interconnected networks of pores of different shapes and sizes. Type H2 loops have a characteristic broad loop with flat plateau accompanied by a steep desorption branch. In contrast to types H1 and H2, types H3 and H4 loops do not terminate in a plateau at high p/p_0 , making the limiting desorption boundary curve more difficult to establish. Nevertheless, both types H3 and H4 hysteresis contain a characteristic step-down in the desorption branch, associated with the closure of the hysteresis loop. Isotherms with type H3 hysteresis do not exhibit any limiting adsorption at high relative pressure, thus indicating the presence of slit-shaped pores. Similarly, H4 hysteresis loops are associated with narrow slit pores but are generally observed with more complex materials which contain both micropores and mesopores.

1.6.9 Thermogravimetric Analysis

Thermogravimetric analysis (TGA) is a method of thermal analysis where the mass of a sample is measured over time as the temperature changes. This measurement can be used to provide information on a wide range of physical and chemical phenomena, such as, phase transitions and thermal decomposition.^[142]

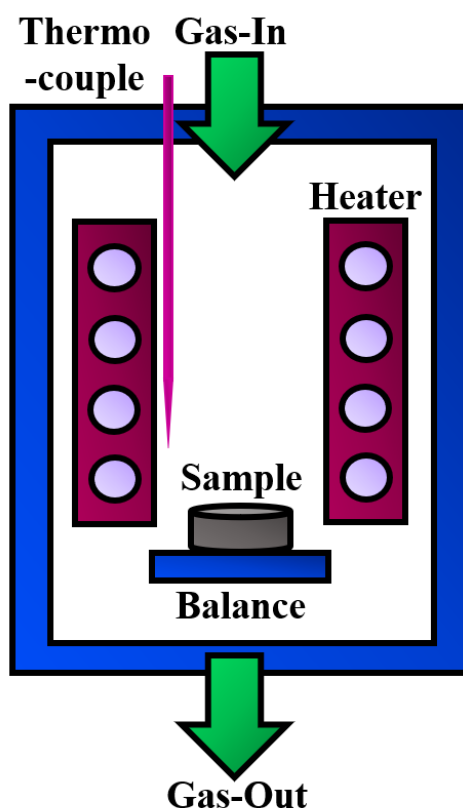


Figure 1.8. Generic instrumentation associated with thermogravimetric analysis.

A thermogravimetric analyser consists of a sample pan, supported by a precision balance. The sample pan resides inside a furnace with programmable temperature control. A sample purge gas is used to control the sample environment. This gas may be inert or reactive and flows over the sample whilst the temperature is increased at a constant rate and exits *via* an exhaust. A schematic diagram of the hardware associated with a thermogravimetric analyser is presented in Figure 1.8. In the determination of thermal stability, if no mass change is observed, then the material is stable within that particular temperature range. Negligible mass loss will consequently correspond to a plateau on the TGA trace.

1.6.10 High Performance Liquid Chromatography

High Performance Liquid Chromatography (HPLC) - sometimes referred to as High Pressure Liquid Chromatography - has proved to be a useful analytical technique. It is used widely as a means of identifying and quantifying the components of mixtures which are often complex in nature.^[143] In general, chromatography involves the movement of a sample through the system over a stationary phase.^[144] In the case of HPLC, the stationary phase is the packing material of the column whilst the mobile phase is a liquid solvent.^[134] The hardware required, seen schematically in Figure 1.9, includes a solvent reservoir, a degasser, a pump, an injection system, a column, a detector, and a method of data acquisition.

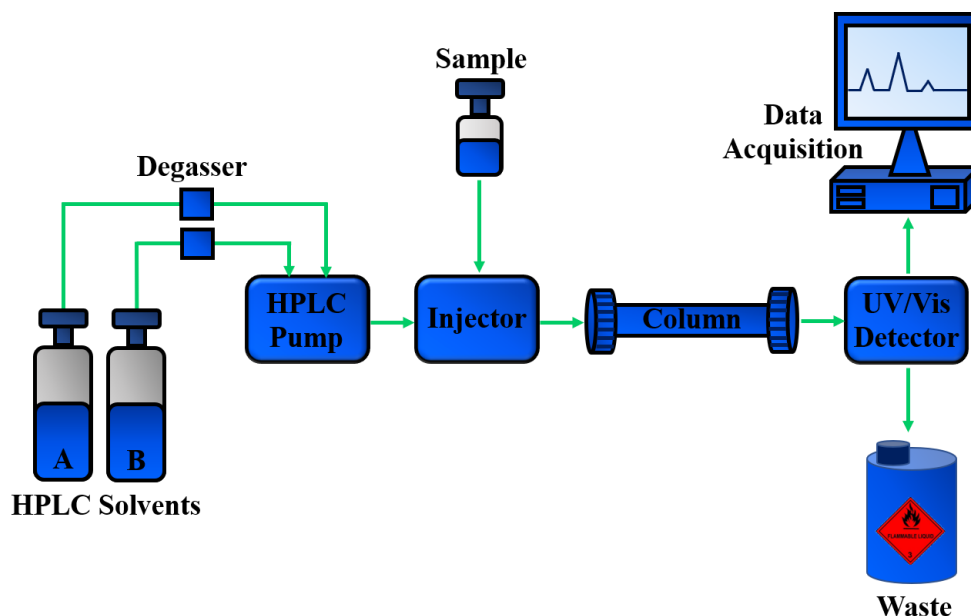


Figure 1.9. Schematic representation of a high performance liquid chromatography set-up.

HPLC solvents are stored in a solvent reservoir and must be completely free from dust and dissolved air. As such, the solvents are filtered *via* a membrane filter and degassed for approximately 30 minutes prior to use. Owing to their improved purity, the use of analytical grade solvents is advocated. A pump is then used to drive the solvent through the system at a specified rate. A gradient valve can be used to simultaneously pump multiple solvents. This is typically between two and four solvents. The injector valve temporarily switches the flow from the pump through a loop of tubing which contains the

sample. The sample is injected, either manually or *via* an autosampler, from a vial into this loop. Insertion of the liquid sample into the injector, located at the end of the column, commences the chromatographic process. Columns are typically made from stainless steel tubing, approximately 10–25 cm in length and 5 mm in diameter. The column packing is kept in place by metal frits. The stationary phase is composed of micron-sized porous particles and, therefore, high pressures are required to force the solvent through the column. After leaving the column, the sample passes to a detector, most commonly a UV detector. UV wavelength can either be fixed, typically at 254 nm, or variable. The detector is highly sensitive and able to detect concentrations down to the $\mu\text{L/mL}$ range for some aromatic substances. The response is linear with concentration.^[143–144]

Each of the sample components will possess a different affinity for the stationary phase, and so, will have a different interaction with it, thus providing basis for separation. The sample components which interact with greater strength to the stationary phase will travel through the column at a slower rate than components which have weaker interactions.^[134] Peak resolution is determined by the interaction of the solute with the mobile and the stationary phases and can be tailored through the choice of solvents (mobile phase) and column (stationary phase). Fine tuning of these conditions can therefore be achieved, and as a result, HPLC has a somewhat higher degree of versatility over other chromatographic methods.^[145]

1.6.11 Nuclear Magnetic Resonance Spectroscopy

Nuclear magnetic resonance (NMR) spectroscopy is an analytical technique used to observe local magnetic fields around atomic nuclei.^[146–147] For a nucleus to be investigated by NMR it must have a nuclear spin quantum number (I) that does not equal zero. The nuclear spin arises from unpaired proton and neutron spins present in the nucleus. NMR spectroscopy monitors the resultant absorption and emission of the transmissions between nuclear spin energy levels of the system which occur as the result of excitation. The energy levels arise from the interaction of the nuclear spin with the magnetic field of the spectrometer and with the magnetic fields set up by other nuclear spins and electrons.^[146–147]

Quantum mechanics dictates that the nuclear spin is quantised and can take integral or half-integral values, depending on the number of unpaired protons and neutrons.^[146] In

the absence of an external magnetic field (B_0), all of the energy levels (m_I states) are degenerate as there is nothing with which the nuclear magnetic moment can interact.^[147–148] As such, the orientation of the nuclear magnetic moment in space will not have an effect on the energy of the system. When the nucleus is placed in a magnetic field, however, different orientations arise, each with a different energy.^[148] Nevertheless, as nuclear spin is quantised, only certain orientations of the nuclear magnetic moment, with respect to the applied field, are allowed, resulting in $2I+1$ discrete energy levels – a phenomenon known as the Zeeman splitting.^[146] For spin $1/2$ nuclei, such as ^1H and ^{13}C , two discrete energy levels are possible, corresponding to $m_I = +1/2$ and $m_I = -1/2$ states.^[147]

When a magnetic field is applied the spin polarisation begins to precess around the magnetic field at the Larmor frequency. Owing to the precessional motions of the nuclei, as well as the wandering motion of the molecule in a sample, more magnetic moments adopt lower energy orientations. The bulk magnetisation vector is then tilted away from the z-axis. Following this, the bulk magnetisation vector precesses about the magnetic field, again at the Larmor frequency.^[148–149] A receiver coil measures the signal as the spins come into equilibrium with the magnetic field. The magnetisation grows along the z-axis in a process called longitudinal relaxation.^[148]

1.6.12 Mass Spectrometry

Mass spectrometry is an analytical technique which measures the mass to charge ratio of ions. A very basic representation of a mass spectrometer is shown in Figure 1.10. The sample is first vaporised before being introduced into the ionisation chamber at very low pressure. The vaporised sample is then bombarded by high energy electrons. The collision between an electron and the molecule (M) causes an electron to be ejected from the sample, leaving a positively charged ion (M^+). The sample molecule may break into charged fragments or simply become charged without fragmenting. The ions are attracted by an applied electrostatic potential and are hence accelerated towards a negative plate. The ions then pass into a magnetic field. The positive ions are then deflected by an amount dependant on their mass (m) and charge (z). The lighter the ion and the greater the charge, the more significant its deflection. Thus, the ions are separated according to their mass to charge ratio.

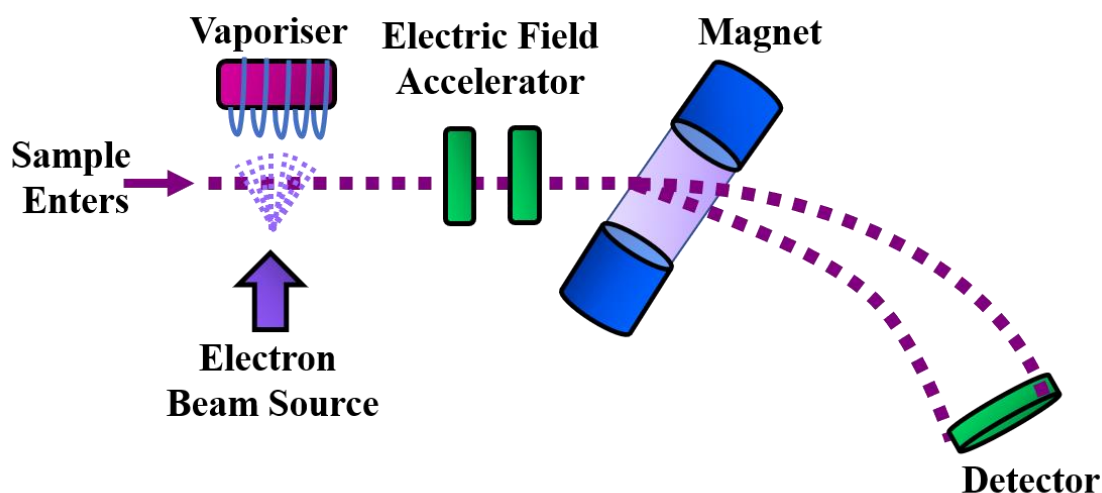


Figure 1.10. Basic features of a mass spectrometer.

1.7 Project Background

The research documented in this thesis represents the findings of a third-stage PhD project undertaken at the University of Glasgow in collaboration with Syngenta, a global agrichemical company specialising in crop protection measures. The project relates to a specific nitrile hydrogenation transformation, mediated by a Pd/C catalyst, involved in the production of a non-specified agrichemical. Specifically, catalyst deactivation issues associated with the fed batch hydrogenation reaction of a ring-substituted aromatic cyanohydrin, to form a primary amine, were identified at the industrial centre. Complications associated with this particular step led to a compromise in the industrial viability of the whole synthesis.

Due to sensitivity issues regarding intellectual property, model compounds were utilised at the University of Glasgow. The first stage of the project conducted by McMillan (2008–2012) examined a series of model compounds to gain a general understanding of aromatic nitrile hydrogenation reactions.^[150] The majority of McMillan's work focused on benzonitrile as a substrate. Benzonitrile was found to be hydrogenated to the valuable benzylamine before undergoing a subsequent hydrogenolysis reaction, yielding toluene and ammonia. At the time, this outcome was somewhat unexpected. The literature has since well documented the production of toluene by this means and many imaginative

ways of suppressing its formation, such that, production of the desired primary amine may be favoured.^[3, 68] When examining the prospect of hydrogenolysis further, gas-phase infrared studies clearly showed the formation of the ammonia by-product. Closer scrutiny of the reaction revealed a consecutive process, encompassing a first order hydrogenation reaction followed by a zero order hydrogenolysis reaction.^[36] Additional co-adsorption studies suggested that these two distinct reactions occurred independently, on discrete palladium sites.^[35] Moving away from the benzonitrile studies, the aliphatic chain length was extended, examining substrates benzyl cyanide, 3-phenylpropionitrile, and cinnamionitrile. Whilst conversion was observed for benzyl cyanide, an increase in the length of the aliphatic chain resulted in a complete loss of reactivity.^[35]

Efforts were then moved to a more complex substrate, the cyanohydrin mandelonitrile. The mandelonitrile hydrogenation reaction was found to require an acid additive, with no reaction observed in a neutral environment. Repeat use of the catalyst showed a dramatically poor outcome, with significant deactivation observed after only one cycle of use. In the mandelonitrile hydrogenation reaction, no imine intermediates were observable in the liquid phase. Thus, additional functionality was added to the aromatic ring, allowing stabilised imine species to be observed in the liquid phase. The nature of the substituent was shown to affect the product distribution, suggesting a role for electronic factors.

The second stage of the project, conducted by Gilpin (2012–2016), focused exclusively on the hydrogenation reaction of mandelonitrile.^[151] In this instance, however, focus was brought to the significant deactivation issues experienced when the catalyst was cycled. It was thought that a build-up of oligomeric species on the surface of the catalyst was responsible for the observed deactivation. Inelastic neutron scattering measurements were used to probe the surface of the catalyst. The results of which were found to corroborate the proposed theory. The yield of phenethylamine achieved when the catalyst was cycled was improved by increasing the hydrogen availability in the reactor through alterations to temperature, hydrogen pressure, and agitation speed. Examination of 4 reagent additions over the same un-regenerated catalyst showed vast improvements in terms of product yield and catalyst durability as a result of these alterations.

It was proposed that high energy edge sites on the palladium crystallites were responsible for the observed deactivation. Thus, investigation into the removal of the edge sites *via* a high temperature annealing process was conducted. The resultant alteration of the catalyst

morphology afforded larger palladium particles which, having fewer edge sites, were more spherical in nature. These morphological alterations resulted in a reduced reaction rate. Moreover, no significant selectivity issues occurred. Infrared studies using CO as a probe molecule were subsequently explored to examine the active sites available at the catalyst surface. To do this, a 5% Pd/ γ -Al₂O₃ catalyst was employed due to the highly absorbing nature of carbon supports, rendering them unsuitable for such measurements.^[153] Unfortunately, it was identified that the annealing process was ineffective in the removal of the high energy edge sites.

1.8 Project Aims

It can therefore be surmised that the heterogeneously catalysed hydrogenation of aromatic nitriles to selectively afford primary amines requires further investigation. Previous work within the Lennon Group has culminated in a thorough understanding of the benzonitrile hydrogenation reaction. However, whilst preliminary investigations into the hydrogenation reaction of mandelonitrile have been undertaken, detailed mechanistic insight for this substrate system is lacking. Against this background, the following project aims are proposed:

- To make a link between the well understood benzonitrile reaction system and the more complex mandelonitrile reaction system, the hydrogenation of 4-hydroxybenzyl cyanide is investigated. This represents a simple reaction system with well-defined chemistry which can be used to probe the effects of various reaction conditions on product selectivity.
- The hydrogenation reaction of mandelonitrile will then be investigated, using a single batch set-up in the first instance, to enhance the mechanistic awareness of this reaction system. Analysis of the resultant reaction mixture will be conducted using HPLC.
- To compliment the mandelonitrile hydrogenation reaction studies, the corresponding deuteration reaction will be investigated. In order to fully analyse the resultant data, appropriate analytical technology must be developed and employed. The use of multinuclear NMR spectroscopy and mass spectrometry

will therefore be utilised for the analysis of the isotopologue distribution resulting from the mandelonitrile deuteration reaction.

- Once mechanistic refinement has been achieved, it is necessary to consider a product scale-up methodology such that the reaction may progress from single batch to a continuous production. To do this, repeat batch technology which mimics the fed batch technology used in the industrial operation will be employed. For this to be as effective as possible, it is essential that optimal reaction conditions are employed. Thus, a variety of changes to the experiential conditions will be implemented to establish optimum operation.
- On cycling the catalyst, it was identified by previous investigations that significant deactivation occurs. It is thus proposed that the mechanistic information gleaned in the first part of the study may be applied to the repeat batch process to alleviate some of the deactivation issues. As equipment and safety limitations are likely to be incurred at the University of Glasgow, it is crucial that the understanding of the deactivation is as comprehensive as possible. This will allow predictions regarding further possible improvements to be made. These enhancements may then be implemented at the industrial site.
- It is hoped that the nitrile hydrogenation knowledge gained from the 4-hydroxybenzyl cyanide and mandelonitrile reaction systems can be extended to yet more complex substrate systems. Exploration into the hydrogenation reaction of a dinitrile species (1,2-dicyanobenzene) is thus considered as part of a future project.
- Overall, a more comprehensive global view of aromatic nitrile and cyanohydrin hydrogenation reactions is sought, so that it may be effectively applied at the industrial complex.

CHAPTER 2

Experimental

2.1 Materials

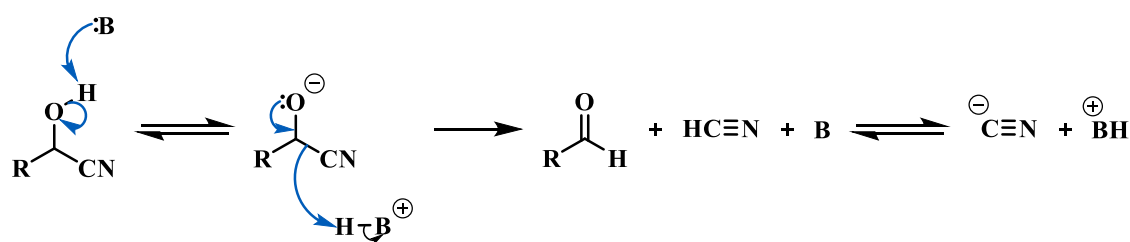
For the hydrogenation reactions of model substrates (4-hydroxybenzyl cyanide, mandelonitrile and 1,2-dicyanobenzene), a generic, commercially available, fine chemicals catalyst (5% Pd/C, Sigma Aldrich, GU-1) was employed in all instances. This catalyst was benchmarked against the technical 5% Pd/C catalyst used in the associated industrial process and found to perform comparably.^[150] Additionally, a second commercially available catalyst was investigated (5% Pd/ γ -Al₂O₃, Alfa Aesar, GU-2). This was used for comparison purposes in the mandelonitrile hydrogenation reaction. Characterisation of both catalysts (GU-1 and GU-2) is reported in Chapter 3.

A variety of substrates, including 4-hydroxybenzyl cyanide (Tokyo Chemical Industry, >99% purity), racemic mandelonitrile (Tokyo Chemical Industry, >97% purity), 2-amino-1-phenylethanol (Sigma Aldrich, 98% purity), 2-aminoacetophenone hydrochloride (Alfa Aesar, 97% purity), 1,2-dicyanobenzene (Sigma-Aldrich, 98% purity) and 2-cyanobenzylamine hydrochloride (Sigma Aldrich, 97% purity) were investigated. A sulphuric acid additive (Fischer Scientific, nominally 95–98%) was typically included in the reaction mixture. However, a variety of acid additives, including hydrochloric acid (Sigma-Aldrich, 36.5–38%), acetic acid (Sigma-Aldrich, 99%), and phosphoric acid (Fluka, 49–51%) were also considered. The liquid phase hydrogenation reactions were primarily conducted in methanol (Riedel-de Haën, 99.9% purity), however, several other solvents were also considered. The additionally investigated solvents included ethanol (VWR, 99.97% purity), butan-1-ol (Alfa Aesar, 99% purity), and tetrahydrofuran (Fischer, 99.8% purity). All reagents have been used, as received, without further purification.

An automated gas flow controller (BPC 1202) allowed delivery of inert (N₂, BOC, 99.9% purity) and active (H₂, BOC, \geq 99.8% purity/D₂, BOC, \geq 99.8% purity) gases to the reactor *via* a gas reservoir. Helium gas (BOC, 99.9% purity) was also employed for reagent degassing.

2.1.1 Cyanohydrin Safety Considerations

As a side note, a degree of experimental caution is documented here. This relates specifically to the chemical hazard associated with cyanohydrin hydrogenation reactions in the presence of base. Under basic conditions it is possible for the cyanohydrin molecule to break down and release hydrogen cyanide gas as shown in Scheme 2.1. Against this rationale, the use of an acid additive is selected as a suitable means of attempting to improve selectivity towards the primary amine.



Scheme 2.1. Cyanohydrin breakdown under basic conditions. [B = base].

2.2 Hydrogenation/Deuteration Reaction Procedure (University of Glasgow)

The majority of the experimental work was conducted at the University of Glasgow using a Büchi stirred autoclave and operated in one of two modes: single batch or repeat batch. Whilst a generic procedure is described here, the specific reaction conditions relating to each experiment are provided in the corresponding figure captions in Chapters 4–8 and 12.

2.2.1 The Büchi Stirred Autoclave

The Büchi reactor is specifically designed for laboratory scale elevated pressure reactions, with a maximum pressure capacity of 12 barg being achievable with this apparatus. However, due to the safety restrictions at the University of Glasgow, the maximum pressure is capped at 6 barg. This apparatus allows for hydrogenation and

deuteration reactions to be carried out whilst a constant pressure of gas is maintained within the system.

The Büchi batch reactor is one system comprising of four interconnecting components: the Büchi autoclave, the press-flow gas controller, the autoclave motor-speed controller, and the Julabo refrigerating and heating circulator. This apparatus is presented schematically in Figure 2.1. All components are located within a fume cupboard that is vented as part of the laboratory (B3-14) extraction system. Thus, in addition to primary containment within the autoclave reactor, the ventilation cabinet afforded secondary containment.

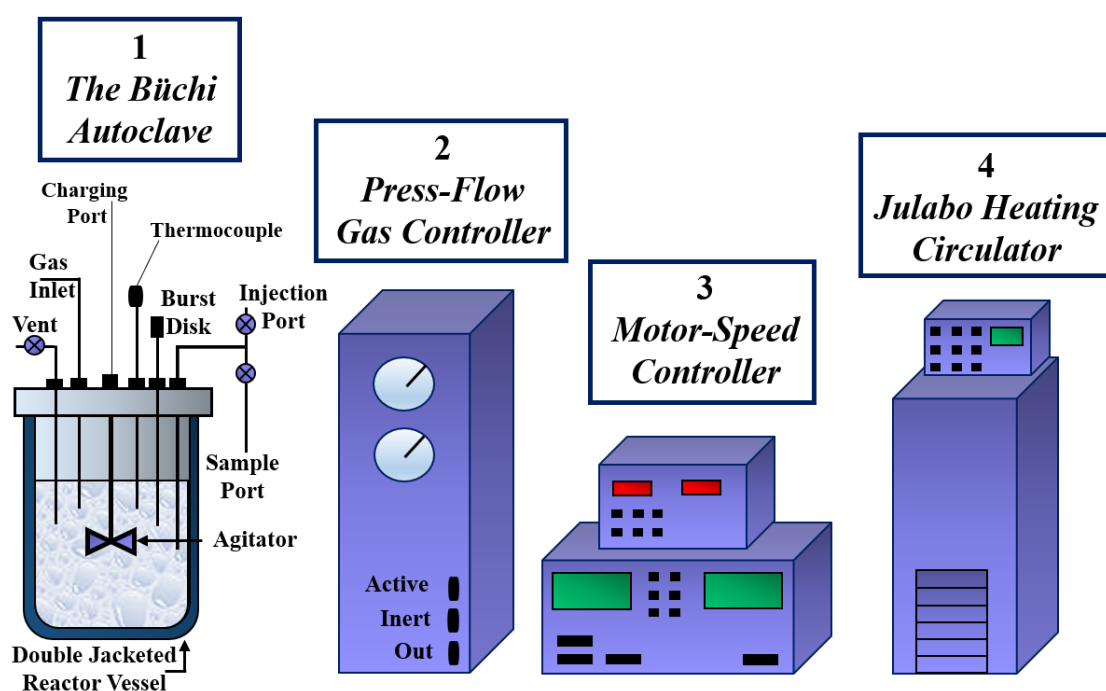


Figure 2.1. Schematic representation of the Büchi autoclave reactor.

1) The Büchi Autoclave

The autoclave is a 500 mL double jacketed glass reaction vessel. Except for the sampling port, which is constructed from $\frac{1}{8}$ inch stainless steel tubing, all piping required for the transport of both active and inert gases is made from $\frac{1}{4}$ inch stainless steel tubing. All additional connections on the reactor are likewise made from stainless steel.

The cover plate of the Büchi autoclave contains seven ports, each with a specific purpose. The introduction of gas (both inert and active) is achieved *via* the gas inlet port. The venting of both active and inert gases from the autoclave is undertaken *via* the scavenge port. Two further ports allow access of the thermocouple and the magnetic stirrer, which are connected to the Julabo heating circulator and motor-speed controller respectively. The main charging port enables the quick addition of catalyst and solvent to the autoclave, *via* a funnel, before the reaction commences. For safety purposes, a rupture element is installed. This is designed to burst at a specified final pressure (8 barg). For additional safety, the reactor is not operated without applying a Perspex shield. The final port is multipurposed, being used for the injection reagents as well as containing the sampling tap. A drain, located on the underside of the autoclave, ensures that the reaction vessel can be rapidly emptied and cleaned at the termination of each reaction.

2) The Büchi Press-Flow Gas Controller

The Büchi press-flow gas controller is a BPC 1202 system consisting of a gas controller and a control box. The gas controller allows the option for either an inert (nitrogen) or an active gas (hydrogen or deuterium) to be supplied, *via* a gas reservoir, to the reaction vessel during purging and reaction. The gas control box is responsible for monitoring the pressure of the active gas, thus allowing the consumption of the active gas to be monitored by the control box.

3) The Autoclave Motor-Speed Controller

The SM 94 autoclave motor-speed controller is connected to the magnetic drive of the stirrer shaft and is utilised to dictate the speed of the magnetic stirrer shaft. Stirring can be controlled up to 1100 rpm.

4) The Julabo Heating Circulator

The Julabo heating circulator enabled temperature control in the reaction vessel up to 170 °C. Silicon oil (47 V 100) is forced by a pressure pump into the lower port of the jacket surrounding the autoclave and is subsequently circulated back to the oil reservoir *via* a suction pump at the top port. Temperature can be monitored by one of two methods, either internally, *via* the oil bath or, externally, *via* the thermocouple in the reaction vessel.

2.2.2 Single Batch Operation

The hydrogenation/deuteration reactions of the various nitrile substrates were carried out in a 500 mL stirred autoclave (Büchi Glas Uster). The reactor was first charged *via* the charging port, with catalyst (wetted with approximately 10 mL of water) and solvent (310 mL). All ports and taps were closed, sealing the reactor. The system was then purged with inert gas (nitrogen). The catalyst/solvent mixture was heated to the reaction temperature and stirred at approximately 300 rpm under a flow of hydrogen/deuterium for 30 minutes in order to reduce the catalyst. The reaction vessel was heated by silicon oil, passed around the reactor *via* the heating circulator (Julabo, F25) and controlled externally *via* the thermocouple in the reactor. In a separate vessel, the substrate was combined with an acid additive, dissolved in the reaction solvent (40 mL) and degassed under helium using a balloon. It should be noted that not all experiments contained an acid additive. This is specified in the appropriate figure captions.

Once the desired temperature was obtained, both the active gas (hydrogen or deuterium) supply and the motor were turned off. The previously degassed reagents were then injected into the reactor *via* the addition valve at the injection port using a 50 mL syringe. The reagents were purged with nitrogen before all taps and ports were closed and the reactor pressurised to the desired value with hydrogen/deuterium. When the required reaction pressure was attained, agitation was initiated at the chosen value. The commencement of the agitation causes a pressure drop in the autoclave due to the solvation of either hydrogen or deuterium gas (active gas dependent) in the solvent.

It is important to note at this juncture that the time taken to reach operational pressure was dependent on the external active gas line pressure. In the hydrogenation study, two hydrogen line pressures were utilised: 6.5 barg and 8.0 barg. For an autoclave operational pressure of 6 barg, respective charging times of 7 and 3.5 minutes were required. When the designated reaction pressure was attained (typically 6 barg), agitation was commenced. The reaction was officially initiated when the pressure of the system stabilised at the chosen value. As the reaction typically commences during the short hydrogen pressure charging process; hydrogen up-take measurements cannot be reliably monitored during this procedure. However, once the reactor pressure is attained, hydrogen up-take measurements can be used to determine relative hydrogen consumption.

The reaction mixture was sampled at regular intervals throughout the course of the reaction coordinate. During sampling, the motor was temporarily stopped, allowing two 1–2 mL aliquots of the reaction mixture, which were obtained *via* the sample tap, to be collected. For each designated sampling time two aliquots were taken with the first being discarded as a washing. The catalyst was removed from the second sample using a 0.22 μm syringe filter (chromatography Direct, cellulose acetate). The residual liquid sample was analysed in the designated manner (HPLC, multinuclear NMR spectroscopy and/or mass spectrometry). Further, the pressure in the reaction vessel, both prior to and after sampling, was recorded, allowing the hydrogen consumption to be measured.

After the reaction was complete, both the agitation and gas supply were stopped, the reactor was cooled to room temperature and depressurised slowly by opening the tap at the scavenge port. The vessel was then purged with nitrogen gas to remove any residual hydrogen. The contents of the autoclave were subsequently released *via* the emptying valve, located at the bottom of the vessel. Gravity filtration of the solution was then carried out, allowing the catalyst and solvent to be disposed of in an appropriate manner. The autoclave was rinsed twice with methanol in preparation for the next reaction.

2.2.3 Repeat Batch Operation

The industrial process associated with the mandelonitrile reaction system operates as a fed batch (or semi-batch) reaction.^[154] Alterations to the single batch hydrogenation protocol were thus executed in order to maximise primary amine product formation. To this end, a repeat batch protocol, employed as a fed batch reactor mimic, was implemented. The repeat batch protocol aims to replicate the industrial experience and to provide information on the durability of the catalyst for the mandelonitrile hydrogenation reaction.

For the repeat batch protocol, an identical procedure to that utilised for a single batch reaction (Section 2.3.1) was initially employed. At reaction completion (taken as a fixed time of 120 minutes) a sample of the reaction mixture was taken. The reactor was then depressurised and a second aliquot of degassed reagent (mandelonitrile and acid), without further catalyst, was added to the reactor with 10 mL of methanol. Following this, the reactor was purged with nitrogen before being re-charged with hydrogen until the desired pressure was attained and the stirring recommenced. This second reaction was left, again

for 120 minutes, and sampled, as before, at reaction completion. This process was repeated until the desired number of reagent additions (typically six) had been achieved.

2.2.4 The Determination of Gas-Liquid Mass Transfer Coefficients (K_{La})

Liquid mass transfer coefficients (k_{La}) were determined using the dynamic pressure method.^[155] The reaction solvent was first degassed with nitrogen to obtain an equilibrium whilst the temperature of the vessel was increased. Once the desired temperature (40 °C) was reached, the reactor was pressurised to 6 barg with hydrogen. Following this, the motor controlling the agitation speed was switched on at a set value. Immediately after the agitation commencement, the pressure of the vessel declines as the gas from the head space of the reactor is adsorbed into the liquid. The pressure of the system continues to decline until a saturation point is reached.^[156] By monitoring the pressure variation as the adsorption proceeds the mass transfer coefficient can be calculated by implementing the following equation:^[157]

$$\frac{P_f - P_0}{P_i - P_0} \ln \left(\frac{P_i - P_f}{P - P_f} \right) = k_{La} t \quad \text{Equation 2.1.}$$

P_0 represents the solvent vapour pressure, P_f and P_i denote final and initial pressures respectively, whilst P indicates the pressure at a given time and t is the time taken to reach the final pressure. P_f , P_i and P were obtained experimentally, $P_0 = 0.35$ bar for methanol at 40 °C.^[158] In this way, a plot of $(P_f - P_0/P_i - P_0) \ln(P_i - P_f/P - P_f)$ versus time will then yield a straight line with the gradient defining the mass transfer coefficient that represents the kinetics of the hydrogen solvation process. These measurements provide an indication as to the amount of hydrogen available within the system for a set of conditions.

2.3 Syngenta Hydrogenation Reaction Studies

In addition to the studies conducted at the University of Glasgow, some time (approximately 4 non-consecutive weeks) was spent at the industrial site (Syngenta, Jealott's Hill). The following section provides details relating to the alternative reactor set-ups utilised at Syngenta. Experiments relating to 1,2-dicyanobenzene (single batch) and mandelonitrile (Continuous Stirred Tank Reactor, CSTR) substrates were conducted.

2.3.1 Single Batch Hydrogenation Reactions

The hydrogenation reactions of 1,2-dicyanobenzene and 2-cyanobenzylamine hydrochloride at the industrial site were conducted in a 120 mL Mettler Toledo EasyMax reactor. The reactor was first charged with catalyst (0.034 g, 5% Pd/C), sulphuric acid (0.45 g) and methanol (80 mL). The reaction vessel and reactor lines were leak tested under 25 barg nitrogen. Following the successful maintenance of pressure for 10 minutes, the reaction vessel and the reactor lines were purged, first with nitrogen and, then with hydrogen. The reduction conditions (temperature = 60 °C; pressure = 6 barg; agitation = 1000 rpm) were then set and the catalyst reduced for approximately 30 minutes.

Post catalyst reduction, the reactor was vented of hydrogen and purged with nitrogen. The reactor was then charged with reagent (1,2-dicyanobenzene or 2-cyanobenzylamine, approximately 0.15 g) under a flow of nitrogen to prevent re-oxidation of the catalyst. The reaction vessel was purged again with nitrogen and then with hydrogen. The reactor was pressurised to 2 barg. The start of the agitation at 1000 rpm signified the commencement of the reaction.

The reaction mixture was sampled at regular intervals throughout the course of the reaction. To sample, the first valve of the sampling dipleg, to fill the sampling pipe, was opened. The first valve was then closed and the second opened to release the sample into a collection vial. The sample volume was approximately 1–2 mL and two sample discards were taken to ensure that the reactor tube was clean for sampling. The third sample was used for analysis. The reaction mixture was filtered to remove any residual catalyst and analysed off-line by HPLC.

Once the reaction was complete, the reaction vessel was cooled to room temperature, vented of hydrogen and purged with nitrogen. The residual reaction mixture was removed from the reaction vessel, the catalyst removed by filtration and the waste disposed of by appropriate means. A schematic representation of the reactor vessel is shown in Figure 2.2.

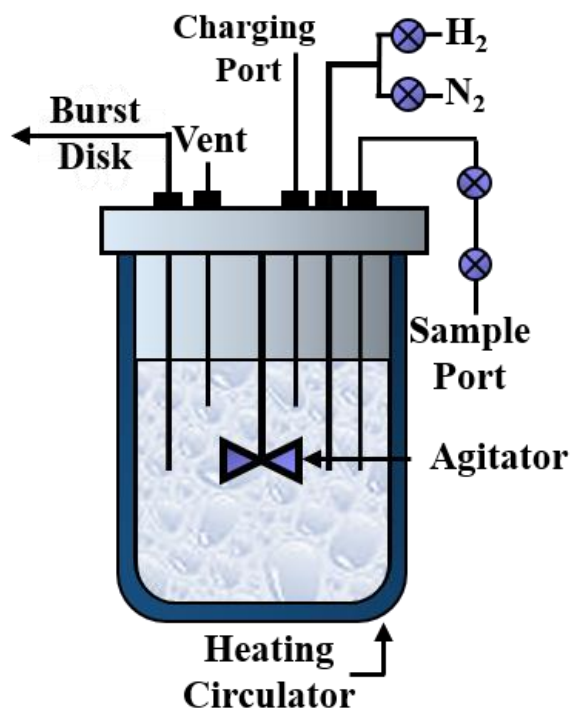


Figure 2.2. EasyMax reactor at Syngenta Jealott's Hill for the hydrogenation reactions of 1,2-dicyanobenzene and 2-cyanobenzylamine hydrochloride.

2.3.2 Continuous Stirred Tank Reactor (CSTR) Reactions

In addition to the single batch and repeat batch reactions conducted at the University of Glasgow, the hydrogenation reaction of mandelonitrile was also conducted at the industrial site as a CSTR arrangement. The reactor (Parr) was first charged with catalyst (0.17 g, 5% Pd/C) and methanol (200 mL) prior to the pre-reduction process. The reaction vessel, reactor lines and the back pressure regulator were all leak tested under 25 barg of nitrogen. Following the successful maintenance of pressure for 10 minutes, each of the components was purged, first with nitrogen and then with hydrogen. The pre-reduction conditions (temperature = 40 °C; pressure = 8 barg; agitation = 1000 rpm) were then set and the catalyst reduced for approximately 30 minutes.

Solutions of mandelonitrile (61.9 mmol L⁻¹) and sulphuric acid (123.9 mmol L⁻¹) in methanol, corresponding to Reservoir A and Reservoir B respectively, were prepared. The feed-in lines were primed by initiating a flow of each reagent *via* the corresponding HPLC pump. The CSTR reaction was initiated by opening valves **7** and **10** (Figure 2.3).

The three HPLC pumps, corresponding to feed-in Reservoirs A and B, and feed-out Reservoir C were initiated. The volume inside the reaction vessel was monitored and maintained at 200 mL by altering the flow rates on each of the HPLC pumps where necessary. Samples were taken at regular intervals and monitored by HPLC. A schematic representation of the CSTR is shown in Figure 2.3.

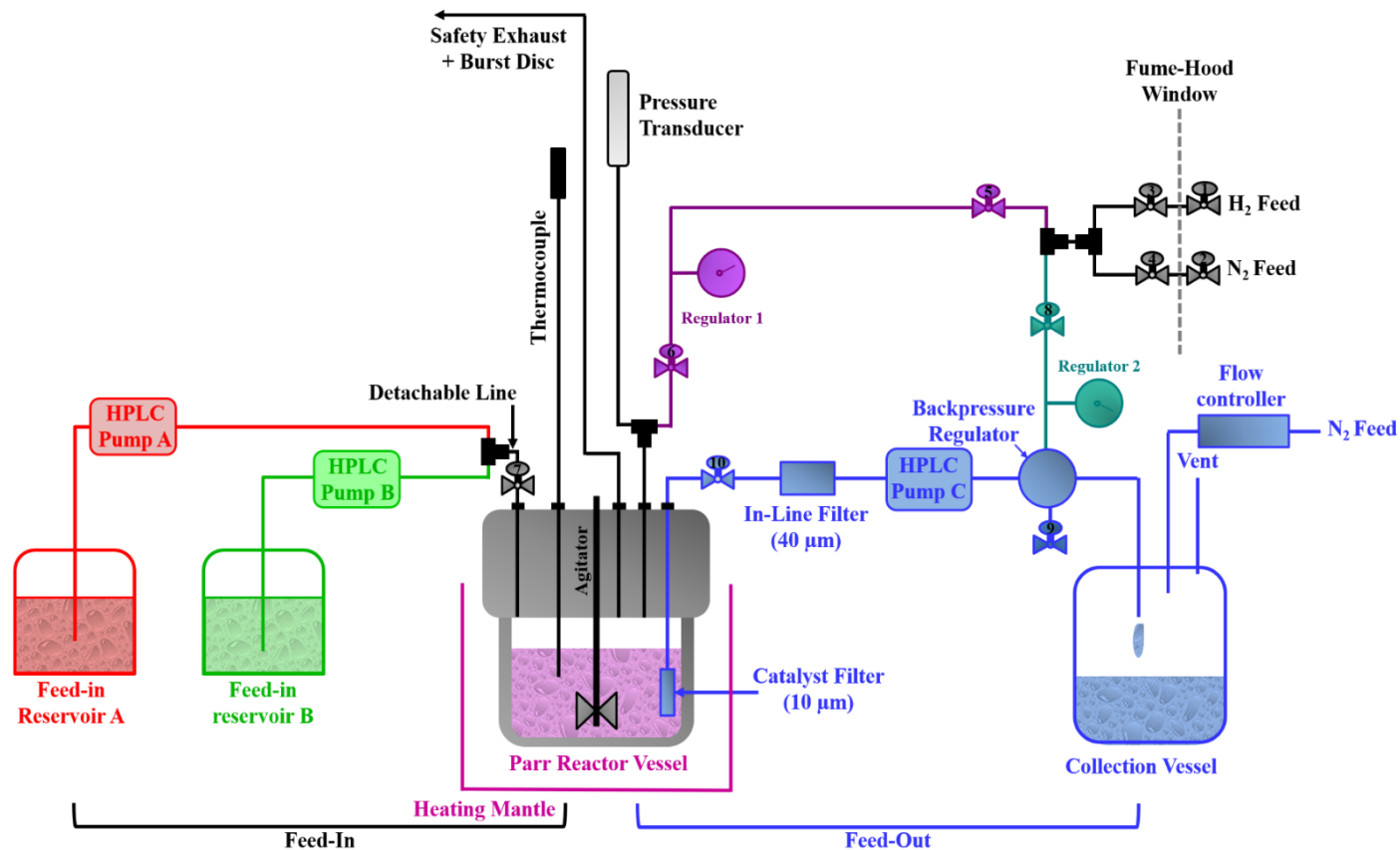


Figure 2.3. CSTR arrangement at Syngenta, Jealott's Hill for the hydrogenation reaction of mandelonitrile. [Feed-in Reservoir A = mandelonitrile; Feed-in Reservoir B = sulphuric acid (2 equivalents)].

2.4 Analytical Techniques

2.4.1 High Performance Liquid Chromatography (HPLC)

Samples of the reaction mixture, collected at regular intervals during reaction, were filtered, using a 0.22 μm syringe filter (Chromatography Direct, cellulose acetate), to remove any catalyst residue. All samples, contained in a sealed vial, were subsequently quenched in an ice bath until it was time for their analysis by high performance liquid chromatography (HPLC).^[151] HPLC analyses were obtained using a Hewlett Packard 1100 Series HPLC fitted with a BDS Hypersil C18 column of dimensions 250x4.6 mm. The solvents utilised, in gradient mode, were analytical grade water (Fischer Scientific, >99.9% purity) acidified with 1% vol phosphoric acid (H_3PO_4 , Sigma Aldrich), prepared in-house, and analytical grade acetonitrile (Fischer Scientific, >99.9% purity). The accompanying eluent method is presented in Table 2.1. With the exception of the 1,2-dicyanobenzene reagent, the details of which are presented in Chapter 12, the accompanying ultraviolet-visible analysis was undertaken at 210 nm. An injection volume of 1 μL was taken for each sample and a flow rate 1.5 mL min^{-1} was employed for all analyses. Further, the thermostat was fixed at 20 $^\circ\text{C}$ ensuring a constant temperature throughout the analysis process. The method reported here represents the optimised form. Further details regarding the optimisation process can be found in Chapter 7.

Table 2.1. The HPLC eluent method utilised for 4-hydroxybenzyl cyanide and mandelonitrile substrate systems.

<i>Time / minutes</i>	0	8	12	16	25
<i>% Water/H_3PO_4</i>	90	80	60	70	90
<i>% Acetonitrile</i>	10	20	40	30	10

Standard solutions of the compounds involved in each of the investigated reaction systems were prepared within an appropriate range for the experiments being conducted in 25 mL standard flasks. Each standard was measured in triplicate on the HPLC for accurate calibration results. Calibration plots could therefore be produced and response factors calculated, allowing quantitative reaction profiles to be achieved. Errors in HPLC output were determined by repeat analysis and found to be below $\pm 5\%$.

2.4.2 Multinuclear Nuclear Magnetic Resonance (NMR) Spectroscopy

For the hydrogenation reactions of the relevant substrates, ^1H and ^{13}C NMR spectroscopies were conducted using a Bruker AVI 400 MHz spectrometer. For the deuteration reaction of mandelonitrile, both 1D NMR (^1H , ^2H and ^{13}C) and 2D (HSQC – Heteronuclear Single Quantum Coherence Spectroscopy) data were acquired. The ^2H analysis was run, without dilution by a deuterated solvent, on a Bruker AVIII 500 MHz spectrometer. Both ^1H NMR and ^{13}C NMR spectra were obtained using a Bruker AVIII 600 MHz with 5 mm TCI cryoprobe (303 K). In order to achieve a quantitative ^{13}C NMR spectra for the deuteration reaction, two parameter changes from the standard were required. Firstly, as the various components of the reaction mixture may have different relaxation times, the relaxation delay (D1) was increased to 30 seconds. This action satisfies system relaxation requirements. Secondly, the decoupling power used during the relaxation delay was reduced to prevent potential build-up of the Nuclear Overhauser Effect (NOE). ^1H - ^{13}C correlation HSQC for the deuterated sample was also undertaken. These data were collected using a DEPT (Distortionless Enhancement by Polarisation Transfer) edited sequence resulting in a different phase for CH/CH₃ and CH₂ signals. To obtain high resolution, this spectrum was run with a reduced ^{13}C sweep width (10 ppm), centred between the signals of interest.^[159] Additionally, for the HSQC experiment, the sample was diluted due to its high ionic strength. In all instances, either deuterium oxide (D₂O) or deuterated methanol (D₃MeOD) was utilised as the deuterated solvent for analysis. Specific details can be found in Chapters 4 and 6. Subsequent data handling was undertaken using the MestReNova program.

2.4.3 Mass Spectrometry

Measurements were performed using a Bruker microTOFq High Resolution Mass Spectrometer. An ESI ion source was used and analysis was performed in positive ionisation mode.

2.5 Catalyst Characterisation

Full characterisation of each of the catalysts was conducted in-house at the University of Glasgow and the associated equipment details provided in Chapter 3. Specific attention is brought here to the catalyst characterisation techniques which were conducted within the Lennon Lab.

2.5.1 CO Chemisorption

Pulsed carbon monoxide chemisorption measurements were conducted on both the 5% Pd/C (GU-1) and the 5% Pd/ γ -Al₂O₃ (GU-2) catalysts in order to determine dispersion and metal particle size. A known quantity of catalyst (approximately 200 mg) was added to a quartz ‘u-tube’ reactor and placed onto the characterisation line. The catalyst was then reduced *in situ* under a flow of He/H₂ (20 mL/30 mL) at 200 °C for 30 minutes. Residual H₂ was removed by passing a flow of solely He over the catalyst at 200 °C for a further 30 minutes before the reactor was cooled to room temperature. A known volume of CO was then pulsed over the reduced catalyst. Any CO that was not adsorbed onto the catalyst surface was detected by gas chromatography (Thermo Finnigan Ultra GC fitted with a thermal conductivity detector). The catalyst was deemed to have saturated once at least three subsequent measurements detected the same quantity of unadsorbed CO. As the pressure and the volume of CO used for each pulse was known, the number of moles of CO adsorbed could be calculated using the ideal gas law and an accompanying calibration plot conducted by pulsing CO over a blank reactor tube. The characterisation line used to conduct the CO chemisorption measurements is shown in Figure 2.4.

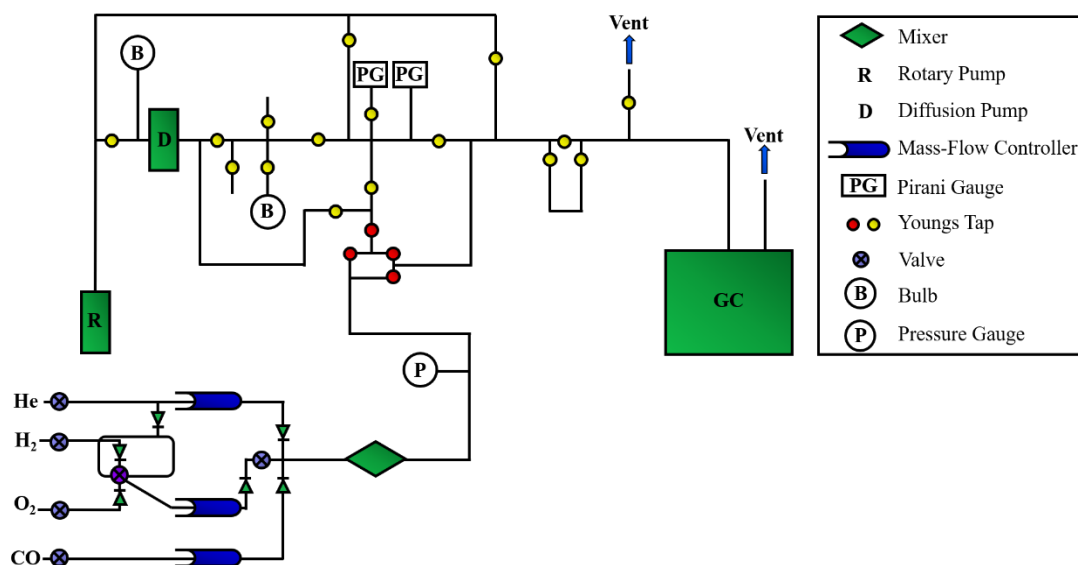


Figure 2.4. Schematic of the characterisation line located within the Lennon Lab on which the CO chemisorption experiments were conducted.

The concentration of surface palladium atoms can be determined by assuming a surface stoichiometry of 1CO:2Pd.^[160–161] The dispersion of the catalyst can then be calculated using the following equation:

$$\text{Dispersion (\%)} = \frac{\text{number of surface Pd atoms}}{\text{total number of palladium atoms}} \times 100 \quad \text{Equation 2.2.}$$

Assuming the metal particles to be spherical and of equal size,^[162] particle size (d) can be calculated from the dispersion value using the following equation:

$$D = \frac{6A}{\rho S_a N_a d} \quad \text{Equation 2.3.}$$

Where D represents dispersion; A is atomic weight (106.92 g mol⁻¹); ρ is the density of the metal (12.02x10⁻²¹ g nm⁻³); S_a is the average surface area occupied by one atom (0.0806 nm²); N_a is Avogadro's constant (6.022x10²³ mol⁻¹) and; d is average particle diameter (nm).^[160, 162–163] The numbers included in brackets relate specifically to palladium. Therefore, for palladium catalysts, Equation 2.3 can thus be simplified, allowing particle size to be determined by:

$$d = \frac{D}{109} \quad \text{Equation 2.4.}$$

2.5.2 Temperature Programmed Infrared (TPIR) Spectroscopy

Diffuse Reflectance Infrared Fourier Transform spectroscopy (DRIFTS) was performed on a Nicolet Nexus FTIR spectrometer equipped with a high D* MCT detector. In this instance it was exclusively the 5% Pd/ γ -Al₂O₃ catalyst which was analysed due to the unsuitability of the carbon support for this particular technique.^[152–153]

The catalyst (approximately 25 mg) was first inserted into a SpectraTech Smart diffuse reflectance cell and environmental chamber. The catalyst was then reduced at 60 °C, under a flow of hydrogen for 30 minutes. Once cooled, an ambient temperature background was obtained and CO was then pulsed over the catalyst (approximately 5 μ mol) with a continuous flow of helium (35 mL min⁻¹). Sufficient time (15 minutes) was then allowed to remove any residual CO from the cell before a spectrum, with background subtraction, was acquired. The cell was then heated to 50 °C (the temperature was controlled by a Thermo SpectraTech heater), held at 50 °C for 10 minutes, before being cooled to room temperature. Once room temperature was reached, a spectrum was collected. This heating, cooling and spectral acquisition process was repeated for 50 °C temperature increments until 450 °C was obtained.

CHAPTER 3

Catalyst Characterisation

3.1 Introduction

The primary catalyst utilised throughout the course of this study is a commercially available 5% Pd/C material (GU-1). As such, the characteristics of this catalyst should conform to the manufacturer's standard. It is, however, essential that there is an appreciation of the materials used in this study. Therefore, general catalyst characterisation has been conducted on the 5% Pd/C catalyst, as well as on another commercially available 5% Pd/ γ -Al₂O₃ catalyst (GU-2), which has been included for comparative purposes. The catalytic activity of the 5% Pd/ γ -Al₂O₃ catalyst for the hydrogenation reaction of mandelonitrile has been tested and compared to the benchmark obtained using the 5% Pd/C catalyst. Details regarding the outcome of these reactions can be found in Sections 5.3 and 7.3 for the 5% Pd/C and 5% Pd/ γ -Al₂O₃ catalysts, respectively.

3.2 Atomic Adsorption Spectroscopy

Atomic adsorption spectroscopy (AAS) was conducted on both catalyst samples in order to determine the percentage loading of the metal on the catalyst. Analyses were performed on a PerkinElmer AAnalyst 100 Atomic Absorption Spectrometer at 244.8 nm with an acetylene flame in order to determine the concentration of palladium in each of the catalysts.

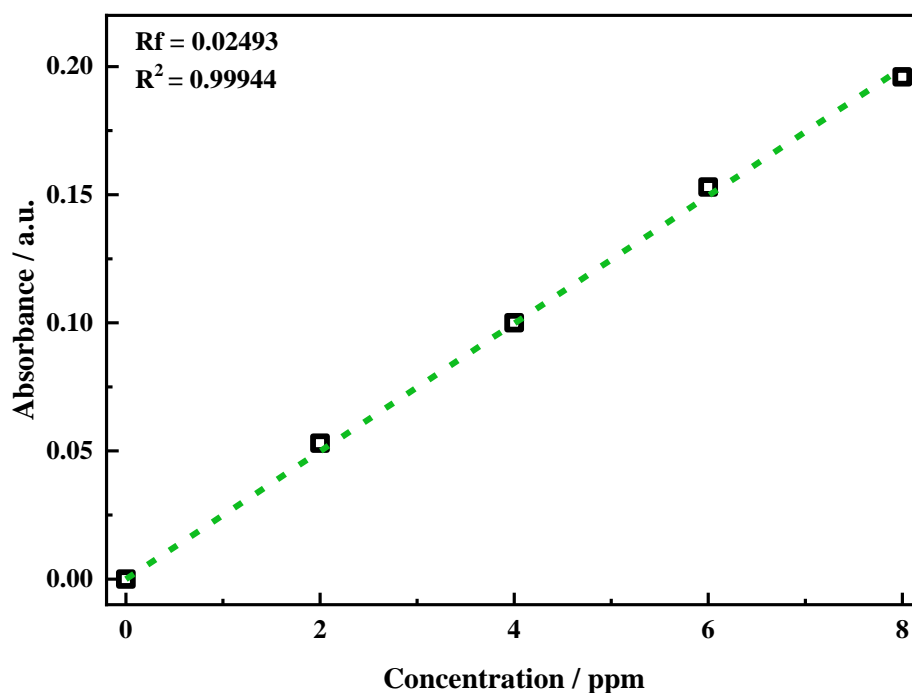


Figure 3.1. Atomic absorption spectroscopy calibration curve obtained using a series of palladium standard solutions, of known concentration, for the determination of palladium content within each of the catalysts.

A commercially available 1000 ppm palladium in 5% HCl standard (Sigma-Aldrich) was used to prepare a set of palladium standards within the 0–8 ppm range. The solutions were subsequently used to calibrate the spectrometer. The resultant calibration curve is presented in Figure 3.1. Before the palladium content of the catalysts could be measured the metal had to be extracted from the support matrix.^[164] Aqua regia (1:3, hydrochloric acid: nitric acid) was prepared and added to a known mass of the catalyst. The mixture was heated at 120 °C for approximately 30 minutes to digest the catalyst. The resultant solution of palladium from each of the catalysts was measured on the atomic absorption spectrometer to acquire an absorbance. Using the response factor (Rf) obtained from the calibration graph (Figure 3.1) the concentration of palladium in the sample was calculated. Once determined, the mass of palladium, and subsequently the percentage loading of palladium could be calculated. The results of these calculations are summarised in Table 3.1.

Table 3.1. Percentage metal loading of the examined catalysts, as calculated by atomic absorption spectroscopy.

<i>Catalyst</i>	<i>Absorbance</i>	<i>Concentration</i>	<i>Mass of Pd in Sample</i>	<i>% Loading of Pd in Catalyst</i>
5% Pd/C	0.156 a.u.	6.24 ppm	0.390 mg	3.7%
5% Pd/ γ -Al ₂ O ₃	0.178 a.u.	7.14 ppm	0.446 mg	3.5%

Interestingly, Table 3.1 shows that the percentage loading, as determined by AAS, is below the commercially quoted value of 5% for both catalysts. It is proposed that this discrepancy could be due to an insufficiently harsh digestion method, with some of the palladium being retained on the support of the catalyst. Further, it is noted that the technique only analyses a small mass of catalyst (approximately 10 mg). Therefore, whilst the measurement was performed in duplicate, the sample analysed may not be a true representation of the bulk material.

3.3 Inductively Coupled Plasma Optical Emission Spectroscopy

Inductively coupled plasma-optical emission spectroscopy (ICP-OES) was conducted on both catalyst samples as an alternative method for the determination of the percentage metal loading. An Agilent 5100 spectrometer, calibrated to a range of known concentration palladium reference solutions, revealed respective percentage metal loadings of 4.12% and 3.65% for the 5% Pd/C and the 5% Pd/ γ -Al₂O₃ catalysts. These results correlate well with the findings of AAS, particularly for the alumina supported catalyst. Again, both catalysts are calculated to have a percentage metal loading lower than that quoted by the manufacturer.

3.4 Scanning Electron Microscopy and Energy Dispersive X-Ray Spectroscopy

Scanning electron microscopy (SEM) was carried out on the catalyst using a Philips XL30 ESEM instrument with an Oxford instruments X-act spectrometer for Energy Dispersive X-ray Spectroscopy (EDX) measurements. The EDX was calibrated using the INCA EDX software with Cu as the calibrated standard. The sample was coated in gold using a sputter coating procedure to improve the contrast. Representative SEM micrographs for both catalysts are presented in Figure 3.2.

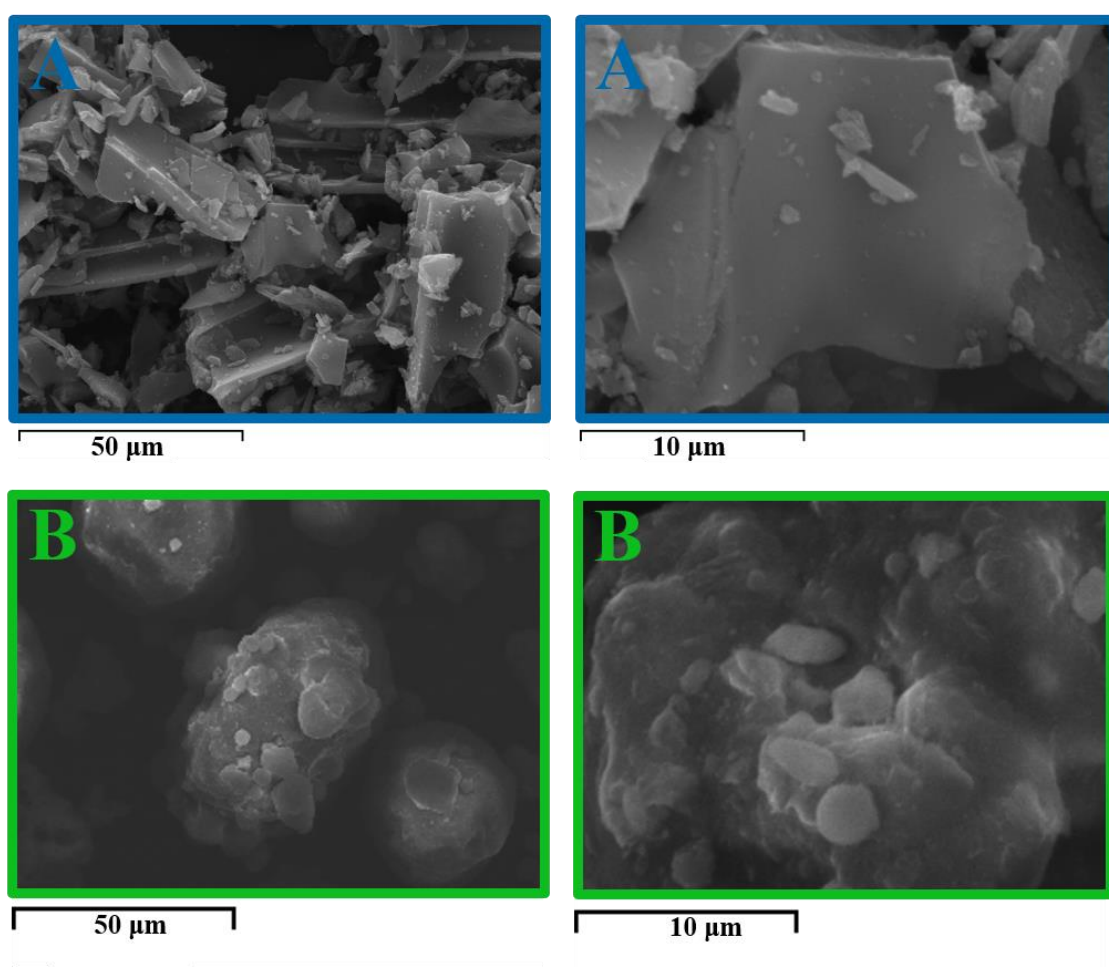


Figure 3.2. Representative SEM micrographs for: **A**, the 5% Pd/C catalyst; and **B**, the 5% Pd/γ-Al₂O₃ catalyst.

The micrographs show the carbon supported catalyst to be composed of irregular plate-like structures, ranging in size from approximately 4 μm to 55 μm . In contrast to this the alumina supported catalyst exhibits a different morphology, being composed of more agglomerated spherical particles ranging in size from 1.1 μm to 64.8 μm .

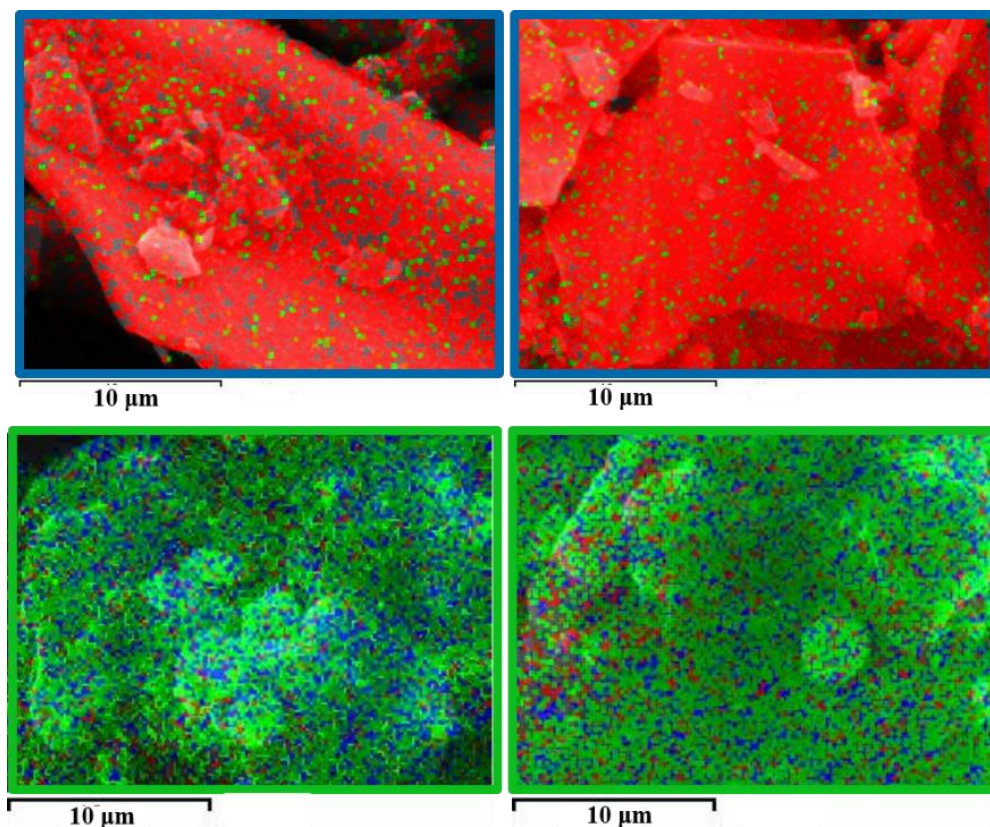


Figure 3.3. Representative EDX maps for the 5% Pd/C catalyst (top) and the 5% Pd/ γ -Al₂O₃ catalyst (bottom). [5% Pd/C: Pd green and C red; 5% Pd/ γ -Al₂O₃: Pd red, Al green and O blue].

The corresponding energy dispersive X-ray spectroscopy allowed the distribution of the elements within the sample to be mapped (Figure 3.3). From this method the percentage loading of the 5% Pd/C on the catalyst was found, from two areas, to be $3.12 \pm 1.2\%$. Using the same methodology, the percentage loading of the 5% Pd/ γ -Al₂O₃ catalyst was found to be $5.87\% \pm 1.4\%$. Moreover, the EDX maps show the palladium to be evenly dispersed on both catalysts.

3.5 Transmission Electron Microscopy

Transmission Electron Microscopy (TEM) analysis was conducted using a Tecnai G2T20 STWIN fitted with a tungsten filament operating at an acceleration voltage of 200 kV. Representative TEM micrographs for the 5% Pd/C catalyst can be seen in Figure 3.4 **A**. Also shown (Figure 3.4 **B**) is the corresponding particle size distribution histogram conducted on 200 particles. A narrow particle size distribution is revealed, with the majority of the palladium particles being found to be within the 2–3 nm range.

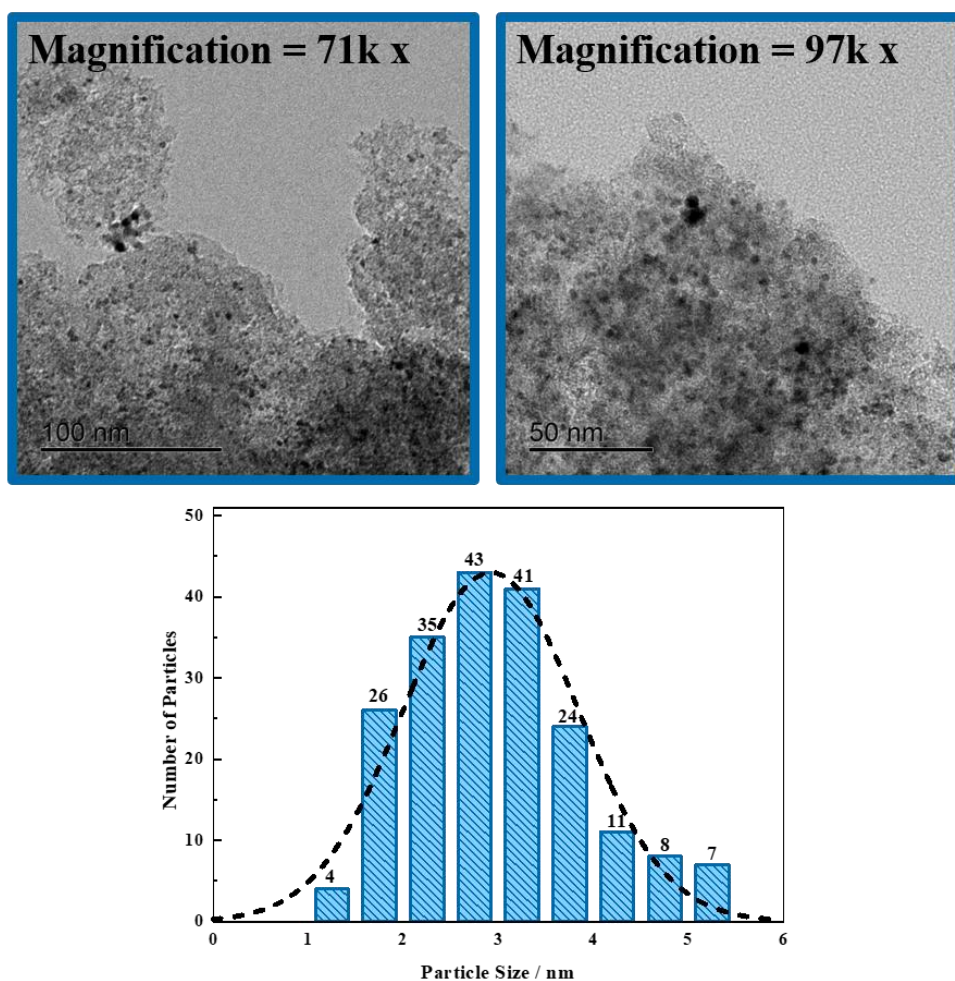


Figure 3.4. Representative TEM images for the 5% Pd/C catalyst collected under an electron beam intensity of 200 kV (A). The magnification associated with each image has been specified in the corresponding image. Particle size distribution histogram (B), as determined by a particles size count of the corresponding TEM images using the Gatan Microscopy Suite Software (bin size = 0.5 nm).

Although TEM is a useful tool for the determination of particle size and shape it is only effective when the metal particles exhibit sufficient contrast with the support. Whilst acceptable contrast for the 5% Pd/C catalyst allowed a particle size distribution to be determined, this was not the case for the alumina supported catalyst. As a potential means of improvement, the intensity of the electron beam was reduced from 200 kV (Figure 3.5 A) to 80 kV (Figure 3.5 B). Nevertheless, there were still uncertainties regarding the observed dark spots on the images. As such, it was not possible to determine whether they were palladium particles or simply thick sample spots. Consequently, no accurate particle size data for the 5% Pd/ γ -Al₂O₃ catalyst was obtained from the TEM measurements.

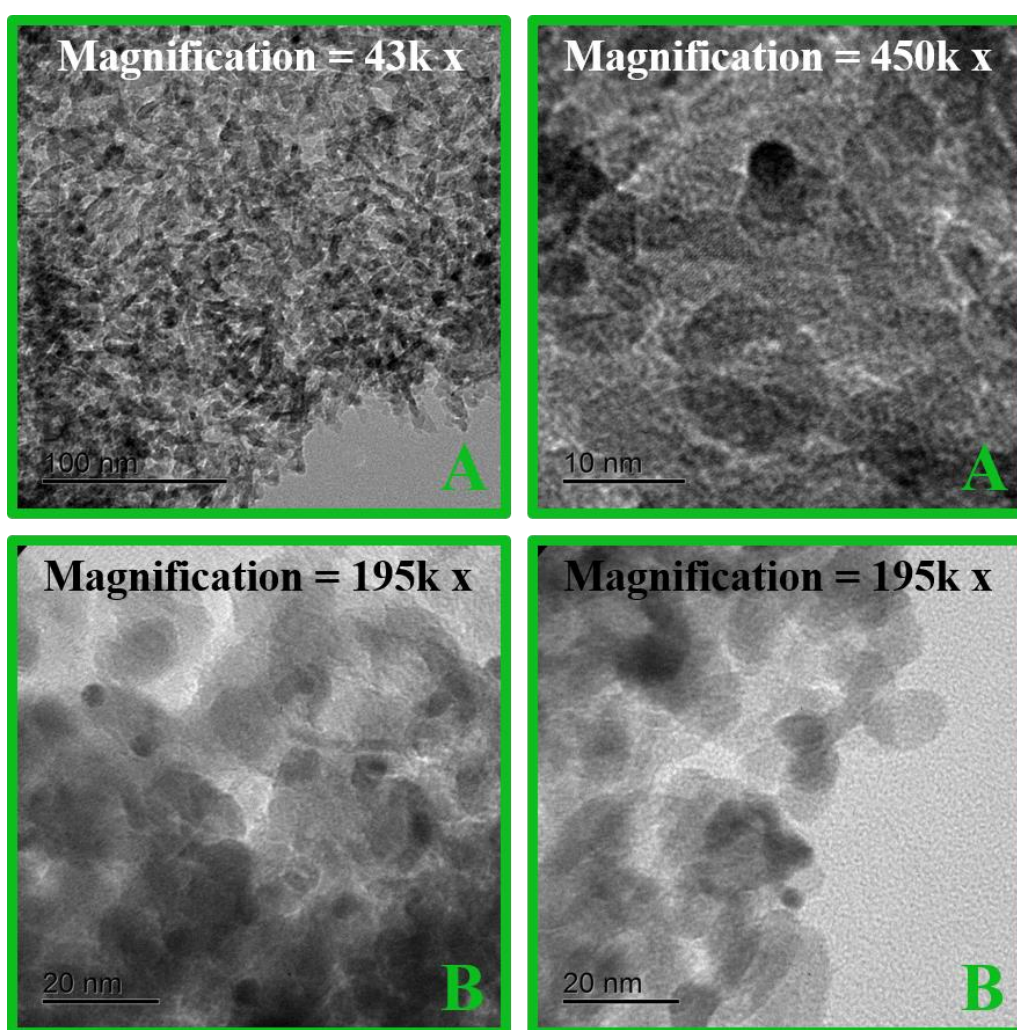


Figure 3.5. Representative TEM images for the 5% Pd/ γ -Al₂O₃ catalyst at an electron beam intensity of **A** 200 kV and, **B** 80 kV. The magnification associated with each image has been specified.

3.6 CO Chemisorption

CO chemisorption was conducted on both catalysts in order to determine dispersion and mean particle size. The apparatus used has been described previously in Section 2.5.1. Representative adsorption isotherms are shown in Figure 3.6. After exposure to a quantity of CO (unique to each catalyst), saturation occurs, resulting in no further uptake of CO by the catalyst. Saturation is designated by the dashed boxes in Figure 3.6.

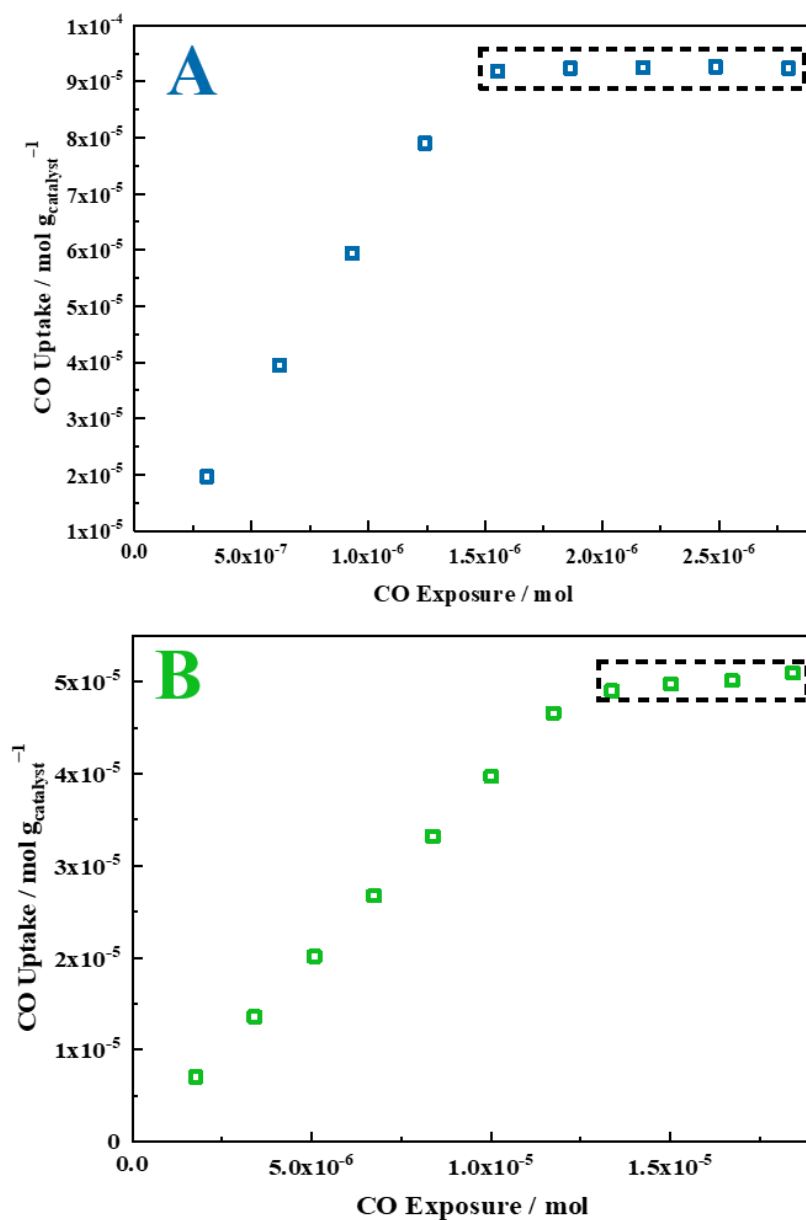


Figure 3.6. CO adsorption isotherms for: **A**, the 5% Pd/C catalyst and **B**, the 5% Pd/ γ -Al₂O₃ catalyst.

The outcome of these measurements are summarised in Table 3.2. From Table 3.2 it is shown that the 5% Pd/ γ -Al₂O₃ catalyst contained, on average, larger particles than the 5% Pd/C catalyst which corresponds to a lower dispersion. Moreover, the mean particle size determined by CO chemisorption (2.8 nm) is in good agreement with the particle size distribution revealed by TEM (2–3 nm). Unfortunately, in this instance, as no TEM particle size distribution histogram was obtained for the 5% Pd/ γ -Al₂O₃ catalyst the CO chemisorption results could not be compared. Additionally, using the number of surface palladium atoms per gram of catalyst, calculated from the CO chemisorption measurements (Table 3.2), the mole ratio of palladium surface atoms to substrate used for the hydrogenation reactions in this study can be determined. This is calculated to be 0.3 mol % for the 5% Pd/C catalyst and 0.5 mol % for the 5% Pd/ γ -Al₂O₃.

Table 3.2. Summary of the CO adsorption isotherm outcomes for both the 5% Pd/C and the 5% Pd/ γ -Al₂O₃ catalysts.

<i>Catalyst</i>	<i>CO Uptake / mol_{g_{catalyst}}⁻¹</i>	<i>No. of Surface Pd Atoms g_{catalyst}</i>	<i>Dispersion / %</i>	<i>Mean Particle Size / nm</i>
5% Pd/C	9.24x10 ⁻⁵	5.99x10 ¹⁹	39	2.8
5% Pd/ γ -Al ₂ O ₃	9.24x10 ⁻⁵	1.11x10 ²⁰	21	5.2

3.7 Powder X-Ray Diffraction

Powder X-ray diffraction (PXRD) was carried out on both catalyst samples using a Panalytical X'Pert PRO MPD diffractometer equipped with a Cu sealed X-ray source in the $2\theta = 5\text{--}85^\circ$ range with a step size of 0.017° . It is, however, important to note that X-ray diffraction is not suitable for the examination of very small metal crystallites or clusters of approximately less than 2.5 nm in size. These objects give diffuse X-ray scattering which spreads to the background making them difficult to detect.^[165–167] As determined by TEM (Section 3.5) and CO chemisorption (Section 3.6) the average particle size for both examined catalysts is within this region, meaning that it is unlikely that strong signals for the palladium will be determined with this method.

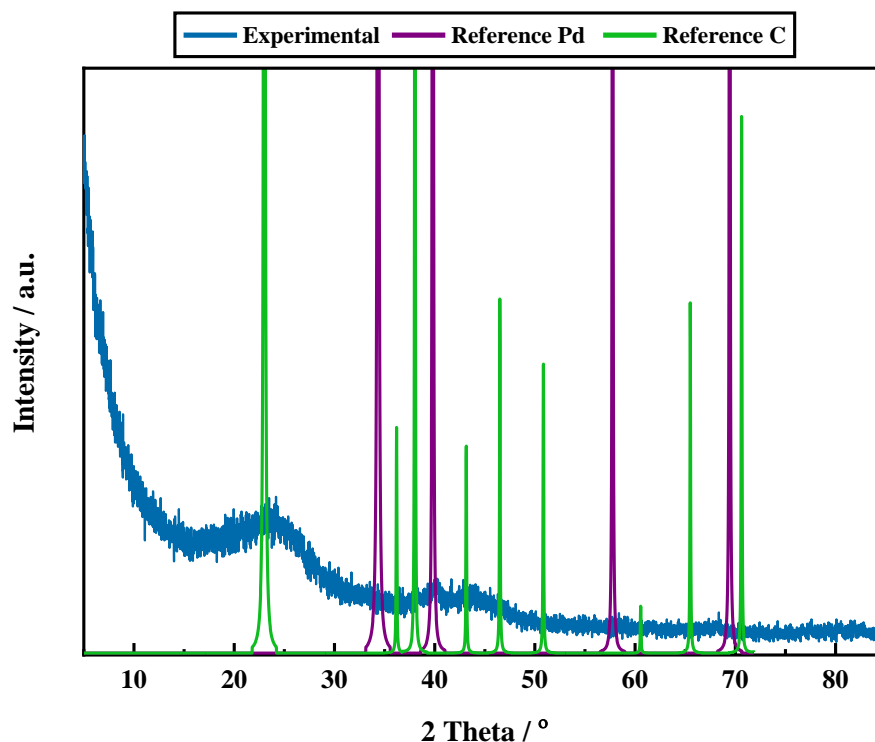


Figure 3.7. Powder X-ray diffraction pattern, including reference palladium and carbon patterns for the 5% Pd/C catalyst used in the hydrogenation reaction of mandelonitrile.

The resultant PXRD pattern for the 5% Pd/C catalyst can be visualised in Figure 3.7 alongside reference patterns obtained from the Inorganic Crystal Structure Database (ICSD) for both carbon (card number: 76767) and palladium (card number: 52251). Figure 3.7 largely shows the amorphous nature of the carbon support, with negligible contribution from the palladium crystallites.

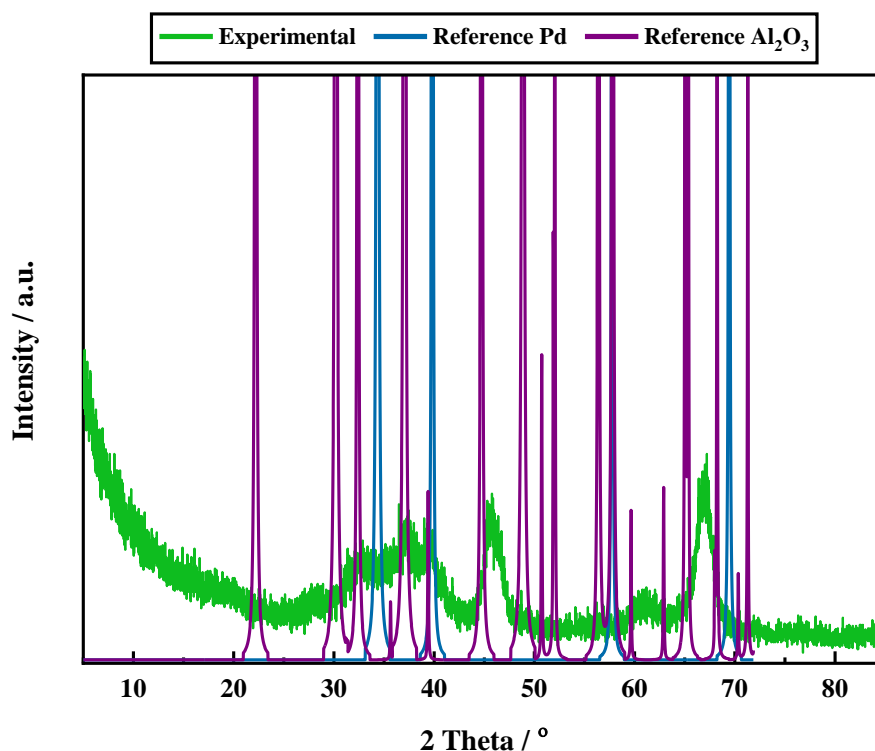


Figure 3.8. Powder X-ray diffraction pattern, including reference palladium and gamma alumina patterns for the 5% Pd/ γ -Al₂O₃ catalyst used in the hydrogenation reaction of mandelonitrile.

The PXRD pattern for the 5% Pd/ γ -Al₂O₃ catalyst is presented in Figure 3.8 alongside reference patterns obtained from the ICSD for both palladium (card number: 52251) and gamma alumina (card number: 68216). Similar to the 5% Pd/C catalyst, minimal contribution from the palladium is observed. In contrast, the predicted pattern for the catalyst support does not exhibit such a good fit suggesting the presence of another phase of alumina. This is perhaps unsurprising as, depending on the synthesis conditions, γ -Al₂O₃ may contain significant amounts of other transition aluminas.^[168–169]

3.8 Raman Spectroscopy

Raman spectroscopy was conducted on both catalyst samples using a Horiba John-Yvon LabRam Raman Spectrometer (HR800) fitted with a 532 nm laser. In order to prevent sample degradation, an aperture size of 100 μm and a 1% filter were employed.

As metallic elements have only one atom in the primitive unit cell they have no vibrational modes. Consequently, the Raman spectrum is forbidden for palladium.^[170] Nevertheless, whilst palladium is not Raman active, the catalyst supports are. It is documented that the inelastic scattering of protons by carbonaceous material results in the occurrence of ‘D’ and ‘G’ bands with a Raman shift within the 1200 to 1600 cm^{-1} range.^[171–173] These bands are listed and assigned in Table 3.3.

Table 3.3. The ‘D’ and ‘G’ bands observed from the Raman spectrum of carbonaceous materials and the corresponding assignments.^[171–172, 174–175]

<i>Carbon Peak</i>	<i>Raman Shift</i>	<i>Assignment</i>
G	<i>ca.</i> 1580 cm^{-1}	ideal graphitic lattice
D1	<i>ca.</i> 1350 cm^{-1}	disordered graphitic lattice (graphene layer edges)
D2	<i>ca.</i> 1620 cm^{-1}	disordered graphitic lattice (surface graphene layers)
D3	<i>ca.</i> 1500 cm^{-1}	amorphous carbon
D4	<i>ca.</i> 1200 cm^{-1}	disordered graphitic lattice

Figure 3.9 therefore clearly shows the presence of carbonaceous material. Namely, disordered carbon (D1, D2 and D4), amorphous carbon (D3) and, ordered carbon (G).^[171, 173, 176] The fitting of Gaussian curves in the 1000 to 1750 cm^{-1} region affords the following assignments: D1 (1336 cm^{-1}), D3 (1520 cm^{-1}), D4 (1219 cm^{-1}) and G (1600 cm^{-1}). The presence of the D2 band, located at approximately 1620 cm^{-1} is understood to have a positive correlation with the D3 band,^[177] and therefore is difficult to observe.^[178]

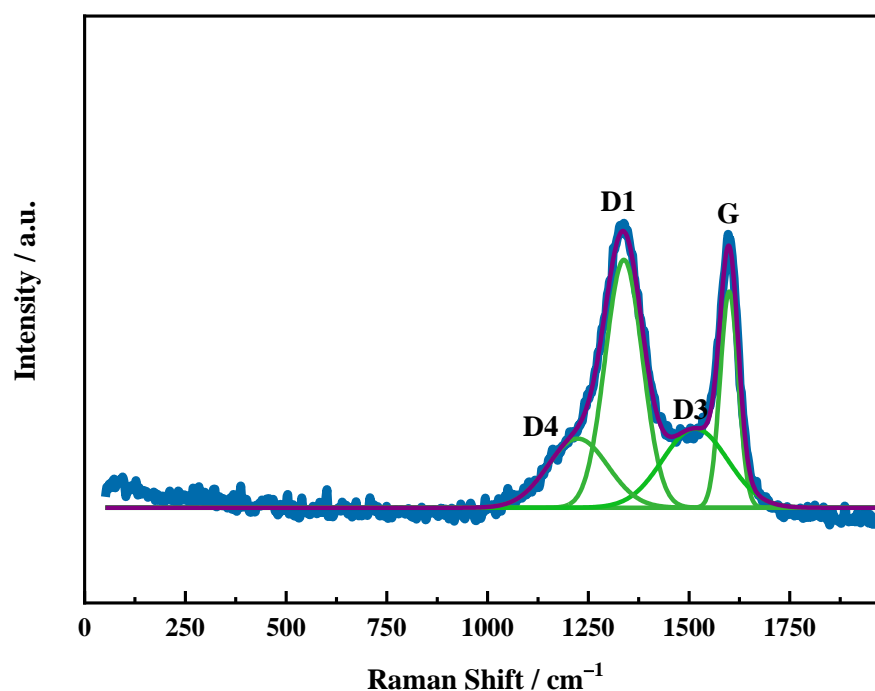


Figure 3.9. Raman spectrum of the 5% Pd/C catalyst. The ‘D’ and ‘G’ bands are defined in Table 3.3. The ‘D’ and ‘G’ bands have been fitted with Gaussian curves (green). The blue line is representative of the experimentally obtained data with the purple line indicating the cumulative fit.

In contrast to the distinctive ‘D’ and ‘G’ bands observed for the 5% Pd/C catalyst the Raman spectrum for the 5% Pd/ γ -Al₂O₃ catalyst (Figure 3.10) is significantly harder to interpret. It is recurrently documented in the literature that γ -alumina does not show any Raman features within the 100–1100 cm⁻¹ region.^[179–182] Indeed, Krishnan reports the Raman spectra of γ -alumina to be “feeble”.^[180] Contrastingly, δ -alumina is reported to have seven active phonon modes at frequencies of 378, 418, 432, 451, 587, 645 and 751 cm⁻¹.^[183] These modes have been included on the Raman spectrum collected for the 5% Pd/ γ -Al₂O₃ catalyst (Figure 3.10). With reference to Figure 3.10, it is only a minimal correlation between these reference bands and the observed bands which is apparent. However, as evidenced by a strong band at 645 cm⁻¹, the presence of δ -alumina in the support is alluded to. Nevertheless, it is apparent that in the study of alumina, the strong background signal produced by Raman spectroscopy renders this an unsuitable method to analyse this support.^[184–185]

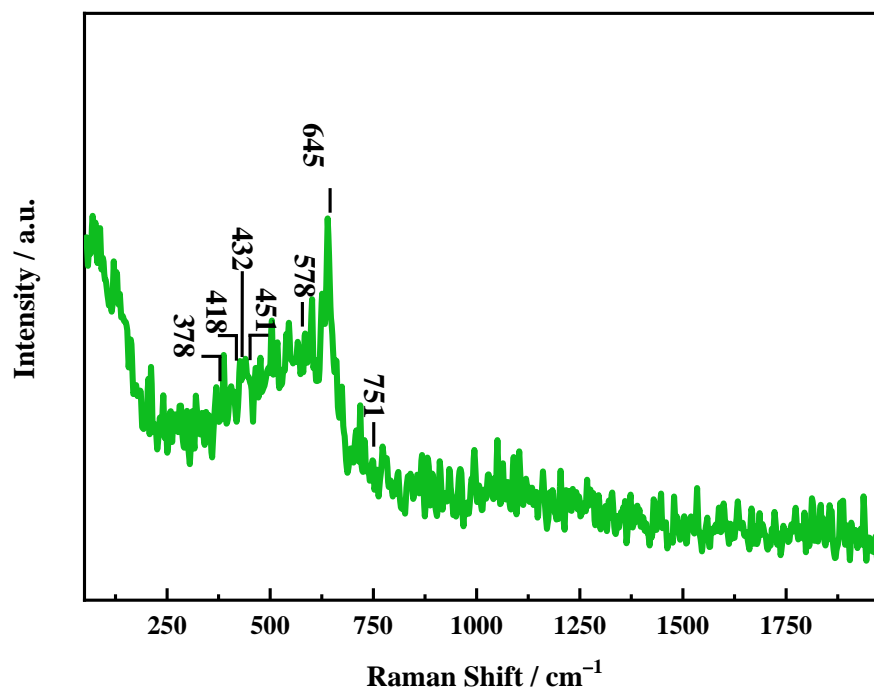


Figure 3.10. Raman spectrum of the 5% Pd/ γ -Al₂O₃ catalyst. Reference Raman active bands associated with δ -alumina have been included.^[183]

3.9 Nitrogen Physisorption

Specific surface areas and textural data for both catalysts were measured on a Quantachrome Evo instrument after degassing (overnight *ca.* 20 hours) on a Quantachrome FloVac degasser. Data analysis was conducted using the Quadrawin software package.

Nitrogen physisorption of the 5% Pd/C catalyst revealed a specific surface area of $775 \pm 19 \text{ m}^2 \text{ g}^{-1}$, significantly larger than the $113 \pm 20 \text{ m}^2 \text{ g}^{-1}$ obtained for the 5% Pd/ γ -Al₂O₃ catalyst. Specific surface areas for both carbon and alumina vary wildly in the literature and are largely dependent on the synthesis method and post treatments applied to the material. Nevertheless, the surface area of carbon is reported to range from 100–1000 $\text{m}^2 \text{ g}^{-1}$;^[186] however, this can be significantly larger.^[187] Alumina as a support has a significantly lower specific surface area within the range of 100–200 $\text{m}^2 \text{ g}^{-1}$.^[188] The experimentally obtained surface areas for both catalysts are tabulated in Table 3.4.

Nitrogen adsorption isotherms for both samples are presented in Figure 3.11, with both catalyst samples being found to exhibit type IV isotherms, as classified by Brunauer^[189] and identified by the characteristic hysteresis loop. Hysteresis loops appear in the

multilayer range of physisorption isotherms and are generally associated with the filling and emptying of mesopores.^[189–190] Thus, it is deduced that both catalysts contain pores within the 2–50 nm range. As there is a correlation between the shape of the hysteresis loop and the pore texture additional details regarding the structure of the pores can be determined. Analysis of the hysteresis loop shapes associated with the isotherms for both catalysts indicates that, despite having the same type of isotherm, the two samples differ in pore structure. For the 5% Pd/C, the hysteresis loop is identified as H4 which is indicative of narrow, slit pores or pores within the microporous region.^[191] In contrast, the 5% Pd/ γ -Al₂O₃ catalyst exhibits H1 hysteresis which is associated with a porous material consisting of well-defined uniform cylindrical pore channels.

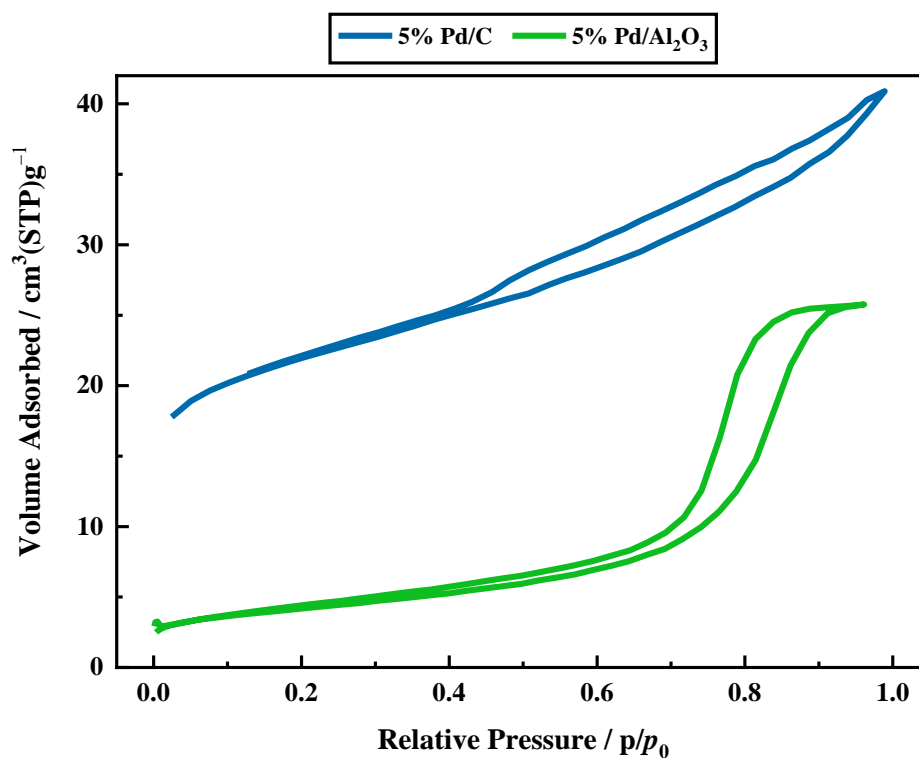


Figure 3.11. Nitrogen adsorption-desorption isotherms for the 5% Pd/C and 5% Pd/ γ -Al₂O₃ catalysts used in the hydrogenation reaction of mandelonitrile.

The Barrett-Joyner-Halenda (BJH) method uses the modified Kelvin equation to relate the amount of adsorbate removed from the pores of the material to the size of the pores. BJH analysis is employed for the determination of pore area and specific pore volume, thus characterising a pore size distribution which is independent of external surface area.^[139] Care must be taken when this analysis is applied to micropores with pores less than 2 nm in size.

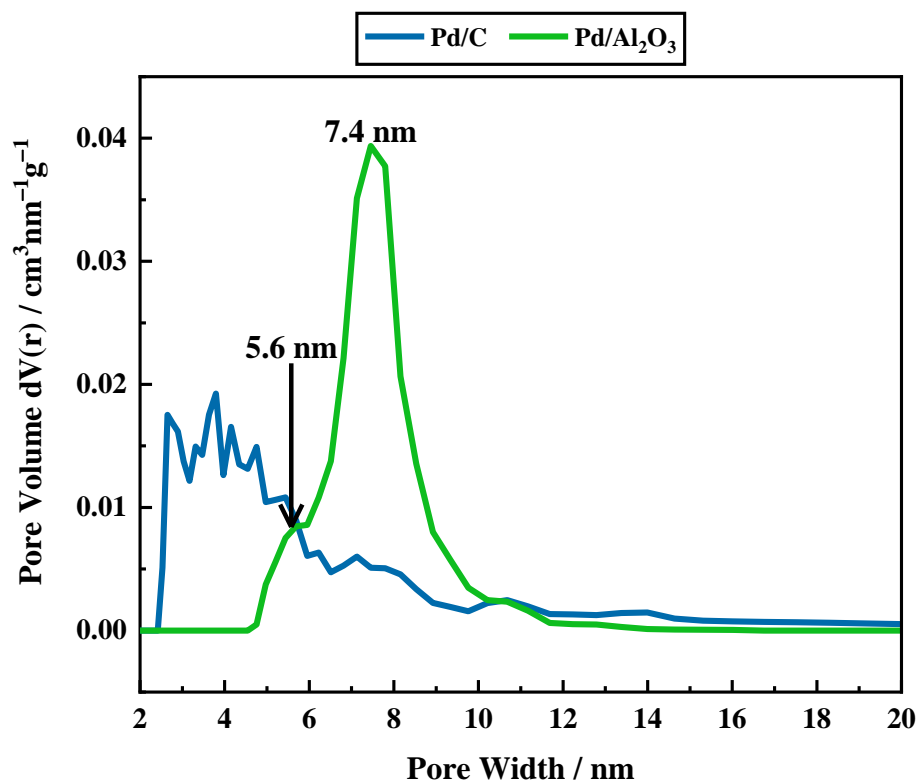


Figure 3.12. BJH pore size distributions for the 5% Pd/C and 5% Pd/ γ -Al₂O₃ catalysts used in the hydrogenation reaction of mandelonitrile.

The accompanying pore size distribution curves are shown in Figure 3.12 to be distinctive for each of the catalysts. As the carbon supported catalyst exhibits pores within the 1–6 nm range, the presence of microporous pores as well as some small mesopores is indicated. Conversely, the alumina supported catalyst exhibits slightly larger mesopores within the 5–12 nm range; the majority being approximately 8 nm in diameter. Total pore volume for each of the catalysts is presented in Table 3.4.

Table 3.4. Summary of surface area and total pore volume for the 5% Pd/C and the 5% Pd/ γ -Al₂O₃ catalysts.

<i>Catalyst</i>	<i>Surface Area / m²g⁻¹</i>	<i>Total Pore Volume / cm³g⁻¹</i>
5% Pd/C	774.7 \pm 19.2	0.693 \pm 0.02
5% Pd/ γ -Al ₂ O ₃	133.2 \pm 20.4	0.429 \pm 0.03

3.10 CO Temperature Programmed Infrared Spectroscopy

Temperature Programmed Infrared spectroscopy (TPIRs) was conducted on *only* the Pd/ γ -Al₂O₃ catalyst due to the unsuitability of the carbon support, detailed in Section 2.5.2. The experimental protocol has been described in Section 2.5.2. This technique is used to monitor how probe molecules, in this instance CO, are perturbed upon adsorption on the metal crystallites of the catalyst. Information on the active sites of the catalyst can thus be provided.

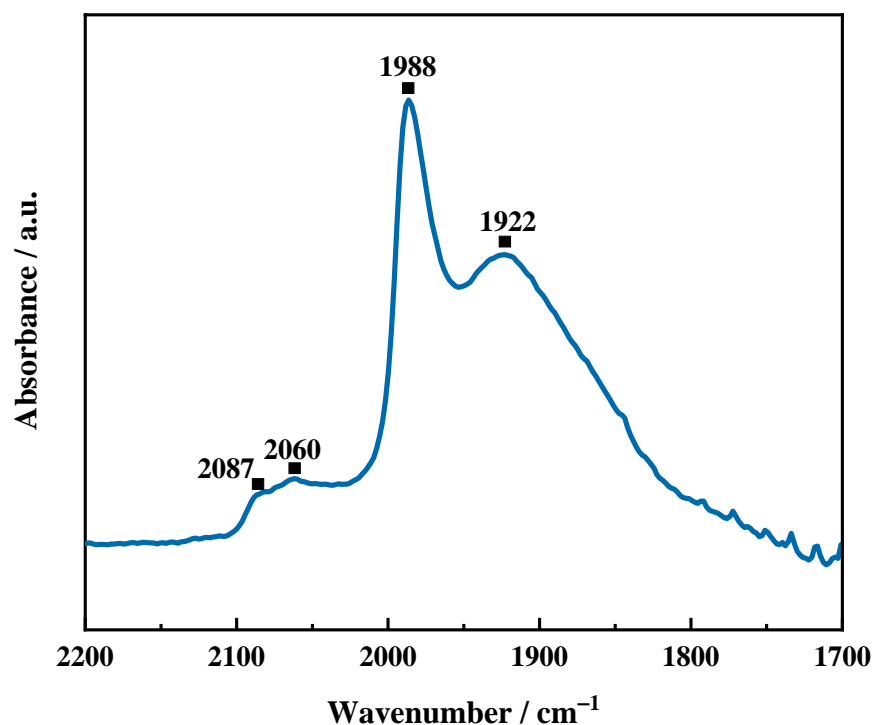


Figure 3.13. Room temperature spectrum of the chemisorbed CO in the 5% Pd/ γ -Al₂O₃ catalyst obtained using the Nicolet Nexus DRIFTS cell.

The background subtracted diffuse reflectance spectrum in the region 1700–2200 cm⁻¹ for a saturation coverage of CO on the 5% Pd/ γ -Al₂O₃ catalyst is presented in Figure 3.13, displaying four characteristic bands for the adsorption of CO onto the palladium crystallites. With basis on CO adsorption studies on metal single crystal and nanoparticle mode catalysts,^[192–195] the 1922 cm⁻¹ band is assigned to μ_3 hollow bonded and CO μ_2 bridge bonded CO on the (111) planes of the palladium particles. The origin of the 1988 cm⁻¹ feature is attributed to μ_2 bonded CO on the (100) palladium facets.^[196] CO linearly bound to the edge sites is observed at 2060 cm⁻¹. The shoulder at 2087 cm⁻¹ is assigned as chemisorbed CO residing on the corner sites.^[160] These assignments have been summarised in Table 3.5.

Table 3.5. Summary of the characteristic bands associated with the adsorption of CO onto the 5% Pd/ γ -Al₂O₃ catalyst.

<i>Wavenumber / cm⁻¹</i>	<i>Assignment</i>	<i>T_{desorption} / °C</i>
2087	Linear Corner	50–100
2060	Linear Edge	250–300
1988	μ_2 , Pd(100)	400–450
1922	μ_3 , Pd(111)	400–450

Figure 3.14 presents the infrared spectra obtained from the progressive warming of a saturated overlayer of CO. Gradual heating of the DRIFTS cell means that a desorption temperature of CO from each of the assigned sites can be identified. Desorption temperatures, as determined from Figure 3.14, are summarised in Table 3.5. The lower the temperature at which the CO desorbs the weaker the binding of CO at that particular site.

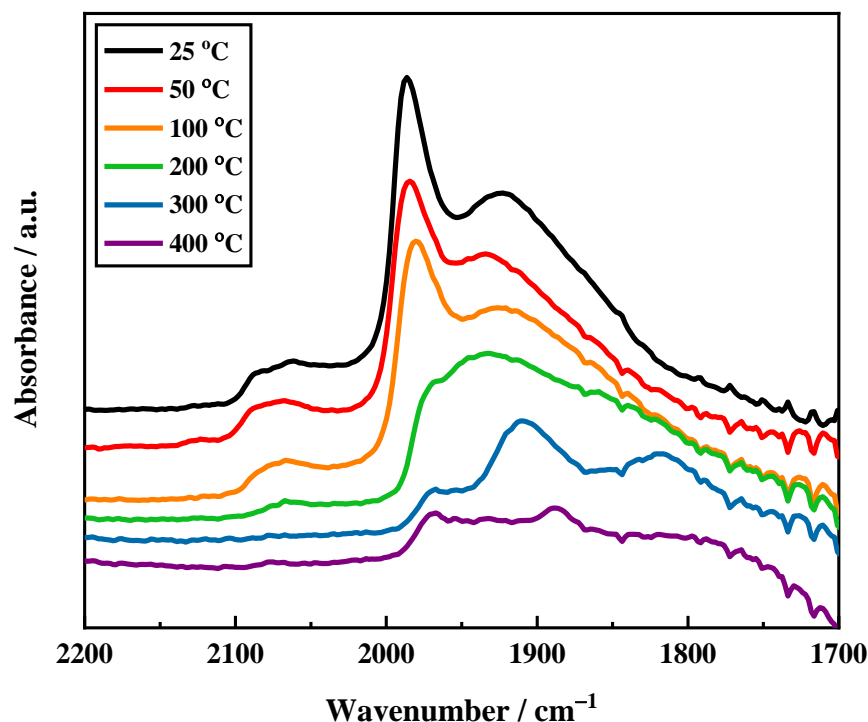


Figure 3.14. Background subtracted diffuse reflectance infrared spectrum of a saturated chemisorbed layer of CO as a function of temperature. The saturation spectrum was dosed at room temperature (25 °C). The 5% Pd/ γ -Al₂O₃ sample was then progressively warmed to 50, 100, 200, 300 and 400 °C.

3.11 Thermogravimetric Analysis

Thermogravimetric analysis (TGA) was conducted using an SDT Q 600 thermogravimetric analyser (TA Instruments), ramping from 0–1000 °C at a rate of 10 °C min⁻¹ under a flow of argon (100 mL min⁻¹), to determine the thermal stability of the catalysts.

From the thermal analysis curves shown in Figure 3.15 a weight loss of approximately 5% is observed within the 0–100 °C temperature range for both catalysts. This is likely caused by the loss of adsorbed water.^[197–198] No further thermogravimetric reaction was observed for the alumina supported catalyst. This suggests that alumina has excellent thermal stability, as is reported in the literature.^[199–202] Indeed, the phase transition from θ -alumina to α -alumina takes place in the temperature range of 1050–1200 °C.^[203–204] For the carbon catalyst; however, a further 22% weight loss was observed at approximately

600 °C (Figure 3.15). This profile indicates the 5% Pd/C catalyst to be structurally stable up to temperatures of approximately 500 °C.

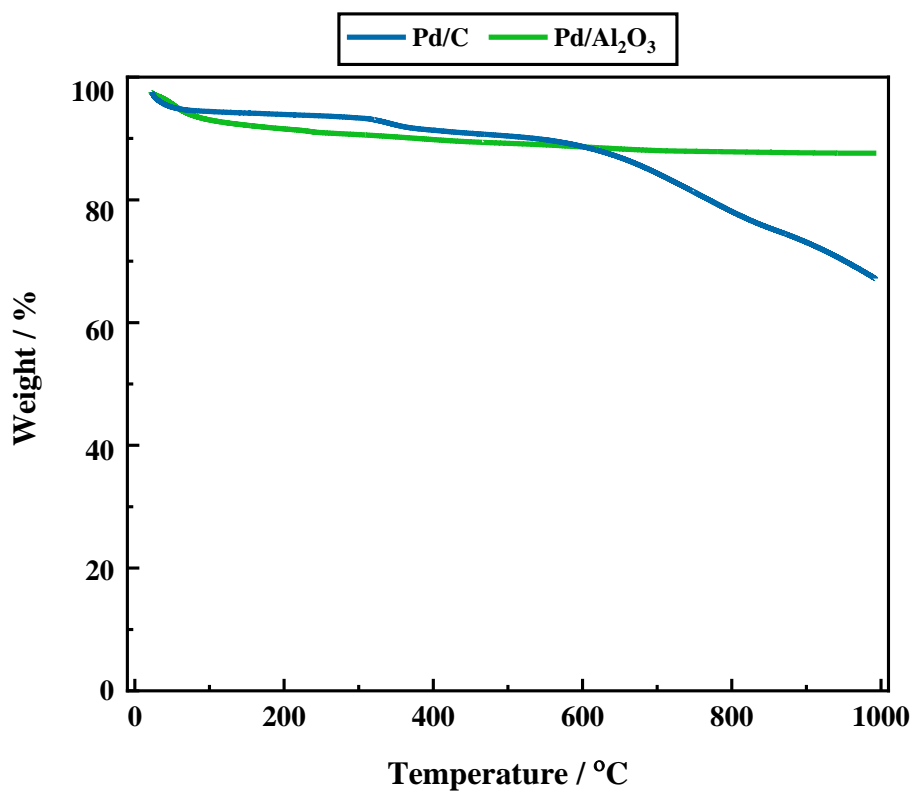


Figure 3.15. Thermogravimetric analysis of both the 5% Pd/C catalyst and the 5% Pd/ γ -Al₂O₃ catalyst from 0–1000 °C ramped at a rate of 10 °C min⁻¹ under a flow of argon.

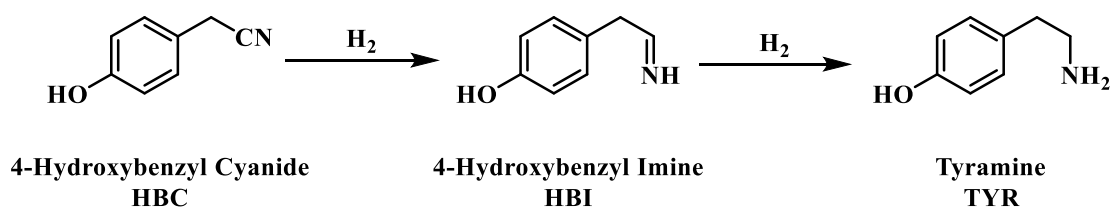
CHAPTER 4

*The Production of Tyramine via the
Selective Hydrogenation of 4-
Hydroxybenzyl Cyanide over a
Carbon-Supported Palladium
Catalyst*

4.1 Introduction

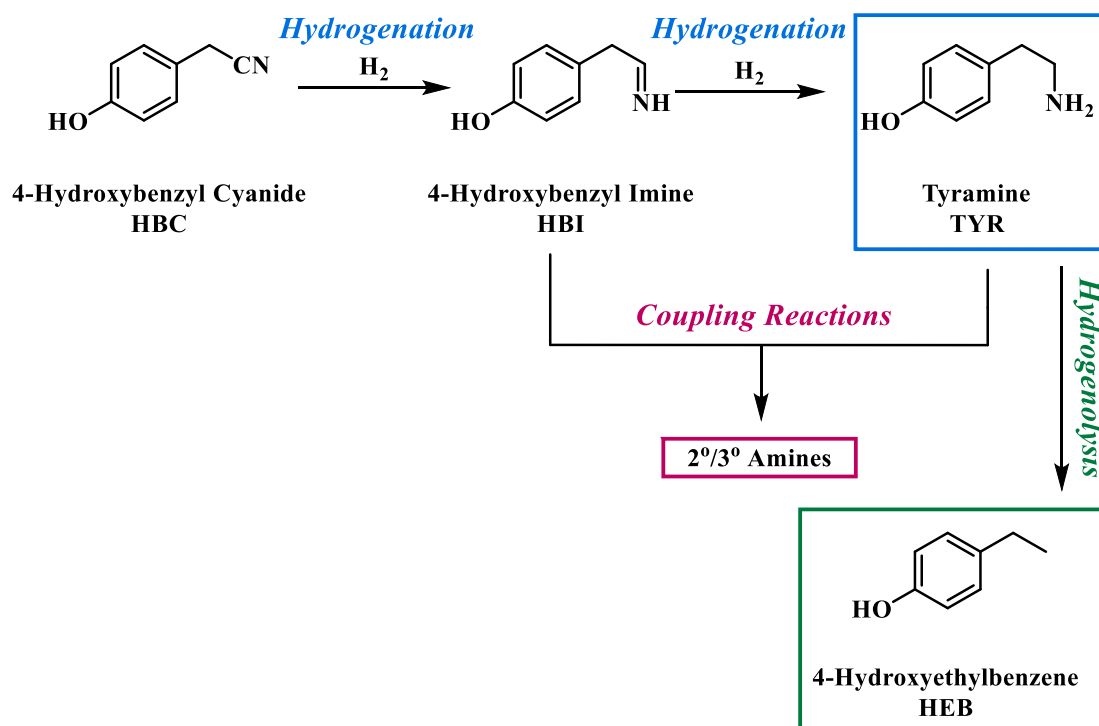
The substrate 4-hydroxybenzyl cyanide ($\text{HOC}_6\text{H}_5\text{CH}_2\text{CN}$), selected for its simple molecular structure, is utilised to provide a preliminary understanding of factors that contribute to the presence, or absence, of hydrogenation and hydrogenolysis pathways in the matter of aromatic nitrile hydrogenation reactions. Care was taken to explore the various experimental parameters that could potentially impede or enhance product formation. For example, the role of acid as an auxiliary agent to minimise amine/metal interactions,^[35] and the issue of efficient hydrogen supply,^[117] were examined in order to maximise product yields. Furthermore, considering these factors, the matter of accessibility to a hydrogenolysis pathway can be usefully explored.

4-hydroxybenzyl cyanide was selected as a reagent for two reasons. Firstly, in certain agri-chemical production chains, selective nitrile hydrogenation is often required in the presence of other ring substituents. To a degree, the inclusion of the hydroxyl group *para* to the nitrile chain addresses this requirement. Secondly, selective hydrogenation of 4-hydroxybenzyl cyanide will yield 4-(2-aminoethyl)phenol ($\text{HOC}_6\text{H}_5\text{CH}_2\text{CH}_2\text{NH}_2$), also known as tyramine. Tyramine is a molecule of some considerable interest due to its biological activity in the human body, where it may be accessed *via* foods as diverse as cheese, red wine, sausages and chocolate.^[205] In addition to involvement in a range of biochemical pathways within mammals, trace amines such as tyramine and its analogues are also thought to influence aspects of brain chemistry. Biochemically, tyramine may be produced by the action of the enzyme tyrosine hydroxylase to form tyrosine ($\text{HOC}_6\text{H}_5\text{CH}_2\text{CH}(\text{CO}_2\text{H})(\text{NH}_2)$) which, subsequently, undergoes decarboxylation *via* the action of the enzyme tyrosine decarboxylase to form tyramine. The matter of the pharmacology and therapeutics of trace amines have been comprehensively reviewed by Broadley.^[206] Following on from the early work of Buck using a platinum dioxide catalyst,^[117] there are surprisingly few accounts of the chemical synthesis of this trace amine.^[66, 96, 207–208]



Scheme 4.1. The hydrogenation reaction of 4-hydroxybenzyl cyanide over a 5% Pd/C catalyst to afford tyramine via the 4-hydroxybenzyl imine intermediate.

Against this background, 4-hydroxybenzyl cyanide is hydrogenated with the aim of selectively producing the biologically relevant primary amine tyramine. Scheme 4.1 highlights the reaction sequence under investigation. The selected reaction system aims to provide a preliminary understanding of aromatic nitrile hydrogenation reactions over a 5% Pd/C catalyst. It should, however, be noted that it is likely that Scheme 4.1 portrays an overly simplistic representation of the reaction system. As such, the scheme may be expanded to include additional reaction processes often shown in the relevant nitrile hydrogenation literature (Scheme 4.1). These additional processes are reported to occur alongside hydrogenation of the nitrile functionality.^[17, 21]



Scheme 4.2. The hydrogenation reaction of 4-hydroxybenzyl cyanide over a 5% Pd/C catalyst to afford tyramine. Additional chemistry which may be available within this reaction system (hydrogenolysis and coupling reactions) are also shown.

Scheme 4.2 highlights that each postulated reaction (hydrogenation, hydrogenolysis or imine/amine coupling) culminates in a different product. Specifically, if only the desired hydrogenation reaction were to occur, tyramine would be the sole detectable product. However, if hydrogenolysis or the coupling pathways were operational, production of 4-hydroxyethylbenzene and secondary/tertiary amines, respectively, would be observable alongside the desired primary amine. Analysis of the product distribution can therefore be used as a means of providing valuable insight into the reaction system. In this study, various parameter changes (acid additive presence, agitation, hydrogen pressure and temperature) are employed as a means of fine tuning the product distribution such that tyramine is selectively produced.

4.2 Hydrogenation Reaction of 4-Hydroxybenzyl Cyanide in the Absence of Chemical Modifiers Affords an Unfavourable Product Mixture

The liquid phase hydrogenation reaction of 4-hydroxybenzyl cyanide was initially conducted under relatively mild hydrogenation reaction conditions in the absence of any chemical modifiers. The conditions utilised mimic those employed successfully for other nitrile hydrogenation reaction systems previously explored within the Lennon Group.^[35, 150–151] Figure 4.1 is a representative reaction profile highlighting the initial outcome of this study.

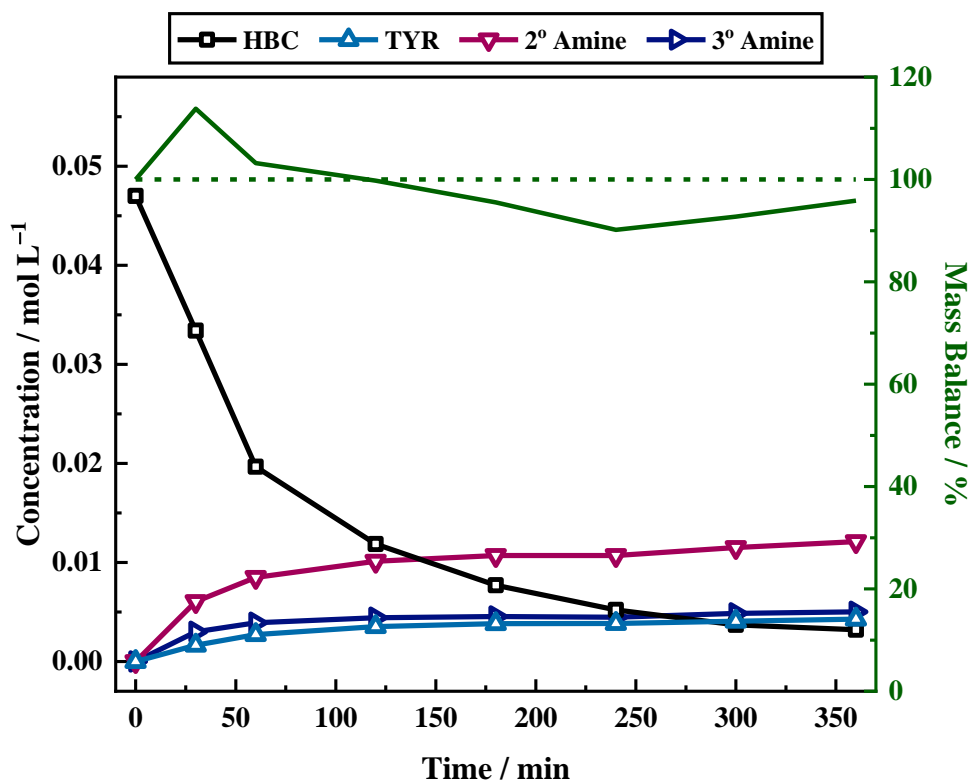
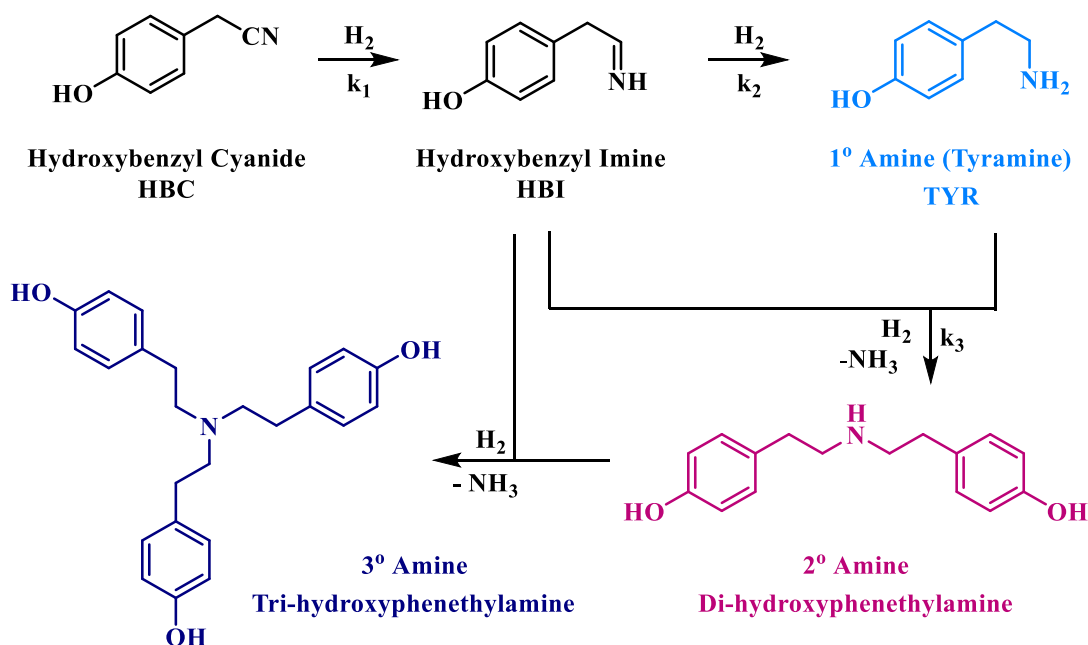


Figure 4.1. Reaction profile and mass balance plot for the liquid phase hydrogenation reaction of 4-hydroxybenzyl cyanide (49 mmol L^{-1}) over a 5% Pd/C catalyst (500 mg) in the absence of acid in methanol. The reaction was conducted at 60°C under 4 barg hydrogen pressure with an external line pressure of 6.5 barg and an agitation speed of 450 rpm. Mass balance is plotted as a percentage on the second y-axis with the solid and dashed lines representing observed and calculated mass balance respectively. [HBC = 4-hydroxybenzyl cyanide; TYR = tyramine; 2° Amine = di-hydroxyphenylamine; 3° Amine = tri-hydroxyphenylamine].

Figure 4.1 illustrates that nitrile conversion was found to be relatively rapid for the initial portion of the reaction, with 58% conversion achieved within 60 minutes. The rate thereafter, progressively decreased with only 93% conversion of the nitrile being achieved at extended reaction times (360 minutes). Further to negligible quantities of the desired product being formed (tyramine selectivity *ca.* 11%), two unknown products, with retention times of 7 minutes and 8 minutes, were observed *via* liquid chromatography. Despite reference standards for these materials being unavailable, liquid chromatography-mass spectrometry (LC-MS) analysis of the reaction mixture conducted at the industrial site (Syngenta, Jealott's Hill) identified the unknown peaks as the corresponding secondary and tertiary amines (di-hydroxyphenylamine and tri-hydroxyphenylamine, respectively). The associated LC-MS data has been published but is not reproduced here

for conciseness.^[37] Due to the lack of commercial availability of these compounds, calibration by HPLC, as employed for 4-hydroxybenzyl cyanide and tyramine, could not be achieved. As an alternative, and with basis on the integration of the associated peaks relative to a known standard (tyramine, concentration determined chromatographically), ¹H NMR spectroscopy was used as a means of calculating a response factor for both the secondary and the tertiary amines. Consequently, a full concentration profile, including a mass balance, for the hydrogenation of 4-hydroxybenzylcyanide under neutral conditions was achievable, as shown in Figure 4.1.



Scheme 4.3. Schematic representation of the imine/amine coupling reactions available within the 4-hydroxybenzyl cyanide hydrogenation system which result in the formation of secondary and tertiary amines.

It is assumed that the higher amines observed in Figure 4.1 are formed by the coupling of imine and amine species by the routes indicated in Scheme 4.3.^[21, 65] Here it is shown that formation of tyramine occurs *via* an imine intermediate, 4-hydroxybenzyl imine. The secondary amine, di-hydroxyphenethylamine, can subsequently be formed by the coupling of this imine intermediate with tyramine in a condensation reaction which is accompanied by the elimination of ammonia. It is then possible for the 4-hydroxybenzyl imine to couple with this secondary amine in a similar process to yield the tertiary amine, tri-hydroxyphenethylamine. In this instance, no imine species were detected in the liquid phase

suggesting that these species are present on the catalyst surface as highly reactive intermediates. The absence of imine species, alongside the poor tyramine yield (11% yield at 93% conversion, as achieved at a reaction time of 360 minutes), indicates that the condensation reactions are fast in comparison to the hydrogenation pathway that yields the primary amine. Interestingly, when the case of benzonitrile was considered under similar reaction conditions, it was the hydrogenation pathway, with a successive hydrogenolysis step, which was faster than the coupling reactions to form higher amines. This was evidenced by the selective production of toluene.^[35–36]

4.3 Inclusion of an Acid Additive Enhances Tyramine Selectivity

The aforementioned selectivity issues associated with this type of chemistry are demonstrated in Figure 4.1 through the undesirable formation of the secondary and tertiary amines. Invoking a technique which reduces the production of secondary and tertiary amines is therefore essential in order to enhance selectivity towards the primary amine. Several authors report the use of auxillary agents to enhance primary amine yields in nitrile reduction reactions. Amongst other methods, and as previously described, both acidic (*e.g.* HCl)^[96, 208–209] and basic (*e.g.* NH₃)^[30] conditions have been used for such a purpose.

Nevertheless, whilst the application of a base additive has been shown to be successful for many nitrile reduction reactions, care must be taken when cyanohydrins are considered. It is noted that, as 4-hydroxybenzyl cyanide does not possess a carbon atom attached to *both* a cyanide group and a hydroxyl group, it is not classified as a cyanohydrin. However, within the overall scope of this project, it is hoped that a suitable methodology for cyanohydrin hydrogenation reaction will be developed, and thus, the associated hazards cannot be ignored. The risk associated with the use of cyanohydrins in the presence of a base additive has been discussed in Section 2.1.1.

On the assumption that protonation of the amine will reduce its reactivity as a nucleophile, therefore hindering condensation reactions, subsequent experiments included an acid additive.^[65] In this instance, sulphuric acid was selected; an excess of a diprotic acid should ensure protonation of the amine functionality throughout the full reaction coordinate and, moreover, the anion (HSO₄[−]) is not expected to cause metal complexation problems as might be the case if, for example, HCl was used. Further details regarding

acid selection will be provided in Chapter 7. Moreover, the protonation of the amine to form a salt should keep this species in the liquid phase, and in doing so, prevent its coordination to the active sites of the catalyst, which could be detrimental to the conversion of the nitrile/imine.^[65] The strong chemisorption of the nitrogen lone pair to the palladium surface is therefore thwarted by the presence of the acid and, as such, poisoning of the catalyst should be reduced.

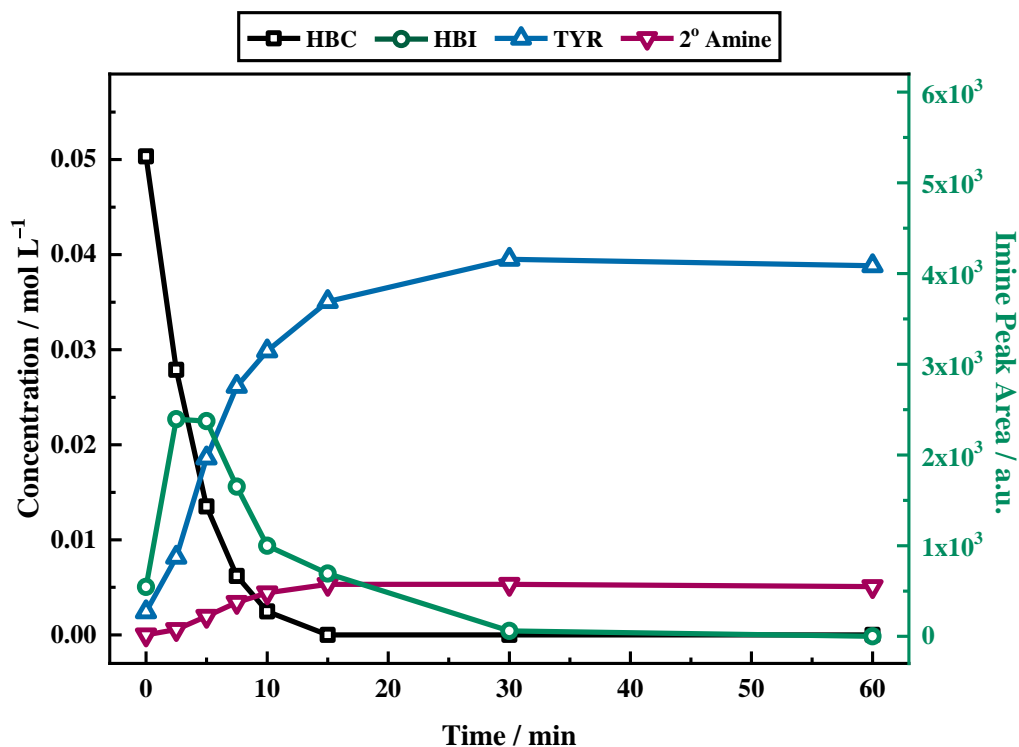


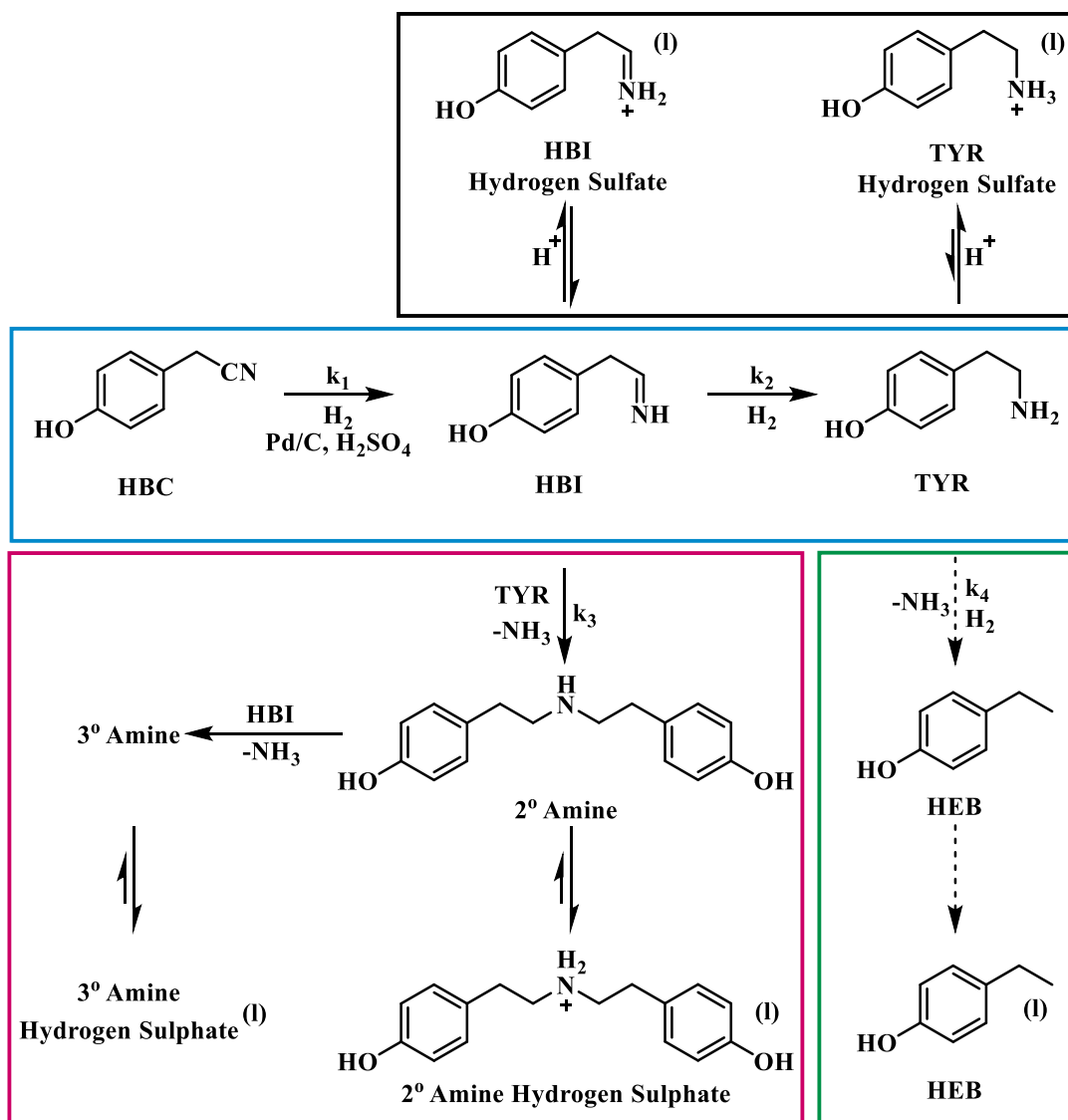
Figure 4.2. Reaction profile for the liquid phase hydrogenation reaction of 4-hydroxybenzyl cyanide (49 mmol L^{-1}) over a 5% Pd/C catalyst (500 mg) in the presence of 2 equivalents of sulphuric acid in methanol. The reaction was conducted at 60°C under 4 barg hydrogen pressure with an external line pressure of 6.5 barg and an agitation speed of 450 rpm. The hydroxybenzyl imine was not quantified, and thus plotted as peak area on the second y-axis. [HBC = 4-hydroxybenzyl cyanide; HBI = 4-hydroxybenzyl imine; TYR = tyramine; 2° Amine = di-hydroxyphenylamine].

Figure 4.2 shows the reaction profile for the hydrogenation reaction of 4-hydroxybenzyl cyanide in the presence of a 2-fold excess (relative to the initial nitrile concentration) of a sulphuric acid additive under identical conditions to those presented in Figure 4.1. Complete conversion of the starting material was achieved within approximately 15 minutes, significantly faster than in the absence of the acid additive (Figure 4.1).

Additionally observed, was a drastic alteration in product distribution. Specifically, it is shown in Figure 4.2 that there are now only two products, a major and a minor, as production of the tertiary amine has been prevented by the presence of the sulphuric acid additive. Further, 4-hydroxybenzyl imine is detectable in the liquid phase as an intermediate of the reaction. It is essential to note that, under the acidic conditions presented here and throughout, the imine and amine species detectable in the liquid phase are the associated hydrogen sulphate salts.

As before, ^1H NMR spectroscopy was employed for the quantification of the secondary amine. However, as a consequence of the highly reactive nature of imines,^[21, 30] it was not possible to determine a response factor for the 4-hydroxybenzyl imine intermediate by this method. As such, the imine intermediate was not quantified, and thus, the imine peak area was plotted separately from all other reaction species on the secondary y-axis. This is the case for all future figures involving the 4-hydroxybenzyl imine species.

It is observed in Figure 4.2 that the inclusion of acid additive has significantly enhanced the desired reaction pathway, with the hydrogenation product, tyramine, produced with a selectivity of *ca.* 82% at reaction completion, time = 60 minutes (*cf.* a tyramine selectivity of 14%, corresponding to a conversion of 58% was observed at the same reaction time in the absence of acid). In contrast to the enhancement of the hydrogenation pathway, and as evidenced by the absence of the tertiary amine, the imine/amine coupling pathways were suppressed. Production of the secondary amine with a selectivity of 18% by reaction completion closed the mass balance (not shown). It is, however, recognised that the unsuccessful quantification of the imine results in an apparent mass imbalance at the beginning of the reaction. For completeness, it is also noted that, as with the neutral conditions, there was no hydrogenolysis of the amine functionality of tyramine to afford 4-hydroxyethyl benzene.



Scheme 4.4. Full schematic representation for all of the interconnecting reactions available within an acidic medium for the hydrogenation reaction of 4-hydroxybenzyl cyanide. Available pathways can be separated into three main categories (hydrogenation, hydrogenolysis and coupling reactions). Additionally shown are the equilibria of the relevant species showing their partitioning between the catalyst surface and the liquid phase (l). [HBC = 4-hydroxybenzyl cyanide; HBI = 4-hydroxybenzyl imine; TYR = tyramine; HEB = 4-hydroxyethylbenzene; 2° Amine = di-hydroxyphenylamine; 3° Amine = tri-hydroxyphenylamine].

The inclusion of the acid additive clearly results in a more complex reaction environment. The original reaction scheme (Scheme 4.1) can therefore be expanded further to show the partitioning of the reaction species between the surface and the liquid phase, consequently highlighting the effects of the acid additive. The resulting scheme (Scheme 4.4) shows the unwanted route to the secondary and tertiary amines and the inactive hydrogenolysis route alongside the desired hydrogenation pathway to tyramine.

Moreover, due to the presence of the sulphuric acid additive, salt formation in the liquid phase is also possible. Scheme 4.4 indicates that both imine and amine species are susceptible to formation of the corresponding conjugate acid when released into the liquid phase. The imine, however, has a lower $pK_a(H)$ than the amines, and therefore has a stronger affinity for proton donation making it a stronger conjugate acid. Conversely, although not observed on this occasion, the hydrogenolysis product 4-hydroxyethylbenzene is not likely to form the conjugate acid when released into the liquid phase. In this instance, as the $pK_a(H)$ of the phenol associated with 4-hydroxyethylbenzene is higher than that of methanol (reaction solvent), protonation of the methanol will be favourable.

4.4 Mass Transport Restrictions Limit the Achievable Selectivity Towards Tyramine

Despite removal of the tertiary amine from the reaction mixture (Figure 4.2), imine/amine coupling reactions to form the secondary amine remain accessible. Complete selectivity towards the primary amine is thus restricted. Accordingly, alternative techniques must also be considered if the selective production of tyramine is to be achieved.

Scheme 4.4 highlights that the hydrogenation pathway to afford tyramine requires two equivalents of hydrogen. Therefore, it is essential that there is ample hydrogen available to rapidly afford the desired product such that the hydrogen sulphate salt of the tyramine may be released into the liquid phase before coupling reactions can occur. To ensure that this is achieved, the hydrogen availability within the system must be considered. As a three-phase reaction system, there is significant potential for mass transfer restrictions at the interfacial barriers that exist between the phases. A restriction at either one, or both of the gas-liquid, or the liquid-solid interfaces may result in a limited hydrogen supply within the reactor thereby hindering tyramine production.

Present as a gaseous reagent, molecules of hydrogen must first pass through the gas-liquid interface to dissolve into the liquid phase. These molecules must then migrate through the solution and pass the liquid-solid barrier before they can reach the catalyst. From here, the hydrogen molecules must find an active site on the catalyst on which to adsorb. If the active sites are not on the surface of the catalyst then it is possible that the hydrogen will have to migrate further, through the pores of the support, before reaching an active site for adsorption. Moreover, the liquid phase reagents, whilst in solution and so do not have to pass through a gas-liquid barrier, also have to pass the liquid-solid interface and migrate through the catalyst particle to reach the active sites before a reaction can take place.^[39]

When a gaseous reactant such as hydrogen is employed, agitation is of great importance in facilitating the transportation of the gas through the gas-liquid interface. The greater the rate of agitation, the larger the liquid surface area exposed to the gas, and thus, the more gas molecules that can pass through the interface into solution. By operating under optimal mixing conditions, gradientless in terms of concentration and temperature throughout the reactor volume, mass transfer restrictions at the gas-liquid interface can be minimised. To assess if perfect mixing has been obtained, a simple ‘agitation test’ may be conducted. The test aims to identify the minimum stirring rate required to achieve perfect mixing. Keeping all other variables constant, the rate of reagent conversion is measured as the stirring speed is altered. Perfect mixing is obtained when the conversion rate is found to be independent of agitation speed.^[39, 210]

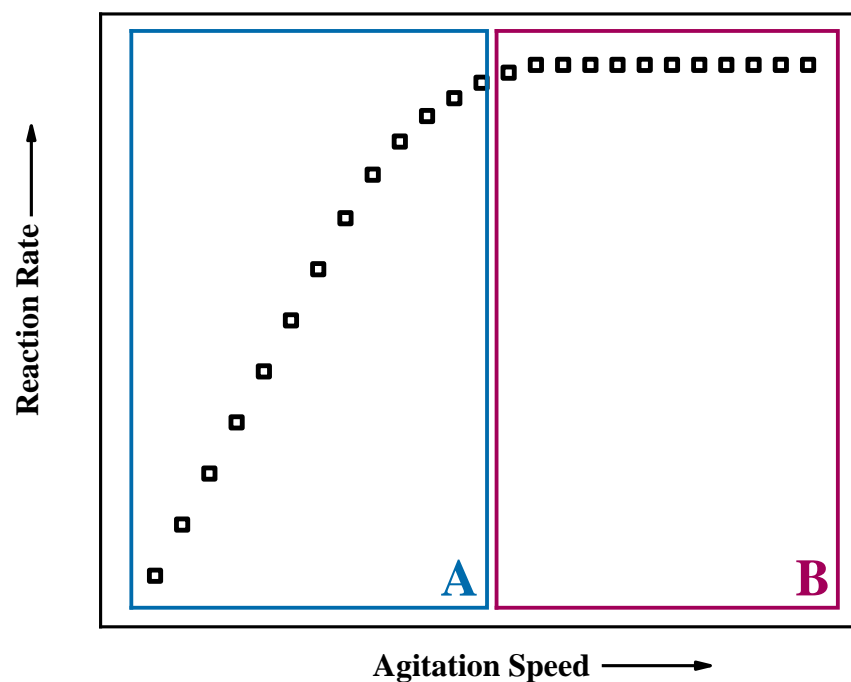


Figure 4.3. Idealised representation of the effect of agitation speed on the rate of a heterogeneously catalysed three-phase reaction. Figure reproduced from reference 39.

With reference to Figure 4.3, where a generic rate *versus* agitation plot for an unspecified three-phase heterogeneously catalysed reaction is presented, it can be seen that a reaction system may be in one of two regimes (designated as **A** and **B** in Figure 4.3). When changes in agitation speed result in different observed rates, as is depicted in Section **A** of Figure 4.3, it can be concluded that gas-liquid mass transport limits the reaction. However, once a certain agitation speed has been reached, increasing this parameter further has no effect on the observed rate. Section **B** of Figure 4.3 corresponds to this observation and represents a set of conditions that are free from such diffusional constraints and hence indicate kinetic control. It is consequently desirable that the operational agitation speed is found to be contained within Section **B** of Figure 4.3 to ensure that the aforementioned mass transport limitations do not interrupt optimal operation.

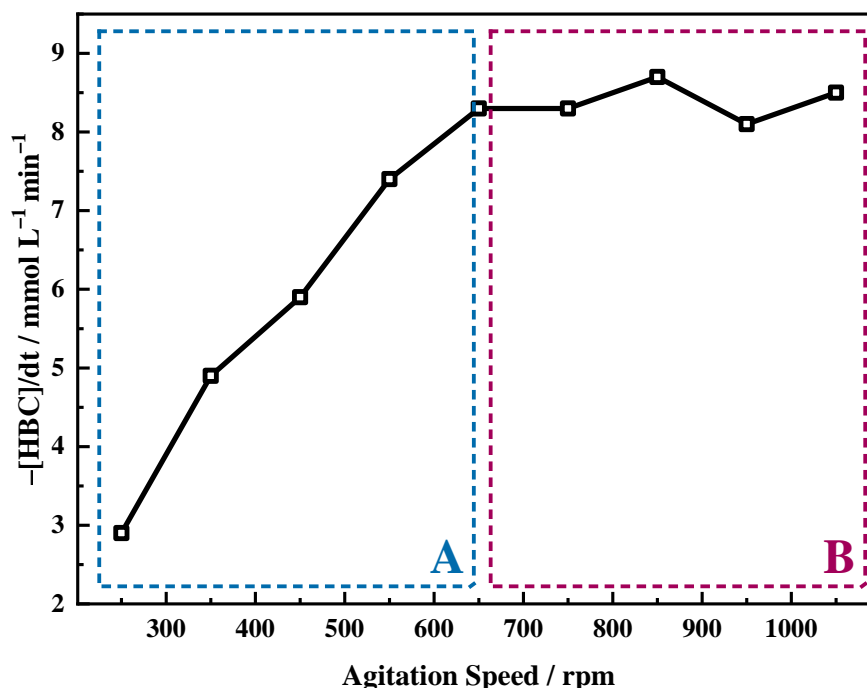


Figure 4.4. Influence of agitation speed on the rate of conversion of 4-hydroxybenzyl cyanide (49 mmol L⁻¹) over a 5% Pd/C catalyst (500 mg) in the presence of 2 equivalents of sulphuric acid in methanol. The reaction was conducted at 60 °C under 4 barg hydrogen pressure with an external line pressure of 6.5 barg and an agitation speed of 450 rpm. [HBC = hydroxybenzyl cyanide].

In order to evaluate the possibility of mass transport restrictions in the reaction system of interest, the effect of agitation speed on the rate of consumption of the starting material was considered. The outcome of the agitation test is presented in Figure 4.4, and, as with the hypothetical example (Figure 4.3) shows two distinctive regimes.

At agitations below *ca.* 650 rpm the reaction exhibits the characteristics of a mass transport limitation (reaction rate \propto stirring speed, *i.e.* first order with respect to agitation rate). Figure 4.4 thus shows that in region A (0–650 rpm), operation is under diffusion control; presumably as a result of inefficient mass transport at the gas-liquid interface. Figure 4.4, however, also shows a plateau dependence of reagent consumption as a function of agitation rate at higher mixing speeds. Over the agitation range 650–1050 rpm, increasing the stirring speed leads to no real increase in the 4-hydroxybenzyl cyanide hydrogenation rate (zero order dependence on agitation rate). This is indicative of the reaction being under kinetic control and free of mass transport restrictions.

Given that Figures 4.1 and 4.2 were performed at 450 rpm, these profiles are deemed to be characteristic of the system operating with a constrained hydrogen supply to the palladium surface. Clearly, it is necessary to investigate the reaction in the absence of mass transport restrictions.

4.5 Increased Agitation Speed Affords Increased Selectivity Towards Tyramine

As discussed in Section 4.4, operation at an agitation speed of greater than or equal to 650 rpm should be sufficient to overcome poor mixing and the associated diffusion constraints at the gas-liquid interface. From here it can be predicted that an increase in agitation speed from the diffusion control region (450 rpm, as shown in Figure 4.5) to the kinetic control region (≥ 650 rpm, again as shown in Figure 4.5) will result in the enhancement of tyramine selectivity as a consequence of improved hydrogen availability. As such, the effect of agitation speed on tyramine selectivity is investigated.

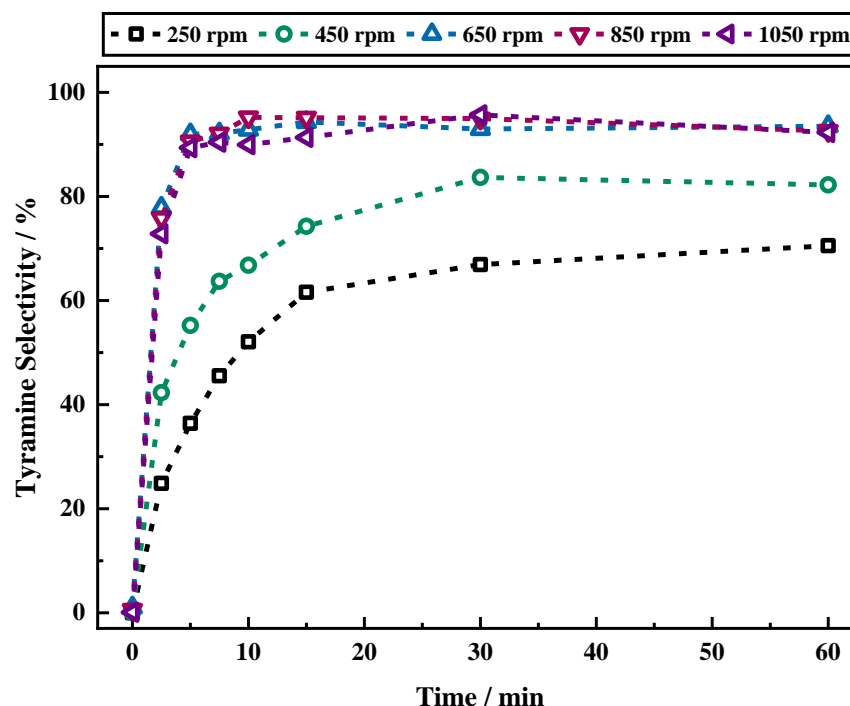


Figure 4.5. Influence of agitation speed on tyramine selectivity for the liquid phase hydrogenation reaction of 4-hydroxybenzyl cyanide (49 mmol L^{-1}) over a 5% Pd/C catalyst (500 mg) in the presence of 2 equivalents of sulphuric acid in methanol. The reaction was conducted at 60°C under 4 barg hydrogen pressure with an external line pressure of 6.5 barg.

Figure 4.5 shows tyramine selectivity throughout the reaction coordinate (0–60 minutes) for a number of different agitation speeds over the 250–1050 rpm range. The observations of the rate *versus* agitation plot for nitrile consumption (Figure 4.4) are clearly mirrored in Figure 4.5. It is revealed that, below approximately 650 rpm, improvements in tyramine selectivity can be made by increasing stirring speed, but, at speeds greater than this value, selectivity is shown to reach a maximum value of approximately 92%.

Although not commonly conducted, the effect of agitation speed on the rate of product and by-product formation was also considered (Figure 4.6). With reference first to Figure 4.6 **A**, it is shown that the rate of tyramine formation shows a similar trend to that observed for the consumption of 4-hydroxybenzyl cyanide. In this instance a rate of formation plateau, indicating kinetic control, is observed at agitation speeds ≥ 550 rpm (*cf.* ≥ 650 rpm for the consumption of 4-hydroxybenzyl cyanide). Interestingly, however, Figure 4.6 **B** shows that the rate of formation of the secondary amine does not vary significantly with agitation speed. This observation endorses Scheme 4.4, which indicates that coupling of the imine intermediate with the amine products does not require a hydrogen supply. Indeed, whilst the rate of secondary amine formation is slower than the rate of tyramine formation by a factor of 10, this finding indicates that a limitation in hydrogen supply will not hinder the formation of the secondary amine product. However, the opposite is true for tyramine formation. Therefore, for selective tyramine production, it is imperative that an adequate hydrogen supply is maintained throughout the reaction coordinate.

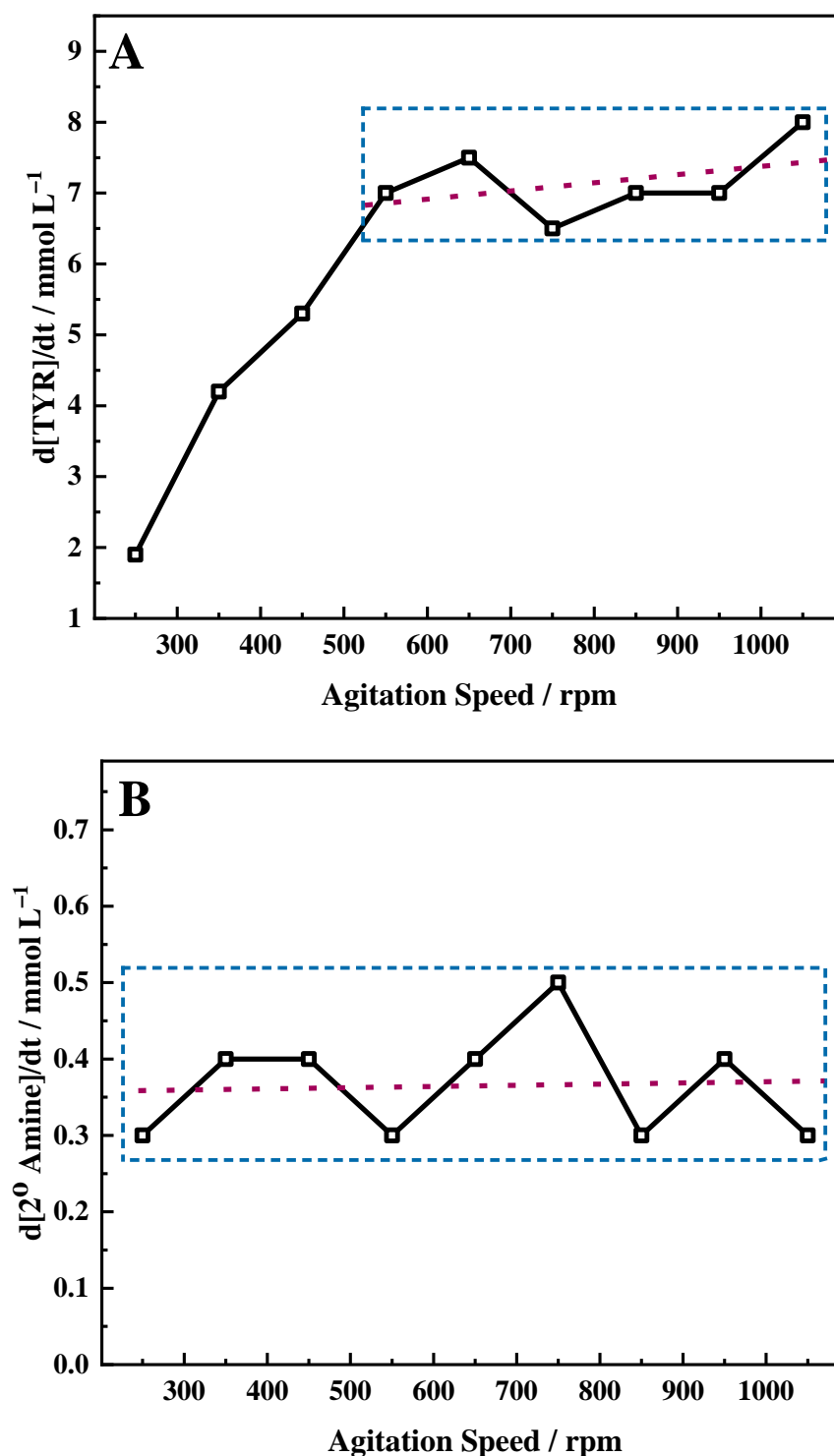


Figure 4.6. Influence of agitation speed on **A**, the rate of production of tyramine, and **B**, the rate of production of the 2° amine for the liquid phase hydrogenation reaction of 4-hydroxybenzyl cyanide (49 mmol L^{-1}) over a 5% Pd/C catalyst (500 mg) in the presence of 2 equivalents of sulphuric acid in methanol. The reaction was conducted at 60°C under 4 barg hydrogen pressure with an external line pressure of 6.5 barg and an agitation speed of 450 rpm. [TYR = tyramine; 2° Amine = di-hydroxyphenylamine].

Collectively, the findings of Figures 4.4 and 4.5 indicate that, at 450 rpm, the current operational agitation speed is likely to be limited by mass transport constraints at the gas-liquid interface. Consequently, it is found to be prudent to increase the stirring speed to a value within the plateau region (650–1050 rpm) in order to avoid this.

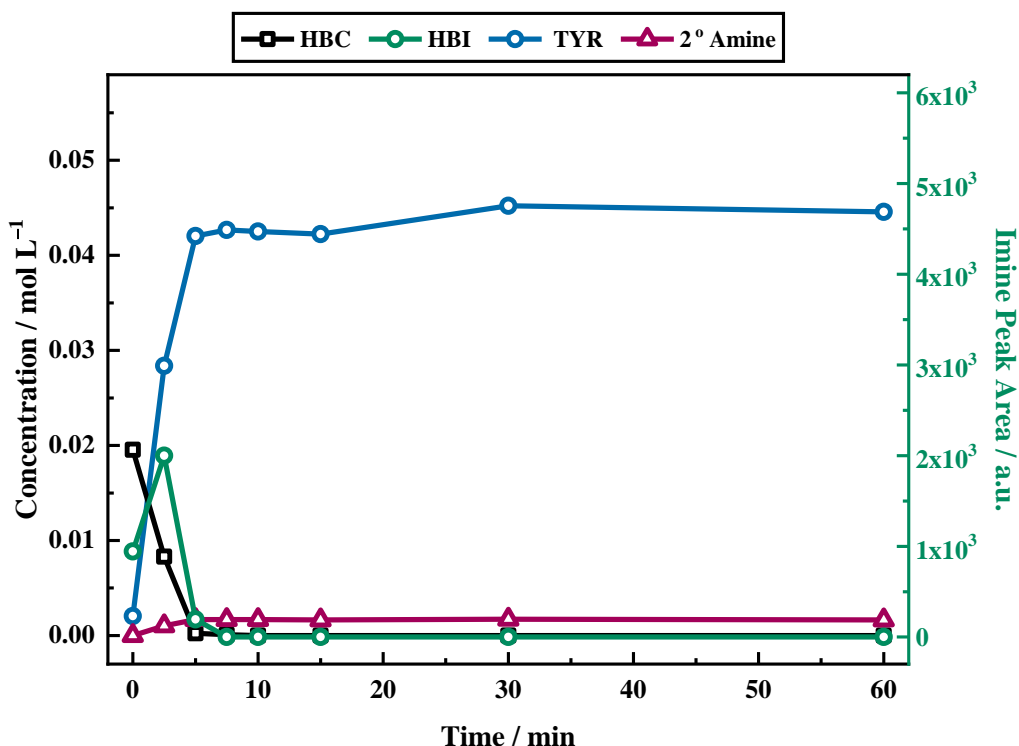


Figure 4.7. Reaction profile for the liquid phase hydrogenation reaction of 4-hydroxybenzyl cyanide (49 mmol L^{-1}) over a 5% Pd/C catalyst (500 mg) in the presence of 2 equivalents of sulphuric acid in methanol. The reaction was conducted at 60°C under 4 barg hydrogen pressure with an external line pressure of 6.5 barg and an agitation speed of 1050 rpm. The hydroxybenzyl imine was not quantified, and thus plotted as peak area on the second y-axis. [HBC = 4-hydroxybenzyl cyanide; HBI = 4-hydroxybenzyl imine; TYR = tyramine; 2° Amine = di-hydroxyphenylamine].

In line with the findings of the rate *versus* agitation plots, Figure 4.7 shows the reaction profile for the hydrogenation reaction of 4-hydroxybenzyl cyanide under acidic conditions at the increased stirring speed of 1050 rpm. As anticipated, the rate of nitrile consumption has hastened but, more significantly, a change in product selectivity is also observed. Whilst the secondary amine is still produced, it is in much lower quantities (selectivity *ca.* 8% on completion of the reaction) than observed during the reaction conducted under conditions associated with diffusion control (Figure 4.2).

The combination of employing an acid auxiliary agent plus operation within a kinetic regime effectively free from gas-liquid mass transport limitations has led to significant improvements in returnable yield of the primary amine salt (tyramine hydrogen sulphate). Nonetheless, in order to further improve the rate of hydrogen supply to the palladium active sites such that it exceeds the hydrogen consumption rate, two further factors were examined. Firstly, the influence of hydrogen overpressure in the autoclave was investigated and then, secondly, the matter of reaction temperature was explored.

4.6 Pressure Alterations

For any industrial process, selectivity towards the desired product is pivotal in the success of the process.^[39] Whilst marked improvements to this were made through the increase in stirring speed, production of the secondary amine was still observed (Figure 4.7). Nevertheless, there are a number of additional factors which can play an important role in achieving a completely selective process.^[21] One such example is hydrogen pressure.^[39] Consequently, the effect of this parameter on the hydrogenation of 4-hydroxybenzyl cyanide was investigated.

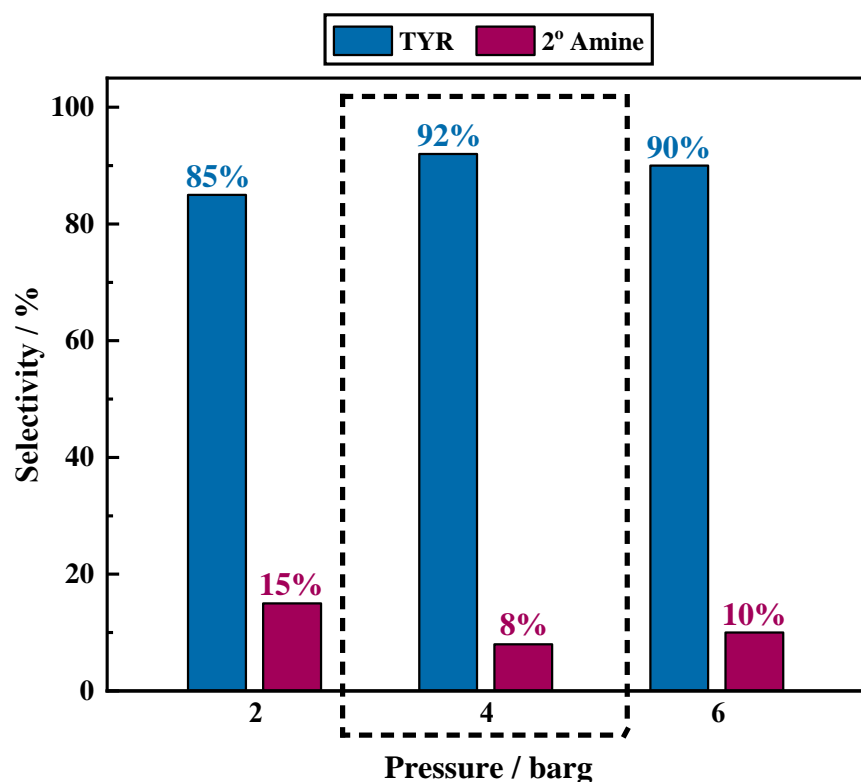


Figure 4.8. Influence of hydrogen pressure on the selectivity at reaction completion (time = 60 minutes) for the liquid phase hydrogenation reaction of 4-hydroxybenzyl cyanide (49 mmol L^{-1}) over a 5% Pd/C catalyst (500 mg) in the presence of 2 equivalents of sulphuric acid in methanol. The reaction was conducted at 60°C at various hydrogen pressures but with a constant external line pressure of 6.5 barg and an agitation speed of 1050 rpm. Highlighted in the dashed black box is the standard operational hydrogen pressure (4 barg). [TYR = tyramine; 2° Amine = di-hydroxyphenethylamine].

Figure 4.8 shows a plot of tyramine hydrogen sulphate selectivity as a function of hydrogen pressure in the headspace of the autoclave. Increasing hydrogen pressure resulted in faster hydrogenation rates; notably complete conversion of 4-hydroxybenzyl cyanide was attained at 10, 5 and 2.5 minutes at respective hydrogen overpressures of 2, 4, and 6 barg. Regardless of this change in rate, the product distribution at reaction completion was largely unaffected with both tyramine hydrogen sulphate and the secondary amine, di-hydroxyphenethylamine, being detectable in the liquid phase alongside the imine intermediate (4-hydroxybenzyl iminium hydrogen sulphate).

Irrespective of the change in hydrogen availability associated with a pressure alteration, Figure 4.8 shows that the resultant selectivity is largely comparable over the monitored pressure range. This suggests that the reaction is more sensitive to agitation speed than

hydrogen pressure. Nonetheless, out-with the error associated with the analytical measurement, minor effects to the reactions selectivity are incurred with the hydrogen pressure alterations. Specifically, increasing the operational pressure from 2 to 4 barg increases tyramine hydrogen sulphate selectivity at reaction completion from 85% to 92%. A further increase in pressure to 6 barg, however, was found to be approximately equal to the 4 barg reaction. Further increases to hydrogen pressure could not be monitored within the safety constraints of the laboratory. Despite this apparent insensitivity, it was identified that there was a minimum hydrogen requirement to afford complete conversion of the starting material within the monitored time frame of this reaction (60 minutes).

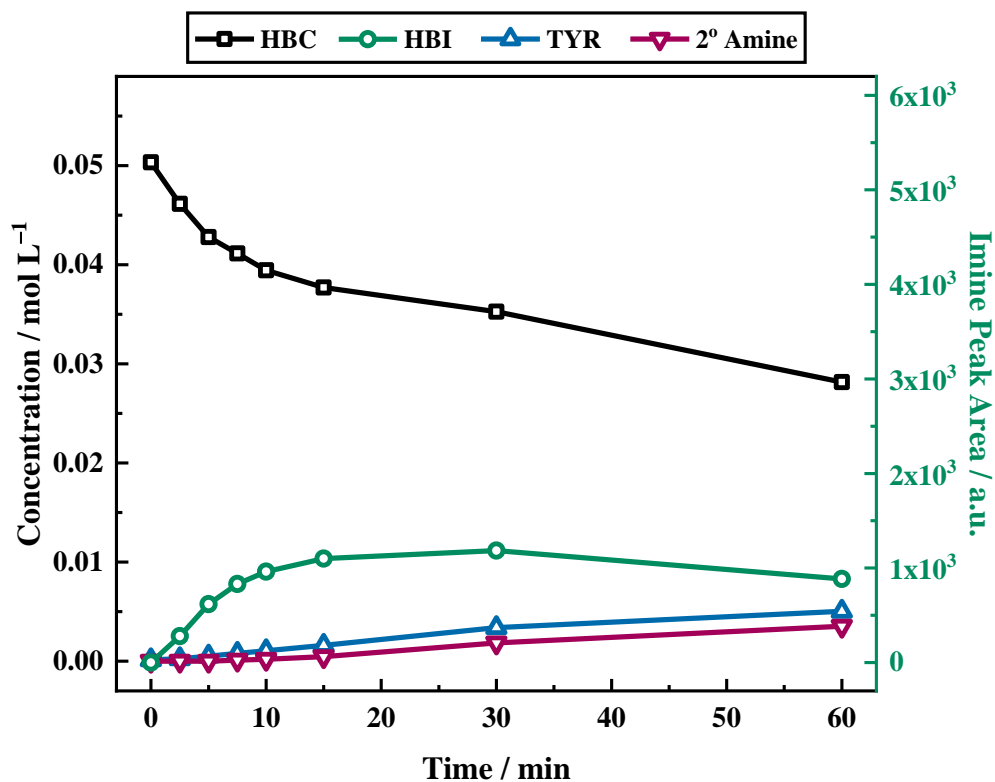


Figure 4.9. Reaction profile for the liquid phase hydrogenation reaction of 4-hydroxybenzyl cyanide (49 mmol L^{-1}) over a 5% Pd/C catalyst (500 mg) in the presence of 2 equivalents of sulphuric acid in methanol. The reaction was conducted at 60°C under 1 barg hydrogen pressure with an external line pressure of 6.5 barg and an agitation speed of 1050 rpm. The hydroxybenzyl imine was not quantified and so plotted as peak area on the second y-axis. [HBC = 4-hydroxybenzyl cyanide; HBI = 4-hydroxybenzyl imine; TYR = tyramine; 2° Amine = di-hydroxyphenylamine].

Shown in Figure 4.9 is the resultant reaction profile for the hydrogenation of 4-hydroxybenzyl cyanide at 1 barg hydrogen pressure. Whilst some of the starting material is consumed, only 44% conversion is achieved after a period of 60 minutes (*cf.* complete conversion was achieved by approximately 5 minutes at 4 barg hydrogen pressure, Figure 4.7). As with the elevated pressure reactions both tyramine and the secondary amine were observed in the liquid phase alongside the imine intermediate. The poor outcome regarding conversion and tyramine selectivity, linked to Figure 4.8, indicates that there is a minimum hydrogen pressure requirement that must be met. The reaction then becomes less dependent on hydrogen pressure once the pre-defined threshold pressure of 4 barg has been met and maintained.

4.7 Temperature Alterations

Arrhenius theory indicates that the rate of most chemical reactions increases rapidly with temperature.^[154] Thus, whilst a temperature increase can be used to enhance the rate of the desired reaction pathway, the effects are often not localised. This is of particular importance for a reaction system where more than one pathway is accessible but only one product is desirable. Indeed, given the breadth of pathways accessible to this reaction system, as presented in Scheme 4.4, this is an important factor to consider.

Further interwoven into the complexity of the reaction matrix is the matter of hydrogen solubility in the reaction solvent: hydrogen solubility in methanol is enhanced at elevated temperatures.^[211–212] Temperature, therefore, is also closely linked to the hydrogen availability issues considered prior (Sections 4.4–4.6). Accordingly, it is necessary to identify an optimal temperature that will facilitate effective solubility of hydrogen in the reaction solvent, whilst also maintaining a reasonable reaction rate and selectivity towards the desired product.

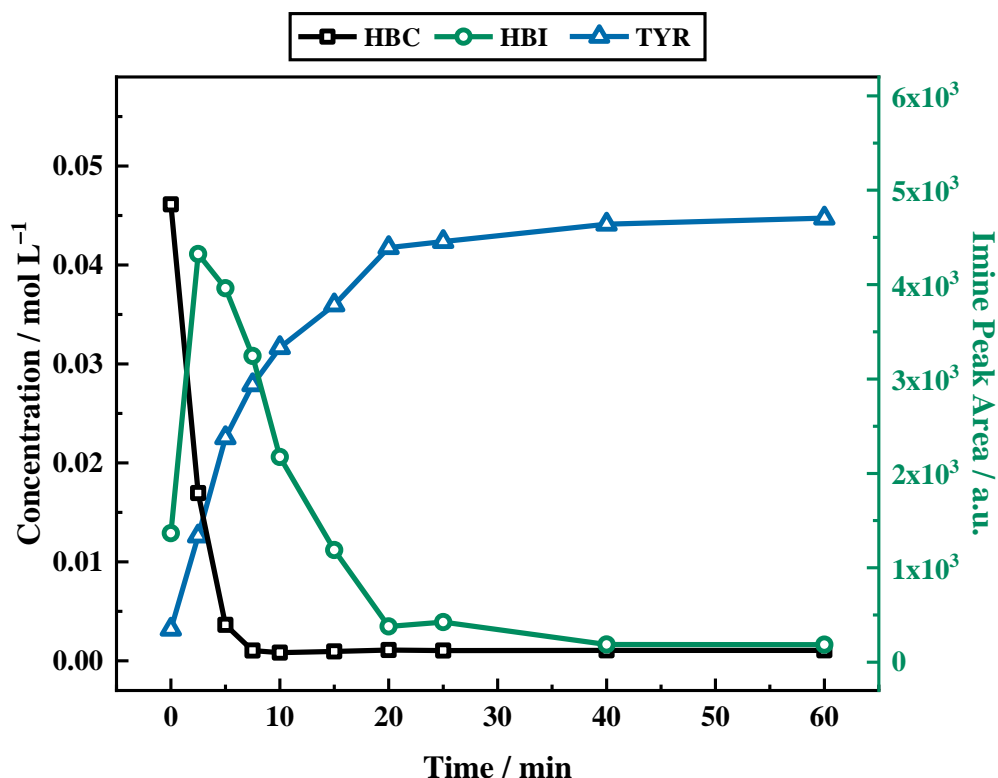


Figure 4.10. Reaction profile for the liquid phase hydrogenation reaction of 4-hydroxybenzyl cyanide (49 mmol L^{-1}) over a 5% Pd/C catalyst (500 mg) in the presence of 2 equivalents of sulphuric acid in methanol. The reaction was conducted at 30°C under 4 barg hydrogen pressure with an external line pressure of 6.5 barg and an agitation speed of 1050 rpm. The hydroxybenzyl imine was not quantified and so plotted as peak area on the second y-axis. [HBC = 4-hydroxybenzyl cyanide; HBI = 4-hydroxybenzyl imine; TYR = tyramine; 2° Amine = di-hydroxyphenylamine].

Figure 4.10 shows the resultant reaction profile for the hydrogenation reaction of 4-hydroxybenzyl cyanide under acidic conditions at the reduced reaction temperature of 30°C . When combined with the pressure and agitation adjustments previously undertaken (Figures 4.7 and 4.9), the reduction in temperature, executed in Figure 4.10, allowed the reaction profile to be further improved. As before, the nitrile unit is rapidly consumed with complete conversion to form the tyramine hydrogen sulphate salt *via* the 4-hydroxybenzyl iminium intermediate. However, no secondary or tertiary amine products were identified chromatographically in this case, indicating that the primary amine was selectively produced. Thus, Figure 4.10 represents the truly selective conversion of 4-hydroxybenzyl cyanide in an acidic medium to form tyramine hydrogen sulphate in the liquid phase.

The reaction profile exhibits the form of a consecutive reaction. 4-Hydroxybenzyl cyanide conversion is rapid, being complete within a reaction time of approximately 8 minutes; with the complete conversion of 4-hydroxybenzyl cyanide corresponding to a turnover number of 184. Hydrogenation of the hydroxybenzyl imine to produce tyramine is clearly a much slower process. The product is formed on commencement of reaction and progressively increases thereafter; the reaction is complete by approximately 40 minutes. This sequence indicates the imine hydrogenation step to be rate limiting under the designated reaction conditions.

With reference to Scheme 4.4, the selectivity of the reaction (S) can be expressed in terms of the kinetics of primary amine formation *versus* the coupling reactions to form the secondary and tertiary amines: $S = k_2[H_2]/k_3[\text{primary amine}]$. Lowering the reaction temperature will affect both rate constants (k_2 and k_3) and is therefore reflective of differing activation energies for these competing reactions. Hence, a lower activation energy for the hydrogenation reaction than for the coupling reactions could provide preliminary reasoning for the improved selectivity towards tyramine that is observed at lower temperatures.

Another explanation, however, may be formulated. Whilst the hydrogen supply in the system has been optimised to avoid gas-to-liquid mass transport limitations, allowing a fixed concentration of hydrogen in solution, it is possible that there is a mass transport limitation at the liquid-solid interface. In this particular case it is conceivable that the rate of hydrogenation at 60 °C is too fast with respect to the provision of surface hydrogen (H_{ads}) causing a hold-up at the liquid-solid interface. However, at 30 °C the rate of reaction is slower, and thus the rate of provision of surface hydrogen is more in balance with the rate of hydrogenation. As a consequence, superior selectivity is observed under these conditions.

4.8 The Selective Production of Tyramine is Achieved Through Fine Tuning of the Reaction Parameters

Despite the favourable selectivity towards tyramine achieved in Figure 4.10, tuning of the reaction conditions and parameters was essential for this outcome to be realised. A summary of the optimisation process showing the effect of key parameter changes and their subsequent effect on selectivity is presented in Table 4.1. The most notable

improvement was detected upon inclusion of an acid additive. The addition of sulphuric acid to the reaction mixture effectively removed the tertiary amine from the system and drastically enhanced tyramine production. Further, at low stirring speeds, outside the kinetic regime for this system (Figure 4.4), the hydrogen supply was found to be limited, thus resulting in an unoptimised selectivity. This can be evidenced by the marked improvement in tyramine production (82% → 92%) upon elevation of the agitation rate. Further, a reduction in reaction temperature resulted in the completely selective formation of the desired primary amine. Thus, the combination of employing an acid as an auxiliary agent, operation within a kinetic regime effectively free from gas-liquid mass transport limitations, and utilising effective temperature control led to significant improvements in the returnable yield of the primary amine salt (tyramine hydrogen sulphate). These alterations illustrate the intricate nature of the process involved in achieving the completely selective production of a primary amine.

Table 4.1. Selectivity towards the primary, secondary and tertiary amines as a result of various parameter alterations. In all instances the following were constant: 4 barg hydrogen pressure with an external line pressure of 6.5 barg; 49 mmol L⁻¹ starting nitrile concentration in the presence of 2 equivalents of sulphuric acid in methanol. [1° Amine = tyramine; 2° Amine = di-hydroxyphenylamine; 3° Amine = tri-hydroxyphenylamine].

CONDITIONS			SELECTIVITY		
H ₂ SO ₄ / mol. equivalents	Stirring / rpm	Temp. / °C	1° Amine	2° Amine	3° Amine
0	450	60	14%	44%	30%
2	450	60	82%	18%	0%
2	1050	60	92%	8%	0%
2	1050	30	100%	0%	0%

4.9 Quantification of the Imine Intermediate was Attempted using the Mass Balance Relationship

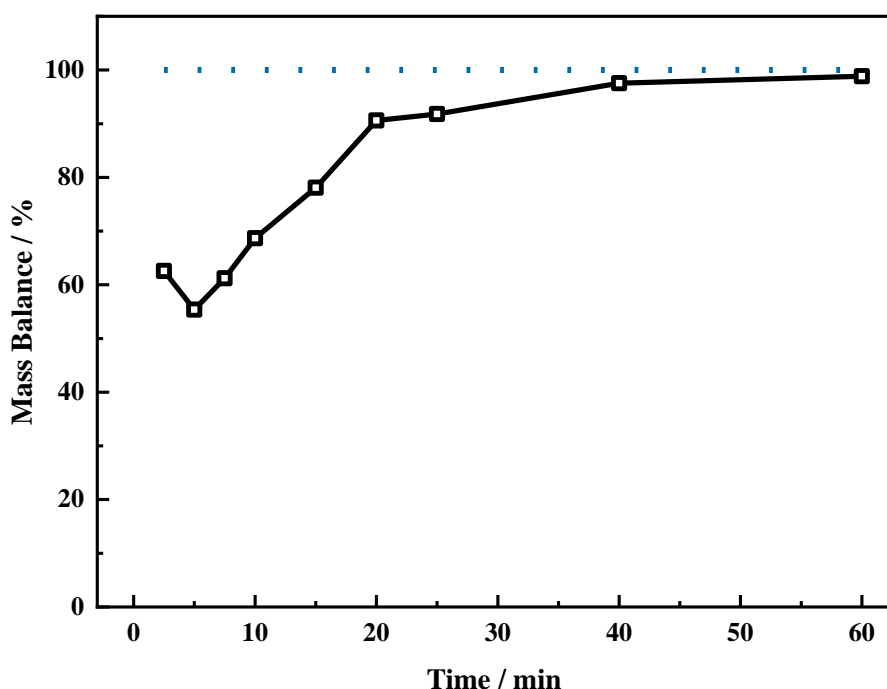


Figure 4.11. Mass balance plot associated with Figure 4.10 which shows the reaction profile for the liquid phase hydrogenation reaction of 4-hydroxybenzyl cyanide (49 mmol L^{-1}) over a 5% Pd/C catalyst (500 mg) in the presence of 2 equivalents of sulphuric acid in methanol. The reaction was conducted at 30°C under 4 barg hydrogen pressure with an external line pressure of 6.5 barg and an agitation speed of 1050 rpm. The solid black line defines the experimental mass balance whilst the dashed blue line represents a complete mass balance.

Figure 4.11 presents the mass balance plot associated with the reaction profile for the hydrogenation reaction of 4-hydroxybenzyl cyanide, conducted at 30°C , 4 barg hydrogen pressure and an agitation speed of 1050 rpm (reaction profile shown in Figure 4.10). Upon commencement of reaction there is a clear mass imbalance for the first 25 minutes of reaction. With reference to Figure 4.10, this corresponds to the period in which chromatography detects the presence of 4-hydroxybenzyl iminium hydrogen sulphate in the liquid phase. The mass imbalance reaches a maximum at 3 minutes, before progressively reducing until, by approximately 40 minutes, a closed mass balance is obtained. Collectively, Figures 4.10 and 4.11 suggest that during the earlier stages of the

reaction coordinate (0–25 minutes) it is the unquantified 4-hydroxybenzyl imine intermediate which is responsible for the mass imbalance.

As discussed in Section 4.2, the short-lived nature of the imine intermediate resulted in issues associated with the quantification of this reaction species. It is hence proposed that, if thought of in terms of concentration, the missing mass observed in Figure 4.11 can be used as a potential means of quantifying the imine intermediate. As the imine intermediate has been plotted thus far in the form of peak area, quantification would add further value to the reaction profile.

The mass balance relationship indicates that reagent starting concentration (A_0) should be equal to the sum of all concentration components of the reaction mixture at any given time in the reaction. A closed mass balance throughout the reaction coordinate is expected. Therefore, the missing mass detected in Figure 4.11, can be calculated as follows:

$$\text{Missing Concentration (Imine)} = [A_0] - [HBC] - [TYR] \quad \text{Equation 4.1.}$$

It should be noted that the above equation can only be applied to Figure 4.10, where no contribution from either the secondary or the tertiary amine is observed. In all other instances, the presence of the secondary amine or both secondary and tertiary amines must be considered. Following calculation of the missing concentration, a response factor for the imine species may be determined at any specific point in the reaction coordinate:

$$R_{ft} = \frac{\text{Peak Area}_t}{\text{Concentration}_t} \quad \text{Equation 4.2.}$$

The response factor (R_f) at time t can be calculated from peak area and concentration at time t . In this instance, peak area corresponds to the value obtained by HPLC analysis whilst concentration refers to the ‘missing’ concentration previously calculated (Figure 4.11). Repeating this process for all data points associated with the full reaction coordinate should result in a consistent R_f value regardless of the reaction time.

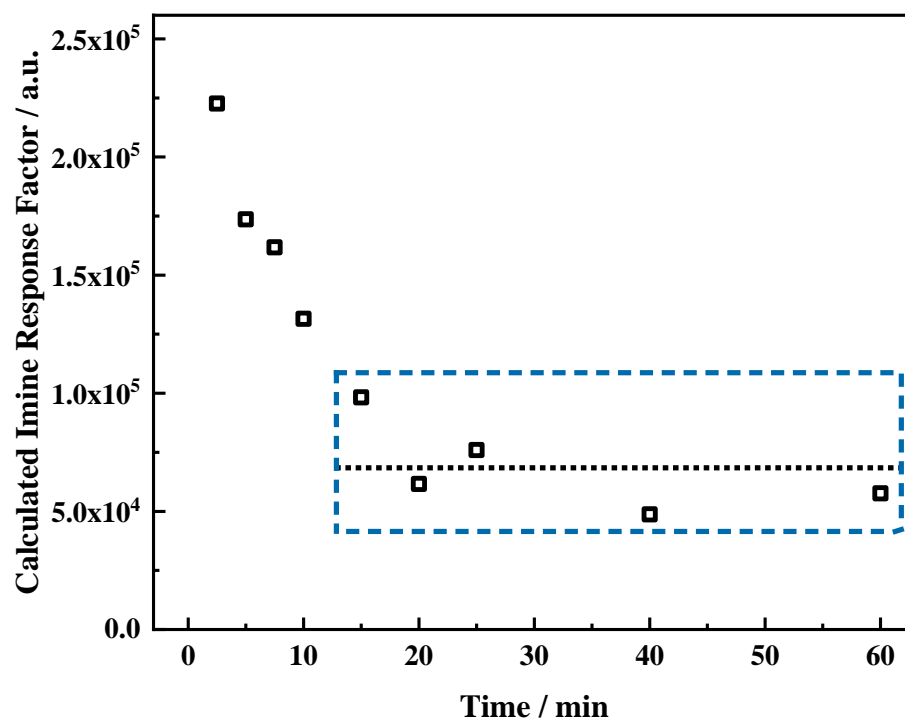


Figure 4.12. Calculated response factor for the imine intermediate based on the concentration data presented in Figure 4.10 for the liquid phase hydrogenation reaction of 4-hydroxybenzyl cyanide (49 mmol L^{-1}) over a 5% Pd/C catalyst (500 mg) in the presence of 2 equivalents of sulphuric acid in methanol. The reaction was conducted at 30°C under 4 barg hydrogen pressure with an external line pressure of 6.5 barg and an agitation speed of 1050 rpm. The dotted black line represents the average response factor associated with data points contained within the blue box.

Figure 4.12 shows the calculated response factor for the imine intermediate as a function of time. It is clearly observed that there is a noteworthy degree of variability in the calculated value throughout the reaction coordinate (0–60 minutes) making it unsuitable for use in the quantification of the intermediate species. Figure 4.12 shows the response factor to be significantly higher in the initial stages of the reaction (approximately 0–15 minutes). At times greater than 15 minutes, however, a more stable response factor for the imine intermediate is determined ($68432 \pm 7\%$).

The implication here is that a portion of the imine is retained on the surface of the catalyst, and thus, not available in the liquid phase for detection by HPLC. If it is, however, considered essential for the imine to be on the surface to facilitate product formation, this finding can be effectively rationalised. Nevertheless, the relative stability of the imine response factor observed towards the close of the reaction indicates that a decreasing quantity of the imine is bound to the surface as the reaction proceeds. This observation is

perhaps linked to the absence of 4-hydroxybenzyl cyanide in the system after approximately 10 minutes. Once complete conversion of the starting material is achieved, no further production of the 4-hydroxybenzyl imine will be facilitated, meaning that it cannot continue to build-up on the surface of the catalyst. Instead, the remaining imine will be hydrogenated to tyramine and released into the liquid phase resulting in the more stable response factor as observed in Figure 4.12 (blue box).

4.10 Selective Tyramine Production is Confirmed by ^1H NMR Spectroscopy

^1H NMR spectroscopy has been used within this substrate system for the quantification of the commercially unavailable secondary and tertiary amine by-products. However, due to the presence of distinctive ^1H NMR signals for both the substrate (4-hydroxybenzyl cyanide) and the desired product (tyramine) of this reaction, this technique is also found to be a suitable probe to monitor the progress of the reaction. This therefore allows the findings to be compared with those obtained by HPLC (Figure 4.10). As such, the experimental conditions connected with a high tyramine selectivity were also analysed by ^1H NMR spectroscopy. These conditions were: the presence of an acid additive at 30 °C; 4 barg hydrogen pressure; and an agitation of 1050 rpm. Accordingly, ^1H NMR spectra were collected at various points throughout the reaction coordinate.

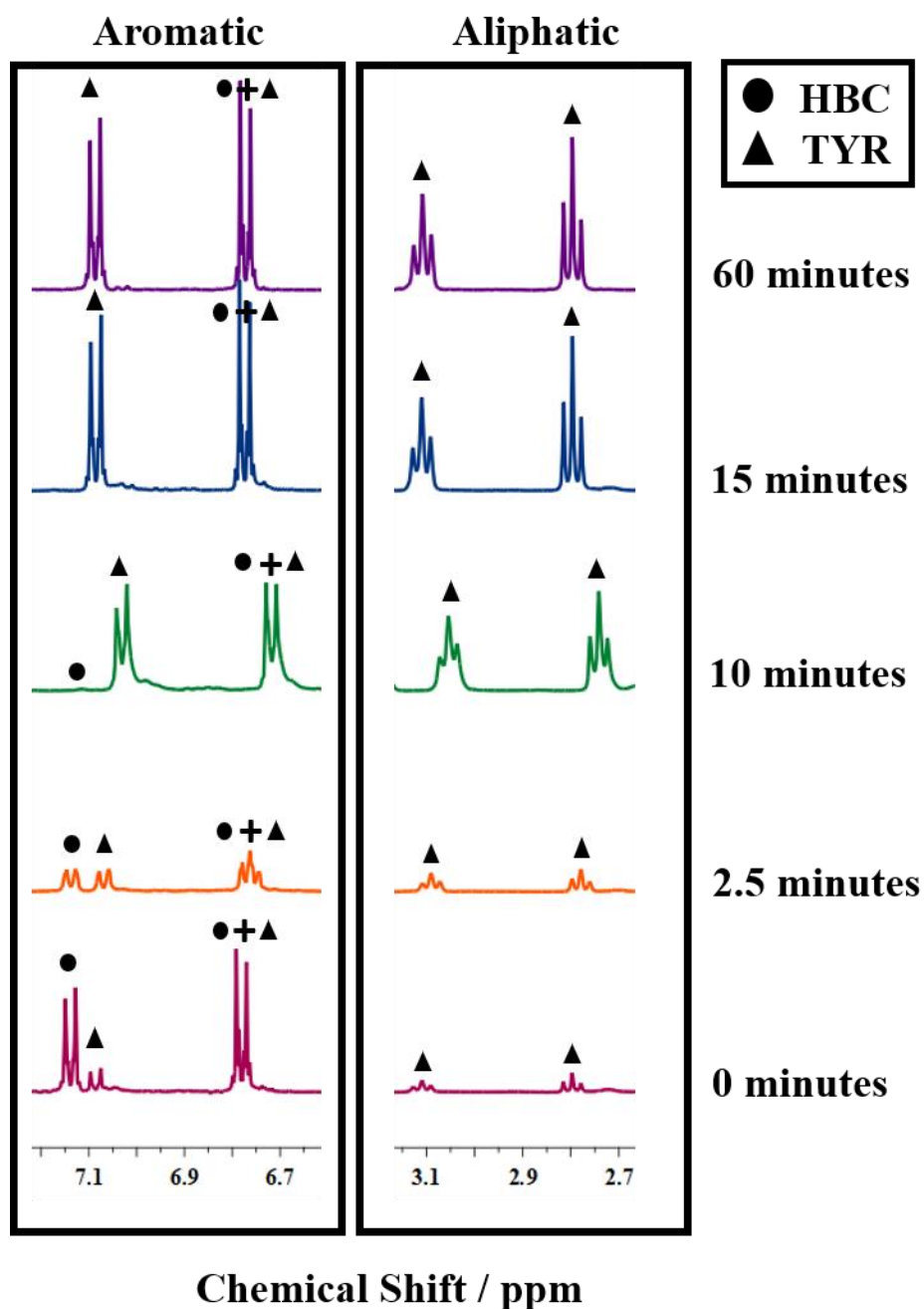


Figure 4.13. ^1H NMR spectra, with focus on the aliphatic and aromatic regions, for the liquid phase hydrogenation reaction of 4-hydroxybenzyl cyanide (49 mmol L^{-1}) over a 5% Pd/C catalyst (500 mg) in the presence of 2 equivalents of sulphuric acid in methanol. The reaction was conducted at 30°C under 4 barg hydrogen pressure with an external line pressure of 6.5 barg and an agitation speed of 1050 rpm. NMR solvent = D_2O . Peaks representative of the starting material and the product are indicated by circles and triangles respectively. [HBC = 4-hydroxybenzyl cyanide; TYR = tyramine].

Figure 4.13 shows a stack-plot of ^1H NMR spectra for the hydrogenation of 4-hydroxybenzyl cyanide. Measurements were taken at regular intervals up to reaction completion (time = 60 minutes) and the resulting spectra show peaks in both the aliphatic (2.7–3.1 ppm) and the aromatic (6.7–7.1 ppm) regions. Inclusion of a known concentration of ethylene glycol (0.49 mol L^{-1} , 1 equivalent), used here as an internal standard, was undertaken to facilitate the quantification of both reagent and product. Deuterium oxide, selected for its effective peak resolution in this particular system, was utilised as the deuterated solvent required for ^1H NMR analysis. Integration of the relevant peaks clearly shows consumption of reagent and production of product.

All chemical shifts were normalised relative to the residual methanol solvent peak at 3.34 ppm.^[213] Nevertheless, due to the presence of acid in the reaction mixture the signals were liable to drift. This effect was most notably observed in the deuterium oxide signal at 4.79 ppm.^[213] The internal standard ethylene glycol appeared at 3.65 ppm, thus avoiding overlap with peaks associated with either the reagent or the product. ^1H NMR spectral assignments for 4-hydroxybenzyl cyanide and tyramine are presented in Figure 4.14.

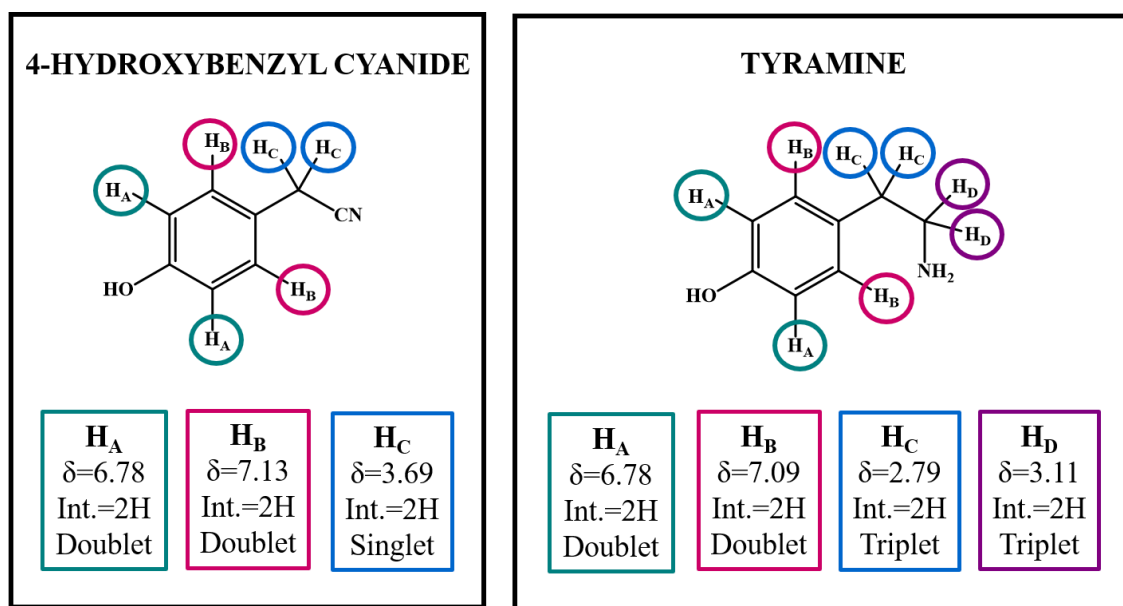


Figure 4.14. ^1H NMR spectroscopy assignments for 4-hydroxybenzyl cyanide (time = 0 minutes) and tyramine (time = 60 minutes). [δ = chemical shift (ppm); Int. = integration].

Interestingly, however, no obvious peaks associated with the imine intermediate (4-hydroxybenzyl iminium hydrogen sulphate), detectable by chromatographic means, were observed in any of the collected ^1H NMR spectra. It is postulated that this observation is a consequence of the practicalities of the technique. Methanol is required to be removed from the sample in order to obtain solvent-free spectra. This was achieved by conducting an overnight evaporation process. A vial containing approximately 3 mL of reaction mixture was covered with pin-pricked parafilm and left in a fumehood for evaporation to occur. Thus, the inherent reactivity of the imine means that these notoriously unstable molecules may be too short lived to be present during analysis. Closer spectral examination does reveal peaks in trace quantities of the imine at the relevant chemical shifts. As the imine was not observed in any appreciable quantity, however, it is probable that there is another rationale for its absence. It is suggested that, as the imine does not appear to tautomerise to its more stable enamine form, as evidenced by the absence of the associated ^1H NMR peaks, the imine itself is perhaps insoluble in the NMR solvent of choice (D_2O).

To improve the outcome, alternative methods of solvent removal, such as rotary evaporation, should be explored as well as the application of a different NMR solvent, such as dimethyl sulfoxide (DMSO). Further, the use of *in situ* ^1H NMR spectroscopy, using deuterated methanol and deuterated sulphuric acid, as a means of following the progress of the reaction, was additionally considered. This, however, was found not to be possible due to the hydrogen availability and hydrodynamic limitations present within the NMR vessel.

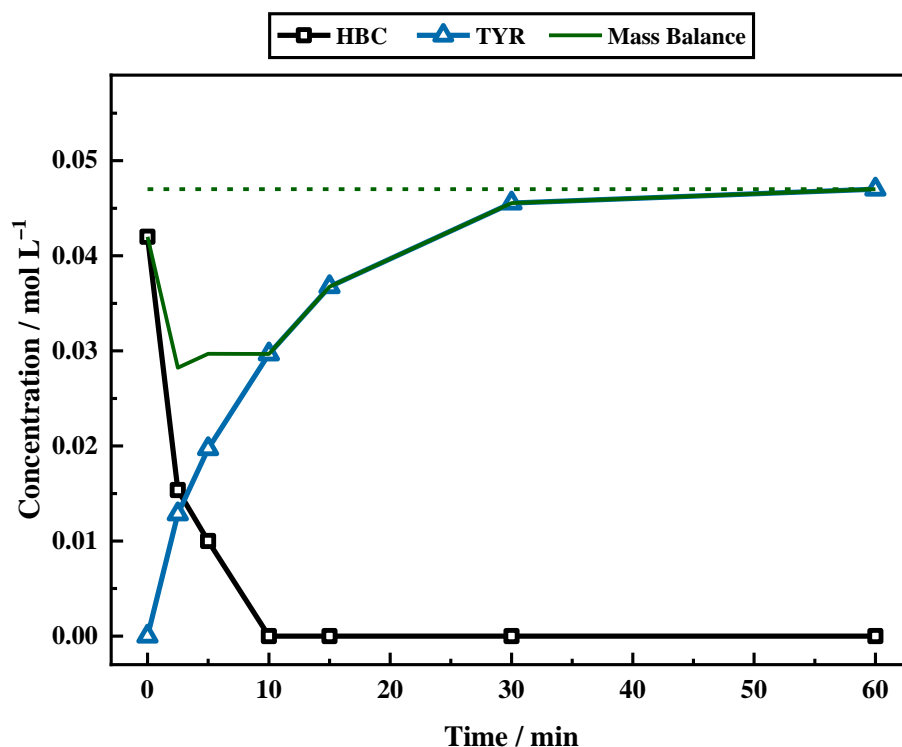


Figure 4.15. Reaction profile and mass balance obtained from the series of ¹H NMR spectra presented in Figure 4.13 for the liquid phase hydrogenation reaction of 4-hydroxybenzyl cyanide (49 mmol L⁻¹) over a 5% Pd/C catalyst (500 mg) in the presence of 2 equivalents of sulphuric acid in methanol. The reaction was conducted at 30 °C under 4 barg hydrogen pressure with an external line pressure of 6.5 barg and an agitation speed of 1050 rpm. [HBC = 4-hydroxybenzyl cyanide; TYR = tyramine; the dashed green line represents a complete mass balance].

Integration of the highlighted reagent and product peaks in Figure 4.13, referenced to the internal standard (ethylene glycol), enables the production of a quantitative reaction profile (Figure 4.15). This is in good agreement with the reaction profile obtained by HPLC analysis (Figure 4.10). As determined by ¹H NMR spectroscopy, Figure 4.15 shows 4-hydroxybenzyl cyanide to be consumed within 10 minutes and tyramine production to be complete at approximately 40 minutes reaction time.

Also highlighted in Figure 4.15 is the mass balance obtained by ¹H NMR spectroscopy. The trend observed by HPLC (Figure 4.11), typified by an initial mass imbalance that slowly recovers over time to ultimately return a complete mass balance once hydrogen consumption is terminated, is replicated by ¹H NMR spectroscopy in Figure 4.15. Despite the absence of definitive spectral evidence for the imine intermediate, the mass imbalance

observed in Figure 4.15 was tentatively assigned as an indicator of the presence of the imine.

Further analysis of the ^1H NMR spectrum reveals that, with the exception of features connected with reaction solvent (CH_3OH), NMR solvent (D_2O) and the internal standard (ethylene glycol), only peaks associated with 4-hydroxybenzyl cyanide and tyramine hydrogen sulphate are present. No other features are detected. Thus, Figure 4.15 endorses the outcome of Figure 4.10; namely, the selective formation of the primary aromatic amine hydrogen sulphate salt from the hydrogenation of 4-hydroxybenzyl cyanide.

One further point worthwhile noting relates to the possibility of homogeneous reactions occurring within this reaction system. The reaction profile depicted in Figure 4.10 shows a total absence of secondary and tertiary amine by-products after 60 minutes reaction time. The ^1H NMR spectra presented in Figure 4.15 validates this outcome. However, when sample vials containing the colourless analyte were left for an extended period of time (overnight) under ambient conditions, certain samples exhibited a distinct colour change. Specifically, samples corresponding to the reaction period 5–15 minutes, *i.e.* containing both 4-hydroxybenzyl iminium hydrogen sulphate and tyramine hydrogen sulphate, developed a brown colouration. Contrastingly, samples taken at reaction times where the imine was absent (20–60 minutes) remained colourless. The colouration is assumed to reflect homogeneous chemistry that results in the formation of higher molecular weight conjugated molecules. These are typically formed from a reaction between solvated 4-hydroxybenzyl iminium hydrogen sulphate and the tyramine hydrogen sulphate entities. This action highlights the reactive nature of the imine species. Nonetheless, given the relatively short reaction time of the heterogeneous chemistry illustrated in Figure 4.10 (≤ 60 minutes) compared to the long period of the homogeneous process (≥ 12 hours), the observed homogeneous chemistry is not a major concern for the heterogeneously catalysed selective production of tyramine under consideration here.

4.11 Positioning of the α -Carbon Relative to the Aromatic Ring System Dictates the Accessibility of the Hydrogenolysis Process

Given that this is exactly the same 5% Pd/C catalyst and experimental apparatus as used by McMillan *et al.*,^[35] the inability of this catalyst to support the proposed hydrogenolysis reaction, outlined in Scheme 4.4, is a surprising result. Indeed, for the benzonitrile hydrogenation reaction over the catalyst, hydrogenolysis was a dominant pathway to such a degree that, ultimately, toluene was produced with complete selectivity.^[35] This particular reactivity was interpreted with a 3-site model for the catalyst. Namely, one site for the hydrogenation of nitrile/imine, one site for the hydrogenolysis and a final site for the dissociative adsorption of dihydrogen (which can also encompass the other sites). This model was consistent with co-adsorption studies.^[35] Therefore, given that the catalyst has been shown to facilitate hydrogenolysis, this raises the question of why the hydrogenolysis reaction is inaccessible under the presented reaction conditions for the hydrogenation of 4-hydroxybenzyl cyanide.

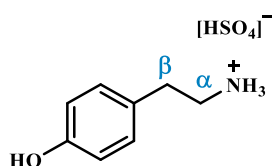


Figure 4.16. Molecular structure of the tyramine hydrogen sulphate salt. The α and β methylene units of the substituent arm are referenced relative to the amine functionality.

Figure 4.16 presents the molecular structure of tyramine hydrogen sulphate and identifies the aliphatic carbon atoms as the α and β positions relative to the amine functionality. The facile hydrogenolysis of benzylamine over this catalyst^[35] suggests that, for hydrogenolysis to be supported, the α -carbon must be adjacent to the aromatic ring. Indeed, Maschmeyer *et al.* suggest exactly that; explicitly, that it is the presence of an aromatic group adjacent to the α -carbon that facilitates hydrogenolysis.^[32] Thus, it is suggested that the ammonium leaving group needs to be connected to the aromatic ring *via* a single methylene group in order to facilitate the hydrogenolysis step. In the case of the tyramine hydrogen sulphate salt, the additional methylene linker in the substituent arm does not meet this molecular requirement. As such, it was predicted, and subsequently found to be in line with the experimental findings, that hydrogenolysis of

tyramine to afford 4-hydroxyethylbenzene will not occur. This scenario implies that the site-selective hydrogenation/hydrogenolysis chemistry invoked by McMillan *et al.* [35] is molecule specific.

Computational calculations conducted by Kieboom *et al.* [214] on the hydrogenolysis of benzyl alcohol derivatives over Pd/C suggest that the aromatic ring is π -bonded to the catalyst surface. Here it is postulated that when hydrogenolysis occurs the transition state facilitates overlap between the electron deficient p-orbital of the α -carbon and the π -orbitals of the benzene ring. The necessity for this orbital overlap rationalises, on account of geometry, why the additional methylene linker present in 4-hydroxybenzyl cyanide is not conducive to a hydrogenolytic process.^[214]

4.12 Conclusions

A 5% Pd/C catalyst has been used to affect the hydrogenation of 4-hydroxybenzyl cyanide within a three-phase reactor. Adjustment of various experimental parameters has led to improved catalytic performance, such that the desired tyramine salt can be produced in quantitative yield. The major findings of which have been summarised in Table 4.1 and the following conclusions drawn:

- In the absence of an acid additive a mixture of products, including the primary, secondary and tertiary amines, was produced resulting in a poor selectivity towards the desired product (14%).
- Inclusion of 2 equivalents of sulphuric acid afforded major improvements, with tertiary amine production being prevented and secondary amine formation considerably hindered. Combined, this resulted in an increase in tyramine selectivity to 82%.
- Though not quantified, the imine intermediate becomes observable in the presence of the acid additive.
- Primary amine selectivity was further enhanced by increasing agitation speed through minimisation of gas-to-liquid mass transfer constraints.

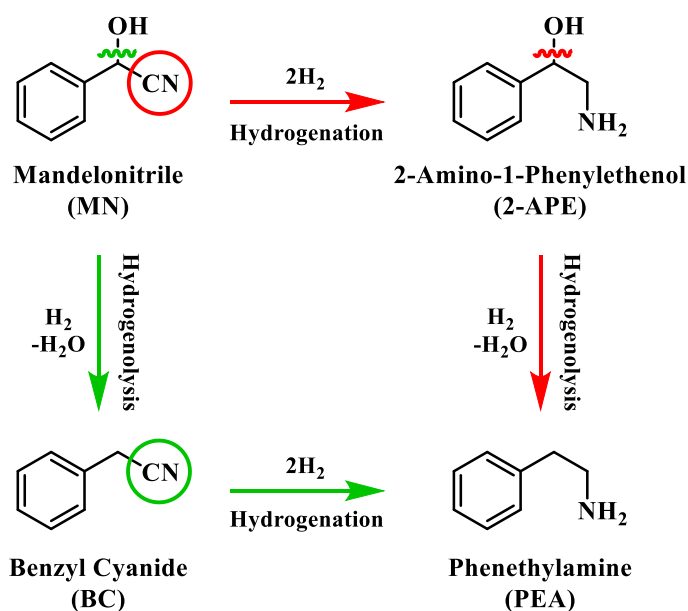
- Increasing the hydrogen pressure increases the selectivity towards tyramine until a critical pressure (4 barg). A further increase in hydrogen pressure from this value, however, does not facilitate any enhancement in the selectivity towards tyramine.
- A reduction in reaction temperature was shown to enhance the rate of hydrogenation over the rate of the coupling reactions to afford tyramine in 100% selectivity.
- The selective production of tyramine under optimised reaction conditions is confirmed by ^1H NMR spectroscopy.
- Hydrogenolysis of the tyramine salt was not observed under any of the presented reaction conditions.
- It is tentatively suggested that the hydrogenolysis process of a substituent protonated amine moiety requires there to be a single methylene unit between the aromatic ring and the leaving group.

CHAPTER 5

*The Liquid Phase Hydrogenation
Reaction of Mandelonitrile:
Towards a Mechanistic
Understanding*

5.1 Introduction

Using the insight gleaned from the 4-hydroxybenzyl cyanide system (Chapter 4), investigation of a new substrate system was initiated. Hydrogenation of the cyanohydrin mandelonitrile, over the same carbon supported palladium catalyst as was employed in the previous chapter, was utilised to afford the desired primary amine, phenethylamine. The increased molecular complexity of this substrate – owing to the presence of both the hydroxyl and cyanide functionalities on the same carbon atom – affords a reaction system which can be used as an effective model for a Syngenta process. As such, this chapter encompasses the preliminary experimental and analytical hurdles as well as the early mechanistic information regarding the hydrogenation reaction of mandelonitrile.



Scheme 5.1. Proposed reaction scheme for the hydrogenation reaction of mandelonitrile, showing two available routes, highlighted in red and green, to afford phenethylamine.

The transformation of mandelonitrile to phenethylamine requires release of the hydroxyl group; a process that may be attributed to a dehydration reaction, forming water as a by-product. However, based on previous investigations into the hydrogenolysis of benzylamine by McMillan and co-workers within the Lennon group, where the loss of ammonia was shown to be facilitated by a hydrogenolytic step, it is proposed that for the mandelonitrile system there is a corresponding hydrogenolysis mechanism which facilitates the loss of water.^[35–36, 150–151] Thus, with reference to Scheme 5.1, two possible

routes to the desired product may be considered.^[110] To successfully produce phenethylamine, both hydrogenation of the nitrile functionality and hydrogenolysis of the hydroxyl group are required. Scheme 5.1 therefore highlights that the order in which the hydrogenation and hydrogenolysis steps take place dictates the intermediate species observed. This intermediate may be either 2-amino-1-phenylethanol (red route) or benzyl cyanide (green route). With a thorough exploration of the hydrogenation reaction of benzonitrile already undertaken,^[35–36] and using the routes suggested in Scheme 5.1 as a basis, a simple consecutive process from the nitrile to the target amine was initially envisaged. To this end, the mechanism for the mandelonitrile hydrogenation reaction is investigated.

5.2 Understanding the Mandelonitrile Hydrogenation Reaction Profile

As the mandelonitrile substrate system had been examined previously by both McMillan^[150] and Gilpin^[151] a benchmarking exercise was conducted. This was undertaken to ensure that the correct methodology was employed, and to document a smooth transition between PhD projects. Figure 5.1 shows the reaction profile for the liquid phase hydrogenation reaction of mandelonitrile over a 5% Pd/C catalyst reported by Gilpin (2012–2016).

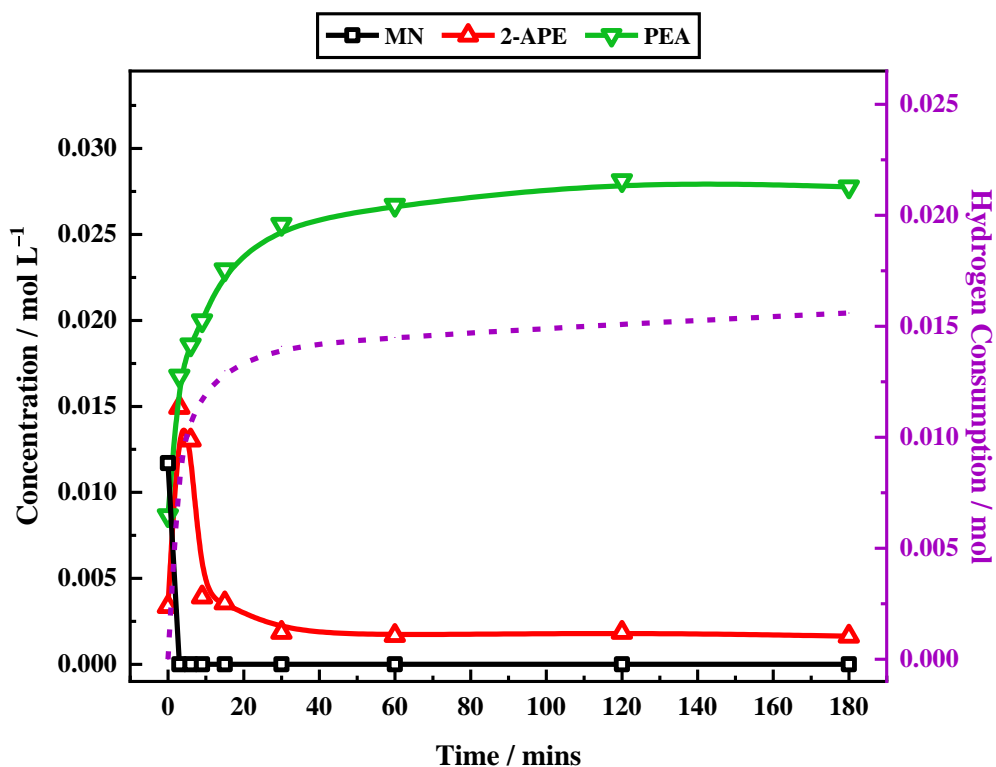


Figure 5.1. The reaction profile and hydrogen uptake curve (dashed purple line on the second y-axis) for the liquid phase hydrogenation reaction of mandelonitrile (35 mmol L^{-1}) over a 5% Pd/C catalyst (300 mg) in the presence of 2 equivalents of sulphuric acid in methanol achieved by Gilpin. The reaction was conducted at 40°C under 6 barg hydrogen pressure with an external line pressure of 6.5 barg and an agitation speed of 1050 rpm. [MN = mandelonitrile; 2-APE = 2-amino-1-phenylethanol; PEA = phenethylamine]. This figure has been reproduced from reference 151.

Figure 5.1 shows rapid and complete consumption of the mandelonitrile, with 100% conversion obtained within the first few minutes of the reaction. Production of the desired primary amine (phenethylamine) is observed from the inception of the reaction, with a selectivity of 87% obtained by reaction completion (time = 120 minutes). Additionally, Figure 5.1 shows the reaction to proceed exclusively *via* 2-amino-1-phenylethanol as an intermediate (selectivity = 8% at reaction completion). No benzyl cyanide was observed. By reaction completion, as indicated by a plateau in the accompanying hydrogen uptake curve, a near complete mass balance (not shown) was achieved (95%), suggesting the absence of additional chemistry.

Initially, however, the occurrence of undesirable homogeneous reactions was found to complicate the analysis method giving misleading results. Analysis of the reaction mixture at ambient temperature revealed a peak area inconsistency at the elution time of

2-amino-1-phenylethanol. The peak area determined by HPLC was found to be variable. Subsequent investigation of sample stability was undertaken by extracting a large aliquot (approximately 20 mL) of reaction mixture from a standard mandelonitrile hydrogenation reaction. This aliquot was removed at a time where the species, identified as the source of the variable peak output, was known to be present (time = approximately 5 minutes). Residual catalyst was then filtered off and the sample divided into equal parts. Each vial was then placed in the HPLC auto-sampler with a time delay between the analyses of each sample. This allowed the area of the 2-amino-1-phenylethanol peak to be measured with respect to time. As each vial contained a sample taken from the autoclave at the same time, each chromatograph should produce an identical trace. Concentration, however, was shown to be inconsistent (Figure 5.2, blue bars). Instead it was shown to increase with time indicating that the reaction mixture was not stable at room temperature.

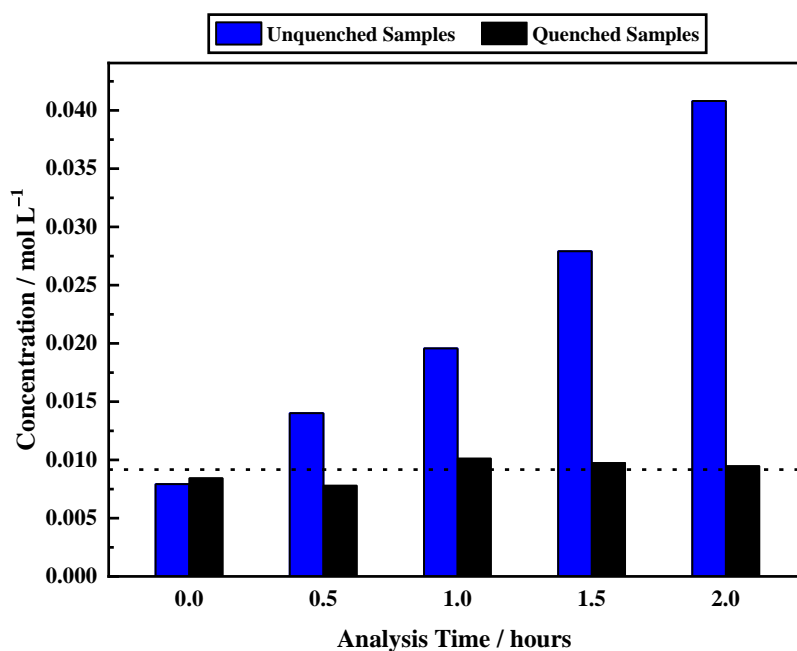


Figure 5.2. Concentration values obtained chromatographically for the '2-amino-1-phenylethanol' peak with increasing time post-extraction from the autoclave; comparing quenched (black) with unquenched (blue) samples. The dashed line represents the average concentration of the quenched samples (9 mmol L⁻¹). Figure adapted from reference 151.

The occurrence of homogeneous chemistry in the sample vials, in the form of acid catalysed reactions, would account for the observed peak growth. Specific reactions taking place under these conditions were not identified, but their occurrence indicates the existence of underlying complexity within the homogeneous phase of this reaction system. Subsequent alteration of the experimental protocol, involving the quenching of all reaction sample vials in ice prior to HPLC analysis, alleviated this problem with a significantly more consistent concentration being obtained (Figure 5.2, black bars). For a single batch run, the issues associated with homogeneous chemistry were eliminated utilising the quenching protocol, with the resultant reaction profile representing solely the palladium catalysed hydrogenation reaction. Nonetheless, the essential nature of this protocol highlights that there is a degree of mechanistic complexity associated with this system which is not currently highlighted within the reaction scheme (Scheme 5.1).

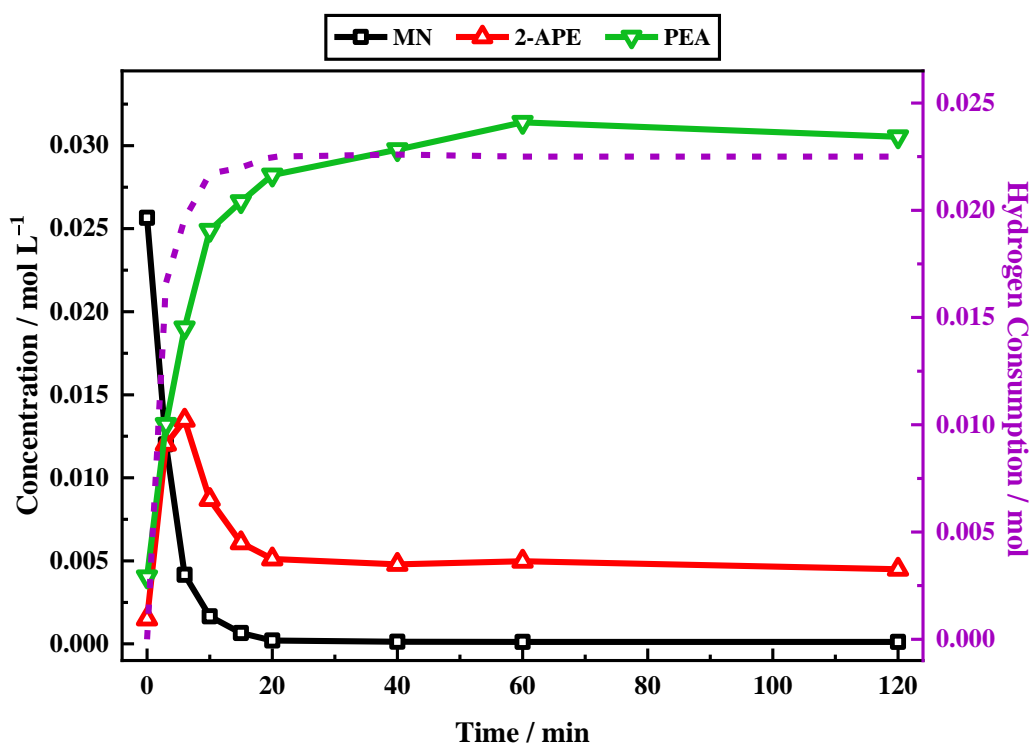


Figure 5.3. Reaction profile and hydrogen uptake curve (dashed purple line on the second y-axis) for the liquid phase hydrogenation reaction of mandelonitrile (35 mmol L^{-1}) over a 5% Pd/C catalyst (300 mg) in the presence of 2 equivalents of sulphuric acid in methanol. The reaction was conducted at 40°C under 6 barg hydrogen pressure with an external line pressure of 6.5 barg and an agitation speed of 1050 rpm. [MN = mandelonitrile; 2-APE = 2-amino-1-phenylethanol; PEA = phenethylamine].

Figure 5.3 shows the reaction profile and hydrogen uptake curve for the hydrogenation reaction of mandelonitrile under analogous conditions to those employed by Gilpin and demonstrates a comparable outcome to that observed in Figure 5.1. As before, the mandelonitrile is rapidly converted within approximately 20 minutes (*cf.* the Gilpin profile which reached complete conversion within 4 minutes). With regard to product distribution at reaction completion (time = 120 minutes), the desired product, phenethylamine, and the by-product, 2-amino-1-phenylethanol, are observable under both sets of conditions (Figures 5.1 and 5.3). Nevertheless, whilst a comparable selectivity towards phenethylamine was observed (Gilpin 89%; McAllister 87%), the 2-amino-1-phenylethanol selectivity shows a more notable difference (Gilpin 8%; McAllister 13%). It is important to note that different analytical equipment, namely different HPLC instruments, with different sensitivity levels have been employed to achieve the two reaction profiles (compare Figure 5.1 with Figure 5.3). The variances associated with both sets of equipment may be the cause of the differing reaction profiles observed. Consequently, direct comparisons cannot be made. Overall, however, the same general trends were observed for both profiles indicating that the benchmarking exercise was successful.

Despite the successful benchmarking procedure, it is essential that advantage of the more sensitive analytical equipment employed on this project is taken. Consequently, alteration of the analytical protocol to that previously used is explored as a means of gleaning further details regarding the mandelonitrile hydrogenation reaction mechanism.

5.3 Exploration of the Analytical Protocol Allowed Further Chromatographic Details to be Revealed

Chromatographically, at approximately 4 minutes, an indistinct peak was observed. From the calibration work necessary for quantification, it was established that this corresponded to the time 2-amino-1-phenylethanol eluted from the column. As previously documented (Section 5.2), Gilpin also reported chromatographic issues at this retention time. Nonetheless, alteration of the experimental procedure appeared to alleviate this problem (Section 5.2).^[151] Further investigation at that time was not undertaken.

The aforementioned indistinct peak was integrated under the assumption that it was composed entirely of 2-amino-1-phenylethanol (Figures 5.1 and 5.3, red trace). However,

due to the enhanced analytical sensitivity of the HPLC unit associated with this project, an investigation of the current analytical protocol was undertaken to ascertain whether improvements could be made.

The wavelength of the absorbance of the ultraviolet-visible detector was changed from the standard 254 nm to 210 nm. The shorter wavelength allowed for greater analytical sensitivity to be achieved due to an improved absorbance and resulted in the detection of increased peak areas. This alteration highlighted the fact that there was in fact the co-elution of two peaks occurring at the retention time of interest. Whilst closer inspection of previous chromatographs showed that this observation was also detectable at 254 nm, it can be seen with greater clarity where this other species is entering and departing the system at 210 nm.

Following the analytical wavelength alteration, changes to the solvent gradient timetable were implemented to afford better separation of the two co-eluting peaks. The analysis time was extended from 15 to 24 minutes, allowing for a more gradual release of the reaction components from the column. These changes afforded a chromatogram with two distinct peaks appearing at an analysis time of approximately 3–4 minutes. The separate integration of these two similarly eluting species culminated in the production of an alternative reaction profile. It is thus observed that the changes to the chromatographic analysis presented here have allowed a more precise representation of the reaction mixture throughout the course of the hydrogenation reaction to be determined.

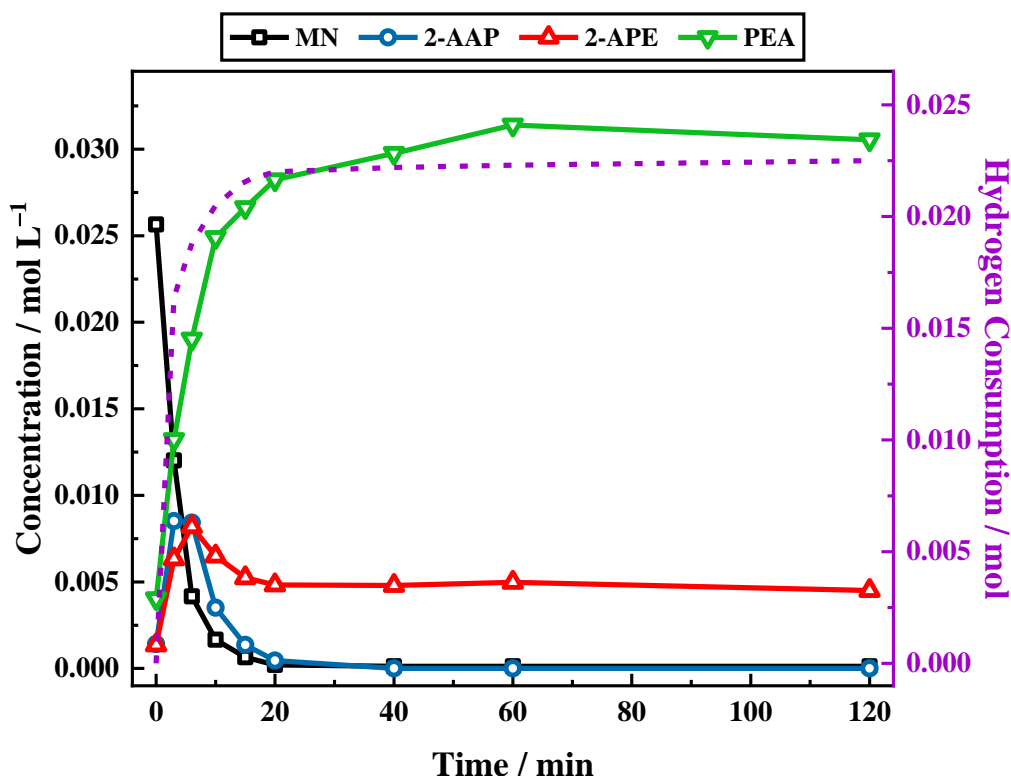


Figure 5.4. Reaction profile and hydrogen uptake curve (dashed purple line on the second y-axis) for the liquid phase hydrogenation reaction of mandelonitrile (35 mmol L^{-1}) over a 5% Pd/C catalyst (300 mg) in the presence of 2 equivalents of sulphuric acid in methanol. The reaction was conducted at 40°C under 6 barg hydrogen pressure with an external line pressure of 6.5 barg and an agitation speed of 1050 rpm. [MN = mandelonitrile; 2-AAP = 2-aminoacetophenone; 2-APE = 2-amino-1-phenylethanol; PEA = phenethylamine]. 2-aminoacetophenone is identified and quantified here for succinctness; however, during the discussed analysis these details were unknown.

Figure 5.4 shows the resultant reaction profile for the hydrogenation reaction of mandelonitrile using the improved analytical procedure. As shown in Figure 5.4, peak resolution has afforded the observation of two separate molecular entities in the place of the single trace for 2-amino-1-phenylethanol. Figure 5.4 assigns 2-amino-1-phenylethanol as the by-product of the reaction whilst the intermediate has been denoted ‘2-AAP’ and defined as 2-aminoacetophenone in the figure caption. The 2-aminoacetophenone intermediate has been included as a quantified molecule in Figure 5.4, however, during the initial analysis, this molecule was treated as an ‘unknown’. The identification of 2-aminoacetophenone as a reaction intermediate will be elaborated on in Section 5.5.

Ignoring the aforementioned assignments and as inferred by Scheme 5.1, it was initially proposed that 2-amino-1-phenylethanol was the sole detectable reaction intermediate. This would then imply that it was the by-product of the reaction which was ‘unknown’. Nevertheless, further investigation indicated that these initial assumptions were incorrect, with 2-amino-1-phenylethanol being definitively identified, by LC-MS, as the by-product. Scheme 5.1 therefore does not sufficiently convey the observable chemistry associated with this reaction, and rather provides a simplified version. Following these findings, identification of the ‘unknown’ intermediate was essential. A series of experiments were therefore commissioned to identify this molecule. As part of this process, different reaction conditions were tested to ascertain whether the acid additive played a role in the formation of the ‘unknown’ molecule. In essence, investigation was required to determine whether the formation of the ‘unknown’ reaction component was a result of palladium catalysed chemistry or of a homogeneous reaction.

5.4 Neutral Conditions are Found not to be Conducive for Phenethylamine Production

Unlike the 4-hydroxybenzyl cyanide system, which showed moderate conversion of the starting material under neutral reaction conditions (Figure 4.1), the cyanohydrin mandelonitrile proved problematic to convert in the absence of acid. It was initially proposed by McMillan ^[150] and Gilpin ^[151] that the hydrogenation reaction of mandelonitrile was a self-poisoning reaction where the 2-amino-1-phenylethanol reaction intermediate bound more strongly to the catalyst surface than the mandelonitrile, therefore blocking the palladium sites and causing cessation of the reaction.^[150–151]

Investigation of the 4-hydroxybenzyl cyanide system (Chapter 4) has allowed the role of the acid in nitrile hydrogenation reactions to be defined with greater clarity. Firmly established as an essential component of the reaction mixture for amine protonation purposes (Section 5.2), the sulphuric acid additive was removed from the mandelonitrile hydrogenation reaction to establish if the acid additive had any additional roles in this reaction system (Figure 5.5). Comparing the same set of reaction conditions, both with and without acid (Figures 5.4 and 5.5 respectively), a stark contrast is observed.

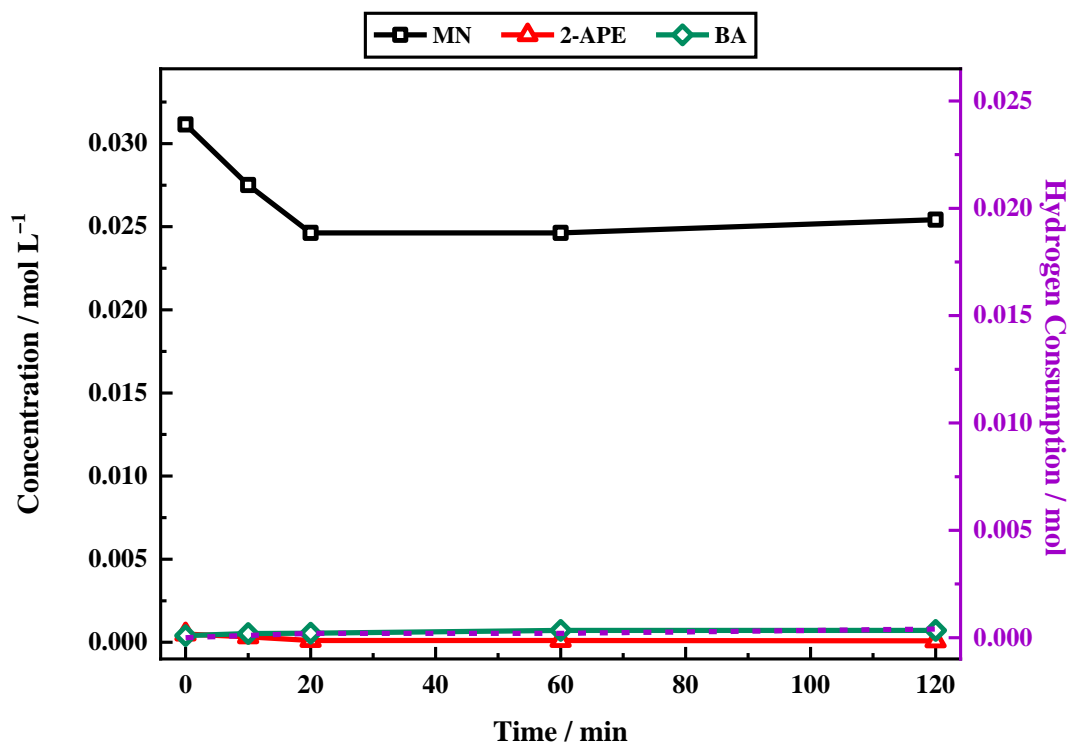


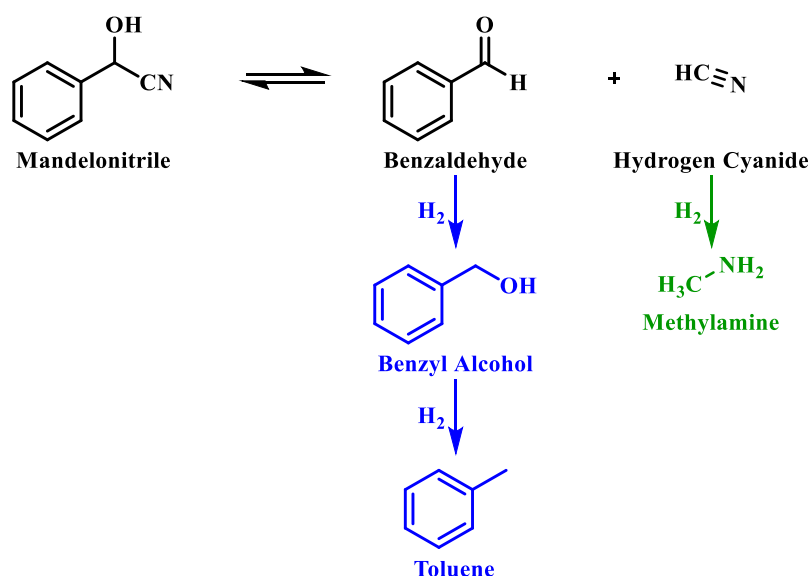
Figure 5.5. Reaction profile and hydrogen uptake curve (dashed purple line on the second y-axis) for the liquid phase hydrogenation reaction of mandelonitrile (35 mmol L^{-1}) over a 5% Pd/C catalyst (300 mg) in the **absence** of an acid additive in methanol. The reaction was conducted at 40°C under 6 barg hydrogen pressure with an external line pressure of 6.5 barg and an agitation speed of 1050 rpm. [MN = mandelonitrile; 2-APE = 2-amino-1-phenylethanol; BA = benzyl alcohol].

Figure 5.5 shows that, in the absence of an acid additive, only minimal mandelonitrile conversion is achieved, with the reaction being incomplete within the 120 minutes monitored time frame (*cf.* complete mandelonitrile conversion in 20 minutes is achieved in the presence of acid, Figure 5.4). Interestingly, however, whilst at a slower rate, moderate conversion (19%) of mandelonitrile is observed for the first 20 minutes of the reaction before a plateau is reached. This plateau could indicate poisoning of the catalyst by the amine products of the reaction, 2-amino-1-phenylethanol and phenethylamine. Despite this postulate, neither of these molecules were detectable in appreciable quantities chromatographically. Nevertheless, trace amounts of 2-amino-1-phenylethanol were observable (Figure 5.5). This finding, in combination with a reduced hydrogen uptake (2% of that detected in an acidic environment), indicates that the proposed reaction chemistry (Scheme 5.1) was not favourable under neutral reaction conditions.

The chromatographic output did, however, provide some useful results. At the elution time of interest (approximately 4 minutes), only one peak was present as opposed to the two closely eluting molecules observed under acidic conditions. The observed chromatographic peak was subsequently identified as 2-amino-1-phenylethanol. The absence of the ‘unknown’ species under neutral conditions is therefore indicative of its formation being an acid catalysed process.

Furthermore, and rather unprecedented, was consumption of the starting material far in excess of the detectable product yield, such that, a missing mass of 16% is detectable at reaction completion (time = 120 minutes). One postulate for the observed missing mass is the presence of surface bound 2-amino-1-phenylethanol and/or phenethylamine. If indeed the amine products were acting as a catalyst poison, it is likely that a portion of these would be present on the surface of the catalyst, hence accounting for some of the missing mass observed.

A further consideration is that, under neutral conditions, literature studies have reported mandelonitrile to be unstable and susceptible to spontaneous decomposition into its starting materials, namely, benzaldehyde and hydrogen cyanide.^[215] Benzaldehyde, whilst detectable by HPLC, was found to co-elute with mandelonitrile using the method reported in this work. Accordingly, the occurrence of this process was challenging to detect.



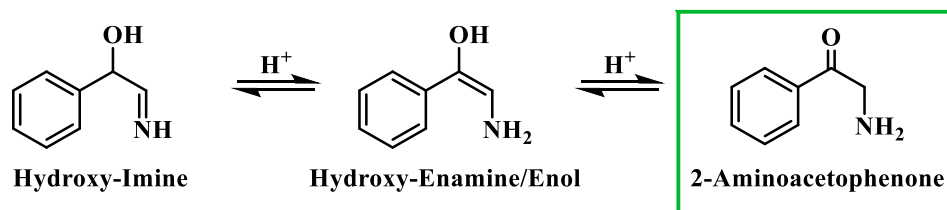
Scheme 5.2. Proposed reaction scheme for a potential side reaction in the hydrogenation reaction of mandelonitrile under neutral conditions.

Nevertheless, due to the necessary hydrogen presence in the reactor for the reduction of mandelonitrile, it is possible that benzaldehyde was also hydrogenated. In a reducing environment, benzaldehyde would be hydrogenated to toluene in a two-step process *via* benzyl alcohol, as is shown in Scheme 5.2. Supporting this hypothesis is the production, albeit in negligible quantities, of benzyl alcohol in the hydrogenation reaction of mandelonitrile under neutral conditions (Figure 5.5). Unfortunately, toluene was undetectable using the HPLC method employed. As such, this decomposition pathway culminating in toluene may be a contributor to the missing mass detected at reaction completion.

Inopportunately, the expected by-product of the decomposition of mandelonitrile is the highly undesirable hydrogen cyanide. It is, however, possible that this species could also be hydrogenated to the significantly less hazardous methylamine which, as a gaseous species, would not be detectable in the liquid phase.^[216] Precautions taken to prevent the release of the harmful hydrogen cyanide are detailed in the experimental section (Section 2.2.1).

5.5 2-Aminoacetophenone is Identified as a Reaction Intermediate

Alongside the production of phenethylamine and 2-amino-1-phenylethanol, another molecule was detectable in the liquid phase. Behaving as an intermediate (Figure 5.4), this molecule was identified by LC-MS as the ketone 2-aminoacetophenone (2-AAP: $\text{C}_6\text{H}_5\text{C}(\text{O})\text{CH}_2\text{NH}_2$).^[217] The formation of this species is found to be acid catalysed, as evidenced by its absence under neutral conditions (Section 5.4). The acid requirement provides rationalisation for the proposal of a tautomeric pathway in the mandelonitrile reaction system (Scheme 5.3). It is important to note at this juncture that no imine or enamine species are observable in the liquid phase, indicating that they exist as assumed adsorbed species. Within this constraint, their presence is implied and/or inferred within mechanistic considerations but, under the stated arrangements, cannot be verified experimentally.



Scheme 5.3. Proposed formation of 2-aminoacetophenone via a two-step tautomeric pathway originating at the hydroxy-imine intermediate. Hydrogenation of the nitrile moiety of mandelonitrile to form the hydroxy-imine precedes this tautomeric pathway. This step, however, has been excluded from the scheme for clarity.

Referring to Scheme 5.3, it can be seen that the hydroxy-imine can undergo an acid catalysed tautomerisation to form 2-aminoacetophenone in a two-step process. The hydroxy-imine is first transformed to a hydroxy-enamine, which, due to the presence of the alcohol functionality can also be classified as an enol. This enol can then be readily converted to its keto form, 2-aminoacetophenone, in the presence of acid. Typically, at equilibrium, it is the keto form of the carbonyl species which is lower in energy,^[109] and thus predominates. Therefore, the formation of 2-aminoacetophenone is demonstrated to be energetically favourable. Moreover, the acid catalysed nature of these tautomerisation reactions provides reasoning for the absence of 2-aminoacetophenone under neutral reaction conditions (Figure 5.5).

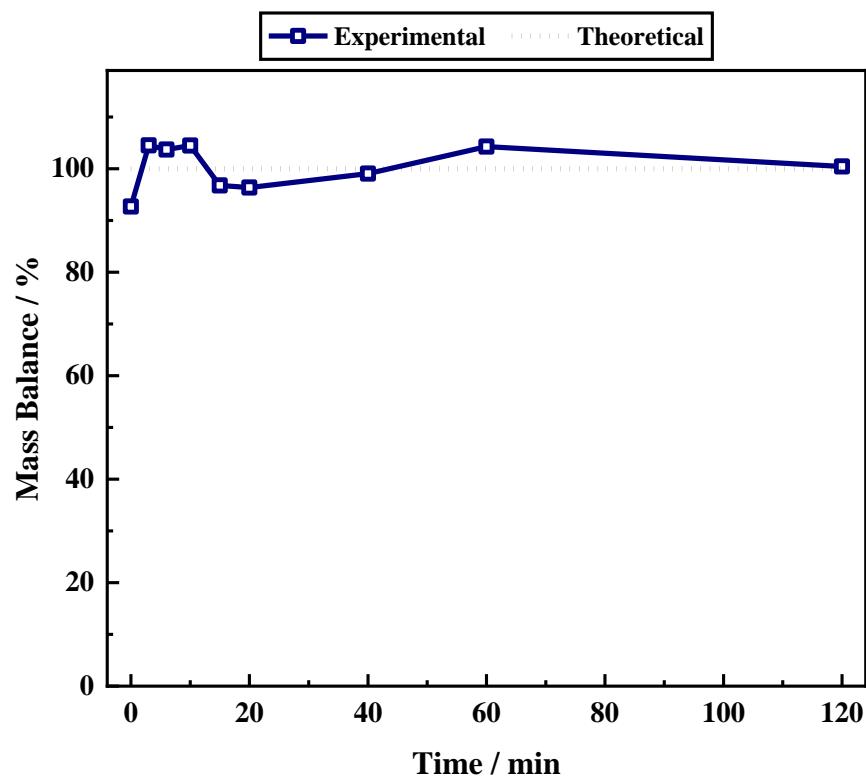
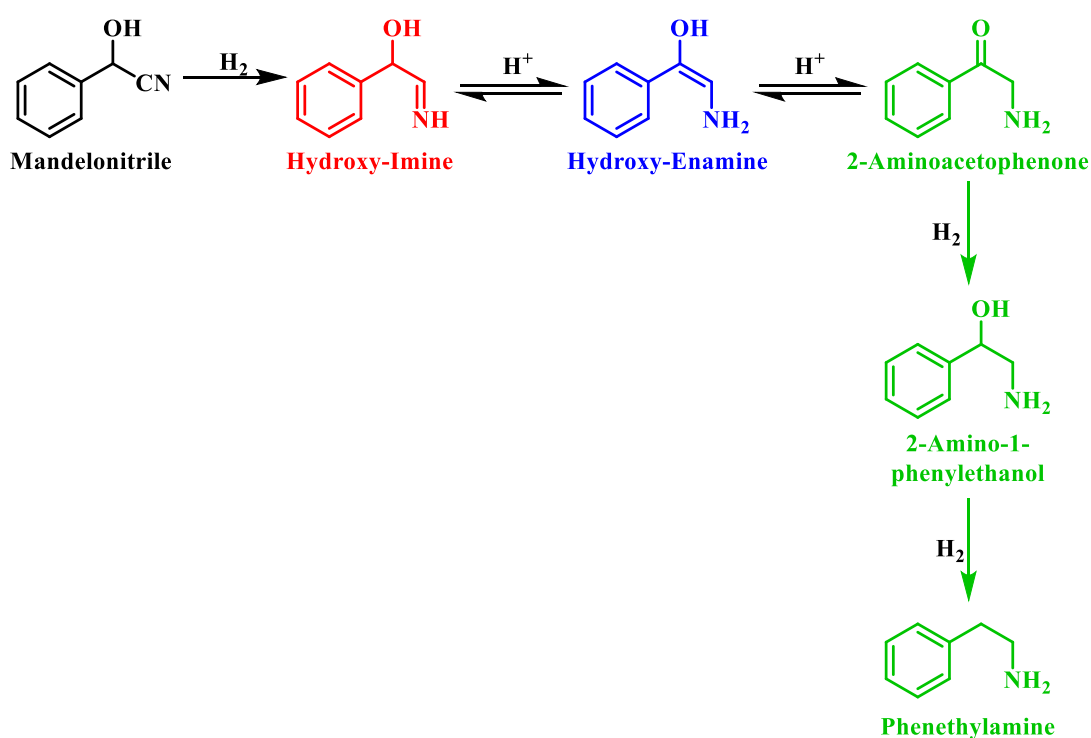


Figure 5.6. Mass balance plot for the liquid phase hydrogenation reaction of mandelonitrile (35 mmol L^{-1}), over a 5% Pd/C catalyst (300 mg) in the presence of 2 equivalents of sulphuric acid in methanol. The reaction was conducted at 40°C under 6 barg hydrogen pressure with an external line pressure of 6.5 barg and an agitation speed of 1050 rpm. The corresponding reaction profile is presented in Figure 5.4.

Adding further complexity to the reaction system, it is acknowledged that, similar to 2-aminoacetophenone, the hydroxy-imine and the hydroxy-enamine are likely to be susceptible to both hydrogenation and hydrogenolysis reactions. Assuming the imine and enamine intermediates exist as adsorbed species further enhances this possibility. No other acid catalysed homogeneous reactions for the batch conditions presented here were detected. Thus, a degree of control over the reaction, as evidenced by a complete mass balance, is demonstrated (Figure 5.6). At reaction termination (time = 120 minutes) the selectivity towards phenethylamine and 2-amino-1-phenylethanol was 87% and 13%, respectively.

5.6 Development of the Reaction Scheme

The identification of mechanistic complexity within the mandelonitrile hydrogenation reaction system, namely the occurrence of an acid catalysed tautomeric pathway to yield 2-aminoacetophenone, necessitates a greater degree of mechanistic precision than that which is available in the current reaction scheme (Scheme 5.1). It is proposed that a mechanistic study would allow the originally proposed two-step consecutive pathway (Scheme 5.1) to be superseded by a more intricate reaction scheme. This scheme therefore aims to more accurately represent the observed chemistry associated with this reaction system.



Scheme 5.4. Schematic development for the palladium catalysed mandelonitrile hydrogenation reaction system. The updated reaction scheme includes the relevant acid catalysed chemistry which is involved in the formation of the intermediate 2-aminoacetophenone.

Included in Scheme 5.4 is the acid catalysed tautomeric pathway which results in formation of observable intermediate 2-aminoacetophenone. Both 2-aminoacetophenone and its anticipated hydrogenation product (2-amino-1-phenylethanol) are detectable chromatographically. The other proposed intermediate, benzyl cyanide (Scheme 5.1),

however, has not been observed chromatographically, and is therefore excluded from the reaction scheme.

The original findings suggested that 2-amino-1-phenylethanol was a key intermediate of the reaction. Nonetheless, further probing indicated that this was not the case. It is hence proposed that examination of the hydrogenation reactions of both 2-amino-1-phenylethanol and 2-aminoacetophenone would deliver valuable mechanistic information regarding their roles in the production of the desired product. At this point in the study it is important to recognise that, whilst it is acknowledged that both the hydroxy-imine and the hydroxy-enamine are likely to possess active chemistry in a hydrogenation environment, the relevant intermediate species are not detected in the liquid phase, thus limiting the mechanistic analysis of these intermediates.

5.7 The Hydrogenolysis Reaction of 2-Amino-1-phenylethanol

Figure 5.7 A presents the reaction profile for the hydrogenolysis reaction of 2-amino-1-phenylethanol, under standard reduction conditions (Section 5.3). As previously shown (Figure 5.4), the conversion of the nitrile functionality was a relatively facile process with desired product formation, coinciding with cessation of hydrogen uptake, reaching a plateau at approximately 20 minutes into the reaction. It would therefore be reasonable to assume that the hydrogenolysis reaction of 2-amino-1-phenylethanol would occur on a similar time scale. Looking solely at section A of Figure 5.7, which represents the first 120 minutes of the reaction, it can be seen that only minimal conversion of 2-amino-1-phenylethanol is achieved under the same reaction conditions. This results in a poor product yield of 5%.

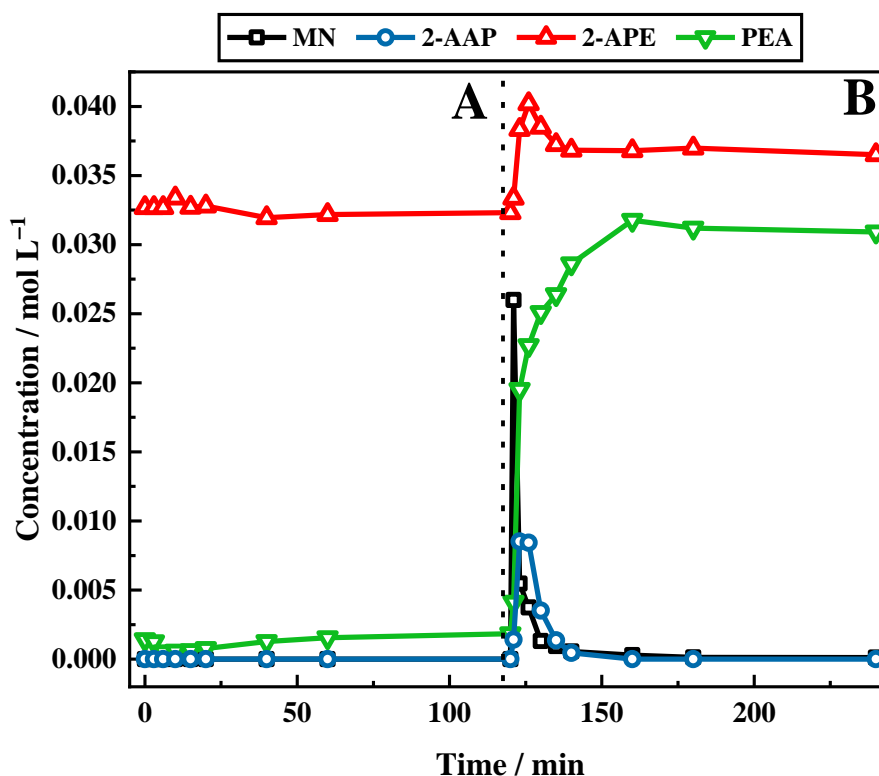


Figure 5.7. A, Reaction profile for the liquid phase hydrogenation reaction of 2-amino-1-phenylethanol (35 mmol L^{-1}) over a 5% Pd/C catalyst (300 mg) in the presence of 2 equivalents of sulphuric acid in methanol, and **B**, reaction profile post introduction of mandelonitrile (35 mmol L^{-1}) in the presence of 2 equivalents of sulphuric acid over the same catalyst. The reaction was conducted at 40°C under 6 barg hydrogen pressure with an external line pressure of 6.5 barg and an agitation rate of 1050 rpm. [MN = mandelonitrile; 2-AAP = 2-aminoacetophenone; 2-APE = 2-amino-1-phenylethanol; PEA = phenethylamine].

In this instance, it may be postulated that blockage of catalytic sites by the reagent occurs; thereby indicating that 2-amino-1-phenylethanol acts as a catalyst poison. This possibility was evaluated by the addition of an aliquot of mandelonitrile and sulphuric acid to the reaction mixture after 120 minutes of reaction without the introduction of any further catalyst. Analysis after the addition of mandelonitrile (Figure 5.7 **B**) showed that the reaction proceeded as observed for the standard mandelonitrile hydrogenation reaction shown in Figure 5.4 from this point. The rate of phenethylamine formation and yield was unaffected by the presence of the excess 2-amino-1-phenylethanol from the first part of the experiment. This observation eliminates the possibility of the hydroxyl-amine poisoning catalyst active sites at the concentration examined. It is therefore suggested that

the route from 2-amino-1-phenylethanol to phenethylamine is kinetically slow when compared to other stages of the overall process. Figure 5.8 considers this possibility.

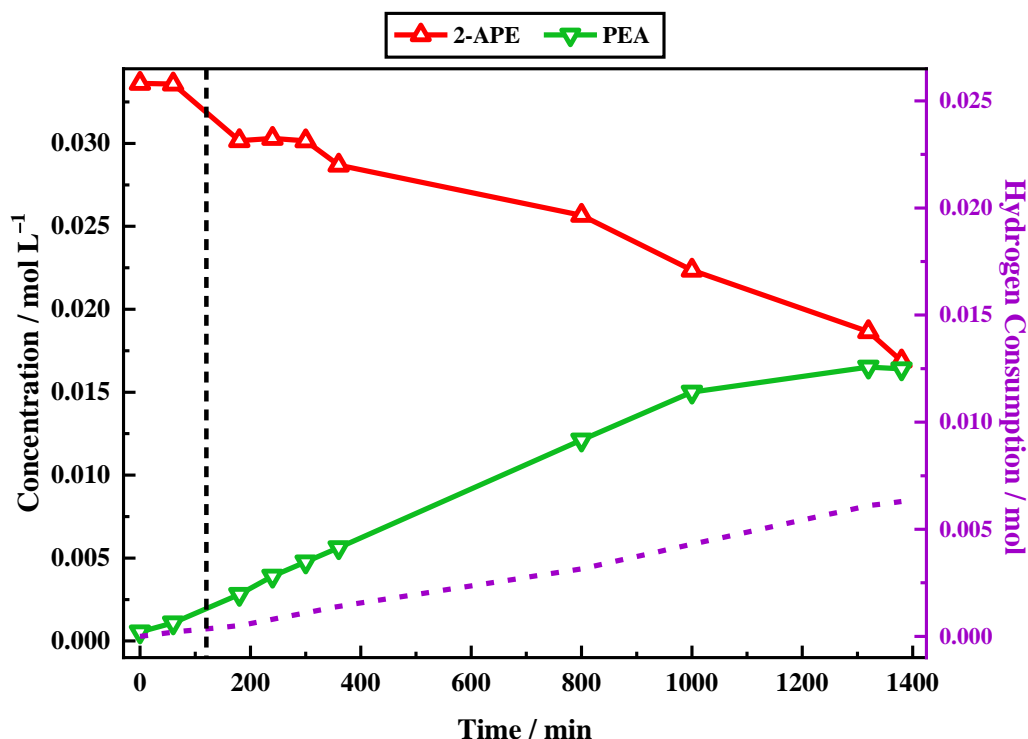


Figure 5.8. Reaction profile and hydrogen uptake curve (dashed purple line on the second y-axis) for the liquid phase hydrogenation reaction of 2-amino-1-phenylethanol (35 mmol L⁻¹) over a 5% Pd/C catalyst (300 mg) in the presence of 2 equivalents of sulphuric acid in methanol. The reaction was conducted at 40 °C under 6 barg hydrogen pressure with an external line pressure of 6.5 barg and an agitation rate of 1050 rpm. [2-APE = 2-amino-1-phenylethanol; PEA = phenethylamine]. The dashed black vertical line denotes a reaction time of 120 minutes.

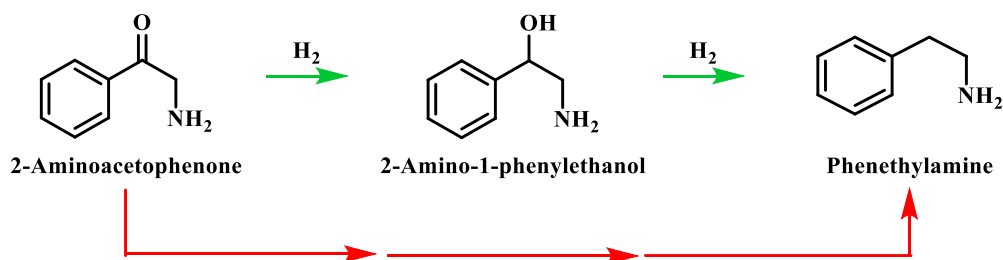
Figure 5.8 shows the hydrogenation reaction of 2-amino-1-phenylethanol over an extended period of 1,380 minutes (23 hours). As shown in Figure 5.7 A, poor phenethylamine production is observed within the first 120 minutes of the reaction. Consistent with this constrained activity, Figure 5.8 shows the hydrogen uptake at 120 minutes to be approximately 0.5 mmol of hydrogen. Assuming that only 1 molar equivalent of hydrogen, with respect to the reagent, is required to achieve complete hydrogenolysis of 2-amino-1-phenylethanol, the observed consumption corresponds to a mere 4% of the expected hydrogen uptake for this reaction (11 mmol).

Nonetheless, as the reaction progressed, an increase in hydrogen consumption was observed as well as conversion of the 2-amino-1-phenylethanol to phenethylamine. This was, however, slow. At 1,380 minutes (23 hours), 2-amino-1-phenylethanol conversion was only 52%, with an accompanying phenethylamine yield of 47%. When the yield of phenethylamine at a reaction time of 20 minutes is compared for the hydrogenation reactions of mandelonitrile and 2-amino-1-phenylethanol, it is found that the yield of the former (81%) is significantly higher than that of the latter (0.9%). The significantly reduced phenethylamine yield associated with the hydrogenolysis reaction of 2-amino-1-phenylethanol indicates this transformation to be unfavourable. Further enhancing this concept is the incomplete conversion of 2-amino-1-phenylethanol within the 1,380 minute monitoring time (Figure 5.8).

The observed build-up of 2-amino-1-phenylethanol in the reaction mixture after 120 minutes for the hydrogenation reaction of mandelonitrile (Figure 5.4) can therefore be rationalised by the slow kinetics of this hydrogenolysis process. Moreover, whilst Figure 5.8 confirms that the hydrogenolysis reaction of 2-amino-1-phenylethanol successfully yields phenethylamine, it also shows that the reaction is too slow to make a significant contribution to product formation within the timescale of the mandelonitrile hydrogenation reaction (120 minutes). Therefore, it is deduced that there must be an alternative chemical pathway, or pathways, that are responsible for accessing phenethylamine.

5.8 The Hydrogenation Reaction of 2-Aminoacetophenone

2-Aminoacetophenone has been identified as an intermediate species in the hydrogenation reaction of mandelonitrile. Thus, the role of this intermediate in the overall reaction process must now be considered. Scheme 5.4 indicates that, in a hydrogenating environment, the ketone functionality of 2-aminoacetophenone will be hydrogenated to the corresponding alcohol, forming 2-amino-1-phenylethanol.^[218–220] Upon formation of 2-amino-1-phenylethanol, it is expected that hydrogenolysis to phenethylamine would occur. The preceding section (Section 5.7), however, has indicated that the hydrogenolysis reaction of 2-amino-1-phenylethanol to form the desired product (phenethylamine) is kinetically unviable.



Scheme 5.5. Postulated pathways for the conversion of 2-aminoacetophenone to the primary amine phenethylamine. The green arrows highlight direct hydrogenation of the 2-aminoacetophenone with subsequent hydrogenolysis of the resultant 2-amino-1-phenylethanol, whilst the red arrows signify an unspecified, multi-step pathway.

Consequently, another route from 2-aminoacetophenone to phenethylamine, that does not proceed *via* 2-amino-1-phenylethanol, must be considered. This alternative route is signified by the red arrows in Scheme 5.5. It should be noted that this pathway may proceed *via* a number of species and does not indicate direct hydrogenolysis of the carbonyl group.

The presence of an acid additive has been shown to be an essential component of the reaction mixture (Section 5.3), and therefore, it is prudent to establish the role of the acid for any transformations incurred when 2-aminoacetophenone is hydrogenated. 2-Aminoacetophenone is commercially available as the 2-aminoacetophenone hydrochloride salt (Section 2.1), providing the opportunity to explore its catalytic conversion both in the absence, and in the presence of the sulphuric acid auxiliary agent. As formerly described in Section 4.3, the sulphuric acid additive was employed in the hydrogenation reaction of mandelonitrile to protonate the amine functionality, thus preventing the strong binding of the nitrogen lone pair to the surface of the catalyst, which can result in catalyst deactivation.^[65, 221] Accordingly, the prerequisite of sulphuric acid inclusion, for protonation purposes, becomes obsolete when the species is present as a salt, as is the case here. The use of the 2-aminoacetophenone hydrochloride salt as a starting material additionally allows the effect of the sulphuric acid to be mimicked without the contribution of its inherent catalytic activity.

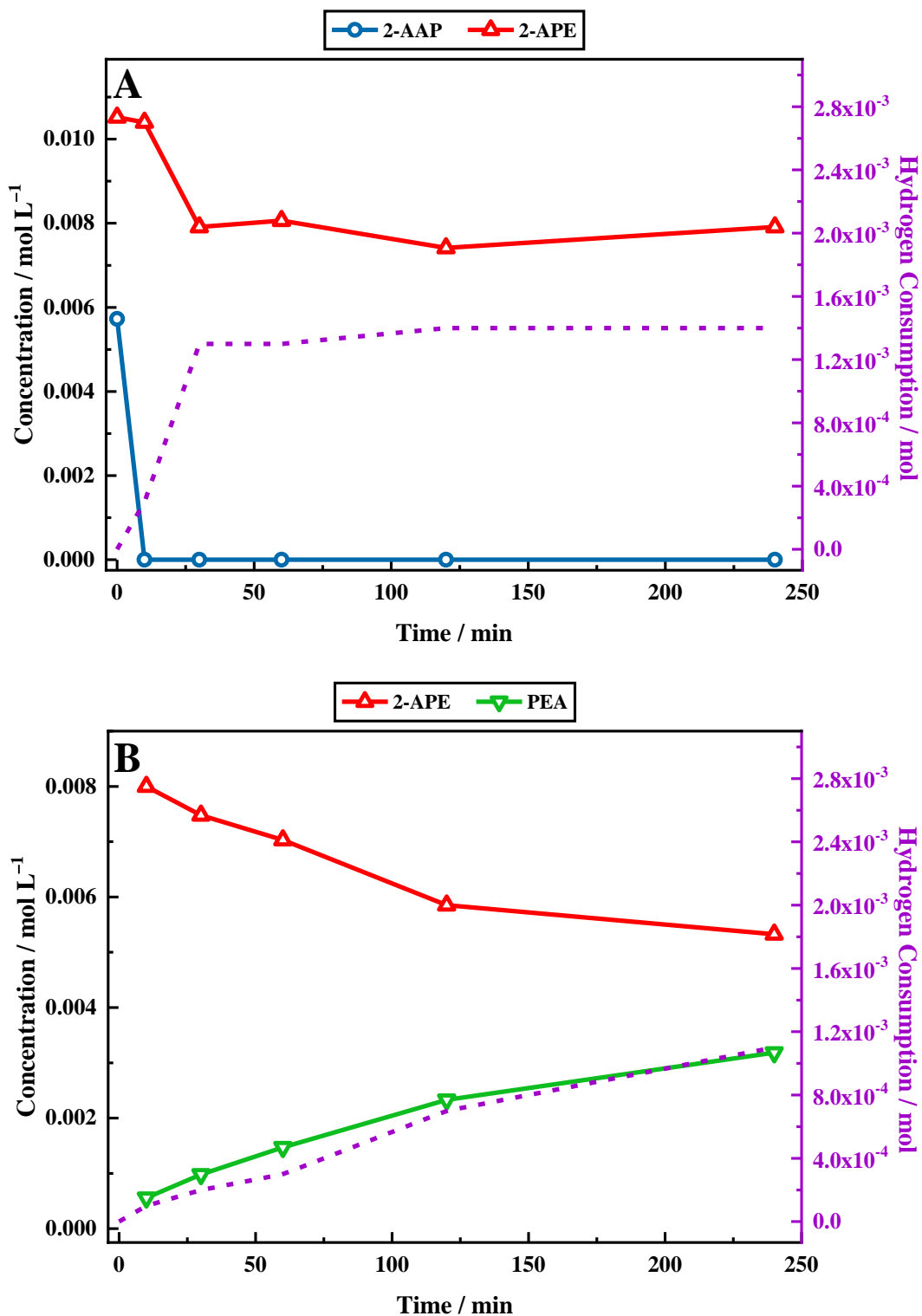
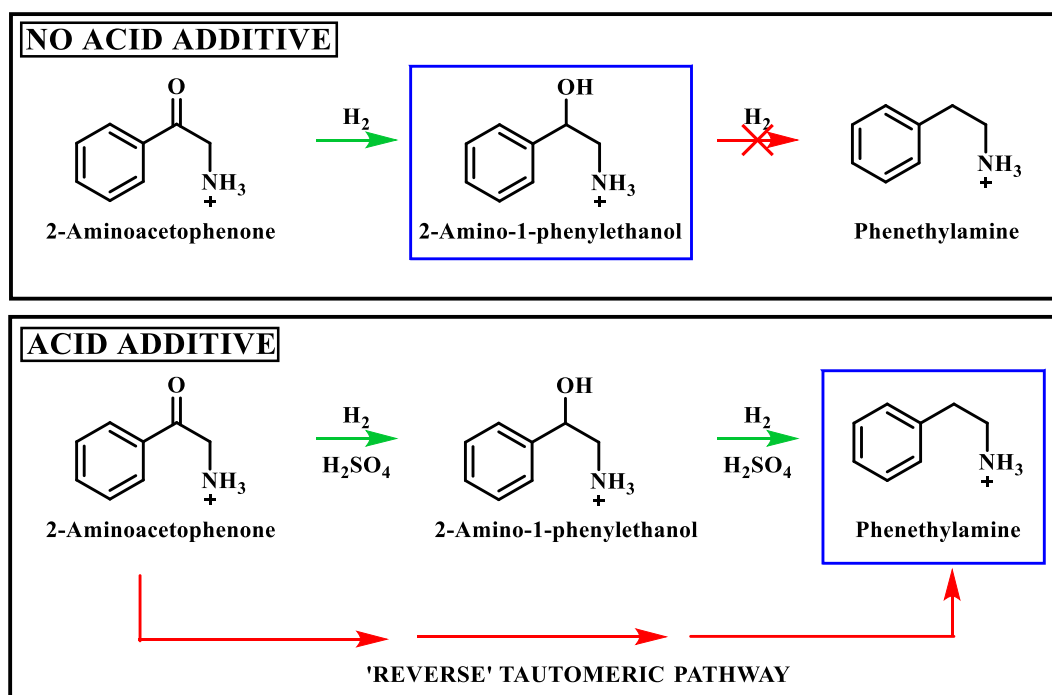


Figure 5.9. Reaction profile and hydrogen uptake curve (dashed purple line on the second y-axis) for the liquid phase hydrogenation reaction of 2-aminoacetophenone hydrochloride (7.6 mmol L^{-1}) over a 5% Pd/C catalyst (300 mg) in **A**, the absence of acid, and **B**, in the presence of 2 equivalents of sulphuric acid, both in methanol. The reaction was conducted at 40°C under 6 barg hydrogen pressure with an external line pressure of 6.5 barg and an agitation rate of 1050 rpm. [2-AAP = 2-aminoacetophenone; 2-APE = 2-amino-1-phenylethanol; PEA = phenethylamine].

Reaction profiles for the hydrogenation reactions of the 2-aminoacetophenone hydrochloride salt both with and without the sulphuric acid additive are presented in Figure 5.9. Upon exploration of the aforementioned experimental conditions, vastly different profiles were obtained. Under both described conditions, the 2-aminoacetophenone hydrochloride salt was rapidly hydrogenated to 2-amino-1-phenylethanol (time \approx 3 minutes), indicating this process to be highly favourable and independent of the catalytic powers of the sulphuric acid additive. The accelerated nature of this transformation meant that no accurate rate data could be obtained. For the neutral environment (Figure 5.9 **A**), the reaction reached completion with 2-amino-1-phenylethanol as the sole detectable product. This observation therefore eliminates a direct hydrogenolytic pathway from 2-aminoacetophenone to phenethylamine.^[219–220, 222]

The addition of sulphuric acid to the reaction mixture, however, afforded a very different profile (Figure 5.9 **B**). In this instance, phenethylamine production is shown to be facilitated by the sulphuric acid additive, with this species detectable alongside 2-amino-1-phenylethanol at the end of the reaction (time = 240 minutes). Continuous hydrogen consumption was evident throughout the reaction with no plateau detected as was previously observed under neutral conditions (Figure 5.5). This is, nevertheless, consistent with the presented profile as Figure 5.9 **B** shows that at 240 minutes, there is residual 2-amino-1-phenylethanol. Interestingly, the yield of phenethylamine at a reaction time of 20 minutes (12%) was higher than the yield obtained for the direct hydrogenation of 2-amino-1-phenylethanol shown prior (0.9%).



Scheme 5.6. Schematic representation of the species detectable in the liquid phase hydrogenation reaction of 2-aminoacetophenone hydrochloride (7.6 mmol L^{-1}) over a 5% Pd/C catalyst (300 mg) both with and without 2 equivalents of sulphuric acid in methanol. Reaction carried out at 40°C , 6 barg hydrogen pressure with an external line pressure of 6.5 barg and an agitation rate of 1050 rpm. The final product of each reaction is highlighted by a blue box.

The results of the experimental findings for the hydrogenation reaction of the 2-aminoacetophenone hydrochloride salt under both discussed conditions are summarised in Scheme 5.6. With reference to Scheme 5.6, these results establish that, in addition to preventing amine groups from site blocking at the palladium surface, the sulphuric acid facilitates phenethylamine production. It is proposed that the inherent reversible nature of the tautomeric equilibria between firstly, the hydroxy-imine and the hydroxy-enamine, and secondly, the hydroxy-enamine and the 2-aminoacetophenone, will provide a tautomeric route, in the 'reverse' direction, from the 2-aminoacetophenone to phenethylamine.

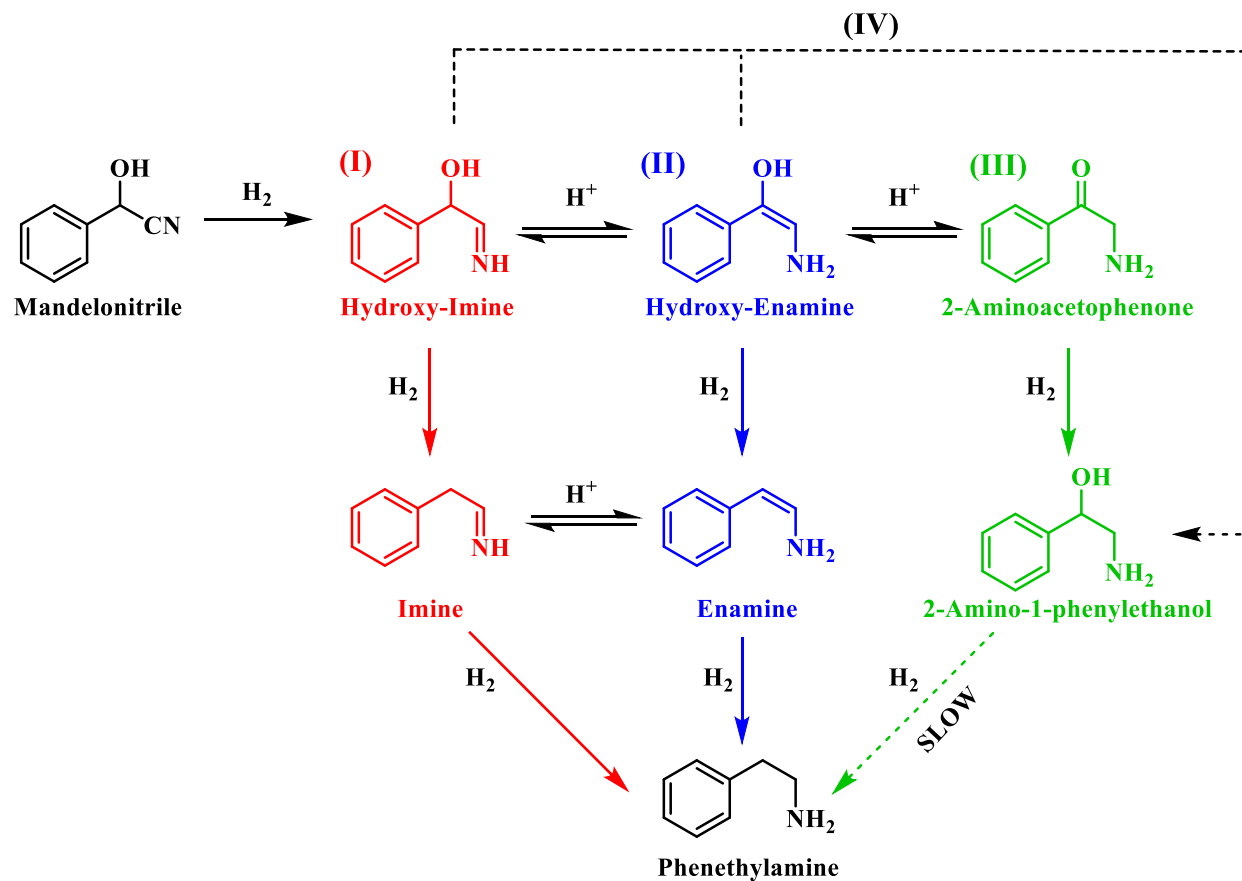
5.9 Full Elucidation of the Reaction Pathway is not Possible by HPLC

The reaction profile for the mandelonitrile hydrogenation reaction over the reported 5% Pd/C catalyst identifies phenethylamine as the principle product (selectivity 87%), 2-amino-1-phenylethanol as a by-product (selectivity 13%) and 2-aminoacetophenone as a reaction intermediate (Figure 5.4). The reaction sequence does not conform to a simple consecutive reaction as envisaged in Scheme 5.1, not least because Section 5.7 establishes that the hydrogenolysis reaction of 2-amino-1-phenylethanol to form phenethylamine is kinetically slow. Moreover, Section 5.8 shows that under the specified reaction conditions, explicitly in the presence of a sulphuric acid auxiliary agent, the desired primary amine product (phenethylamine) can be produced from 2-aminoacetophenone under conditions of continuous hydrogen consumption. The above considerations involve all the chemical entities detectable by HPLC. Further development of the mechanism, however, is thwarted by the participation of reactive species, assumed to be adsorbed, and thus not observable in the liquid phase. Consequently, additional chemical pathways, which can account for the reaction profile presented in Figure 5.4, must be brought forward for consideration.

Section 5.5 introduced the availability of a tautomeric pathway, originating at the hydroxy-imine entity, and culminating at 2-aminoacetophenone (Scheme 5.3). Whilst not detectable chromatographically, the hydroxy-imine and hydroxy-enamine species are believed to be essential intermediates in the production of 2-aminoacetophenone. Mentioned prior (Section 5.5), and as is the case for 2-aminoacetophenone, both the hydroxy-imine and the hydroxy-enamine are chemically susceptible to both hydrogenation and hydrogenolysis reactions. Therefore, in order to construct a reaction scheme that contains chemically viable reaction pathways, the following deductions/observations need to be accounted for:

- (i) The hydrogenation reaction of mandelonitrile is fast (Section 5.2).
- (ii) The hydrogenation reaction of 2-aminoacetophenone to produce 2-amino-1-phenylethanol is fast (Section 5.8).
- (iii) The hydrogenolysis reaction of 2-amino-1-phenylethanol to produce phenethylamine is prohibitively slow (Section 5.7).
- (iv) As a consequence of (iii), 2-amino-1-phenylethanol is observed as a by-product of the reaction (Section 5.3).

- (v) 2-Aminoacetophenone is a reaction intermediate, the formation of which is associated with a reversible, acid catalysed tautomeric pathway (Section 5.5).
- (vi) There is potential for either, or both the hydroxy-imine and hydroxy-enamine entities to undergo direct hydrogenation to form 2-amino-1-phenylethanol (Section 5.5).



Scheme 5.7. Proposed reaction scheme for the liquid phase hydrogenation reaction of mandelonitrile over a 5% Pd/C catalyst. The scheme builds on Scheme 5.4 to include the assumed chemistry associated with the hydroxy-imine and the hydroxy-enamine intermediates. Further, highlighted are postulated pathways (I–IV) showing the multiple routes available to the desired product phenethylamine.

On the basis of this perspective, Scheme 5.7 is provisionally proposed as a global reaction scheme for the hydrogenation reaction of mandelonitrile over a 5% Pd/C catalyst to produce the primary amine phenethylamine. Scheme 5.7 indicates that, far from the simple consecutive pathway initially envisaged (Scheme 5.1), there are now at least four potential routes from reagent to desired product. These pathways are highlighted as **I**, **II**, **III** and **IV** in Scheme 5.7. Pathways **I–III** proceed exclusively in the forward direction and originate at each of the species involved in the tautomeric equilibria shown in Scheme 5.3 (hydroxy-imine, **I**; hydroxy-enamine, **II**; and 2-aminoacetophenone, **III**). Pathway **III** has been explored in greater detail in Sections 5.7 and 5.8. It is proposed that the hydroxy-imine (Pathway **I**) and hydroxy-enamine (Pathway **II**) undergo hydrogenolysis to form the corresponding imine and enamine species, before undergoing a final hydrogenation step to afford phenethylamine in both cases. Additionally considered in Scheme 5.7 is Pathway **IV** which represents the potential for direct hydrogenation of either the hydroxy-imine or the hydroxy-enamine to afford 2-amino-1-phenylethanol, where the concluding step would be hydrogenolysis of the hydroxyl functionality to yield phenethylamine, as with Pathway **III**.

Prior investigation has indicated that Pathways **III** and **IV** are unlikely to be significant contributors to phenethylamine production due to the 2-amino-1-phenylethanol hydrogenolysis bottleneck (Section 5.7). Indeed, it is this sluggish transformation which results in the formation of 2-amino-1-phenylethanol as a by-product of the reaction. The removal of Pathways **III** and **IV** from consideration directs attention towards Pathways **I** and **II** as potential candidates for the most likely route or routes by which mandelonitrile can be converted to phenethylamine. In addition to the reaction proceeding exclusively in the forward direction, as is depicted in Scheme 5.7, the reversible nature of the tautomeric equilibria provides an additional opportunity for Pathways **I** and **II** to be followed. Specifically, it is proposed that, upon formation of the energetically favourable 2-aminoacetophenone, the reverse tautomeric equilibrium to reform the hydroxy-enamine and the hydroxy-imine species is incurred. From here, Pathways **I** and **II** can be followed to furnish phenethylamine as previously described. Against this reasoning, it is proposed that the reaction proceeds *via* either Pathway **I** and/or Pathway **II**.

Unfortunately, Pathways **I** and **II** cannot be differentiated using the chromatographic methods presented in this chapter as the corresponding intermediates are undetectable in the liquid phase. It is therefore proposed that in the hydrogenation reaction of

mandelonitrile, phenethylamine formation has the potential to proceed *via* either one, or both of these routes. Further investigation into the more conclusive identification of the active pathway or pathways involved in this reaction is explored in the subsequent chapter.

5.10 Conclusions

Mechanistic aspects of the liquid phase hydrogenation reaction of mandelonitrile over a 5% Pd/C catalyst has been investigated and the following conclusions drawn:

- An acid additive (2 equivalents of sulphuric acid) proved not only to be essential for sustained catalytic activity (Section 5.2), but also played a vital role in catalysing the homogeneous reactions responsible for the formation of the ketone intermediate 2-aminoacetophenone (Section 5.8).
- The resultant tautomeric pathway is thought to open-up alternative routes to afford phenethylamine to those originally postulated in Scheme 5.1. These routes have been designated as Pathways **I–IV** in Scheme 5.7.
- A tentative global reaction scheme is proposed (Scheme 5.7) to account for all the possible pathways accessible within this chemical network; the scheme includes contributions from species assumed to be solely adsorbed as well as entities that are partitioned between solvated and adsorbed states at the liquid-solid interface.
- For a single batch reaction, successful production of the primary amine phenethylamine with a selectivity of 87% (Figure 5.4) was achieved alongside full conversion of mandelonitrile. Production of 2-amino-1-phenylethanol as a by-product accounts for the remaining 13% selectivity and closes the mass balance (Figure 5.6).
- When the kinetics of the conversion of the proposed intermediate 2-amino-1-phenylethanol were considered, it was found that this process was significantly slower than the overall production of phenethylamine. This finding excluded the possibility that 2-amino-1-phenylethanol is an intermediate and is instead

designated as a by-product of the reaction. Moreover, it was indicated that an alternative route from reagent to product must be operational.

- It was consequently proposed that the hydrogenolytic cleavage of the C-OH bond occurs on either one, or both, of the highly reactive hydroxy-imine and hydroxy-enamine species. Differentiation between these two proposed pathways, however, was not possible by the chromatographic procedures employed here, rendering further investigation desirable.

CHAPTER 6

*Isotopic Substitution Experiments in
the Hydrogenation Reaction of
Mandelonitrile over a Supported Pd
Catalyst: A Nuclear Magnetic
Resonance Study*

6.1 Introduction to the Catalytic Deuteration Reaction of Mandelonitrile

Previous studies on the mandelonitrile hydrogenation reaction system, detailed in Chapter 5, utilised HPLC as an analytical tool to provide useful information on the reaction mechanism.^[217] Despite gleaned useful insight, the reported analytical method did not allow for the identification of short-lived intermediates or surface species, namely, imines and/or enamines. As such, the mechanistic understanding was restricted.

It was first demonstrated in 1935 by Morikawa, Benedict and Taylor that transition metals were capable of catalytically exchanging their C-H and C-D bonds in a H/D exchange process following a deuteration procedure.^[223] The application of deuterium labelling has since been recurrently reported in the literature to elucidate reaction mechanisms.^[224–230] Analysis of the resultant product distribution by NMR spectroscopy and mass spectrometry can be employed to reveal information about the number, location and grouping of the deuterium atoms in a molecule.^[229–231] One particular example, reported by Thakar *et al.*, uses such a study to examine the hydrogenolysis of benzylic alcohols over supported palladium catalysts.^[224] In this instance, multinuclear NMR spectroscopy was used to determine the position of deuterium incorporation, identifying that the acidity of the support played a role in determining which pathways were accessible in the hydrogenolysis of 1-(4-isobutylphenyl) ethanol to afford 4-isobutylethylbenzene.^[224] Accordingly, a similar strategy is applied to the mandelonitrile hydrogenation reaction system to overcome the aforementioned limitations.

Herein, the deuteration reaction of mandelonitrile to supplement the corresponding hydrogenation reaction is invoked. Furthermore, the use of isotopic labelling, as a method of following the reaction pathway, provides a potential means to distinguish the postulated pathways and minimise the residual mechanistic uncertainty. Reaction schemes are presented to account for the experimental observations. Analysis of the resultant product distribution is undertaken primarily by multinuclear NMR spectroscopy, but also by mass spectrometry. It is, however, noted that this analysis is principally associated with the desired product, phenethylamine. Though this provides useful insight into the production of this molecule, a more global consideration of the reaction system must not be overlooked.

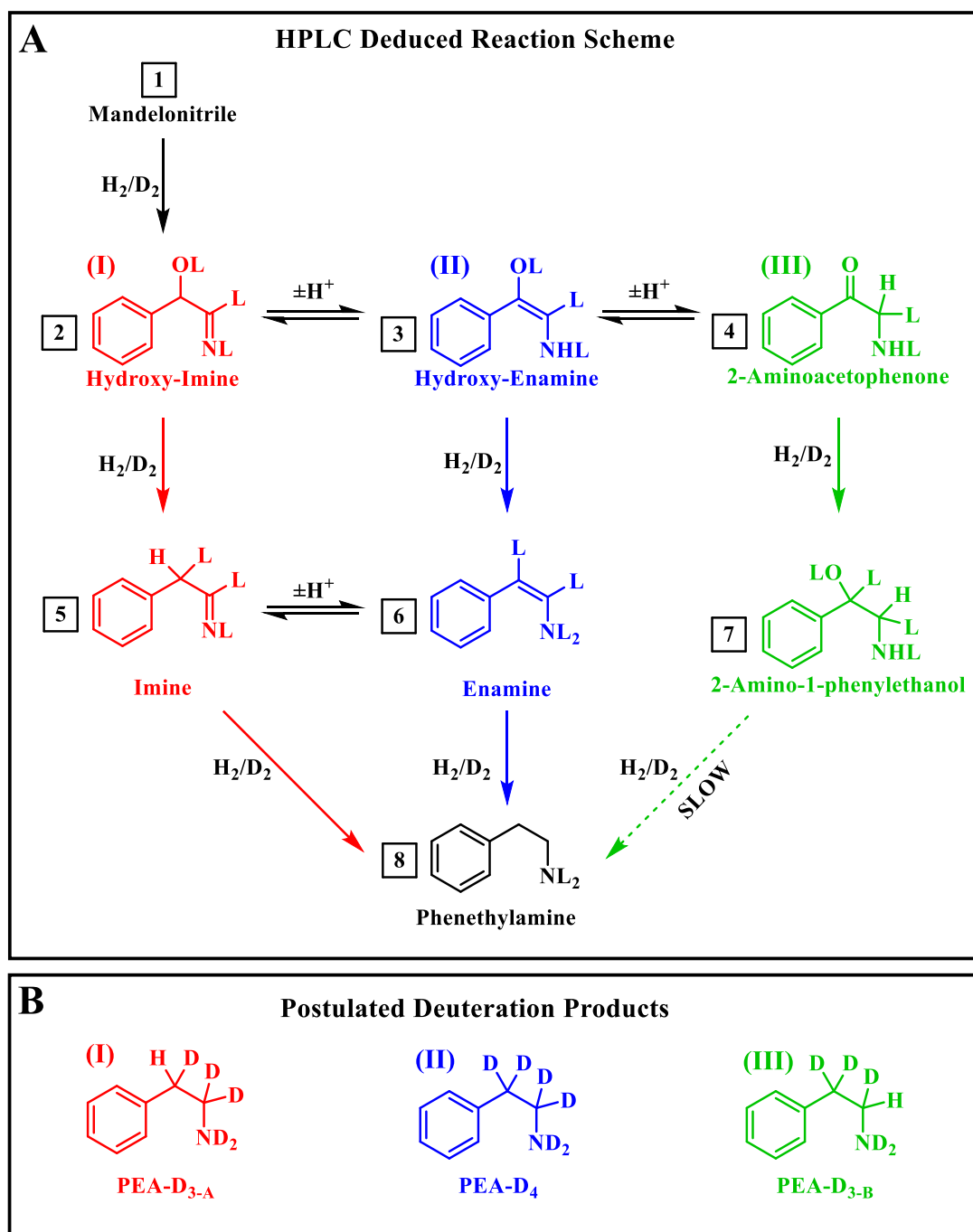
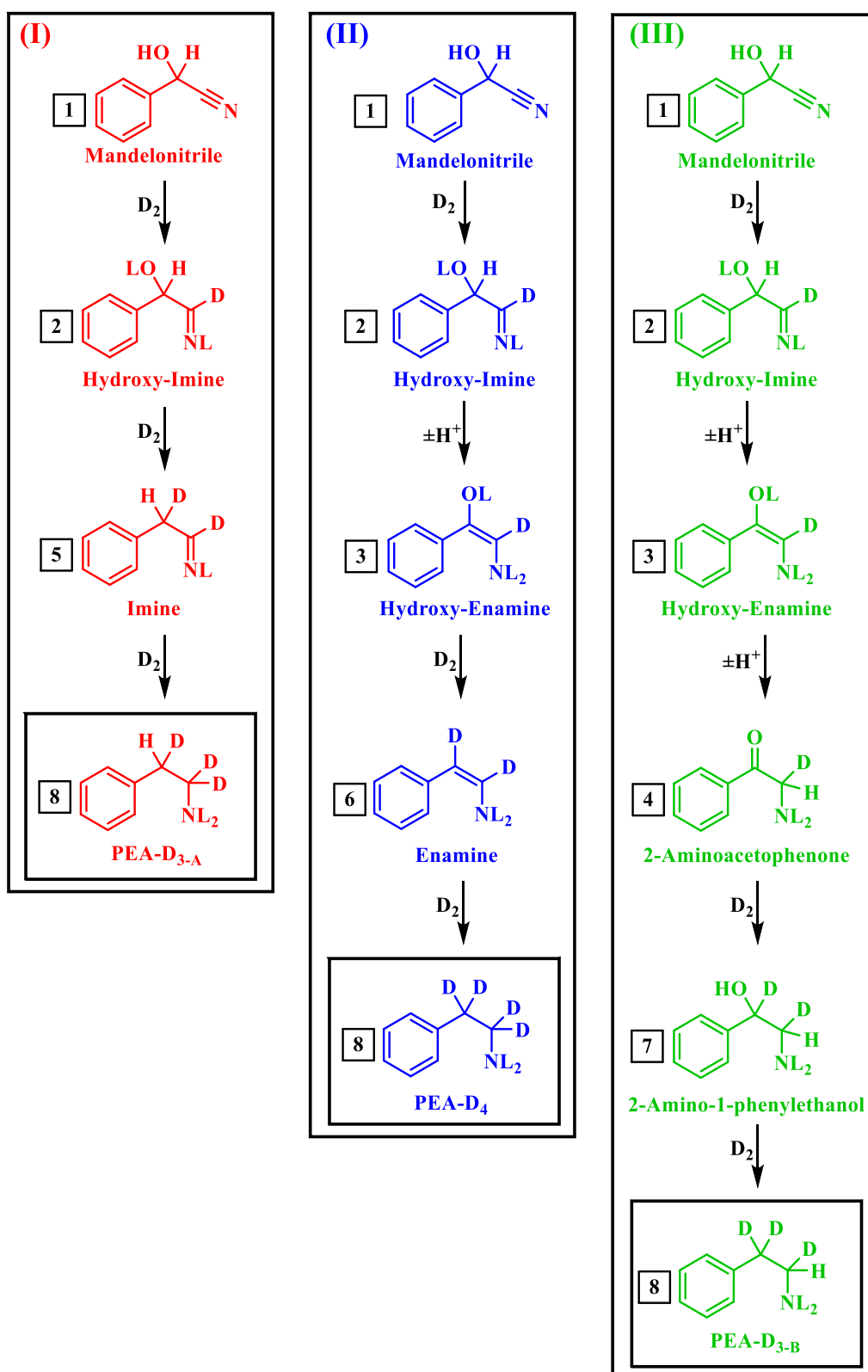


Figure 6.1. (A) Postulated reaction scheme based on previous HPLC analysis (Chapter 5), and (B) the hypothesised deuterated form of the phenethylamine post deuteration reaction for each of the three potential forward reaction pathways (I–III). Pathways I–III have been coloured red, blue and green respectively for lucidity. Numbers have been associated with each species for clarity in later analyses. Subscripts ‘A’ and ‘B’ have been used to highlight positioning of the proton in the relevant deuterated phenethylamine products. Due to the rapid H/D exchange on the amine and alcohol functionalities, L has been used to denote either a hydrogen atom (H) or a deuterium atom (D). [PEA = phenethylamine].

With focus on the preferred product, phenethylamine, three potential forward pathways to afford this molecule, labelled as **I–III** in Figure 6.1 **A**, have been identified. Each pathway must incur two hydrogenation steps, *and* hydrogenolysis of the hydroxyl group in order for phenethylamine to be produced. The presence of a tautomeric pathway, activated as the result of the acid additive which is found to be necessary to prevent catalyst deactivation,^[217] renders it possible for three molecules to undergo the hydrogenolysis step. As such, the molecule undergoing hydrogenolysis is dependent on the pathway taken, the hydroxy-imine (**2**), the hydroxy-enamine (**3**) or, the hydroxy-amine (**7**) for Pathways **I**, **II** and **III** respectively. Also highlighted in Figure 6.1 **B** are the proposed outcomes of the deuteration reaction showing the postulated deuterium incorporation in the major product (phenethylamine) for each of the presented pathways. Full schematic representations, showing the step-wise introduction of deuterium for each Pathway (**I–III**), leading to the corresponding anticipated phenethylamine isotopologue, are presented in Scheme 6.1.



Scheme 6.1. Full schematic representation of Pathways **I–III** upon the deuteration reaction of mandelonitrile showing the deuterium incorporation as the reaction progresses. Due to the rapid H/D exchange on the amine and alcohol functionalities, **L** has been used to denote either a hydrogen atom (H) or a deuterium atom (D). [PEA = phenethylamine].

The slow reaction kinetics of the conversion of 2-amino-1-phenylethanol to furnish phenethylamine, identified previously (Section 5.7), has provided an indication that Pathway **III** (green) is not in occurrence.^[217] For completeness, it should be noted that, to afford 2-amino-1-phenylethanol, the full tautomeric equilibria originating at the hydroxy-imine, as shown in Figure 5.3, may be followed. Alternatively, a direct step from either the hydroxy-imine, or the hydroxy-enamine may also yield 2-amino-1-phenylethanol.^[217]

Against this background, this study aims to confirm that Pathway **III** is not operational within the considered time frame (120 minutes), but also, and more significantly, to provide a means of differentiating between Pathways **I** and **II** in order to identify which route or routes are active.

6.2 NMR Spectroscopic Analysis Defines the Location of Deuterium Incorporation within Phenethylamine

Upon completion of both the hydrogenation and the deuteration reactions of mandelonitrile (time = 120 minutes), ¹³C NMR spectroscopy of the respective reaction mixtures was conducted. Preliminary examination of the ¹³C NMR spectra indicated that, as expected, peaks associated with both 2-amino-1-phenylethanol and phenethylamine were observed. The ¹³C NMR spectra associated with both experiments can be found in Figure 6.2. Here, the aliphatic and quaternary carbons connected with both phenethylamine and 2-amino-1-phenylethanol have been assigned. However, due to the overlapping nature of the aromatic carbon atoms associated with both molecules, peak assignment has not been conducted in this region of the spectra (127–130 ppm). As a reference point, the carbon atoms of benzene appear at 128 ppm with substituted variants occupying a much broader range (110–175 ppm).^[232] Additionally detected is the septet associated with the NMR solvent, deuterated methanol, at 49 ppm.^[213] A further peak, not associated with either phenethylamine or 2-amino-1-phenylethanol, at 56 ppm, was also observed and identified as an impurity of the reaction.

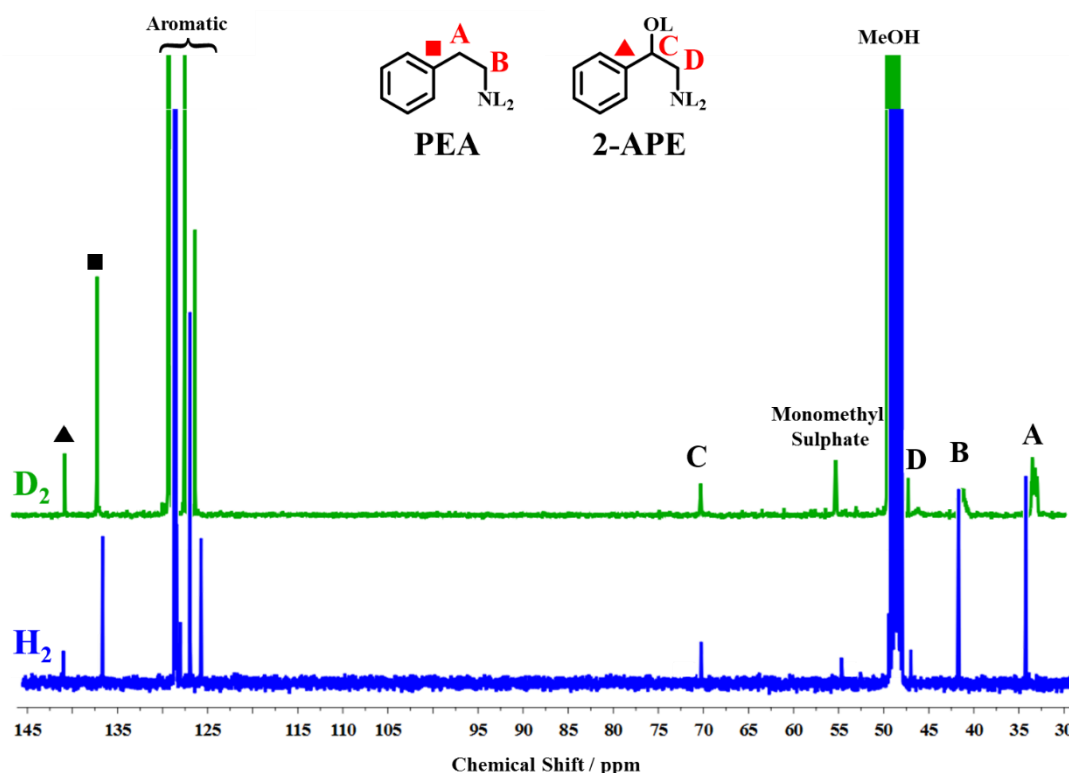
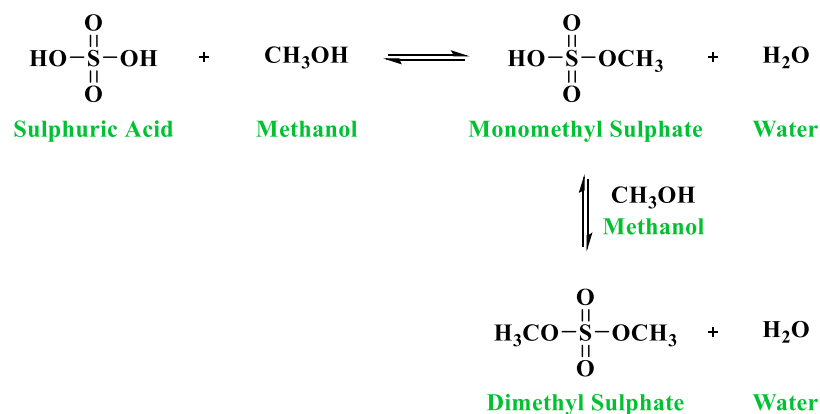


Figure 6.2. ^{13}C NMR spectra for both the hydrogenation reaction (blue) and deuteration reaction (green) of mandelonitrile. NMR solvent = CD_3OD . All peaks have been labelled according to the molecules, phenethylamine (PEA) and 2-amino-1-phenylethanol (2-APE), shown inset. Due to the rapid H/D exchange at the alcohol and amine functionalities, *L* is used to denote either a hydrogen atom (H) or a deuterium atom (D) and is dependent on the active gas used for the experiment.

The impurity observed on the ^{13}C NMR spectra at 56 ppm was identified as monomethyl sulphate. Monomethyl sulphate is formed as the result of methylation of the sulphuric acid additive.^[233] Upon formation, the monomethyl sulphate can either hydrolyse to reform sulphuric acid and methanol, or further react with methanol to form dimethyl sulphate, as is illustrated in Scheme 6.2. Nonetheless, it should be noted that in this instance, no peaks associated with the production of dimethyl sulphate were detected in the spectra. Investigation into this side reaction has been conducted at the industrial site and indicates that the production of this relatively benign impurity (with regard to the reaction itself) does not significantly interfere with the production of phenethylamine.^[234]



Scheme 6.2. Methylation of sulphuric acid resulting in formation of dimethyl sulphate, via monomethyl sulphate, with water produced as a by-product.

For the hydrogenation reaction, the proton-decoupled ^{13}C NMR spectra should show no splitting of the peaks owing to carbon-hydrogen interactions. Further, due to low natural abundance, ^{13}C NMR spectra do not usually show carbon-carbon splitting as the more prevalent ^{12}C does not have a magnetic moment, and thus cannot split the signal of an adjacent ^{13}C . A consequence of this is that a simplified spectrum, containing solely singlets is expected.^[224] Contrastingly, for a deuteration reaction, multiplicity can arise due to the coupling of a carbon nucleus with a deuterium atom.^[226] Multiplicity at a specific chemical shift can then be used as an indicator for deuterium incorporation at the corresponding carbon atom.^[224, 226]

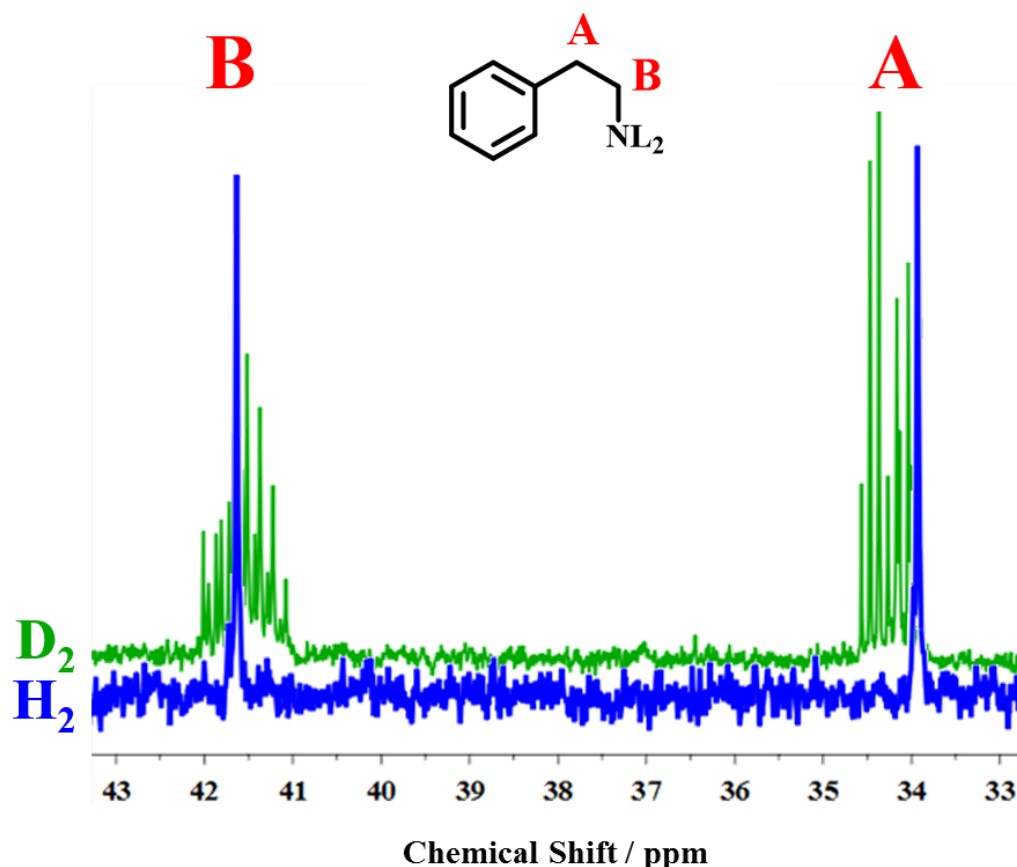


Figure 6.3. ^{13}C NMR spectra for both the hydrogenation reaction (blue) and the deuteration reaction (green) of mandelonitrile collected at reaction completion (time = 120 minutes) in CD_3OD in the 33–43 ppm range. Signals have been assigned according to the labelled phenethylamine molecule shown inset. Due to the rapid H/D exchange at the amine functionality, **L** denotes either a hydrogen atom (H) or a deuterium atom (D).

As previously described, the potential for differing degrees of deuteration at the aliphatic carbons of phenethylamine can be used as a method of differentiating between Pathways **I–III** (Figure 6.1). Analytical emphasis is therefore drawn to carbons **A** and **B**. Figure 6.3 shows the ^{13}C NMR spectra for both the hydrogenation and deuteration reactions of mandelonitrile in the 33–43 ppm range. Deuterium incorporation, as evidenced by peak splitting in ^{13}C NMR spectroscopy, was observed at both aliphatic carbon positions post deuteration reaction (Figure 6.3, green trace). This observation provided an indication that deuterium had been introduced at both locations. As a proof of concept, a ^{13}C NMR spectrum taken post hydrogenation reaction was also collected, and found to be solely comprised of singlets (Figure 6.3, blue trace). However, with reference to Figure 6.1, where it is shown that at least one deuterium atom is expected at both aliphatic positions,

regardless of the route taken, this finding does not in itself provide substantial mechanistic insight. Nonetheless, the successful deuteration reaction of mandelonitrile is confirmed.

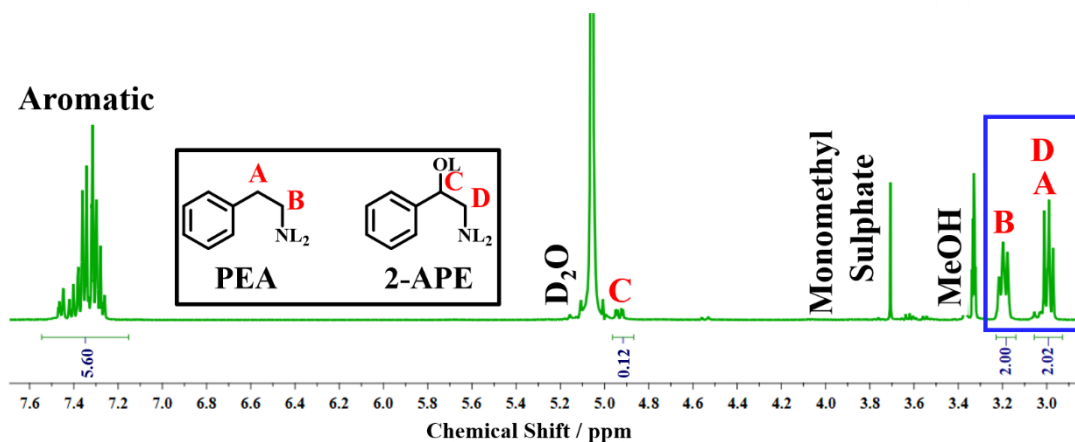


Figure 6.4. ^1H NMR spectrum for the hydrogenation reaction of mandelonitrile collected at reaction completion (time = 120 minutes) in CD_3OD . Signals have been assigned according to labelled phenethylamine (PEA) and 2-amino-1-phenylethanol (2-APE), displayed inset. The aliphatic protons of interest have been highlighted by a blue box. Due to the rapid H/D exchange at the amine and alcohol functionalities, **L** denotes either a hydrogen atom (H) or a deuterium atom (D). The accompanying integrations are shown below each multiplet.

Further examination of the reaction mixture by ^1H NMR spectroscopy does, however, provide some insight into the reaction mechanism. Whilst the main focus of the study is to examine the route from mandelonitrile to phenethylamine, the presence of the by-product 2-amino-1-phenylethanol, and its potential to complicate the resultant spectra, cannot be overlooked. As such, reference spectra, taken under generic hydrogenation conditions, were used to determine the possible interference arising from the product mixture (Figure 6.4).

With reference to Figure 6.4, peak overlap was found to be particularly prevalent in the aromatic region of the spectra (7.25–7.50 ppm). Unfortunately, this was also found to be an issue in the aliphatic region with peak overlap of the protons associated with carbons **A** and **D** found to occur at 2.96 ppm (Figure 6.4). However, this means that spectra must be interpreted with care and an awareness of the associated error (typically $\pm 5\%$ error for the integrations associated with routinely acquired ^1H NMR spectra). The proportion of

2-amino-1-phenylethanol, representing around 6% of the total (as determined by ^1H NMR spectroscopy), can be considered as negligible.

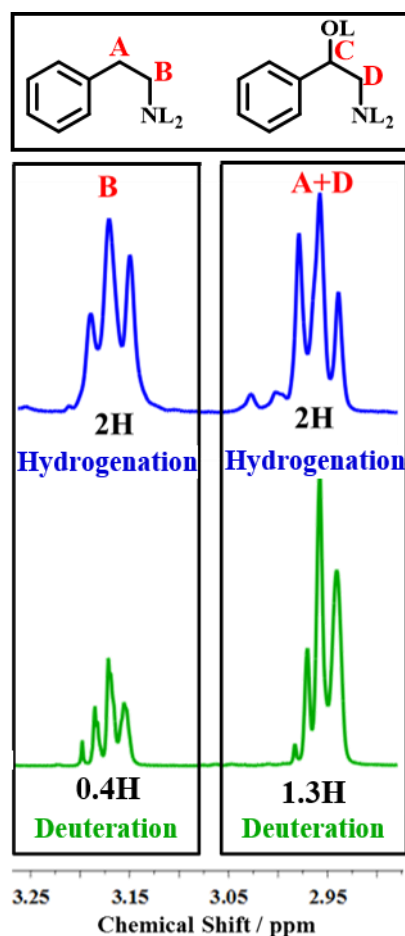


Figure 6.5. 400 MHz ^1H NMR spectra for the hydrogenation (blue) and deuteration (green) reactions of mandelonitrile showing exclusively the 2.90–3.25 ppm range. NMR solvent = CD_3OD . Letter assignments **A** and **B**, and **C** and **D** correspond to aliphatic carbon positions of phenethylamine and 2-amino-1-phenylethanol, respectively. The integration at both aliphatic carbon positions, for both hydrogenation and deuteration reactions, is shown beneath the associated peak. Due to the rapid H/D exchange at the amine and alcohol functionalities, **L** denotes either a hydrogen atom (H) or a deuterium atom (D) for the deuteration reaction and a hydrogen atom (H) for the hydrogenation reaction.

Closer examination of the aliphatic peaks of interest for both the hydrogenation reaction (blue) and the deuteration reaction (green) is shown in Figure 6.5. The integration of the aliphatic carbon peaks is first considered for the hydrogenation reaction spectrum, with each expected to yield an integration of 2H. If the protons associated with carbon **B**, of

known composition (solely phenethylamine), are integrated as 2H, the relative integration of the protons associated with carbon **A** should then also yield an integration of 2H if phenethylamine is the only contributor at this position.

This was found to be the case for the hydrogenation reaction, as would be expected in the absence of 2-amino-1-phenylethanol, described above. This finding adds further value to subsequent results by showing that the 2-amino-1-phenylethanol contribution at carbon **A** is insignificant. It can consequently be assumed that the resultant integration at this position can be attributed solely to phenethylamine, thus simplifying analysis.

Also shown in Figure 6.5 is the ^1H NMR spectroscopy analysis of the deuteration reaction, again focusing on the protons associated with aliphatic carbons **A** and **B**. A fully deuterated compound will not show any peaks in a ^1H NMR spectra, as despite deuterium having nuclear spin ($I \neq 0$) and being NMR active, ^2H and ^1H NMR require vastly different operating frequencies. Therefore, NMR signals for deuterium are not detected under the conditions used for ^1H NMR spectroscopy and *vice versa*. Therefore, deuterium will be ‘silent’ in the ^1H NMR spectrum.^[235] It is consequently postulated that the integration of the aliphatic phenethylamine peaks associated with the deuteration reaction will be lower than that observed for the hydrogenation reaction (2H/2H). As each postulated pathway (**I–III**) is expected to yield a different deuterated product, the resultant integration at each position will be unique to the associated pathway.

Table 6.1. Predicted ^1H NMR spectral integrations for the aliphatic protons associated with carbons **A** and **B** for each of the postulated deuterated products which relate to Pathways **I–III**. Due to the rapid H/D exchange at the amine functionality, **L** is used to denote either a hydrogen atom (H) or a deuterium atom (D).

<i>Pathway</i>	<i>Predicted Product</i>	<i>Predicted Proton Integration at A</i>	<i>Predicted Proton Integration at B</i>
I	PhCH ^{blue} DC ^{red} DDNL ₂	1H	0H
II	PhC ^{red} DDC ^{red} DDNL ₂	0H	0H
III	PhC ^{red} DDC ^{blue} HNL ₂	0H	1H

As predicted, it is observed in Figure 6.5 that integration of the aliphatic protons no longer yields 2H. Instead, due to differing degrees of deuteration at each carbon, integrations of 1.3H and 0.4H were observed at carbons **A** and **B**, respectively. As deuterium atoms are not observed by ^1H NMR spectroscopy, the degree of deuteration at each position is determined by subtracting the experimentally integrated proton component obtained from the deuteration reaction from the expected proton integration at each position (2H). By this method, carbon **A** is found to be only partially deuterated (*ca.* 35% D), whereas carbon **B** is highly deuterated (*ca.* 80% D).

As determined by ^1H NMR spectroscopy, a deuterium presence in the molecule was deduced by the observation of an incomplete 2H aliphatic proton component at both carbon positions, **A** and **B**. To complement this measurement, ^2H NMR spectroscopy was also conducted on the deuterated sample. Whilst ^2H NMR spectroscopy has a similar chemical shift range to ^1H NMR spectroscopy, it has poorer resolution and sensitivity, making it an unsatisfactory substitute for general use.^[235] As a direct consequence of this, deuterium-deuterium couplings are significantly smaller than proton-proton couplings and are therefore not observed. This means that information about the chemical environment of the neighbouring carbons, typically obtained from the splitting pattern, cannot readily be gained from ^2H NMR spectroscopy. Despite these limitations, ^2H NMR spectroscopy may be effectively used to verify the presence of deuterium (*cf.* ^1H NMR spectroscopy where the presence of deuterium was only inferred from reduced peak integrations).

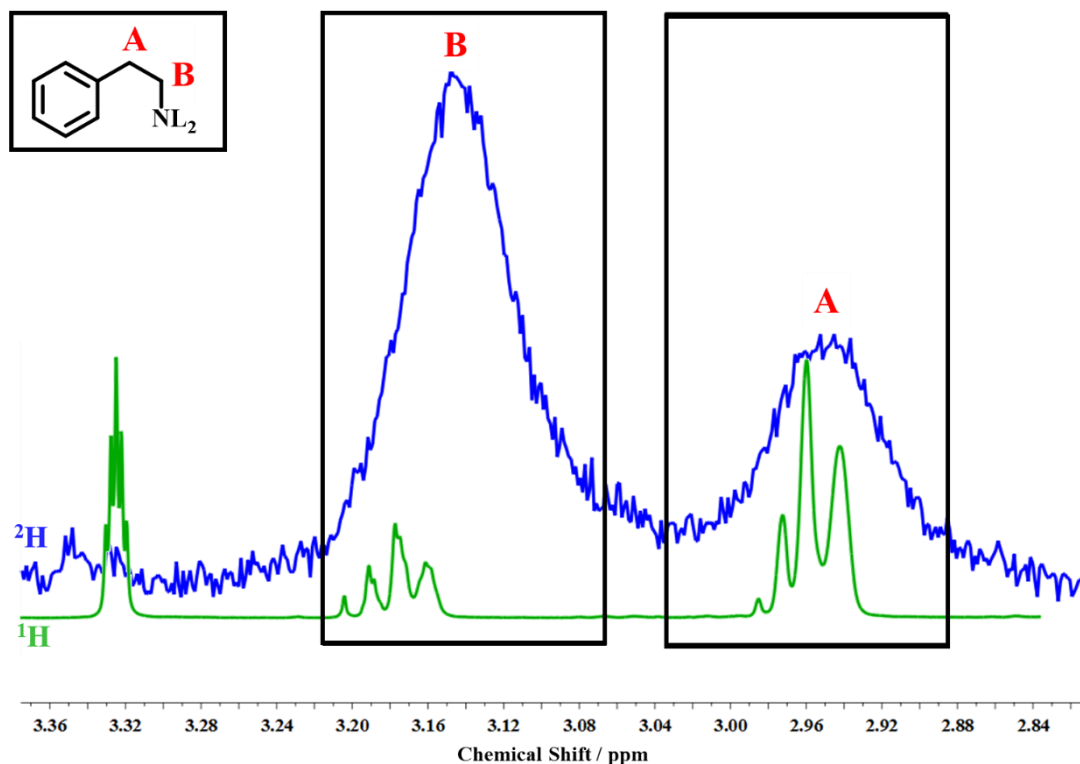


Figure 6.6. ^1H NMR (green) and ^2H NMR (blue) spectral analysis of the mandelonitrile deuteration reaction in the 2.84–3.36 ppm range. The aliphatic carbons of phenethylamine (**A** and **B**) have been assigned against the molecule shown in the inset. Also observed in the ^1H NMR spectrum, at approximately 3.32 ppm, was the residual signal from the solvent, methanol- d_4 .^[213] Due to the rapid H/D exchange at the amine functionality, **L** denotes either a hydrogen atom (H) or a deuterium atom (D).

Figure 6.6 compares the ^1H and ^2H NMR spectra for the deuteration reaction of mandelonitrile. Confirming the presence of deuterium by direct detection, the ^2H NMR spectrum shows the inverse to that obtained by ^1H NMR spectroscopy. Moreover, Figure 6.6 shows that distinctive peaks, indicating deuterium incorporation, are observed by ^2H NMR spectroscopy at *both* aliphatic positions. However, due to the sensitivity issues linked with ^2H NMR spectroscopy, the spectra are not quantitative. It can clearly be seen in Figure 6.6 that the peak for carbon **B** is more intense than the peak representing carbon **A**. In line with the findings of the ^1H NMR spectroscopy relative integrations of 1H and 2H, for carbons **A** and **B**, respectively, are observed.

Table 6.2. Predicted extent of deuteration of the aliphatic protons at carbons **A** and **B** for Pathways **I–III**, as defined in Scheme 6.1. 50% indicates deuteration at one proton whilst 100% indicates deuteration at both protons of carbons **A** and **B** respectively. These predictions are then compared to the experimental findings as determined by ^1H NMR spectroscopy.

<i>Pathway</i>	<i>%D at Carbon A</i>	<i>%D at Carbon B</i>
I	50%	100%
II	100%	100%
III	100%	50%
Experimental	35%	80%

The ^1H NMR and ^2H NMR spectral analysis has allowed the degree of deuteration at both aliphatic positions to be estimated. With reference to Table 6.2, the experimentally determined percentage composition most closely matches the anticipated product of Pathway **I**, where the expected deuteration at carbons **A** and **B** is 50% (experimental *ca.* 35%) and 100% (experimental *ca.* 80%) respectively. Although this result indicates that it is likely that Pathway **I** is favoured, the hydrogen incorporation is shown to be slightly greater than expected. This indicates partial scrambling of H/D within the molecule and suggests the presence of a mixture of isotopologues. In order to further understand this reaction, a more in-depth analysis of the exact product distribution is required.

6.3 Isotopologue Distribution for the Deuteration Reaction of Mandelonitrile is Defined by Mass Spectroscopy

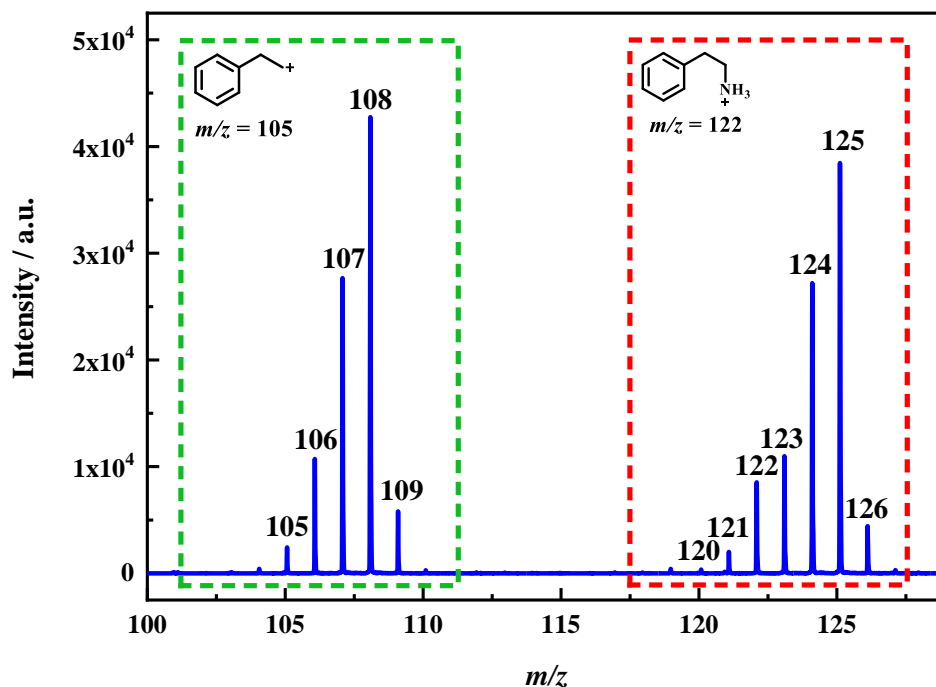


Figure 6.7. Mass spectrometric (ESI⁺) analysis of deuterated mandelonitrile at reaction completion. Highlighted are the two main phenethylamine fragments at $m/z = 122$ ($[\text{C}_6\text{H}_5\text{CH}_2\text{CH}_2\text{NH}_3]^+$, red box) and $m/z = 105$ ($[\text{C}_6\text{H}_5\text{CH}_2\text{CH}_2]^+$, green box).

To achieve a more comprehensive picture of the reaction mixture, mass spectrometry of the deuterated product mixture produced in the mandelonitrile deuteration reaction was performed. Sampling was undertaken at reaction completion (time = 120 minutes). The resultant spectra, presented in Figure 6.7, shows peaks representing the two main fragments of phenethylamine at $m/z = 122$ ($[\text{C}_6\text{H}_5\text{CH}_2\text{CH}_2\text{NH}_3]^+$) and $m/z = 105$ ($[\text{C}_6\text{H}_5\text{CH}_2\text{CH}_2]^+$). The by-product of the reaction, 2-amino-1-phenylethanol, would then be expected to exhibit $[\text{MH}]^+$ at $m/z = 138$ and a $[\text{MN}-\text{H}_2\text{O}]^+$ fragment at $m/z = 120$. Thus, in the deuteration experiment, ions for this fragment may be observed in the $m/z = 120$ –123 range, depending on the level of deuteration observed. Therefore, overlap of phenethylamine and 2-amino-1-phenylethanol in the $m/z = 122$ –126 range is possible. The phenethylamine fragment at $m/z = 122$ (Figure 6.7, red box) was thus excluded from the subsequent analysis. The $m/z = 105$ fragment (Figure 6.7, green box), representative of phenethylamine minus the amine group, is consequently selected for further

examination. The accompanying peaks ($m/z = 106$ – 109) are representative of the isotopic pattern.

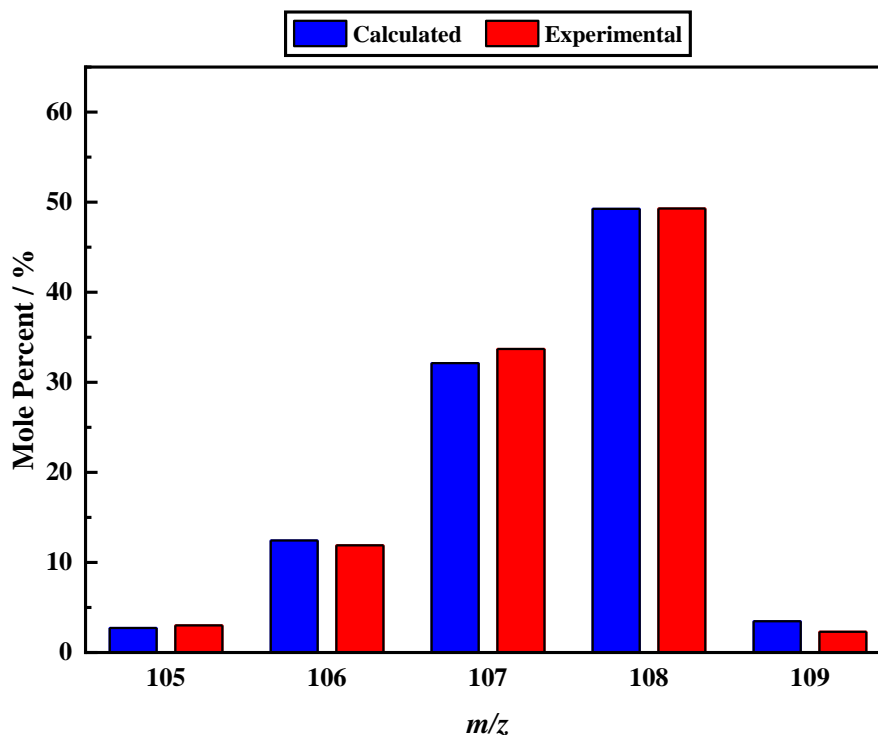


Figure 6.8. Mole percent of each m/z peak (105–109), corresponding to phenethylamine- D_0 – D_4 , normalised to the major peak observed by mass spectrometry. Experimentally obtained data is presented in red and shows good correlation with the calculated values presented in blue.

It is proposed in Section 6.1 that the deuterated sample does not contain a single species, but instead, a mixture of different phenethylamine molecules containing an unknown combination of 0–4 deuterium atoms. Mass spectrometry is therefore used to calculate the isotopic product distribution for the deuteration reaction of mandelonitrile. As the product mixture is comprised of an unknown combination of molecules, the resulting mass spectrum is composed of a linear combination of their respective isotopic patterns. Each isotopic pattern is composed of a major peak (m/z), which is increased by one for the incorporation of each deuterium atom into the phenethylamine- D_0 molecule, and two main satellites at $m/z + 1$ and $m/z + 2$, arising solely from the natural abundance of ^{13}C . The intensities of the satellites, relative to the major peak, are 8.8% and 0.34%, respectively. For a given mixture, a mass spectrum can then be simulated from the linear

combination of each of the phenethylamine-D₀–D₄ molecules. This method is used to calculate the mixture of deuterated phenethylamine molecules which gave the best fit to the experimentally determined spectra. The simulated and experimentally obtained data is shown to correlate well (Figure 6.8), thus allowing for the composition of the deuterated product mixture to be resolved. The resulting composition is given in Table 6.3.

Table 6.3. *Percentage composition of each deuterated phenethylamine species in the reaction mixture as determined by mass spectrometry conducted on the deuterated product mixture at reaction completion (time = 120 minutes).*

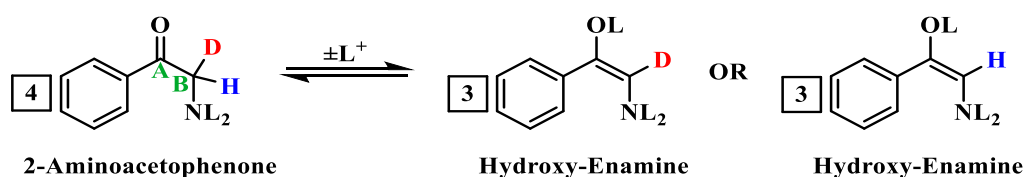
<i>Deuterium Content</i>	D ₀	D ₁	D ₂	D ₃	D ₄
<i>Mole Percent / %</i>	3.0	11.8	33.7	49.2	2.3

From the isotopic distribution calculated by mass spectrometry, it is deduced that the average hydrogen content of carbons **A** and **B** is 0.83H (*cf. ca.* 0.85H by ¹H NMR spectroscopy, Section 6.2). The results obtained by mass spectrometry are therefore in good agreement with the ¹H NMR spectroscopic analysis. The aforementioned analysis, allowing the exact composition of the mixture to be determined, provides valuable mechanistic information. It is shown in Table 6.3 that the deuterated sample is composed predominantly of phenethylamine-D₃ (49.2%), as would be expected from Pathway **I**. Moreover, both the phenethylamine-D₀ and the phenethylamine-D₄ contributions have been found to be ≤3%, and can therefore be considered negligible. It is the absence of phenethylamine-D₄ which enables Pathway **II** *via* the hydroxy-enamine to be eliminated. Despite this evidence which, again suggests favour of Pathway **I**, there is significant production of both phenethylamine-D₁ (11.8%) and phenethylamine-D₂ (33.7%). This finding further complicates analysis as these products cannot be rationalised by Pathways **I–III**.

6.4 To Rationalise the Increased Hydrogen Content the ‘Reverse’ Tautomeric Reactions must be Considered

Postulated Pathways **I–III** (Figure 6.1) do not account for the occurrence of the phenethylamine-D₁ and the phenethylamine-D₂ isotopologues detected by mass spectrometry (Section 6.3). Thus, the presence of more than one aliphatic hydrogen, as implied by the presence of both isotopologues, cannot easily be described. The origin of the observed hydrogen enrichment must therefore be considered further. It should be noted that under the presented reaction conditions, and in the presence of catalyst, phenethylamine-H₄ does not undergo deuterium scrambling. Therefore, any H/D exchange observed *must* occur at the steps incurred prior to product formation. As such, the increased hydrogen contribution is rationalised by a H/D exchange process with either the solvent (methanol) or the acid additive (sulphuric acid), occurring at the equilibria associated with formation of the intermediate species.

It has previously been established that formation of the detectable intermediate species, 2-aminoacetophenone, occurs *via* an acid catalysed tautomeric pathway originating at the hydroxy-imine (Section 5.5). It is therefore suggested that, alongside forward Pathway **I**, there are other pathways which involve the tautomeric equilibria responsible for 2-aminoacetophenone formation in operation. It is proposed that the acid catalysed ‘reverse’ tautomerisation reaction, from the 2-aminoacetophenone (**4**) to the hydroxy-enamine (**3**), and subsequently, the hydroxy-imine (**2**) results in the increased hydrogen incorporation observed (Table 6.3).



Scheme 6.3. Tautomerisation reaction from the ketone 2-aminoacetophenone (**4**) showing the two possible hydroxy-enamine (**3**) isotopologues which may be formed depending on whether a hydrogen (H) atom or a deuterium (D) atom is removed from carbon **B**. Due to the rapid H/D exchange at the amine and alcohol functionalities, **L** denotes either a H atom (H) or a deuterium atom (D).

Scheme 6.3 shows the first step in the abovementioned ‘reverse’ tautomerisation from 2-aminoacetophenone (**4**) to the hydroxy-enamine (**3**). Here it is shown that tautomerisation of 2-aminoacetophenone can yield two hydroxy-enamine isotopologues, based on whether a hydrogen or a deuterium atom is lost from position **B**. The same principle can also be applied to the second equilibria to afford the hydroxy-imine (**2**) from the hydroxy-enamine (**3**) (shown later in Section 6.7). The subsequent hydrogenation reaction of either of the hydroxy-imine (**2**) or the hydroxy-enamine (**3**) isotopologues may then afford a wider product distribution which includes phenethylamine-D₁ and phenethylamine-D₂. The equilibria between species (**2**), (**3**) and (**4**) therefore provides a route for the enhancement of the hydrogen content at aliphatic carbon position **B**. In the same manner, it is believed that the acid catalysed tautomerisation of the imine intermediate (**5**) into the enamine (**6**) allows further hydrogen enhancement at aliphatic carbon position **A** (Figure 6.1).

Tautomerisation along the hydrogen enriching equilibria has been shown to be operational, as evidenced by the production of intermediate 2-aminoacetophenone, however, this process takes a secondary role to direct Pathway **I** which leads to phenethylamine-D_{3-A} as evidenced by the deuterated product distribution (Table 6.3). If the equilibrium reactions were faster than the direct reduction (Pathway **I**), complete scrambling of the deuterium in the molecule would occur resulting in the dominance of either phenethylamine-D₁ or phenethylamine-D₂. As determined by mass spectrometry, this is not the case (Table 6.3). It can hence be understood that the forward (Pathway **I**) and the ‘reverse’ reactions occur concurrently, with the tautomerisation being a reversible side reaction.

6.5 Examination of the Multiplicity Observed in the ¹³C NMR Spectra for the Deuteration Reaction of Mandelonitrile Highlights the Presence of Multiple Phenethylamine Isotopologues

As presented in Figure 6.9, there are a total of five phenethylamine isotopologues, with phenethylamine-D₁, phenethylamine-D₂ and phenethylamine-D₃ each having isotopomers, which can be produced from the deuteration reaction of mandelonitrile, ranging from phenethylamine-D₀ to phenethylamine-D₄. Each isotopologue or isotopomer is given a unique name which acts as a descriptor of its hydrogen and

deuterium composition at the aliphatic carbons of interest (denoted **A** and **B**, as defined in Figure 6.2).

Each isotopologue or isotopomer name shown in Figure 6.9 comprises of a number followed by a series of letters. The number indicates the number of deuterium atoms, out of a possible four, present at the two aliphatic carbon positions. Subscripts **A** and **B** then indicate the presence of a hydrogen atom at aliphatic carbons **A** and **B** respectively. Each letter denotes one hydrogen atom. Therefore, if phenethylamine- $D_1\text{-AAB}$ is considered as an example, D_1 indicates the presence of one deuterium atom. The subsequent sequence of lettering may then be employed to identify the specific arrangement of H and D atoms attached to the aliphatic carbons for this particular isotopologue. $D_1\text{-AAB}$ thus designates HH at carbon **A** and HD at carbon **B**. These rules may be applied to each isotopologue or isotopomer, the accompanying notation is used throughout.

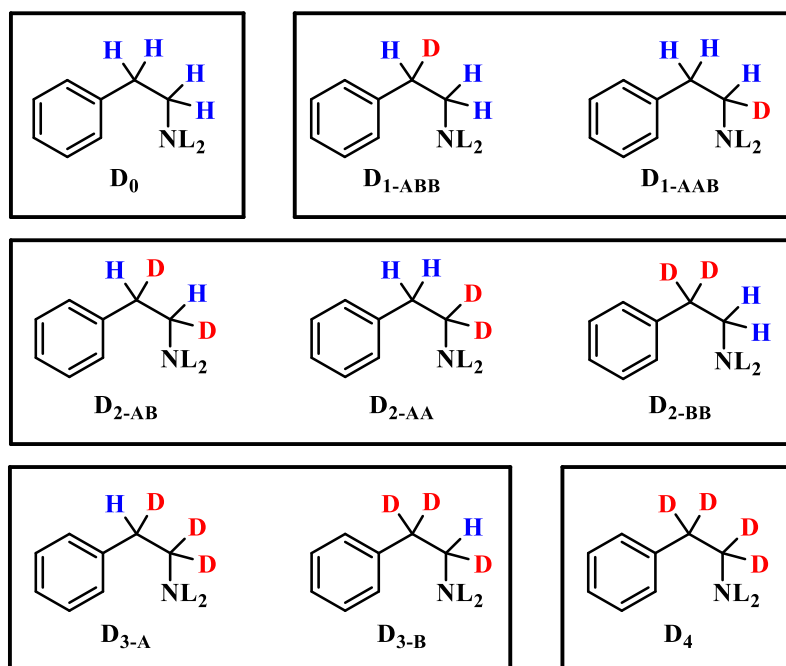


Figure 6.9. The nine phenethylamine isotopologues and isotopomers which can be produced from the deuteration reaction of mandelonitrile. Each isotopologue is given its own unique descriptor based on the positioning of the hydrogen atoms at aliphatic carbons **A** and **B**. Due to the rapid H/D exchange at the amine functionality, **L** denotes either a hydrogen atom (H) or a deuterium atom (D).

Based on the previously described mass spectrometry analysis (Table 6.3), minimal contributions from phenethylamine-D₀ and phenethylamine-D₄ are expected. In addition, Table 6.3 shows phenethylamine-D₃ to be the major product. Phenethylamine-D₃ may manifest itself as one of two isotopomers (phenethylamine-D_{3-A} or phenethylamine-D_{3-B}, as defined in Figure 6.9) depending on the positioning of the aliphatic hydrogen atom. The complementary ¹H NMR spectroscopy studies (Section 6.2), however, have indicated that the greater degree of deuteration is at carbon **B**, thus suggesting that phenethylamine-D_{3-A} is the favoured phenethylamine-D₃ isotopologue.

Following this, the use of ¹³C NMR spectroscopy can be utilised to add a layer of detail to the isotopologue and isotopomer distribution. Analysis of the splitting pattern for the ¹³C NMR spectra obtained from the deuteration reaction of mandelonitrile can be used to provide further information regarding the product distribution for this reaction. As previously discussed, the deuteration reaction of a material may yield a product, or a product mixture, with varying degrees of deuteration. For the ¹³C NMR spectroscopy experiment, whilst the protons have been decoupled from the spectra, the deuterium atoms have not. Therefore, different splitting patterns are to be expected based on the number of deuterium atoms attached to a particular carbon atom in the molecule. As such, interpretation of the resultant splitting pattern may be used as a tool to determine if a single product, or a product mixture, is observed.

Each chemically different magnetic nucleus, or set of nuclei, will give rise to a peak or a multiplet in the corresponding NMR spectra. Coupling of a magnetic nucleus **Z** to *N* equivalent nuclei with spin **I** will split the signal from **Z** into a multiplet consisting of **2NI+1** peaks. Considering that ²H is a spin (**I**) = 1 nuclei, the relative peak intensities for multiplet peaks arising from spin-spin coupling of a nucleus to *N* equivalent nuclei can be determined.

Table 6.4. Multiplicity and expected peak intensity ratio for the peaks associated with *N* equivalent nuclei for a spin = 1 nucleus. In this instance, *N* is representative of the number of deuterium (*D*) atoms attached to each aliphatic carbon in phenethylamine.

<i>N</i> (<i>D</i>)	<i>Expected Peak Intensity Ratio</i>	<i>Multiplicity</i>
0	1	Singlet
1	1:1:1	Triplet
2	1:2:3:2:1	Quintet

At each of phenethylamines' aliphatic carbon positions, **A** and **B**, there are three possible outcomes in terms of composition: HH, HD or DD. Consequently, expected peak intensity for the multiplets corresponding to the degree of deuteration at each aliphatic carbon in the sample (CH₂, CHD or CD₂) can be predicted (Table 6.4). Peak assignment for each carbon can therefore be primarily achieved using the predicted splitting pattern associated with each species at that location (singlet/triplet/quintet, corresponding to CH₂/CHD/CD₂). Moreover, an additional factor to consider is that the presence of deuterium induces an upfield chemical shift on the carbon atoms. This is usually between 0.2–1.5 ppm for a one-bond shift and around 0.1 ppm for a two-bond shift.^[236–237] Accordingly, each isotopologue or isotopomer present in the mixture will be expected to have a unique set of multiplets.

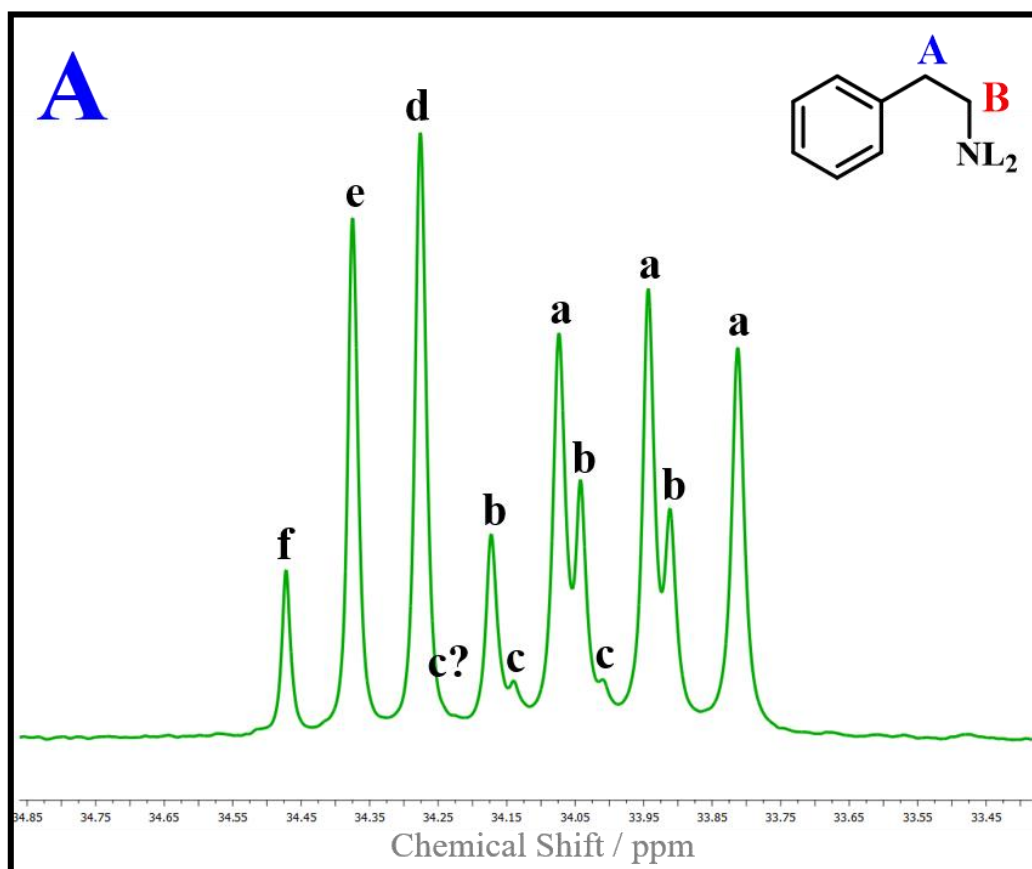


Figure 6.10. Expansion of the splitting pattern observed for aliphatic carbon **A**, assigned against phenethylamine, inset. Assignments **a–f** denote the splitting patterns associated with each phenethylamine isotopologue present in the reaction mixture as detected by proton decoupled ^{13}C NMR spectroscopy. Due to the rapid H/D exchange at the amine functionality, **L** denotes either a hydrogen atom (H) or a deuterium atom (D).

An expansion of the splitting pattern for carbon **A**, which corresponds to the benzylic carbon, can be observed in Figure 6.10. The spectra can be interpreted as a combination of six isotopologues comprised of three triplets (CHD, $\delta = 33.74/33.04/34.14$ ppm) denoted **a**, **b** and **c** and three singlets (CH_2 , $\delta = 34.28/34.38/34.47$ ppm) designated **d**, **e** and **f** in Figure 6.10. Due to the absence of quintet signals, the possibility of two deuterium atoms (DD) at carbon **A** can be eliminated. Therefore, it is deduced that the composition of carbon **A** is either CHD or CH_2 .

The outcome of Figure 6.10 is confirmed by two-dimensional distortionless enhancement by polarisation transfer (DEPT) edited heteronuclear single quantum coherence (HSQC) NMR spectroscopy of the phenethylamine produced by the deuteration reaction of

mandelonitrile. Each peak in an HSQC spectrum corresponds to a peak in the ^1H spectrum and a peak in the ^{13}C spectrum. However, an HSQC peak only occurs when the atoms are directly connected, any carbon atom without an attached hydrogen atom will not give a peak. Further, whilst not relevant here, the same applies to a proton which is not attached to a carbon atom, for example OH or NH.^[238] It will therefore not be possible to observe any isotopologue of phenethylamine which possesses CD_2 at either carbon **A** or **B** by these means.

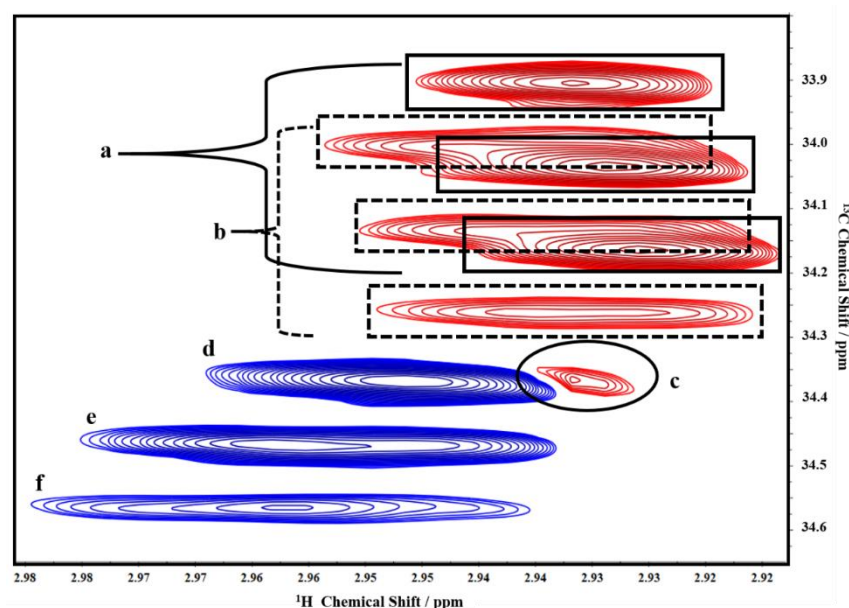


Figure 6.11. Two-dimensional DEPT edited HSQC NMR spectroscopy associated with carbon A. [CH signals = red; CH₂ signals = blue]. Letter assignments **a–f** correspond to the associated signals observed in Figures 6.12.

Figure 6.11 shows the two-dimensional DEPT edited HSQC NMR spectroscopy associated with carbon A. As the data has been collected using a DEPT edited sequence the CH₃ and CH signals are on a different phase (up; red) from the CH₂ signals (down; blue). It should, however, be noted that there are no methyl groups present in this particular example. Highlighted in blue in Figure 6.11 are the CH₂ signals representing the three singlets **d**, **e**, and **f**, as shown in Figure 6.10. Contrastingly, the red signals represent either CH or CH₃. As carbon A is a mid-chain aliphatic carbon, the maximum number of protons present at this position is two. Thus, represented in red are the signals that correspond to CHD. Figure 6.11 therefore shows the three sets of triplet signals,

designated as **a**, **b**, and **c** in Figure 6.10. Although a degree of overlap is observed, three sets of signals are apparent.

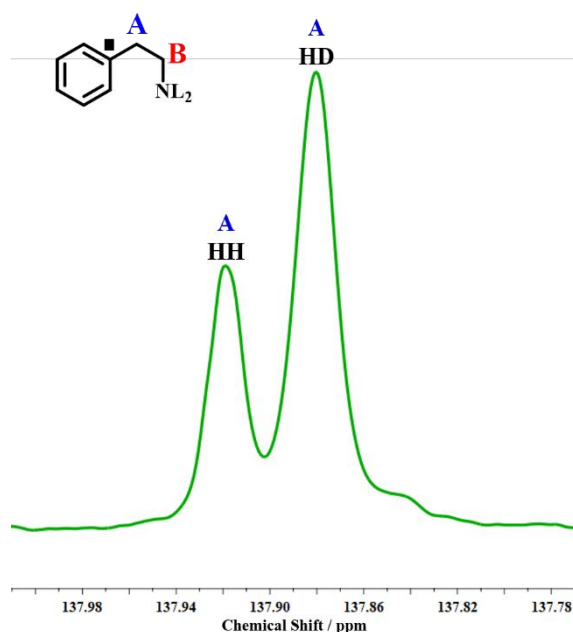


Figure 6.12. ^{13}C NNMR spectra for the deuteration reaction of mandelonitrile in the 137.8–138.0 ppm range showing the signal assigned to the quaternary carbon of phenethylamine (assigned with a square symbol). Two distinct signals are detected due to the isotopic effect which is observed as a result of the varying deuterium substitution at carbon **A** (CH_2/CHD). Due to the rapid exchange at the amine functionality, **L** denotes either a hydrogen atom (*H*) or a deuterium atom (*D*).

Analysis of the multiplet assigned to carbon **A** (Figure 6.10) has allowed identification of six isotopologues or isotopomers each possessing either CH_2 or CHD at this position. Examination of the peak associated with the quaternary carbon adjacent to carbon **A**, denoted by a black square in Figure 6.12, provides confirmation of this. The presence of two distinct signals at this position indicates the presence of two possible isotopic environments at carbon **A**. These environments have previously been identified as CH_2 and CHD (Figure 6.10), thus Figure 6.12 endorses the absence of CD_2 at this position.

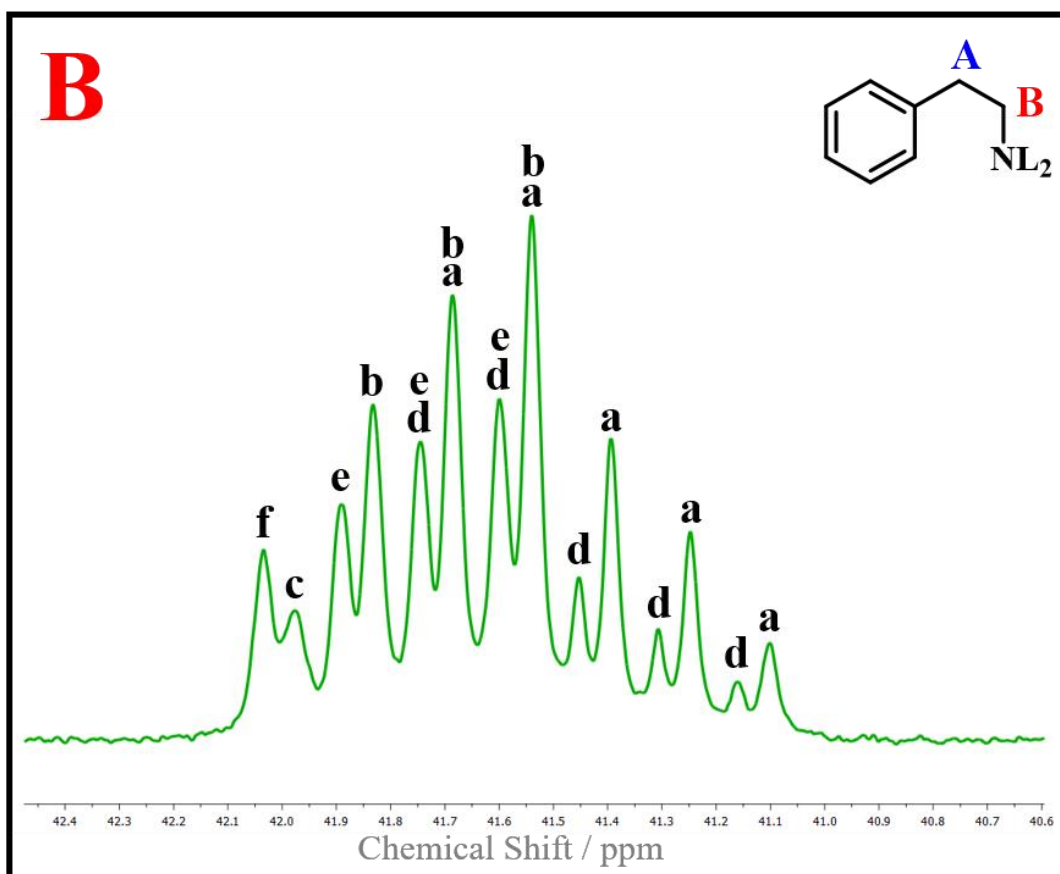


Figure 6.13. Expansion of the splitting pattern observed for aliphatic carbon **B**, assigned against phenethylamine, inset. Assignments **a–f** denote the splitting patterns associated with each phenethylamine isotopologue present in the reaction as determined by proton decoupled ^{13}C NMR spectroscopy. Due to the presence of rapid H/D exchange at the amine functionality, **L** denotes either a hydrogen atom (H) or a deuterium atom (D).

Carbon **B** is initially found to exhibit a slightly more complex splitting pattern than was observed for carbon **A**. Nevertheless, a similar analysis on carbon **B** (Figure 6.13) confirms the aforementioned findings. The splitting pattern of carbon **B** is composed of two quintets (CD_2 , $\delta = 41.39/41.45$ ppm), two triplets (CHD , $\delta = 41.69/41.75$ ppm), and two singlets (CH_2 , $\delta = 41.98/42.03$ ppm). The three signals, corresponding to the three unique compositions of carbon **B** (CD_2 , CHD or CH_2), are each split in two. A chemical shift separation of 0.05 ppm between the signals is observed as a result of the isotope effect experienced due to the two, pre-determined, isotopic options available at carbon **A** (CH_2/CHD). The same effect was observed at the quaternary carbon as shown in Figure 6.12.

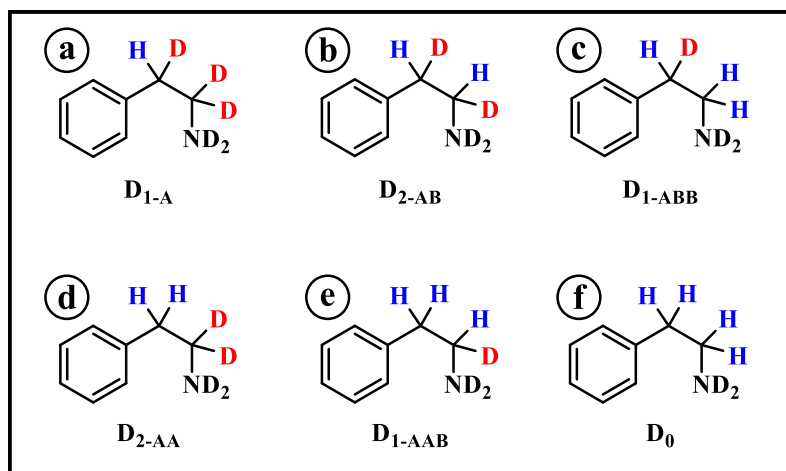


Figure 6.14. The six phenethylamine isotopologues and isotopomers produced in the deuteration reaction of mandelonitrile as identified by ^{13}C NMR spectroscopy. Letter assignments **a–f** correspond to the associated signals observed in Figures 6.10 and 6.13.

Identification of all six isotopologues and isotopomers (**a–f**), based on the isotope effect and the splitting patterns of both aliphatic carbon atoms are presented in Figure 6.14. It should be noted that phenethylamine- D_4 , detected by mass spectrometry in negligible quantities, was not detectable by ^{13}C NMR spectroscopy. Interestingly, however, phenethylamine- D_0 , detectable in similar quantities by mass spectrometry to phenethylamine- D_4 , was observed by ^{13}C NMR spectroscopy.

The deuterium presence greatly reduces the intensity of the signals on the ^{13}C NMR spectra as a consequence of peak splitting (carbons bonded to deuterium are split by residual C-D coupling), making detection harder. Further, an increase in the ^{13}C T_1 relaxation arises as it is the interaction with protons which provides the main relaxation mechanism for the ^{13}C spins. It is therefore possible that the relaxation delay associated with the NMR measurement will not be sufficient to allow full relaxation of the deuterated species which contain a higher deuterium content.^[232] If this is the case, then the highly deuterated isotopologues such as phenethylamine- D_4 , will be underestimated when compared to the isotopologues which have a low deuterium content, for example phenethylamine- D_0 .

6.6 Quantitative ^{13}C NMR Spectroscopy Confirms the Mass Spectrometry Findings

To compliment the mass spectrometry study (Section 6.3), quantitative ^{13}C NMR spectroscopy on the deuterated product mixture was conducted. In order to achieve a quantitative ^{13}C NMR spectra, two parameter changes, which were reported in Section 2.4.2, were required. Firstly, as the various components may have different relaxation times, the relaxation delay (D1) was increased to 30 seconds (*cf.* the standard D1 is 1–1.5 seconds). If the pulsing is too quick, then the slowly relaxing signals will not have the opportunity to recover between scans, leading to a reduction in signal intensity, and thus, poor quantification. It is noted that, whilst the use of ‘normal’ pulsing is typically advocated for the determination of compound ratios in a mixture, such an approach is not suitable for comparing carbon atoms with a different number of attached protons, as is the case for the phenethylamine isotopologue mixture.^[239]

Secondly, the decoupling power used during the relaxation delay was reduced to prevent potential build-up of the Nuclear Overhauser Effect (NOE). The Nuclear Overhauser effect is the transfer of nuclear spin polarisation from one population of spin nuclei to another *via* cross relaxation and is produced during normal decoupling.^[109] As NOE build-up may differ between components, especially if they have a different number of attached protons, its presence could be a further source of inaccurate quantification. In this instance, however, the absence of any significant increase in line width in the relevant spectra indicates the absence of any NOE.

Again, during spectral analysis, care must be given to potential peak overlap. With reference to Figures 6.10 and 6.13, where the splitting pattern associated with aliphatic carbons **A** and **B** are considered, it is observed that there is a greater degree of peak overlap at carbon **B**. Although analysis of both splitting patterns should yield the same result, carbon **A** is selected for quantitative analysis due to the lesser extent of peak overlap at this position. Subtraction of known peaks at overlap regions can be used to determine peak integration of the components of a mixed peak. Nonetheless, this method is less reliable than integration of a lone peak and can decrease the overall accuracy. By applying this method, a percentage of each identified isotopologue or isotopomer of phenethylamine produced in the reaction (Figure 6.14) can be calculated. The results of which are presented in Table 6.5.

Table 6.5. Percentage of each of the six phenethylamine isotopologues and isotopomers produced in the deuteration reaction of mandelonitrile as determined by quantitative ^{13}C NMR spectroscopy.

<i>Isotopologue</i>	a	b	c	d	e	f
<i>Composition</i>	HD DD	HD HD	HD HH	HH DD	HH HD	HH HH
<i>Percentage</i>	39.5%	22.6%	4.2%	16.0%	13.7%	4.0%

Combining the percentages of isotopomers **b** and **d**, and isotopomers **c** and **e** gives the full component of phenethylamine-D₂ and phenethylamine-D₁, respectively. The results can then be compared to the quantitative mass spectrometry findings presented in Section 6.3 (Figure 6.8).

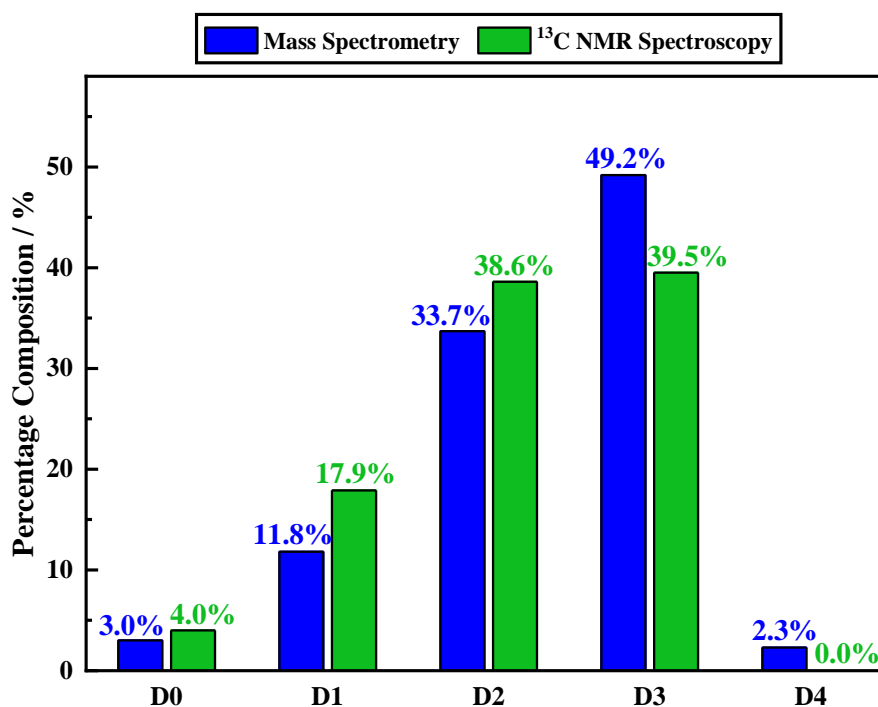


Figure 6.15. Percentage composition of each phenethylamine isotopologue as determined at reaction completion (time = 120 minutes) by mass spectrometry (blue bars) and ^{13}C NMR spectroscopy (green bars). For phenethylamine-D₁, phenethylamine-D₂ and phenethylamine-D₃ the composite isotopomers have been combined to give the isotopologue total.

Figure 6.15 demonstrates that the quantitative mass spectrometry and ^{13}C NMR spectroscopy studies show the same general trends and are thus largely comparable. For both analysis techniques there is minimal contribution from phenethylamine- D_0 and phenethylamine- D_4 . In both instances, production of phenethylamine- D_3 as the major product is additionally observed. Despite these similarities, there are some notable differences between the two techniques. Specifically, these differences in the detected percentages of each isotopologue are found to be correlated to the number of deuterium atoms present.

It is observed that by ^{13}C NMR spectroscopy, there appears to be marginally more phenethylamine- D_1 and phenethylamine- D_2 , but less phenethylamine- D_3 , than detectable by mass spectrometry. This finding could perhaps indicate that H/D scrambling at the tautomeric equilibria is more significant than initially indicated by mass spectrometry. Nevertheless, it is proposed that isotopologues with a higher deuterium content (phenethylamine- D_3 and phenethylamine- D_4 in this instance) are under-represented using this technique. The presence of deuterium in a molecule increases the T_1 relaxation of the ^{13}C nucleus. Thus, for the highly deuterated isotopologues it is possible that the time required to relax all the nuclei will exceed the allotted 30 seconds. This will result in a reduced representation for these isotopologues. As the deuterium content is lowered, it becomes increasingly likely that all the nuclei will relax within 30 seconds. This hypothesis can be effectively used to rationalise the findings of Figure 6.15.

6.7 The Observed Deuterated Phenethylamine Isotopologue and Isotopomer Distribution Allows Refinement of the Reaction Mechanism

Analysis by mass spectrometry (Section 6.3) and ^{13}C NMR spectroscopy (Sections 6.1 and 6.5) has indicated the presence of a mixture of phenethylamine isotopologues ranging from phenethylamine- D_0 to phenethylamine- D_3 . Linking this outcome to the reaction scheme (Scheme 6.1), allows insight into the active pathways to be gleaned.

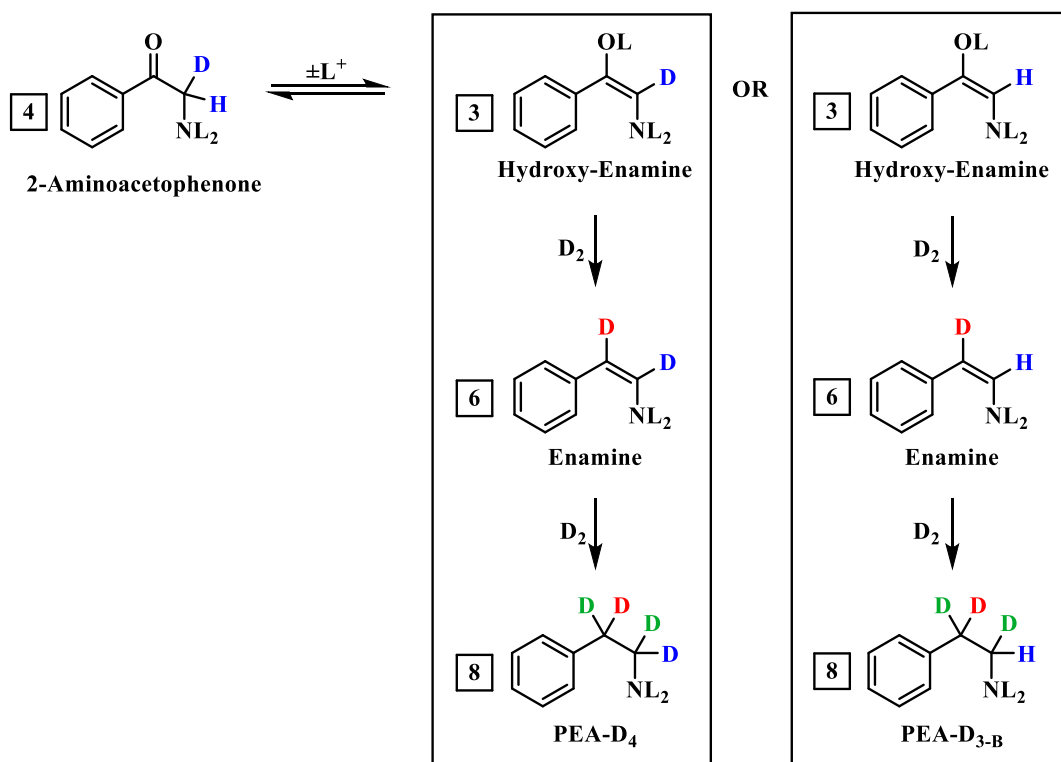
To a first approximation, the negligible quantities of phenethylamine- D_4 detected by mass spectrometry indicate that forward Pathway **II**, *via* the hydroxy-enamine, can be eliminated. Excluding Pathway **III** on kinetic grounds (Section 5.7), this would then imply that the remaining pathway, Pathway **I**, is the active route. Nevertheless, due to the

presence of a complex reaction mixture containing a total of six isotopologues and related isotopomers of phenethylamine and the occurrence of a H/D scrambling process (Sections 6.4 and 6.5), a more intricate reaction mechanism must be considered.

Phenethylamine-D_{3-A} is identified as the major phenethylamine isotopologue (49.2% by mass spectrometry). As such, Pathway **I** is confirmed to be active in the formation of phenethylamine by means of mandelonitrile hydrogenation. The occurrence of the ‘reverse’ acid catalysed tautomeric pathways, resulting in the hydrogen enrichment observed in the isotopologue distribution, are also acknowledged. With reference to Figure 6.1, hydrogen scrambling during the deuteration reaction may *only* occur at two reaction steps and affect *only* one carbon at a time. The equilibria between molecules (**3**) and (**4**) will enrich carbon **B** whilst the equilibria between molecules (**5**) and (**6**) will enrich carbon **A** (Figure 6.1). Moreover, it is essential to note that the remaining equilibrium in the system, between molecules (**2**) and (**3**), is not involved in the H/D scrambling process as it is a hydrogen atom and not a deuterium atom which is removed. Replacement of the hydrogen atom by another hydrogen atom in the enrichment process renders this equilibria hydrogen enrichment neutral.

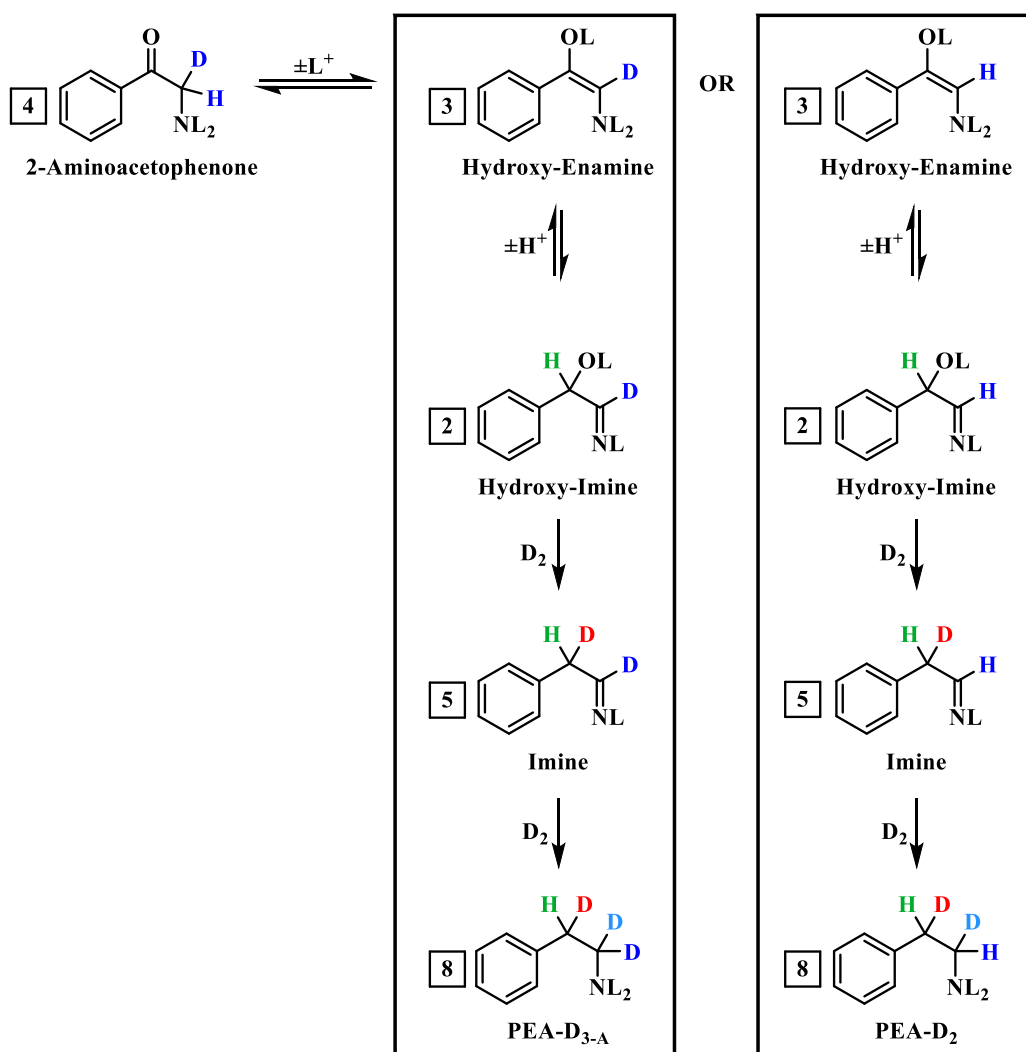
In order to establish what is possible mechanistically, the position of the deuterium and the degree of deuteration within the molecule must be followed for all possible reaction pathways. The expected deuterated product from each potential pathway can then be compared to the known isotopologue and isotopomer distribution (Figure 6.17) to determine whether a pathway is feasible or not.

Pathways **I–III**, linked to the initially proposed forward pathways, have previously been described, and are presented collectively in Scheme 6.1. It was identified that, out of the three routes originally postulated, only Pathway **I** was active. When hydrogen scrambling at the three active equilibria is considered, however, additional pathways (**IV–VI**) may also be considered. Utilising the numbers assigned to each molecule in Figure 6.1, Pathways **IV–VI** may be defined. Common with all three additional pathways (**IV–VI**) are the initial steps: hydrogenation of the mandelonitrile (**1**) to the hydroxy-imine (**2**) followed by tautomerisation to the hydroxy-enamine (**3**), (**1**→**2**→**3**). These initial steps have been removed from each of the schemes for simplicity.



Scheme 6.4. Pathway **IV** – the reaction sequence (1), (2), (3) proceeds (4) in the figure but has been omitted for clarity in this instance. Due to the rapid H/D exchange on the amine and alcohol functionalities, **L** has been used to denote either a hydrogen atom (H) or a deuterium atom (D). [PEA = phenethylamine].

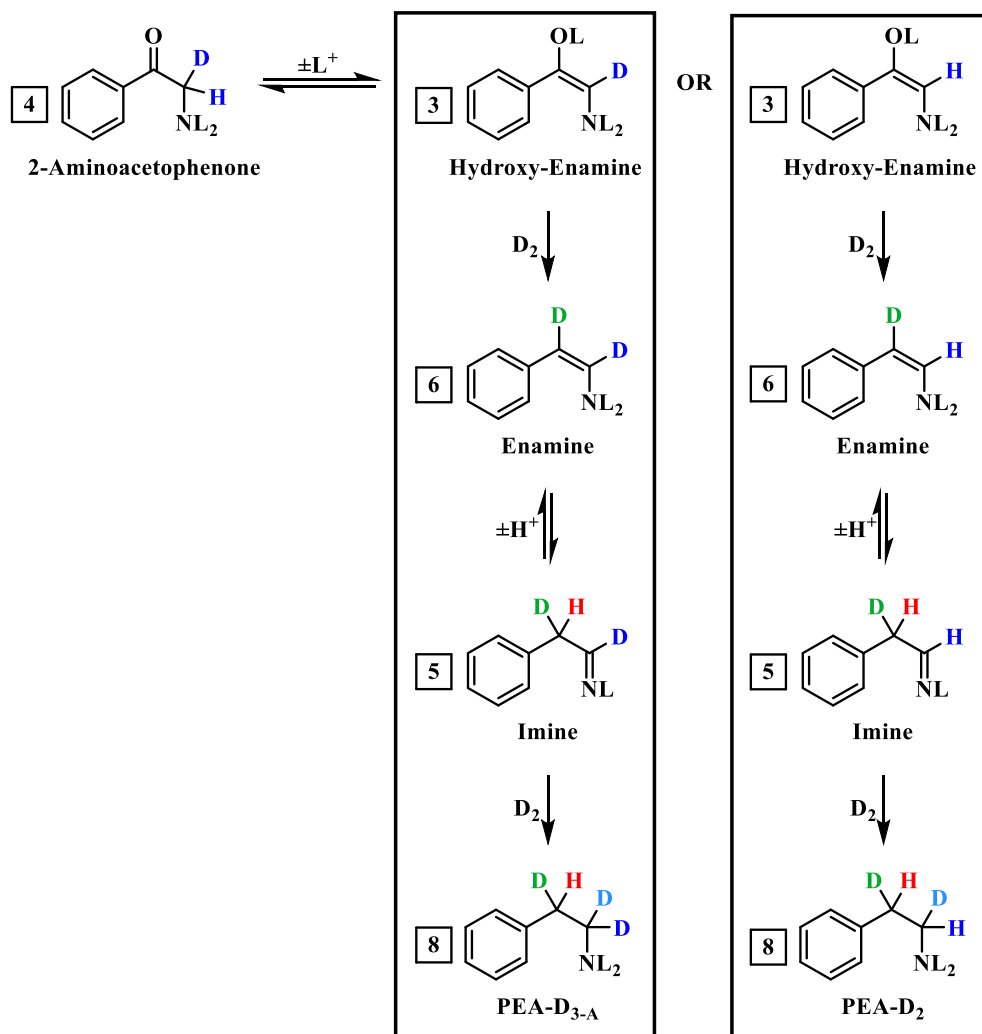
Pathway **IV** is presented in Scheme 6.4 and can be considered as being analogous to Pathway **II**. As shown in Scheme 3.3, the occurrence of the ‘reverse’ tautomeric reaction at ketone (4) may yield two hydroxy-enamine isotopologues depending on whether it is a hydrogen or a deuterium atom which is removed from carbon **B**. This pathway therefore incurs scrambling between molecules (3) and (4) which results in the possibility for hydrogen enrichment at carbon **B**. Direct hydrogenation of the hydroxy-enamine (3) to enamine (6) and finally phenethylamine (8), without any further exchange at the active equilibria, results in either phenethylamine- D_4 or phenethylamine- D_{3-B} . Neither of these isotopologues of phenethylamine were detectable by the analytical methods employed (mass spectrometry and ^{13}C NMR spectroscopy), and so, it can be deduced that Pathway **IV** is inactive.



Scheme 6.5. Pathway V - the reaction sequence (1), (2), (3) proceeds (4) in the figure but has been omitted for clarity in this instance. Due to the rapid H/D exchange on the amine and alcohol functionalities, **L** has been used to denote either a hydrogen atom (H) or a deuterium atom (D). [PEA = phenethylamine].

As Pathway IV is analogous to Pathway II, Pathway V (Scheme 3.5) is analogous to Pathway I. Upon formation of the intermediate 2-aminoacetophenone (4), the ‘reverse’ tautomeric reaction from (4) to the hydroxy-enamine (3) is again invoked. As in Pathway IV, this process allows H/D scrambling leading to the potential for hydrogen enrichment at carbon B. The second ‘reverse’ tautomerisation of the hydroxy-enamine (3) to the hydroxy-imine (2), however, is identified as enrichment neutral, in that, whilst a hydrogen atom is removed, it is also replaced. Pathway V subsequently follows the same route as Pathway I to reach both phenethylamine-D_{3-B} and phenethylamine-D₂. Both of these

phenethylamine isotopologues have been detected by analytical means, and thus, it can be deduced that Pathway **V** is an active route to afford phenethylamine.

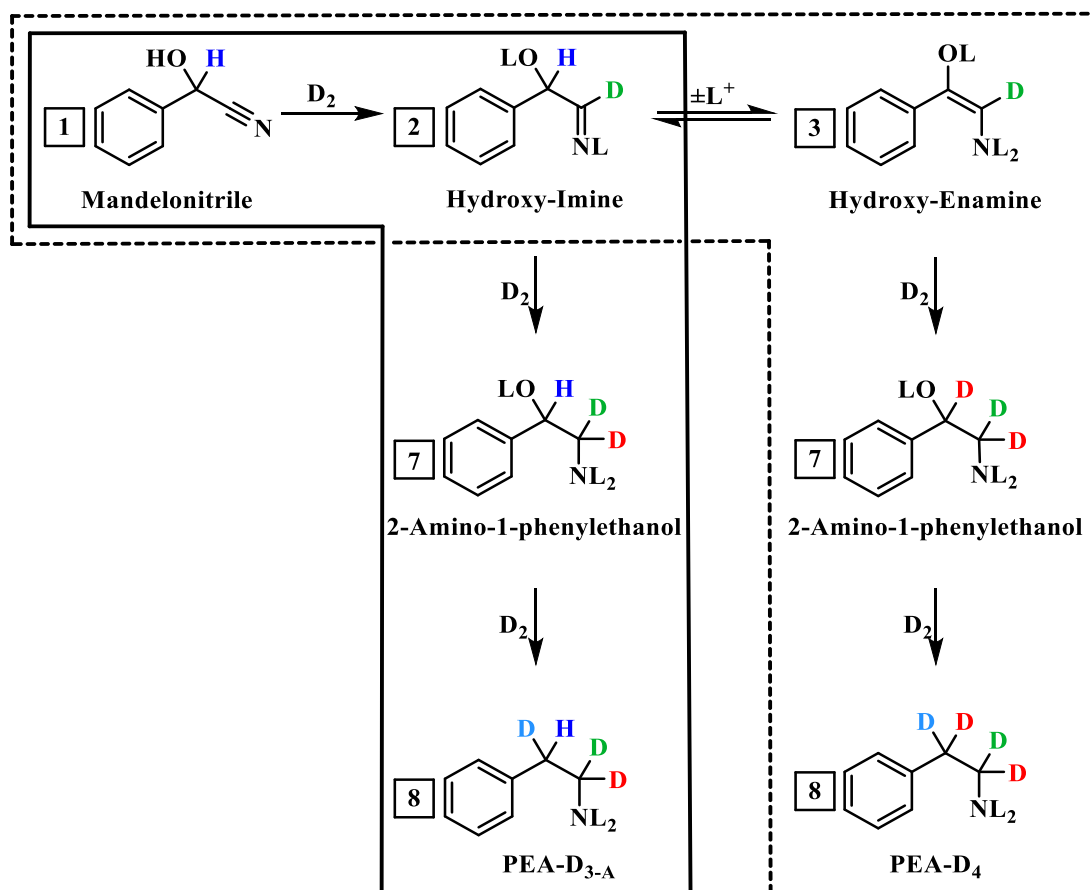


Scheme 6.6. Pathway **VI** - the reaction sequence (1), (2), (3) proceeds (4) in the figure but has been omitted for clarity in this instance. Due to the rapid H/D exchange on the amine and alcohol functionalities, **L** has been used to denote either a hydrogen atom (H) or a deuterium atom (D). [PEA = phenethylamine].

In contrast to Pathways **IV** and **V**, Pathway **VI** (Scheme 3.6) incurs H/D exchange at two equilibria (**3**↔**4** and **5**↔**6**) allowing hydrogen enrichment at both aliphatic carbon positions. Tautomeric exchange between molecules (**3**) and (**4**), as previously described, allows enrichment at carbon **B**, whereas exchange between molecules (**5**) and (**6**) enables enrichment at carbon **A**. Deuteration of imine (**5**) may then yield phenethylamine

isotopologues phenethylamine-D_{3-A} and phenethylamine-D₂, hence Pathway **VI** is also identified as an active pathway.

Included for completeness are two further pathways, Pathways **VII** and **VIII**. Here, direct deuteration from *either* the hydroxy-imine (**2**) (Pathway **VII**, Scheme 3.7, solid box) or the hydroxy-enamine (**3**) (Pathway **VIII**, Scheme 3.7, dashed box) to 2-amino-1-phenylethanol (**7**) are considered. From this juncture hydrogenolysis of 2-amino-1-phenylethanol (**7**) must be incurred in order to afford phenethylamine (**8**). Neither pathway (**VII** or **VIII**) pass through a hydrogen enriching equilibria, and so, only one phenethylamine isotopologue is possible for each pathway.



Scheme 3.7. Pathways **VII** (solid box) and **VIII** (dashed box). Due to the rapid nature of the H/D exchange on the amine and alcohol functionalities, **L** has been used to denote either a hydrogen atom (H) or a deuterium atom (D).

As shown in Scheme 3.7, Pathway **VIII** is predicted to yield phenethylamine-D₄, and consequently, can be excluded from consideration. Pathway **VII**, however, is expected to yield phenethylamine-D_{3-A}. As this particular isotopomer of the phenethylamine-D₃ isotopologue is detected within the observed distribution, Pathway **VII** may therefore be considered as active. Nonetheless, if one contemplates the previous HPLC studies which indicate that the conversion of 2-amino-1-phenylethanol to phenethylamine is kinetically slow (Section 5.7); this route to phenethylamine may also be eliminated.

At reaction completion (time = 120 minutes), the reaction profile (Figure 5.4) shows production of 2-amino-1-phenylethanol as a by-product. By predicting the progress of deuterium incorporation as the reaction proceeds, it is identified that three pathways (Pathways **III**, **VII** and **VIII**) culminate in the formation of 2-amino-1-phenylethanol instead of phenethylamine as a consequence of kinetics. Alongside peaks linked to the aliphatic carbons of phenethylamine (**A** and **B**), the ¹³C NMR spectra for the mandelonitrile deuteration reaction also shows peaks associated with the aliphatic carbons of 2-amino-1-phenylethanol (**C** and **D**). Therefore, it is proposed that analysis of the ¹³C NMR spectroscopy splitting patterns associated with the carbon atoms of 2-amino-1-phenylethanol will provide some insight into the formation of this molecule. Specifically, it can be used to determine whether the 2-amino-1-phenylethanol is formed *via* the acid catalysed tautomeric pathway culminating in hydrogenation of 2-aminoacetopheneone (**4**), or, by direct hydrogenation from either the hydroxy-imine (**2**) or the hydroxy-enamine (**3**).

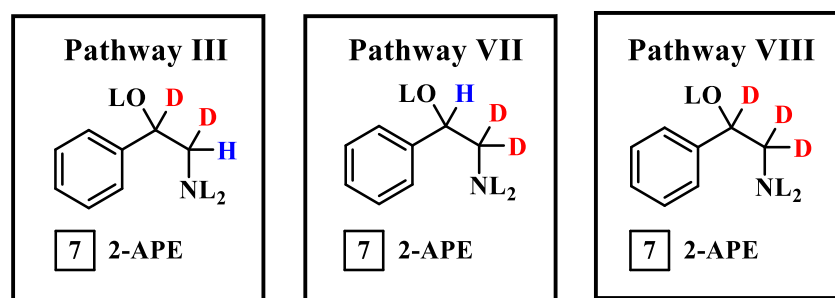


Figure 6.16. Hypothesised deuterated form of 2-amino-1-phenylethanol post deuteration reaction (time = 120 minutes) for Pathways **III**, **VII** and **VIII**. Due to the rapid H/D exchange on the amine and alcohol functionalities, **L** has been used to denote either a hydrogen atom (H) or a deuterium atom (D).

Figure 6.16 shows the predicted form of the deuterated 2-amino-1-phenylethanol resulting from Pathways **III**, **VII** and **VIII**. In this instance there are only four possible isotopologues of 2-amino-1-phenylethanol with 2-amino-1-phenylethanol-D₁ and 2-amino-1-phenylethanol-D₂ each containing two isotopomers (*cf.* nine possible isotopologues and associated isotopomers for phenethylamine) due to the presence of a hydroxyl group at position **C**. Figure 6.17 examines the ¹³C NMR spectra at approximately 70 ppm and 47 ppm showing aliphatic carbons **C** and **D** of 2-amino-1-phenylethanol respectively.

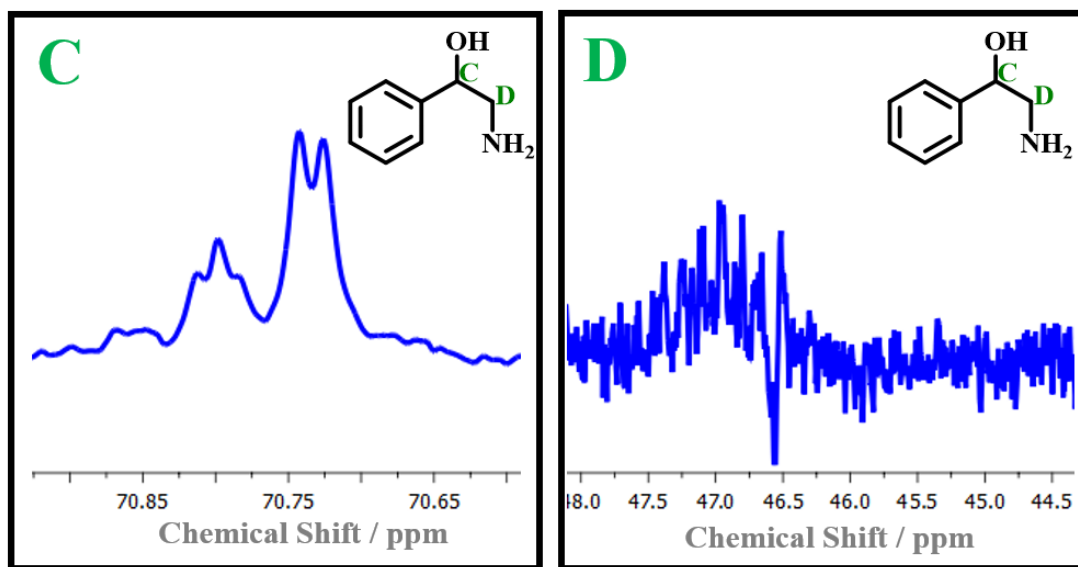


Figure 6.17. Splitting pattern observed in the ¹³C NMR spectra for aliphatic carbons **C** and **D** assigned against 2-amino-1-phenylethanol, inset.

Unfortunately, Figure 6.17 shows that despite a deuterium component being present at both positions (evidenced by the presence of multiplets) clear isotopologue resolution, as was achieved for the analogous aliphatic carbons **A** and **B**, was not possible as a consequence of poor resolution and peak intensity. This is likely due to the reduced concentration of 2-amino-1-phenylethanol in the reaction mixture when compared to that of phenethylamine. Further, 2-amino-1-phenylethanol showed poor solubility in the NMR solvent (methanol-d₄). Signal overlap of carbons **A** and **D** at 2.96 ppm in the ¹H NMR spectrum renders further analysis of carbon **D** impossible. Nevertheless, carbon **C** of 2-amino-1-phenylethanol at 4.92 ppm is clearly resolved. As such, it is possible to compare the integration of this peak for both the hydrogenation and deuteration reactions

of mandelonitrile. From this analysis it is determined that there is an 87% chance that a deuterium atom is present on carbon **C**. The high coincidence of a deuterium presence at carbon **C** narrows down the number of 2-amino-1-phenylethanol isotopologues from six to three, removing all isotopologues with a hydrogen atom at this position. Moreover, out of the three pathways initially proposed to afford 2-amino-1-phenylethanol (Figure 6.16), Pathway **VII** can be eliminated on these grounds. It is therefore tentatively proposed that the probable mixture of isotopologues observed at both carbon positions in Figure 6.16 occurs as the result of activity at the tautomeric equilibria between the hydroxy-imine (**2**), the hydroxy-enamine (**3**) and 2-aminoacetophenone (**4**). Movement between these equilibria is likely to allow hydrogen enrichment at both carbon positions giving rise to the observed isotopologue distribution. Despite this, care must be taken as the quality of the spectra presented in Figure 6.17 is not sufficient to make a definitive conclusion and thus, the mechanistic implications are only proposed.

Comprehensive examination of each of the postulated reaction pathways (**I–VIII**) can be used to provide valuable mechanistic information. This enhanced understanding provides further insight to the reaction scheme, providing a degree of clarity found to be inaccessible by HPLC analysis alone.

6.8 Isotopologue and Isotopomer Analysis is used to Further Enhance the Reaction Mechanism

Initially, three pathways were postulated (Figure 6.1), with Pathways **I–III** expected to yield phenethylamine-D_{3-A}, phenethylamine-D₄ or, phenethylamine-D_{3-B}, respectively. The observed phenethylamine isotopologue or isotopomer in the case phenethylamine-D₃ would therefore ideally provide an indication of the active route from reagent to product in the hydrogenation reaction of mandelonitrile. Through the presence of some of the more hydrogen rich isotopologues (phenethylamine-D₀, phenethylamine-D₁ and phenethylamine-D₂), it became clear that Pathways **I–III** cannot be considered in isolation. The presence of these isotopologues can be rationalised by H/D exchange at each of the three active equilibria resulting in hydrogen enrichment at both aliphatic carbons (Section 6.4). Consequently, additional pathways were proposed. Following the progress of the deuterium incorporation for each of these pathways allowed the prediction

of a unique set of products for each pathway to be determined. Full schematic descriptions of each pathway have already been discussed, with the findings summarised in Table 6.6.

Table 6.6. *Proposed Pathways I–VIII for the deuteration reaction of mandelonitrile to afford phenethylamine. A sequence for each pathway is defined along with the expected deuterated phenethylamine isotopologue or isotopologues and an assessment of the accessibility of each route based on the observed product distribution. Each molecule has previously been assigned a number (Figure 6.1), and it is these numbers which have been employed to define the route. Where two phenethylamine isotopologues are possible (Pathways IV, V and VI), both have been specified. Product subscript notation has been described prior (Section 6.5).*

<i>Path</i>	<i>Sequence</i>	<i>Product(s)</i>	<i>Accessible?</i>
<i>I</i>	<i>1,2,5,8</i>	<i>D_{3-A}</i>	<i>Yes</i>
<i>II</i>	<i>1,2,3,6,8</i>	<i>D₄</i>	<i>No</i>
<i>III</i>	<i>1,2,3,4,7,8</i>	<i>D_{3-B}</i>	<i>No</i>
<i>IV</i>	<i>1,2,3,4,3,6,8</i>	<i>D_{3-B} + D₄</i>	<i>No</i>
<i>V</i>	<i>1,2,3,4,3,2,5,8</i>	<i>D_{2-AB} + D_{3-A}</i>	<i>Yes</i>
<i>VI</i>	<i>1,2,3,4,3,6,5,8</i>	<i>D_{2-AB} + D_{3-A}</i>	<i>Yes</i>
<i>VII</i>	<i>1,2,7,8</i>	<i>D_{3-A}</i>	<i>No</i>
<i>VIII</i>	<i>1,2,3,7,8</i>	<i>D₄</i>	<i>No</i>

The phenethylamine isotopologue and isotopomer distribution, as determined by mass spectrometry and ¹³C NMR spectroscopy, indicates the absence of phenethylamine-D_{2-BB}, phenethylamine-D_{3-B} and phenethylamine-D₄. Pathways which yield these phenethylamine isotopologues can therefore be eliminated. As such, Pathways **II**, **III**, **IV** and **VIII** are removed from consideration. Interestingly, it is noted that each of the absent isotopologues or isotopomers contains DD at aliphatic carbon **A**, thus providing a strong indication that there is a hydrogen component at carbon **A**. This is in line with all experimental findings reported prior.

Predicted to produce phenethylamine-D_{3-A}, Pathway **VII** may technically be considered viable. Nonetheless, this pathway can be disregarded on kinetic grounds, as the conversion of 2-amino-1-phenylethanol (**7**) to phenethylamine (**8**) has been shown to be incredibly slow (Section 5.7). Similar to Pathway **VII**, Pathway **III** also culminates in the kinetically hindered conversion of 2-amino-1-phenylethanol (**7**) to phenethylamine (**8**). Therefore, the absence of products associated with Pathway **III** (phenethylamine-D₄) can be used to provide additional evidence for the exclusion of Pathway **VII**.

The number of active pathways is therefore narrowed down. Accordingly, three active pathways are identified. With reference to Figure 6.1, where all involved species are numbered for clarity, the following pathways can be defined with the sequence of numbered species defining the individual steps:

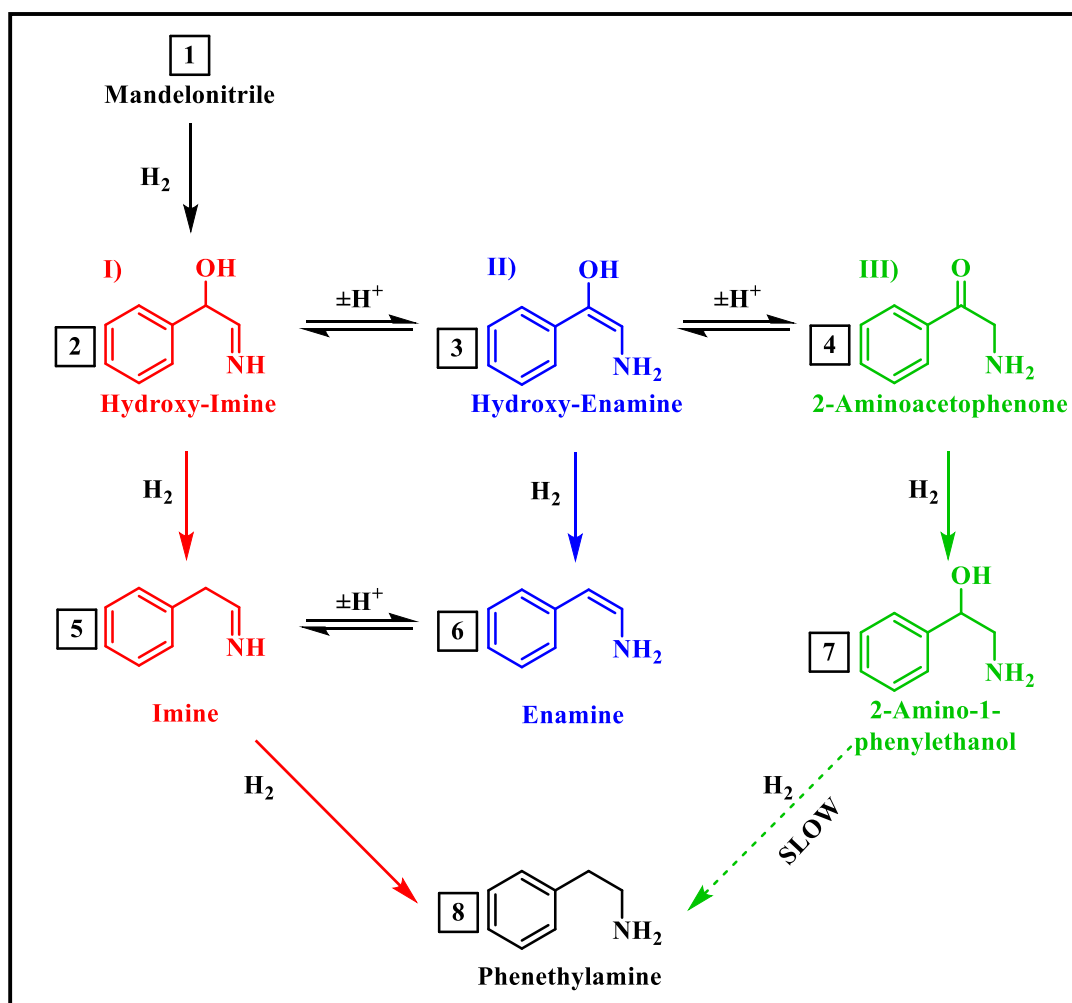
- (i) **1, 2, 5, 8**
- (ii) **1, 2, 3, 4, 3, 2, 5, 8**
- (iii) **1, 2, 3, 4, 3, 6, 5, 8**

Here, path (i), corresponding to Pathway **I**, proceeds exclusively in the forward direction to yield phenethylamine-D_{3-A}, and constitutes the major pathway in this particular reaction system. In contrast to path (i), both paths (ii) and (iii), relating to Pathways **V** and **VI** respectfully, invoke a ‘reverse’ tautomeric reaction upon formation of 2-aminoacetophenone (**4**). The re-formation of the hydroxy-enamine (**3**) represents the branching point between paths (ii) and (iii). Path (ii) undergoes a further ‘reverse’ tautomerisation to the hydroxy-imine (**2**) prior to undergoing hydrogenation to phenethylamine (**8**) *via* imine (**5**), as was observed in path (i). Path (iii), however, first undergoes hydrogenation to the enamine (**6**) before taking the ‘reverse’ tautomeric route to the imine (**5**), from where the final hydrogenation step to phenethylamine (**8**) is completed.

Upon examination of the pathways which contribute to phenethylamine formation, several similarities are identified. Namely, all three hydrogen requiring processes in the reaction (two hydrogenation steps and one hydrogenolysis step) occur in a specified order. The first step of the reaction is hydrogenation of the nitrile moiety of mandelonitrile to furnish the hydroxy-imine (**1**→**2**). Secondly, a hydrogenolysis step resulting in cleavage of the hydroxyl group will occur (**2**→**5** or **3**→**6**). Finally, the concluding step involves the hydrogenation of the imine to phenethylamine (**5**→**8**).

All pathways, whether active or inactive, involve hydrogenation of mandelonitrile (**1**) to the hydroxy-imine (**2**). The hydrogenation of (**1**)→(**2**) can therefore be considered as the unrefuted first step. Regarding the concluding step, three options were available. Hydrogenation of (**7**)→(**8**) is prohibited by kinetic reasoning, leaving two available options: (**5**)→(**8**) or (**6**)→(**8**). The hydrogenation of (**6**)→(**8**) can also be eliminated when Pathways **III** and **IV** are considered. Both pathways conclude in the hydrogenation of the enamine (**6**) to phenethylamine (**8**), and both are rejected as the result of the observed product distribution. It is hence deduced that this hydrogenation step is not operational. Consequently, the final hydrogenation step (**5**)→(**8**), shared by the three active pathways, is confirmed as the concluding step in achieving phenethylamine.

Adding a degree of complexity to this process, the presence of the acid catalysed tautomerisation pathway means that the hydrogenolysis step may occur on either the hydroxy-imine (**2**) or the hydroxy-enamine (**3**). The present experimental findings, however, cannot be used to differentiate between these two options. As there is no direct experimental evidence to suggest that one hydrogenolytic cleavage is more favoured than the other, it is concluded that both are probable. The reaction scheme for the hydrogenation reaction of mandelonitrile over a carbon supported palladium catalyst (Figure 6.1) is hence adapted to include the presented findings (Scheme 6.8).



Scheme 6.8. Advancement of the reaction scheme for the hydrogenation reaction of mandelonitrile showing the results of the isotopologue distribution study.

6.9 Density Functional Theory Proposal Relating to the Hydrogenolysis Reaction in the Hydrogenation Reaction of Mandelonitrile to Afford Phenethylamine

It was established in Section 6.1 that liquid phase analysis has been found to be insufficient in determining which molecule undergoes hydrogenolytic cleavage of the hydroxyl group. Therefore, in order to establish which hydrogenolytic pathway (hydroxy-imine (2) to imine (5), or hydroxy-enamine (3) to enamine (6)) is more energetically favourable, a density functional theory (DFT) study is proposed. Calculation of the activation energies associated with each of the aforementioned steps should provide an

indication of this. It is also proposed that the activation energies associated with two of the potential final hydrogenation steps (imine (**5**) to phenethylamine (**8**) and, enamine (**6**) to phenethylamine (**8**)) are also calculated. As the hydrogenation of the enamine (**6**) to phenethylamine (**8**) has been shown by experimental means to not occur, consistencies between the DFT calculation and the experimental findings for this step would validate the outcomes of the theoretical calculations for the hydrogenolysis reaction. This additional facet of the mandelonitrile hydrogenation reaction investigation constitutes ‘work in progress’ and is being undertaken in collaboration with the University of Cardiff. Those activities, however, are beyond the scope of this thesis.

6.10 Conclusions

Mechanistic aspects of the heterogeneously catalysed hydrogenation and deuteration reactions of mandelonitrile over a 5% Pd/C catalyst to afford the primary amine phenethylamine have been investigated. It was initially proposed that further mechanistic studies could be used to provide an enhanced understanding of the pathways taken from reagent to product. This section of work aimed to differentiate between Pathways **I** and **II**, which could not be achieved by the chromatographic means previously employed, and further, to confirm the inactivity of Pathway **III**. Instead, it was found that the previous scheme was overly simplistic resulting in a trivialised view of the reaction system. Rather, the following, more detailed, mechanistic conclusions have been drawn:

- ^1H and ^2H NMR spectroscopy analysis of the reaction mixture confirms the successful deuteration of the product and provides information on the location of deuterium incorporation within phenethylamine.
- Upon deuteration mass spectrometry and quantitative ^{13}C NMR spectroscopy reveal a similar isotopologue distribution. The detection of phenethylamine- D_3 as the major product is used as a means of proposing that Pathway **I** is favoured. Nevertheless, the significant contribution from phenethylamine- D_1 and phenethylamine- D_2 in the reaction mixture highlights the presence of a hydrogen enrichment process occurring alongside the main pathway.

- To rationalise the increased hydrogen content, the significance of the ‘reverse’ tautomeric reactions along the acid catalysed equilibria are highlighted.
- Examination of the multiplicity observed in the ^{13}C NMR spectra for the deuteration reaction of mandelonitrile indicates the presence of six isotopologues.
- Analysis of the deuterated product distribution allows refinement of the mechanism. The three hydrogen requiring processes involved in the conversion of mandelonitrile to phenethylamine are found to occur in a specified order. Hydrogenation of mandelonitrile to the hydroxy-imine precedes hydrogenolysis of the hydroxyl group with the final step being the hydrogenation of the double bond of the imine to phenethylamine.
- Whilst the predicted products of Pathway **III** have been confirmed to be absent from the isotopologue distribution, complete differentiation between Pathways **II** and **III** was found not to be possible as the result of a more complex reaction mechanism than initially anticipated.

CHAPTER 7

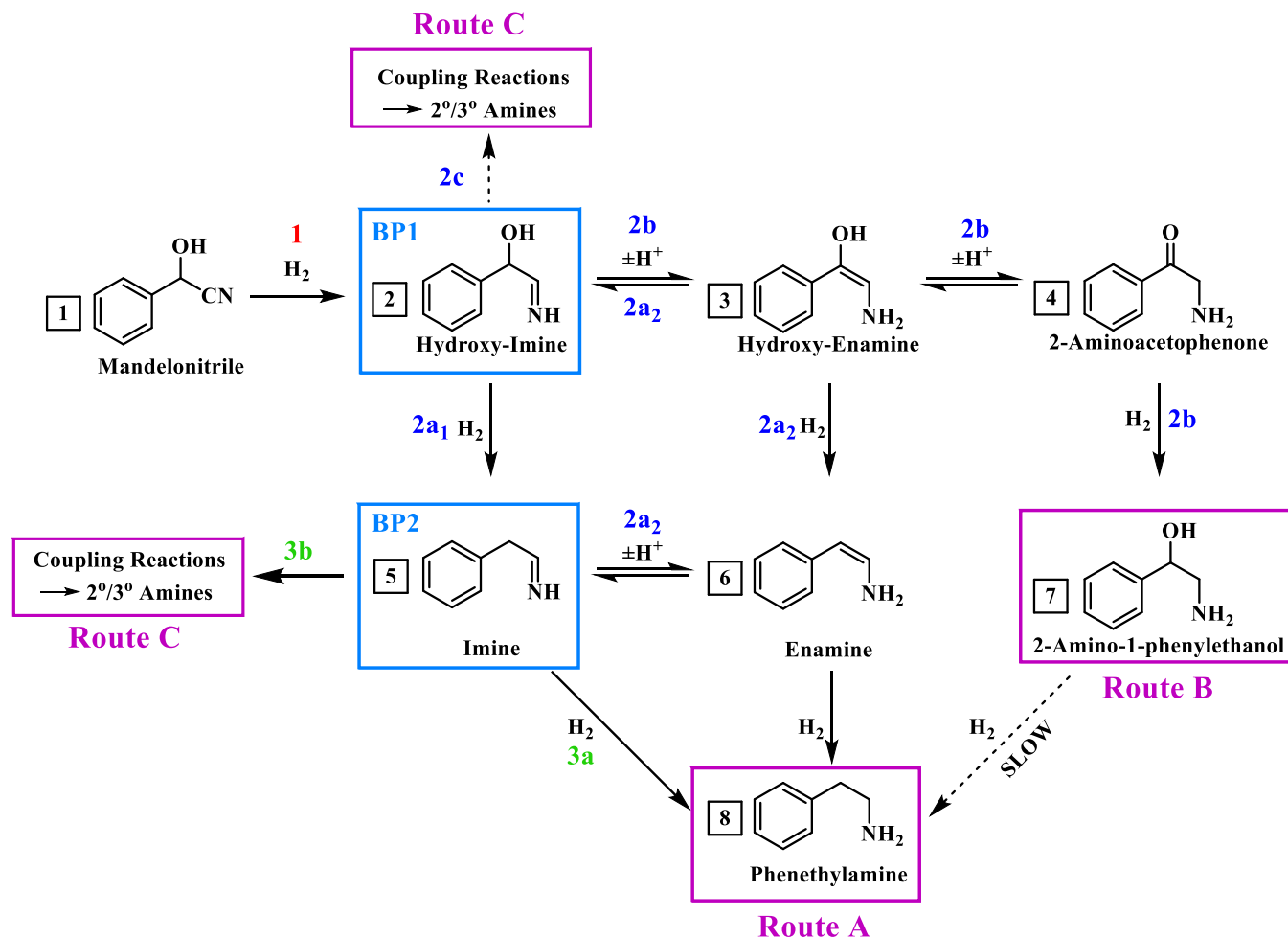
*Exploring Aspects of Reaction
Optimisation for the Liquid Phase
Hydrogenation Reaction of
Mandelonitrile under Single Batch
Conditions*

7.1 Introduction

As detailed in Chapter 1, due to the industrial relevance of the mandelonitrile substrate system, it is essential that production of the desired primary amine is maximised. As such, it is imperative that the single batch conditions employed for the hydrogenation and deuteration reactions of mandelonitrile described in Chapters 5 and 6 are optimised to allow for possible industrial viability. Extensive mechanistic details for this reaction have been discussed in Chapters 5 and 6, where it was identified that, alongside the desired product phenethylamine, a by-product (2-amino-1-phenylethanol) is also observed. Separation costs associated with large scale operations for non-selective processes are often less than desirable. Consequently, the exploration of potential avenues to improve phenethylamine yields is found to be prudent.

Against this background, various reaction parameter alterations were investigated, with particular focus on temperature, solvent, and acid choice. Moreover, to sufficiently analyse the findings, the reaction scheme, developed throughout Chapters 5 and 6, required further expansion. This schematic development includes additional chemistry which is only apparent upon alteration of the reaction conditions. As such, a set of routes within the system, not to be confused with Pathways **I–VIII** detailed in Chapter 6, have been defined to aid analysis. Whilst useful insight into the reaction was obtained, it was found that the current conditions (defined in Section 5.3) were superior. Nonetheless, this chapter aims to provide validity for the selected experimental conditions and, thereby ensure a more complete understanding of the reaction system, allowing an effective method for product scale-up, which is linked to process intensification, to be considered.

7.2 The Reaction Scheme is used to Rationalise the Product Distribution



Scheme 7.1. Expansion of the reaction scheme for the hydrogenation reaction of mandelonitrile highlighting the three major Routes (A–C) which are available to afford phenethylamine. The associated product of each route is highlighted by a purple box. The boxed numbers have been associated with each species for clarity in later analyses. [MN = mandelonitrile; 2-AAP = 2-aminoacetophenone; 2-APE = 2-amino-1-phenylethanol; PEA = phenethylamine. **BP1** and **BP2** denote Branching Points 1 and 2 respectively. **1**, **2** and **3** with subscripts **a** and **b** are representative of the hydrogen supply stages required by the reaction].

Previous mechanistic studies conducted on the mandelonitrile system culminated with the proposal of a complex, multi-step reaction scheme, validated against the outcome of a single batch hydrogenation and deuteration reaction.^[217, 240] However, if the reaction scheme is to be used as a diagnostic tool, slight alterations to that previously presented (Scheme 6.8), are necessary to aid the analysis. A modified reaction scheme (Scheme 7.1) is thus proposed. Additional chemistry, not observed under single batch conditions, is included here and relates to the occurrence of condensation reactions between the imine intermediate and the primary amine products to form secondary and tertiary amines. Analogous reactions were observed in the 4-hydroxybenzyl cyanide system (Section 4.2).

The mechanism proposed for the hydrogenation reaction of mandelonitrile is comprised of several transformations, some acid catalysed, and some hydrogen mediated. Thus far, the primary focus of the study has been production of phenethylamine, however, a more global representation of the reaction system must not be overlooked. Scheme 7.1 therefore highlights that there are additional routes, not resulting in phenethylamine, which the reaction may take. Accordingly, Routes **A–C** are defined; with each route possessing a different hydrogen requirement as well as a unique product.

In the first instance, all three routes commence with a common transformation; namely hydrogenation of the nitrile moiety of mandelonitrile (**1**) to form the hydroxy-imine intermediate (**2**). Upon completion of this first hydrogen-requiring step, the reaction may proceed by three possible major pathways (Routes **A–C**, Scheme 7.1). Consequently, the hydroxy-imine (**2**) represents a Branching Point, denoted **BP1** in Scheme 7.1.

Following this initial transformation, Routes **A–C** can be defined as follows. Route **A** affords the desired primary amine product, phenethylamine (**8**), in a step-wise process requiring three equivalents of hydrogen. With reference to Scheme 7.1, it is observed that at Branching Point 1, Route **A** follows path **2a₁** to form the imine (**5**). It is here that the second Branching Point in the reaction is reached (**BP2**). The concluding step for Route **A** is the occurrence of path **3a** to yield phenethylamine (**8**). Further, for completeness, it should be noted that at Branching Point 1, the hydroxy-imine (**2**) may undergo tautomerisation to form the hydroxy-enamine (**3**) by following path **2a₂**. Hydrogenolysis of the hydroxy-enamine (**3**) to furnish the enamine (**6**), followed by a second ‘reverse’ acid catalysed tautomerisation reaction to form the imine (**5**) then precedes the final step, **3a**, to phenethylamine (**8**). In addition, to rationalise the reported order of events, it has

been evidenced by the previous deuteration study (Chapter 6),^[240] that hydrogenation of the enamine (**6**) to phenethylamine (**8**) is not chemically probable under the presented reaction conditions.

Conversely, if the reaction were to follow Route **B** then, at Branching Point 1, path **2b** is taken. It is noted that tautomerisation of the hydroxy-imine (**2**) to form the hydroxy-enamine (**3**) is labelled as both **2a₂** and **2b**. This transformation is common to Routes **A** and **B** and has been labelled according to both to avoid ambiguity. Once path **2b** has been taken to the hydroxy-enamine (**3**), keto-enol tautomerisation to afford the detectable intermediate 2-aminoacetophenone (**4**) occurs. These tautomeric exchanges happen prior to the second hydrogenation step. Hydrogenation of 2-aminoacetophenone (**4**) rapidly affords by-product 2-amino-1-phenylethanol (**7**), the hydrogenation of which has been shown previously to be kinetically hindered (Section 5.7).

Finally, if following Route **C**, the reaction proceeds to either Branching Point 1 or 2. Instead of incurring a hydrogenation step at either position, however, the hydroxy-imine (**2**) (**BP1**) or, imine (**5**) (**BP2**) intermediates participate in coupling reactions, forming unwanted secondary and tertiary amines, which may, in turn, oligomerise. The production of these higher amine species are frequently reported to reduce selectivity towards the desired product.^[16–17, 21]

In order to establish which routes are operational at any given point in the catalytic reaction, an outcome, specific to each defined Route (**A–C**), must be identified. For Route **A**, Scheme 7.1 shows that phenethylamine (**8**) is the expected product, and so, if Route **A** is operational, the production of phenethylamine (**8**) will be observed. If Route **B** is active, however, a build-up of 2-amino-1-phenylethanol (**7**) will be detected chromatographically. Lastly, if Route **C** is to occur, formation of a carbonaceous over-layer on the catalyst surface is likely to occur due to the production of the oligomeric products associated with coupling reactions. This outcome will manifest itself as missing mass when a mass balance measurement is conducted for two main reasons. Firstly, a portion of the aforementioned oligomeric products are expected to be retained at the catalyst surface and thus, will not be detectable in the liquid phase.^[72–74] Secondly, due to the complex nature of the mandelonitrile system, chromatographic peaks, likely to be associated with higher amines, have not been specifically identified or quantified. Although some molecules suspected of being oligomeric products are found to be present

in the liquid phase, they are not quantified, and therefore will also be manifested as missing mass.

The absence of a definitive identification for these chromatographic species does, however, create a level of ambiguity over their assignment as secondary and tertiary amines. In support of this assignment, the identification and quantification of the corresponding secondary and tertiary amines has been documented for the simpler 4-hydroxybenzyl cyanide substrate system (Section 4.2). Consequently, it is recognised that the route, or routes, the reaction takes will dictate the product outcome. As such, analysis of the product distribution can be used as a diagnostic tool to monitor catalyst activity. Table 7.1 shows the predicted product for each route.

Table 7.1. Selectivity towards each of the routes available (A–C) at reaction completion (time = 120 minutes) for the single batch liquid phase hydrogenation reaction of mandelonitrile (35 mmol L^{-1}) over a 5% Pd/C catalyst (300 mg) in the presence of 2 equivalents of sulphuric acid in methanol. The reaction was conducted at 40 °C under 6 barg hydrogen pressure with an external line pressure of 6.5 barg and an agitation speed of 1050 rpm.

<i>Route</i>	<i>Product</i>	<i>Selectivity</i>
A	Phenethylamine	87%
B	2-Amino-1-phenylethanol	13%
C	Missing Mass	0%

Also shown in Table 7.1 is the prevalence of Routes A–C at reaction completion (time = 120 minutes) for the mandelonitrile hydrogenation reaction. From Table 7.1, Routes A and B are revealed to be active, with Route A showing dominance. Conversely, Route C is shown to be dormant, as evidenced by the complete mass balance detected at reaction cessation (Figure 5.6).

The outcome of the standard single batch mandelonitrile hydrogenation reaction, shown in Table 7.1, can therefore be employed as a benchmark from which the outcomes of the subsequent parameter alterations can be compared. For a specific set of reaction conditions to be considered for the subsequent repeat batch studies associated with

product scale-up, the absence of Route **C** is essential. Further, the enhancement of Route **A** and the diminishment of Route **B**, such that phenethylamine production is completely selective is desirable. Consequently, a series of systematic reaction parameter alterations are implemented, and the subsequent effects monitored using the described Routes (**A–C**).

7.3 Consideration of an Alternative Catalyst

In the first instance, the catalyst was altered. However, it must be noted that extensive catalyst screening was not conducted. For the purpose of this study, a 5% Pd/ γ -Al₂O₃ catalyst was selected as a reference catalyst which could be compared directly to the 5% Pd/C catalyst. This particular catalyst (5% Pd/ γ -Al₂O₃) was chosen as its use has been documented in the Lennon Group for several reactions, and, is therefore well understood.^[241–242] Characterisation of this catalyst, alongside the 5% Pd/C catalyst, has been conducted, with the details provided in Chapter 3. For both catalysts, the active metal and the metal loading are the same, meaning that it is the nature of the support which represents the primary difference. Crucially, the 5% Pd/ γ -Al₂O₃ catalyst provides opportunity for the consideration of the relevance of palladium crystallite morphology.

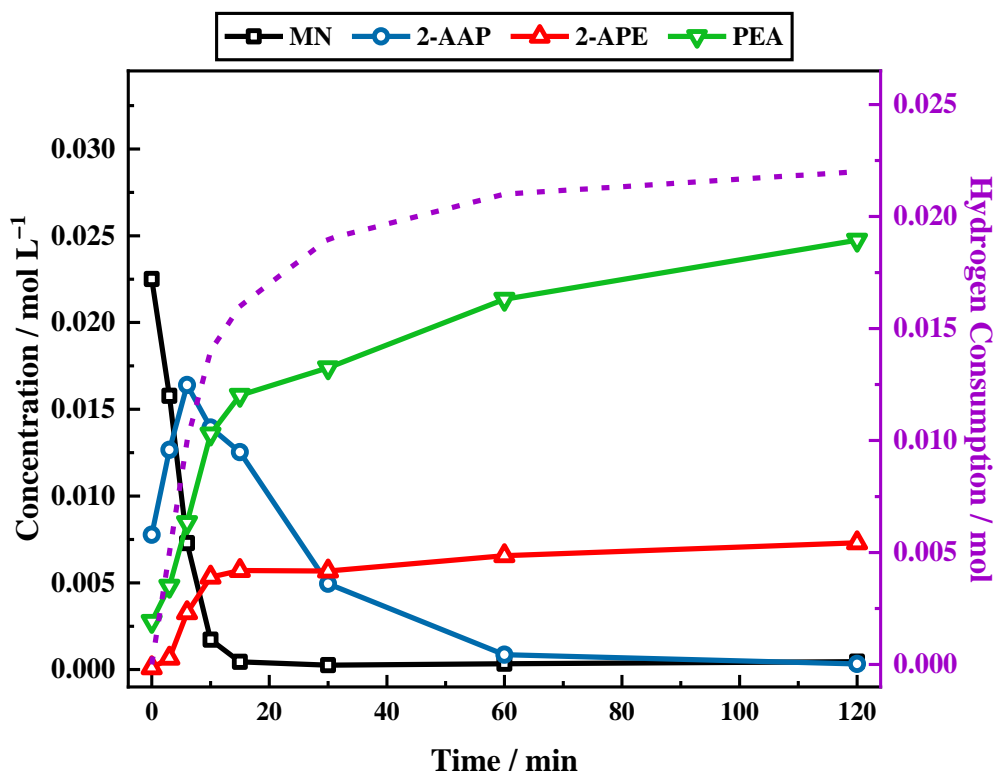


Figure 7.1. Reaction profile and hydrogen uptake curve (dashed purple line on the second y-axis) for the liquid phase hydrogenation reaction of mandelonitrile (35 mmol L^{-1}) over a 5% Pd/ $\gamma\text{-Al}_2\text{O}_3$ catalyst [GU-2] (300 mg) in the presence of 2 equivalents of sulphuric acid in methanol. The reaction was conducted at 40°C under 6 barg hydrogen pressure with an external line pressure of 6.5 barg and an agitation speed of 1050 rpm. [MN = mandelonitrile; 2-AAP = 2-aminoacetophenone; 2-APE = 2-amino-1-phenylethanol; PEA = phenethylamine].

The resulting profile for the hydrogenation reaction of mandelonitrile over the 5% Pd/ $\gamma\text{-Al}_2\text{O}_3$ catalyst is presented in Figure 7.1. When compared directly to the outcome obtained over the 5% Pd/C catalyst (Figure 5.4), the rate of mandelonitrile conversion is shown to be similar, reaching completion within approximately 20 minutes. Further, the production of both 2-amino-1-phenylethanol and phenethylamine again show similar trends. Nevertheless, slight differences in selectivity at reaction completion (time = 120 minutes) are observed. Intriguingly, the trace for intermediate 2-aminoacetophenone reaches a maximum far in excess of that observed in the reaction over 5% Pd/C. The lifetime of this intermediate in the reaction system is also prolonged, not departing until a reaction time of 60 minutes. This finding could be linked to the increased time required for phenethylamine formation to reach completion.

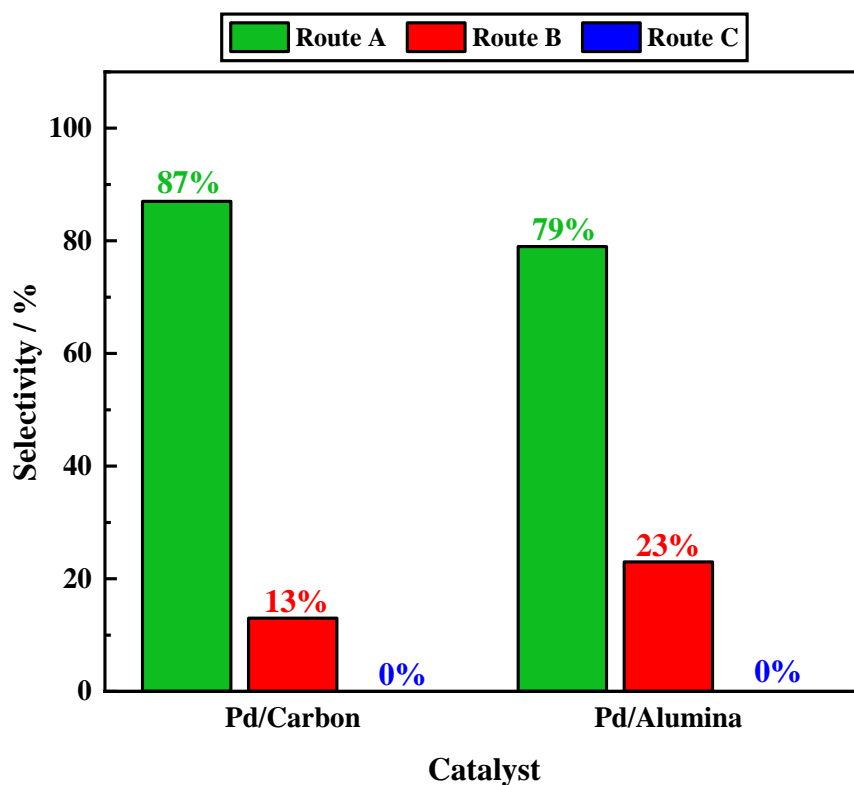


Figure 7.2. Selectivity towards each of the described Routes (A–C), calculated at reaction completion (time = 120 minutes) for the liquid phase hydrogenation reaction of mandelonitrile (35 mmol L^{-1}) in the presence of 2 equivalents of sulphuric acid in methanol. The reaction was conducted at 40°C under 6 barg hydrogen pressure with an external line pressure of 6.5 barg and an agitation speed of 1050 rpm. In this instance catalyst choice is compared. [Route **A** = phenethylamine; Route **B** = 2-amino-1-phenylethanol; Route **C** = missing mass].

Comparing the selectivity for each of the catalysts (Figure 7.2) highlights that performance is similar. For both catalysts, only Routes **A** and **B** are found to be active, with a complete mass balance achieved in both instances. Over the 5% Pd/C catalyst, however, Route **A** is shown to be more dominant, such that an enhanced selectivity towards phenethylamine is afforded compared to the alumina supported catalyst. It must, nevertheless, be noted that the outcomes of Figures 5.4 and 7.1 indicate that a successful outcome for the mandelonitrile hydrogenation reaction to afford phenethylamine is not restricted to a single catalyst. In line with the enhanced phenethylamine production achieved using 5% Pd/C, all further investigations will utilise this catalyst.

7.4 Temperature Alterations

Included within the many effects temperature has on a reaction system is a role in reaction selectivity.^[154] Arrhenius theory states that increasing temperature increases reaction rate.^[39] While this may be favourable in terms of an improved rate of formation of the desired product, the effects are often not localised. Indeed, within the 4-hydroxybenzyl cyanide system, reported in Chapter 4, a temperature decrease was shown to improve selectivity towards tyramine such that this species was formed with 100% selectivity.

Whilst this was found to be beneficial in the prevention of unwanted side reactions in the 4-hydroxybenzyl cyanide system, it must be noted that the mandelonitrile system has a more significant hydrogen demand. As such, the solubility of dihydrogen in the reaction solvent must also be considered to ensure adequate hydrogen supply to afford phenethylamine in high yield. As temperature has an influence on solubility, it can therefore be linked to hydrogen availability.^[211–212] For methanol, the standard reaction solvent, hydrogen solvation has been shown to increase with increasing temperature.^[211–212]

It was therefore considered necessary to identify an optimal reaction temperature that would allow effective solubility of dihydrogen in methanol, whilst maintaining the selectivity of the reaction. Against this background, both an increase, and a decrease, in temperature were considered.

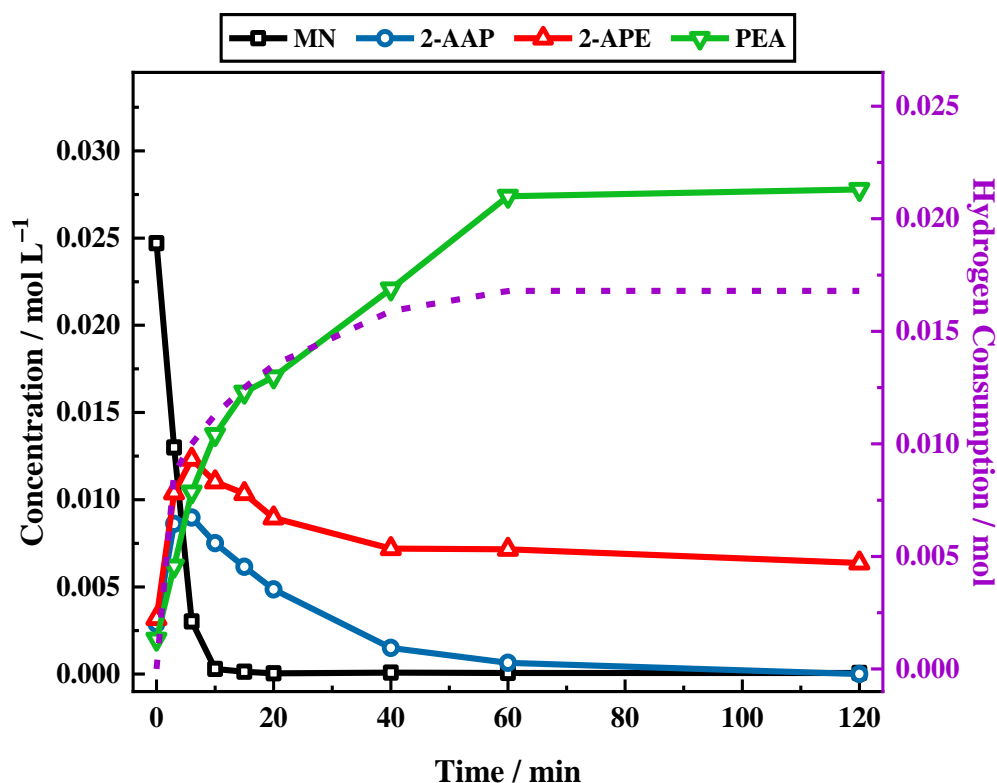


Figure 7.3. Reaction profile and hydrogen uptake curve (dashed purple line on the second y-axis) for the liquid phase hydrogenation reaction of mandelonitrile (35 mmol L^{-1}) over a 5% Pd/C catalyst (300 mg) in the presence of 2 equivalents of sulphuric acid in methanol. The reaction was conducted at 20°C under 6 barg hydrogen pressure with an external line pressure of 6.5 barg and an agitation speed of 1050 rpm. [MN = mandelonitrile; 2-AAP = 2-aminoacetophenone; 2-APE = 2-amino-1-phenylethanol; PEA = phenethylamine].

In line with the findings of the 4-hydroxybenzyl cyanide system, the temperature was first lowered from 40°C (standard conditions) to 20°C . The results (Figure 7.3) are largely similar to that obtained for standard conditions (Figure 5.4). The mandelonitrile undergoes rapid consumption (being completely reduced within *ca.* 10 minutes). 2-Aminoacetophenone is present as an intermediate, and, at reaction completion (time = 120 minutes), both 2-amino-1-phenylethanol and phenethylamine are observed, as by-product and major product, respectively. There is, however, an overall slowing in the rate of 2-aminoacetophenone consumption as evidenced by the increased longevity of this molecule in the system (complete conversion reached within 60 minutes, *cf.* 20 minutes under standard conditions). Further, Figure 7.3 highlights that an extended reaction time was also required for phenethylamine formation to reach saturation (approximately 60

minutes, *cf.* 20 minutes under standard conditions). These observations are in line with what would be expected as the result of a reduced rate associated with a temperature decrease.

Although the outcome of the temperature reduction is largely similar to the standard conditions, the slowed rate results in some of the highly reactive intermediates being longer lived in the system. Consequently, it is proposed that as these species have a longer lifetime in the reaction mixture, there will be greater opportunity for Route **C**, which forms unwanted oligomeric products, to occur. Whilst a complete mass balance, indicating the absence of Route **C**, is obtained for this single batch study, this route is predicted to become more prevalent when a repeat batch protocol is implemented. Further details regarding this can be found in the following chapter.

Considering now a temperature elevation, it is postulated that, in addition to enhancing hydrogen availability, the increased reaction rate associated with a temperature increase may provide sufficient energy to improve the conversion of 2-amino-1-phenylethanol to phenethylamine. This transformation has previously been shown to be kinetically slow (Section 5.7) resulting in the production of 2-amino-1-phenylethanol as an unwanted by product.

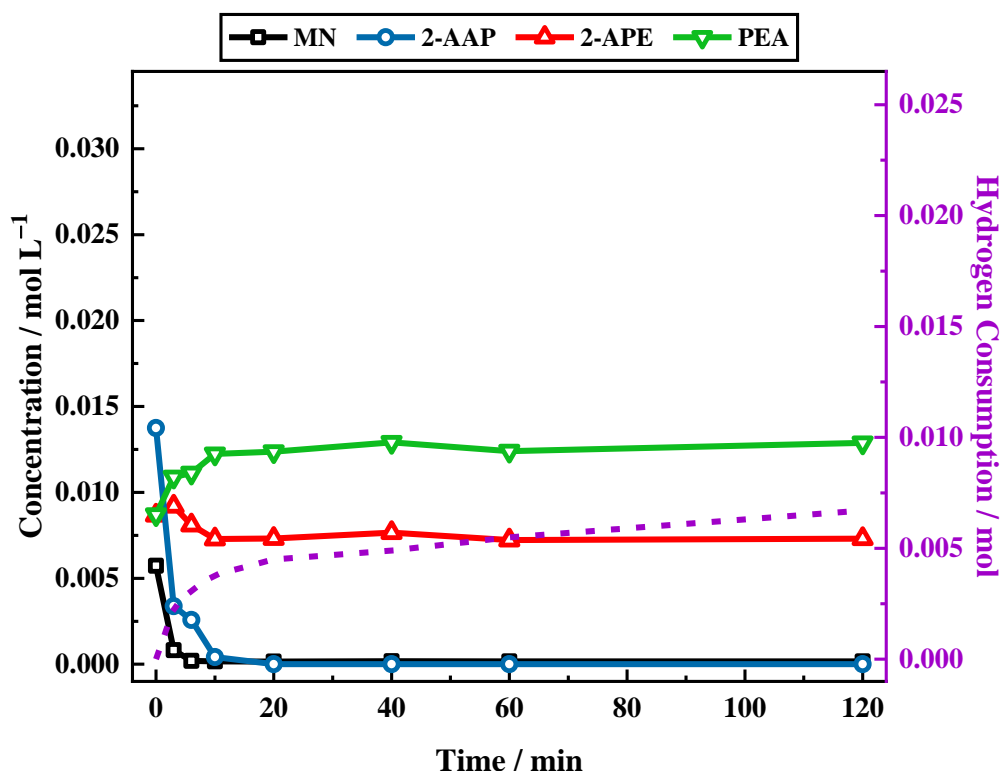


Figure 7.4. Reaction profile and hydrogen uptake curve (dashed purple line on the second y-axis) for the liquid phase hydrogenation reaction of mandelonitrile (35 mmol L^{-1}) over a 5% Pd/C catalyst (300 mg) in the presence of 2 equivalents of sulphuric acid in methanol. The reaction was conducted at 60°C under 6 barg hydrogen pressure with an external line pressure of 6.5 barg and an agitation speed of 1050 rpm. [MN = mandelonitrile; 2-AAP = 2-aminoacetophenone; 2-APE = 2-amino-1-phenylethanol; PEA = phenethylamine].

Figure 7.4 shows that, despite the postulated improvements associated with a temperature increase, the resultant profile does not present a favourable outcome. Whilst both the starting material (mandelonitrile) and the intermediate (2-aminoacetophenone) are rapidly consumed, they are not converted to phenethylamine in significant quantities. As a result, phenethylamine selectivity is tremendously reduced, exhibiting a meagre 41% selectivity at reaction completion (*cf.* 87% at 40°C). Further, a 10% increase in 2-amino-1-phenylethanol selectivity, compared to standard conditions, and a significant missing mass at reaction completion (36%) were observed.

Despite the outcome of Figure 7.4, an attempt was made to reap the benefits of the elevated temperature whilst avoiding the observed selectivity issues. After the reaction appeared to reach completion at 40°C (time = 120 minutes), the temperature was then

increased to 60 °C. This was done to ascertain whether further conversion of the 2-amino-1-phenylethanol by-product to furnish phenethylamine was possible. Unfortunately, after 60 minutes at 60 °C only negligible conversion of 2-amino-1-phenylethanol was observed. This was in line with the findings of Section 5.7. It thus appears that the minor temperature increase of 20 °C does not significantly enhance the rate of this reaction.

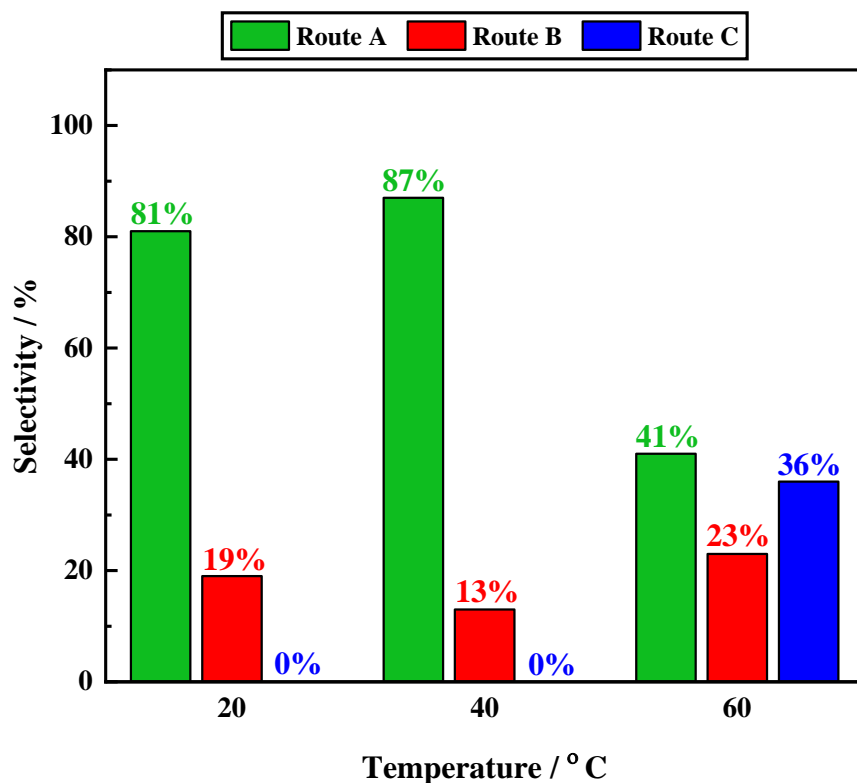


Figure 7.5. Selectivity towards each of the described Routes (A–C), calculated at reaction completion (time = 120 minutes) for the liquid phase hydrogenation reaction of mandelonitrile (35 mmol L^{-1}) over a 5% Pd/C catalyst (300 mg) in the presence of 2 equivalents of sulphuric acid in methanol. The reaction was conducted at 6 barg hydrogen pressure with an external line pressure of 6.5 barg and an agitation speed of 1050 rpm. In this instance reaction temperature is compared. [Route **A** = phenethylamine; Route **B** = 2-amino-1-phenylethanol; Route **C** = missing mass].

Comparing each of the explored reaction temperatures, Figure 7.5 shows the distribution of Routes A–C, previously defined, at reaction completion (time = 120 minutes). Here it is shown that at 20 °C and 40 °C, the product distribution is largely comparable with the presence of both Routes **A** and **B**, but an absence of Route **C**. The product ratio does, however, slightly favour phenethylamine production at 40 °C. In contrast, the reaction

conducted at 60 °C showed a vastly different selectivity profile to that observed at lower temperatures. Most notable was the activation of Route **C**.

Hydrogen consumption for the reactions conducted at each of the reported temperatures are compared in Table 7.2. This illustrates that the amount of hydrogen consumed correlates to the dominance of the routes requiring the greatest hydrogen contribution (Routes **A** and **B**). Further, as Route **A** is more hydrogen demanding than Route **B** this rationalises the increased hydrogen uptake at 40 °C when compared to 20 °C.

Table 7.2. *Hydrogen consumption for each of the monitored temperatures in the liquid phase hydrogenation reaction of mandelonitrile (35 mmol L⁻¹) over a 5% Pd/C catalyst (300 mg) in the presence of 2 equivalents of sulphuric acid in methanol. The reaction was conducted at 6 barg hydrogen pressure with an external line pressure of 6.5 barg and an agitation speed of 1050 rpm.*

<i>Temperature / °C</i>	<i>H₂ Consumption / mmol</i>
20	16.8
40	22.5
60	6.7

7.5 Solvent Alterations

Having an influence over a number of experimental factors, solvents play a critical role in heterogeneously catalysed reactions.^[17, 21 39, 243] Despite the fact that appropriate solvent selection can lead to considerably improved outcomes, this parameter is often overlooked in catalytic studies.

Of specific interest for this study, is the influence of the reaction solvent on the resultant selectivity. The primary function of a reaction solvent is to solubilise the reagents and products so that reaction can occur. Complete solubility, however, is not necessary. Limited solubility, or indeed dilution, can be used to slow the rate of reaction such that certain, unwanted, reactions are hindered or prevented.^[39] Whilst this method may prove

effective, diffusion must also be considered. This factor is particularly important when the reagents are in different phases, as with the mandelonitrile hydrogenation system. It may also be desirable for the products to remain in solution to prevent their precipitation on the catalyst surface. Nonetheless, the insolubility of a by-product in the reaction solvent can provide a means of easy separation (such as filtration). Additionally, solvents can have a pronounced effect on the positioning of the reaction equilibria and indeed on the catalyst itself, with the solvent able to interact with both the metal sites and the support.

The factors considered here regarding the influence of solvent are not exhaustive but serve to demonstrate the complex nature of this parameter. Due to the multifaceted role of the solvent, it is often difficult to select one which satisfies all criteria, with balance and compromise often necessary. Nonetheless, if used correctly, the reaction solvent can be a powerful instrument which can be used towards achieving a highly selective reaction. In line with relevant literature,^[3, 21] a variety of alterations to the reaction solvent have been investigated and are presented forthwith.

7.5.1 Addition of Water to the Reaction Mixture is Reported to Improve Selectivity

It is reported that the addition of water to a reaction solvent may lead to a markedly lower tendency for by-product formation to occur, thus increasing selectivity towards the primary amine for nitrile hydrogenation reactions catalysed by nickel or cobalt.^[21, 93–94] The positive influence was ascribed to solvation of the amine by the water, hence making it unavailable for participation in condensation reactions with the imine intermediate. It is the suppression of imine/amine coupling reactions which provides the basis for the improved selectivity towards the primary amine.^[21] The combined action of water and ammonia is also described to promote high primary amine yields. This appears to be due to the alkaline conditions created when water and ammonia are used in unison. The alkaline conditions inhibit the acidic sites of the catalyst which are likely responsible for the coupling reactions.^[94, 244] Nonetheless, basic conditions, as previously described (Section 2.1.1) are problematic for cyanohydrin systems and so have not been explored in this instance.

Despite the reported selectivity benefits associated with the inclusion of a water component in the reaction solvent, the solubility of hydrogen in the reaction media becomes slightly challenging when the use of water is considered. Hydrogen is not dissolved as effectively in water as it is in alcohols, thus rendering the current reaction solvent, methanol, superior in terms of its potential to deliver hydrogen to the necessary components of the reaction system.^[211, 245–246] Thus, a balance must be struck between ensuring an ample hydrogen supply for the reaction and, producing phenethylamine in high selectivity.

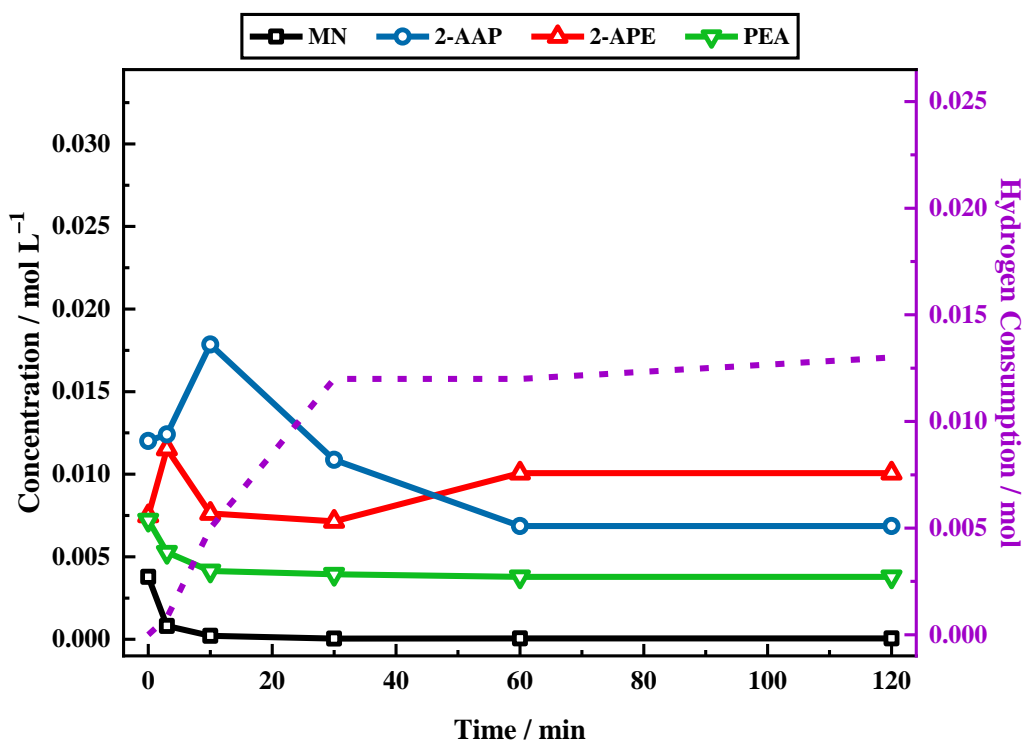


Figure 7.6. Reaction profile and hydrogen uptake curve (dashed purple line on the second y-axis) for the liquid phase hydrogenation reaction of mandelonitrile (35 mmol L^{-1}) over a 5% Pd/C catalyst (300 mg) in the presence of 2 equivalents of sulphuric acid in a reaction solvent of equal methanol-water composition ($\text{MeOH}_{50\%}:\text{H}_2\text{O}_{50\%}$). The reaction was conducted at 40°C under 6 barg hydrogen pressure with an external line pressure of 6.5 barg and an agitation speed of 1050 rpm. [MN = mandelonitrile; 2-AAP = 2-aminoacetophenone; 2-APE = 2-amino-1-phenylethanol; PEA = phenethylamine].

Initially, the use of a solvent mixture composed of equal volumes of water and methanol ($\text{MeOH}_{50\%}:\text{H}_2\text{O}_{50\%}$) was explored. The resultant reaction profile is presented in Figure 7.6 and shows that the inclusion of water as a component of the reaction solvent affords

a dramatic alteration in the observed product distribution. It can be seen in Figure 7.6 that the mandelonitrile was fully and rapidly converted, reaching complete conversion within approximately 10 minutes (*cf.* the reference reaction profile, presented in Figure 5.4, reached complete conversion within 20 minutes). This finding indicates that the inclusion of water enhances the rate of reaction. A similar observation was noted by Rajadhyasha and co-workers for a comparable reaction system.^[247]

However, whilst both the desired product (phenethylamine) and the by-product (2-amino-1-phenylethanol) were still produced, the product ratio was markedly different. In this instance, it was 2-amino-1-phenylethanol, and not phenethylamine, which was observed as the major product at reaction completion. Interestingly, and in contrast to the MeOH_{100%} reference profile (Figure 5.4), 2-aminoacetophenone was shown to be detectable as an additional by-product rather than an intermediate. This outcome therefore indicates that the presence of water has altered the reaction pathway. A significant missing mass (*ca.* 30% at reaction completion, time = 120 minutes) was also observed. As described previously, the missing mass is identified to be the result of higher amine formation, occurring as a consequence of coupling reactions. Therefore, this finding indicates that Route **C** has been activated by the presence of water.

Using the mechanistic insight previously gained for this system, it is possible to rationalise the aforementioned findings. Routes **A–C**, and their associated identifiers, have previously been defined (Table 7.1). With reference to the reaction scheme (Scheme 7.1), the findings of Figure 7.6 can be described in greater detail.

The first step of the process, relating to the hydrogenation of the nitrile functionality to furnish the hydroxy-imine, is successfully undertaken, as evidenced by the complete conversion of mandelonitrile. The product distribution has also indicated that all three Routes (**A–C**) are operational, demonstrating that all pathways from Branching Point 1 are active. Nevertheless, when compared to the MeOH_{100%} reference, phenethylamine production has been shown to be significantly stunted with a selectivity drop of 75% observed. Route **A** can thus be assigned as a minor contributor under these conditions.

The production of 2-amino-1-phenylethanol (selectivity = 33%) provides direct evidence for Route **B**. As an intermediate of Route **B**, the selectivity towards 2-aminoacetophenone (22%) is combined with that obtained for 2-amino-1-phenylethanol, giving Route **B** a selectivity total of 55% at reaction completion. Route **B** is therefore shown to be the

dominant route under the presented experimental conditions. The detection of 2-aminoacetophenone, does, however, complicate the analysis. The hydrogenation reaction of 2-aminoacetophenone to afford 2-amino-1-phenylethanol has previously been shown to be facile (Section 5.8), and thus, the build-up of 2-aminoacetophenone observed in Figure 7.6 implies that this transformation has been mired. Strangely, the production of 2-amino-1-phenylethanol is also shown to be enhanced (33% selectivity, *cf.* 13% selectivity for MeOH_{100%}), suggesting that a further degree of complication is in operation.

To rationalise these outcomes, it is proposed that water binds to the surface of the 5% Pd/C catalyst, attracted by the hydrophilic nature of the carbon support,^[248] and acts as a poison. Blockage of the active sites by water may limit the surface hydrogen supply. As such, a proposed rationale for the observed product distribution can be made. The first step of the process requires hydrogen, but, crucially, is rapid enough to reach full conversion without the interference of a diminishing hydrogen supply. As the reaction proceeds, the build-up of water on the surface reduces the number of sites available for essential surface intermediates to undergo the necessary hydrogenation steps. Consequently, reactions that do not require a hydrogen supply will be favoured. Relying on acid catalysed equilibria, the formation of 2-aminoacetophenone is thus preferred. From here, the 2-aminoacetophenone is rapidly hydrogenated to 2-amino-1-phenylethanol, explaining the enhanced formation of this species. Nevertheless, it is suggested that, in due course, this process will also be hindered as the result of insufficient hydrogen supply. Further, it is proposed that the enhancement of Route C accelerates the surface poisoning process as the resultant higher amines will act as additional surface poisons.

Due to the nature of the carbon support, optical probes cannot, at present, be effectively used to determine the exact composition of the catalyst surface.^[152–153] As such, the surface species postulated here cannot be directly evidenced. Providing a degree of support for this postulate, however, is the reduced hydrogen uptake that accompanied this measurement, approximately 56% of that obtained for the MeOH_{100%} reference experiment. The reasoning here is that if the reaction is limited by hydrogen, then the overall uptake will be reduced, as is observed experimentally (Figure 7.6).

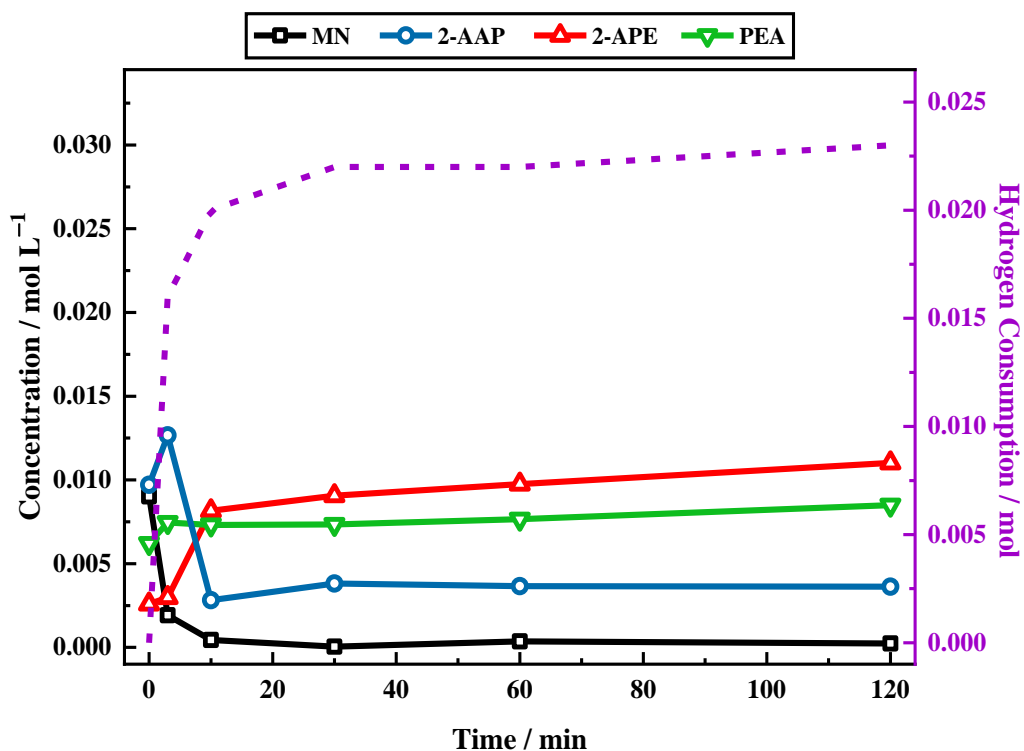


Figure 7.7. Reaction profile and hydrogen uptake curve (dashed purple line on the second y-axis) for the liquid phase hydrogenation reaction of mandelonitrile (35 mmol L^{-1}) over a 5% Pd/C catalyst (300 mg) in the presence of 2 equivalents of sulphuric acid in a reaction solvent of methanol-water composition ($\text{MeOH}_{75\%}:\text{H}_2\text{O}_{25\%}$). The reaction was conducted at 40°C under 6 barg hydrogen pressure with an external line pressure of 6.5 barg and an agitation speed of 1050 rpm. [MN = mandelonitrile; 2-AAP = 2-aminoacetophenone; 2-APE = 2-amino-1-phenylethanol; PEA = phenethylamine].

Unfortunately, instead of improving the selectivity to the desired primary amine, as was the intention, it appears that the presence of water favours the unwanted chemistry which affords the products of Routes **B** and **C**. Hence, attempting to facilitate more favourable reaction conditions, the percentage of water in the reaction mixture was reduced from 50% to 25%, with the remainder comprising of methanol ($\text{MeOH}_{75\%}:\text{H}_2\text{O}_{25\%}$). The resulting reaction profile and the hydrogen uptake curve for this solvent composition are presented in Figure 7.7. As with the 50:50 methanol-water solvent mixture (Figure 7.6), mandelonitrile reaches complete conversion in a rapid manner (complete within approximately 15 minutes). Nevertheless, once again, considerable alterations to the product distribution were observed.

Figure 7.7 represents an intermediary outcome between the MeOH_{100%} and the MeOH_{50%}:H₂O_{50%} reaction profiles (Figure 5.4 and Figure 7.6, respectively), with similarities to both profiles observed. The overall product distribution is largely comparable to the 50:50 mixture (Figure 7.6), however, with subtle differences which indicate an improved hydrogen supply. The postulated rationale for Figure 7.6, which suggests that water acts as a catalyst poison, therefore holds, with the resultant elevated hydrogen availability affording enhanced phenethylamine formation when compared to Figure 7.7. Further, the depleted quantity of residual 2-aminoacetophenone observed at reaction completion (time = 120 minutes) indicates that more of this molecule has been able to convert to 2-amino-1-phenylethanol before the catalyst has been completely shut down.

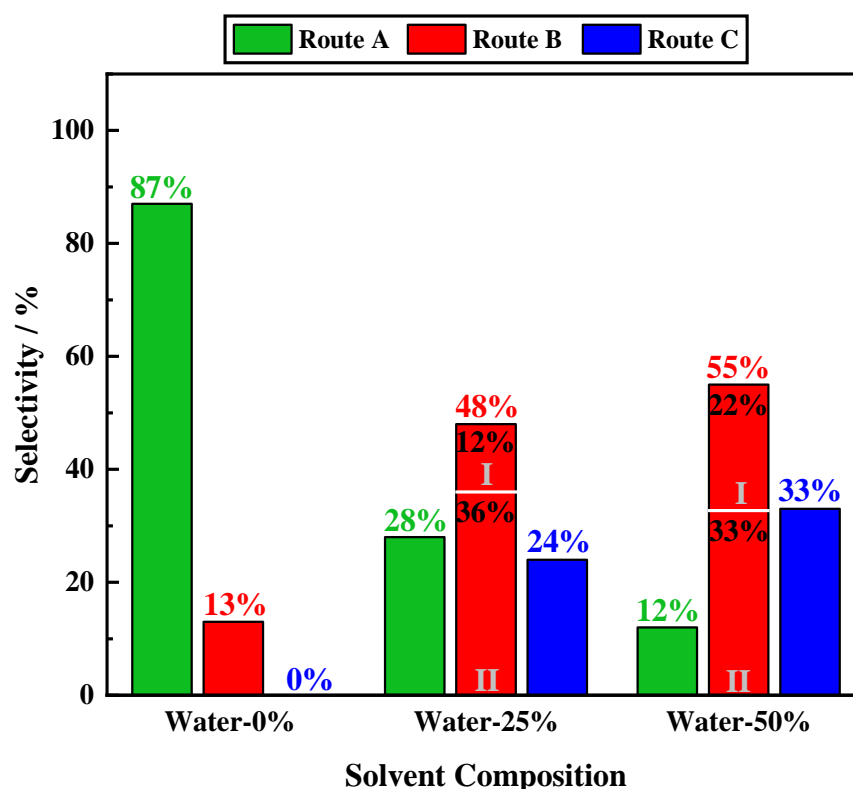


Figure 7.8. Distribution of Routes A–C for the liquid phase hydrogenation reaction of mandelonitrile (35 mmol L^{-1}) over a 5% Pd/C catalyst (300 mg) in the presence of 2 equivalents of sulphuric acid. The reaction was conducted at 40°C under 6 barg hydrogen pressure with an external line pressure of 6.5 barg and an agitation speed of 1050 rpm. In this instance, composition of the reaction solvent, specifically the inclusion of a water component to the methanol, is compared. [Route A = phenethylamine; Route B-I = 2-aminoacetophenone; Route B-II = 2-amino-1-phenylethanol; Route C = missing mass].

The outcomes associated with the inclusion of water in the reaction solvent are summarised in Figure 7.8. Shown, is the resultant selectivity towards each of the identified routes at reaction completion (time = 120 minutes). Clearly observed is the deterioration of the product distribution relative to the desired outcome as the water component of the reaction mixture is increased. It is thus demonstrated that the inclusion of water cannot be used to afford improved selectivity towards the primary amine.

With the addition of water to the reaction mixture proving not to be beneficial, it was deemed necessary to consider a potential conflict between the effects of the water and the sulphuric acid additive. The use of a 50:50 methanol-water solvent ratio under neutral conditions was therefore used to assess, with improved accuracy, the effect of water as a component of the reaction solvent. The resultant reaction profile can be visualised in Figure 7.9.

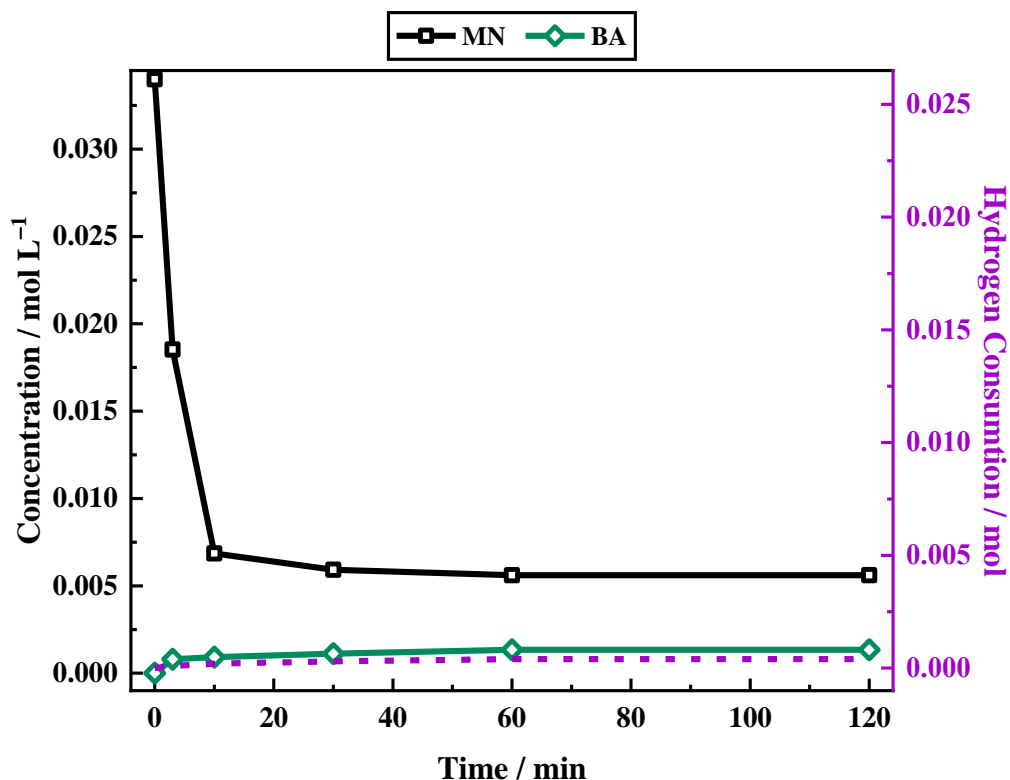


Figure 7.9. Reaction profile and hydrogen uptake curve (dashed purple line on the second y-axis) for the liquid phase hydrogenation reaction of mandelonitrile (35 mmol L^{-1}) over a 5% Pd/C catalyst (300 mg) in the **absence** of sulphuric acid in a reaction solvent of equal methanol-water composition ($\text{MeOH}_{50\%}:\text{H}_2\text{O}_{50\%}$). The reaction was conducted at 40°C under 6 barg hydrogen pressure with an external line pressure of 6.5 barg and an agitation speed of 1050 rpm. [MN = mandelonitrile; BA = benzyl alcohol].

The resultant reaction profile (Figure 7.9) exhibits similarities to the profile obtained from the previously discussed hydrogenation reaction of mandelonitrile in methanol without the use of a sulphuric acid additive (Section 5.4, Figure 5.5). Mirroring the outcome of Figure 5.5, negligible product formation and minimal hydrogen uptake by the system were detected. This was accompanied by an incomplete mass balance (80% at reaction completion). The inclusion of water in the reaction solvent, however, affords increased conversion at a reaction time of 120 minutes (84%, *cf.* 19% in the absence of water under comparable conditions). This indicates that the presence of water enhances the conversion achieved within the 120 minute reaction. Nevertheless, it is likely that the mandelonitrile either undergoes spontaneous decomposition or, produces species which bind irreversibly to the surface of the catalyst and act as poisons.

It can thus be concluded that the inclusion of water greatly reduces the selectivity towards phenethylamine, with an increasing water content further diminishing the selectivity. Furthermore, the use of water, whilst not a suitable substitute for the acid additive, affords a more successful conversion of mandelonitrile than methanol in the absence of acid.

7.5.2 Increasing Alcohol Chain Length is Reported to Increase Hydrogen Solubility

The use of alcohols as reaction solvents for nitrile hydrogenation reactions is shown to dominate in the literature due to the favourable solubility of hydrogen in this media.^[211, 246] The solubility of hydrogen in all alcohols is reported to rise with increasing temperature and pressure.^[249] The role of temperature has been explored previously in Section 7.4, with a temperature increase being found to be detrimental to phenethylamine selectivity. Nevertheless, hydrogen solubility is also shown to increase with increasing chain length for linear alcohol molecules.^[249] The notable exception being ethanol which exhibits a slightly higher solubility than propan-1-ol.^[249] As such, the hydrogenation reaction of mandelonitrile is conducted in ethanol and butan-1-ol and is compared to the methanol standard (Figure 5.4).

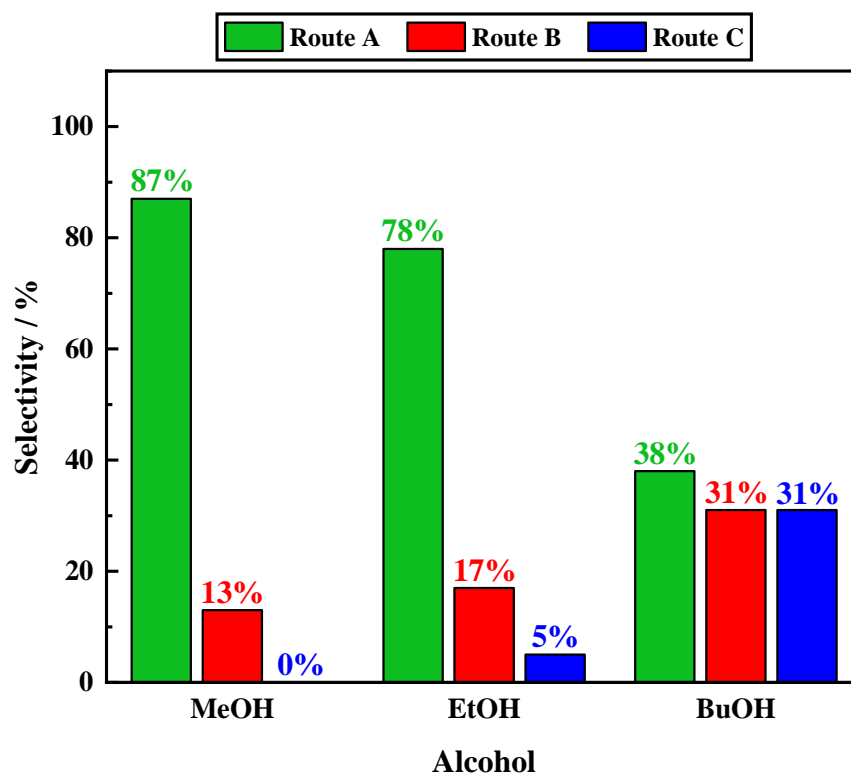


Figure 10. Selectivity towards each of the described Routes (A–C), calculated at reaction completion (time = 120 minutes) for the liquid phase hydrogenation reaction of mandelonitrile (35 mmol L^{-1}) over a 5% Pd/C catalyst (300 mg) in the presence of 2 equivalents of sulphuric acid. The reaction was conducted at 40°C under 6 barg hydrogen pressure with an external line pressure of 6.5 barg and an agitation speed of 1050 rpm. In this instance, alcohol chain length is compared. [Route A = phenethylamine; Route B = 2-amino-1-phenylethanol; Route C = missing mass].

Figure 7.10 shows the observed selectivity towards Routes A–C at reaction completion (time = 120 minutes) for each of the tested alcohols. It is apparent in Figure 7.10 that, as alcohol chain length increases, selectivity towards the desired product (phenethylamine) decreases. Further, whilst Route A is shown to undergo a decline as the alcohol chain length increases, Routes B and C display the opposite trend.

It is proposed that this observation is due to an elevation in viscosity of the alcohol as chain length increases. This trend is observed as the result of the increasing strength of the intermolecular forces which hold the molecule in place and is caused by the entanglement of the hydrocarbon chains. The longer the chain, the more entanglement is possible. Therefore, whilst an increase in alcohol chain length will result in the enhancement of hydrogen solubility, mass transport within the system will be hindered

as a result of the increased viscosity associated with long chain alcohols. This means that, although there is an increased hydrogen presence, the availability of the hydrogen at the surface of the catalyst will be restricted. Consequently, the outcome of Figure 7.10, showing a decline in hydrogen demanding routes (Route **A**) but the enhancement of routes which require less hydrogen (Routes **B** and **C**), is rationalised.

7.5.3 The Consideration of Tetrahydrofuran as an Alternative Reaction Solvent

As mentioned above, alcoholic solvents are shown to dominate in the nitrile hydrogenation literature.^[21, 246] Nevertheless, some more exotic solvents are also used.^[3, 40] As discussed in Section 1.4.1, there is literature precedence for the use of bi-phasic systems which are reported to improve selectivity by trapping the desired product in a particular phase.^[3, 65] The accompanying work-up required to isolate the product does, however, prove to be complicated and labour intensive. Neither of these factors are overly conducive to the necessary scale-up considerations for the mandelonitrile hydrogenation reaction process under consideration here.

Looking towards a simple mono-phasic system, the use of tetrahydrofuran as a reaction solvent is considered. Downing and co-workers report that the use of tetrahydrofuran as a solvent can improve selectivity through elimination of the common by-products formed in the presence of alcohol solvents.^[246, 250] However, no details regarding how the improved selectivity is facilitated are provided.

It was found that, in order to afford phenethylamine, it was necessary for the mandelonitrile hydrogenation reaction to be conducted in the presence of a sulphuric acid additive (Section 5.2). Despite this, tetrahydrofuran is typically used in the reported systems in the absence of additives. Moreover, as a cyclic ether, tetrahydrofuran is known to undergo ring opening reactions at elevated temperatures in the presence of sulphuric acid.^[251] Therefore, when the reaction was conducted in tetrahydrofuran (Figure 7.11), precautions were exercised. Specifically, the reaction was performed at room temperature and in the presence of only 1 equivalent of sulphuric acid (*cf.* standard reactions were conducted at 40 °C to ensure maximum phenethylamine selectivity (Section 7.4) and, in the presence of 2 equivalents of sulphuric acid).

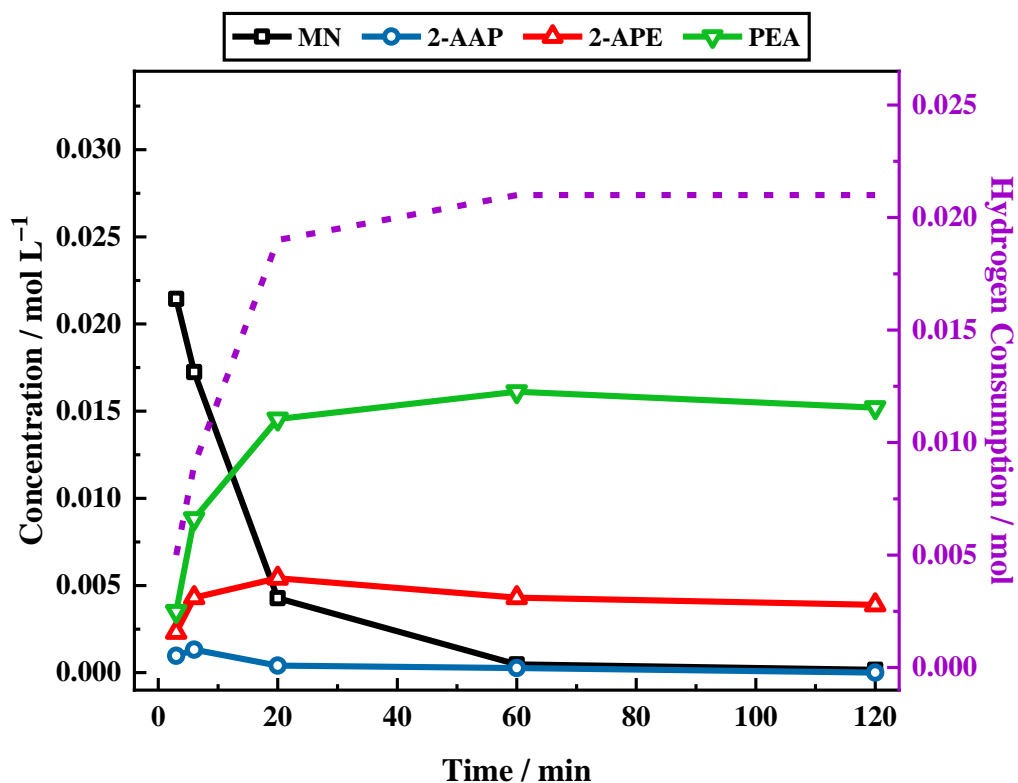


Figure 7.11. Reaction profile and hydrogen uptake curve (dashed purple line on the second y-axis) for the liquid phase hydrogenation reaction of mandelonitrile (35 mmol L^{-1}) over a 5% Pd/C catalyst (300 mg) in the presence of **1** equivalent of sulphuric acid in **tetrahydrofuran**. The reaction was conducted at **room temperature** under 6 barg hydrogen pressure with an external line pressure of 6.5 barg and an agitation speed of 1050 rpm. [MN = mandelonitrile; 2-AAP = 2-aminoacetophenone; 2-APE = 2-amino-1-phenylethanol; PEA = phenethylamine].

Figure 7.11 illustrates that, whilst the use of tetrahydrofuran as a reaction solvent affords a comparable hydrogen uptake (21 mmol, *cf.* 22.5 mmol obtained for standard conditions), the overall product distribution is not favourable. A primary observation would be the slower conversion of mandelonitrile, which does not reach completion until 60 minutes (*cf.* complete conversion achieved within 20 minutes under standard conditions). This is indicative of the first reaction step being hindered under the reported conditions. However, when the profile is compared to that obtained in the absence of acid (Figure 5.5), it may be postulated that it is the reduced acid concentration which causes the slower rate. This hypothesis will be considered further in Section 7.6.

Again, both 2-amino-1-phenylethanol and phenethylamine are observed at reaction completion. When compared directly to the standard conditions, the selectivity towards

2-amino-1-phenylethanol is not altered (13%), whereas phenethylamine selectivity is significantly reduced to 49% (*cf.* 87% for standard conditions). The reduced favour towards phenethylamine is accompanied by a noteworthy missing mass (38%), indicating a strong presence of Route **C**. Interestingly, the trace for 2-aminoacetophenone was shown to go through a maximum at 3 minutes with a concentration of 3.5 mmol L⁻¹. This minimal detection of 2-aminoacetophenone perhaps suggests that the position of the equilibrium no longer favours formation of the thermodynamically favourable ketone intermediate. It is again possible that the reduced acid concentration is responsible for this change in equilibrium favour. Overall, the outcome using tetrahydrofuran as a reaction solvent is stimulating, and something that may be worth pursuing. Nevertheless, in balance, it is likely that this solvent will perhaps be too chemically fragile to be used with the higher acid concentrations required in a product scale-up situation.

7.6 Acid Alteration Considerations

Following on from the findings of the tetrahydrofuran mediated reaction, the role of the acid additive was explored in greater detail. The standard reaction conditions (Section 5.3, Figure 5.4) include 2 equivalents of sulphuric acid with respect to the starting nitrile concentration. As previously described, the acid is found to have several important roles in the reaction system. Briefly, the acid primarily prevents coupling reactions of the imine intermediate and the amine products through protonation of the amine functionality.^[21] Furthermore, the acid also has an essential role in catalysing the tautomeric pathway which is found to be responsible for the formation of the ketone intermediate, 2-aminoacetophenone.^[217]

Nonetheless, as a strong acid, the use of sulphuric acid may be associated with several negative factors. This list includes the acid's ability to react with the reaction solvent to form unwanted by-products. As described in Section 6.2, the reaction between methanol and sulphuric acid affords monomethyl sulphate. Moreover, extended exposure of the reactor to a strong acid can result in corrosive effects, necessitating often costly repairs and maintenance. Alternative acids were therefore considered. Specifically, hydrochloric, acetic, and phosphoric acids were examined for their effectiveness in the hydrogenation reaction of mandelonitrile to afford the primary amine phenethylamine. In addition to

this, the concentration of the sulphuric acid present in the reaction mixture was considered.

7.6.1 Hydrochloric Acid

Despite the absence of any significant contemporary cyanohydrin hydrogenation literature, a report of the hydrogenation reaction of mandelonitrile was published in 1933. J.S. Buck hydrogenated various substituted mandelonitriles in alcohol over a platinum oxide catalyst in the presence of a hydrochloric acid additive.^[117] The reaction afforded a mixture of phenethylamine and 2-amino-1-phenylethanol type products, with the ratio dependent on the substituent used. No attempt to rationalise the findings, however, were made. Moreover, the reaction was reported to be complex and, thus, focus was brought to product isolation rather than the understanding of the mechanism.^[117] Against the literature precedent, the use of hydrochloric acid was considered for the hydrogenation reaction of mandelonitrile, the findings are presented in Figure 7.12.

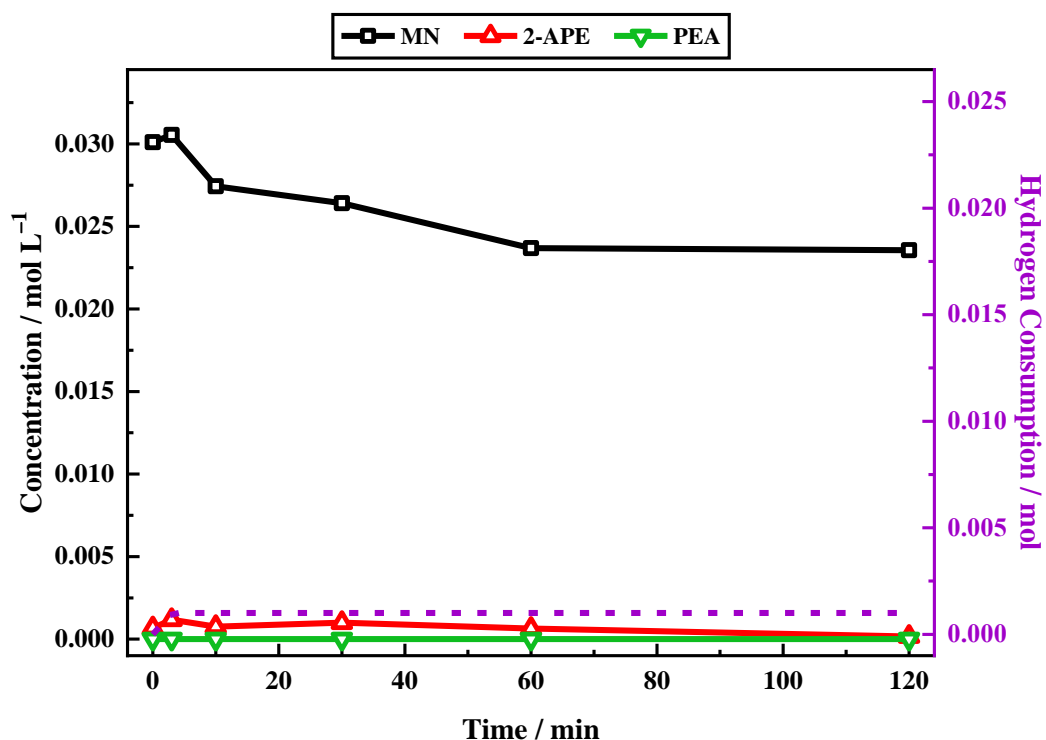


Figure 7.12. Reaction profile and hydrogen uptake curve (dashed purple line on the second y-axis) for the liquid phase hydrogenation reaction of mandelonitrile (31 mmol L^{-1}) over a 5% Pd/C catalyst (300 mg) in the presence of 2 equivalents of **hydrochloric acid** in methanol. The reaction was conducted at 40°C under 6 barg hydrogen pressure with an external line pressure of 6.5 barg and an agitation speed of approximately 1050 rpm. [MN = mandelonitrile; 2-APE = 2-amino-1-phenylethanol; PEA = phenethylamine].

Figure 7.12 shows incomplete mandelonitrile conversion (33%) at reaction termination, time = 120 minutes (*cf.* 100% in the presence of sulphuric acid). Further inspection reveals that no conversion is observed after 60 minutes, perhaps suggesting that the catalyst has been poisoned. Regarding product distribution, no phenethylamine is detected, with only trace quantities of 2-amino-1-phenylethanol being produced. Interestingly, this outcome is found to be comparable to that obtained in the *absence* of acid (Figure 5.5). When compared to the reaction conducted in the absence of acid, Figure 7.12 shows an enhanced mandelonitrile conversion (14% elevation). Moreover, the reaction is shown to proceed for a further 40 minutes before a product formation plateau is observed. Despite these improvements, the hydrochloric acid does not operate as effectively its sulphuric acid counterpart (as indicated in Figure 5.4).

If the catalyst is indeed poisoned, the cause of this must be determined. It is reported that halide ions inhibit palladium. These inhibitory effects are also linked to the corresponding

acid, for chloride ions this would be hydrochloric acid.^[18, 65, 117] In addition, the method by which hydrochloric acid is produced must also be considered. Hydrochloric acid is made by dissolving hydrogen chloride gas in water, resulting in a significant water presence.^[253] As shown in Section 7.5.1, the presence of water is found to be problematic for the production of phenethylamine and so, this may present an additional source of catalyst poisoning. Further, as a strong acid ($\text{pK}_a = -5.9$ for HCl gas), the presence of hydrochloric acid may promote an unwanted side reaction with the methanol solvent to form methyl chloride.^[254] When combined, however, all factors suggest that hydrochloric acid is not a suitable replacement for sulphuric acid.

7.6.2 Acetic Acid

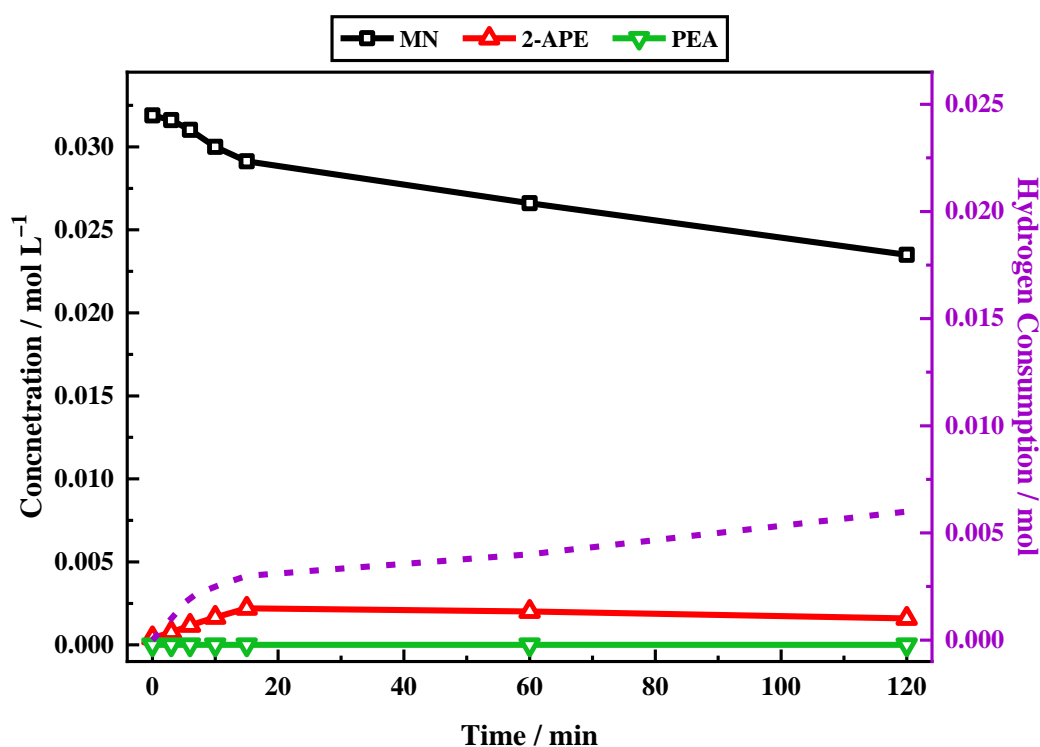


Figure 7.13. Reaction profile and hydrogen uptake curve (dashed purple line on the second y-axis) for the liquid phase hydrogenation reaction of mandelonitrile (31 mmol L^{-1}) over a 5% Pd/C catalyst (300 mg) in the presence of 2 equivalents of **acetic acid** in methanol. The reaction was conducted at 40°C under 6 barg hydrogen pressure with an external line pressure of 6.5 barg and an agitation speed of approximately 1050 rpm. [MN = mandelonitrile; 2-APE = 2-amino-1-phenylethanol; PEA = phenethylamine].

Having a pKa of 4.8, acetic acid is a weaker acid than sulphuric acid. The mandelonitrile hydrogenation reaction in the presence of an acetic acid additive is presented in Figure 7.13. Amongst other benefits, weaker acids are less likely to cause structural damage to the autoclave during reaction.^[65] Nevertheless, as with the use of hydrochloric acid, the outcome is unsatisfactory with regard to phenethylamine production. Again, conversion of mandelonitrile is poor, reaching 32% by reaction termination (time = 120 minutes). In contrast to Figure 7.12, however, the consumption of mandelonitrile is continual and does not plateau. This suggests that it is a slowed conversion instead of catalyst poisoning which results in the observed trend. As with Figure 7.12, no phenethylamine is produced within the allotted 120 minutes, but a slight enhancement in the production of 2-amino-1-phenylethanol is observed, reaching a maximum concentration of 2 mmol L⁻¹ where this molecule reaches a plateau (*cf.* a maximum of 0.9 mmol L⁻¹ was achieved using hydrochloric acid and, 8.2 mmol L⁻¹ using sulphuric acid).

It is postulated that the acetic acid is not sufficiently strong to protonate the full amine product component. As such it is likely that Route **C**'s coupling reactions will become more favourable than Routes **A** and **B**'s production of phenethylamine and 2-amino-1-phenylethanol, respectively. In line with this suggestion, 23% missing mass is detected at reaction completion alongside poor yields of Route **A** and Route **B** products. Therefore, it is predicted that, should the reaction time be extended such that full mandelonitrile conversion is achieved, more obvious signs of catalyst poisoning by amine products would be apparent. If this was the case, however, it is also possible that complete conversion may not be achievable.

7.6.3 Phosphoric Acid

The use of sodium dihydrogen phosphate (NaH₂PO₄) as an acid additive was successfully employed by Hegedűs and co-workers to afford phenethylamine in high selectivity (95%) *via* the hydrogenation reaction of benzyl cyanide over a 10% palladium on carbon catalyst.^[65] Phosphoric acid is a triprotic acid which undergoes a step-wise dissociation process. The use of phosphoric acid for the hydrogenation reaction of mandelonitrile is additionally tested (Figure 7.14).

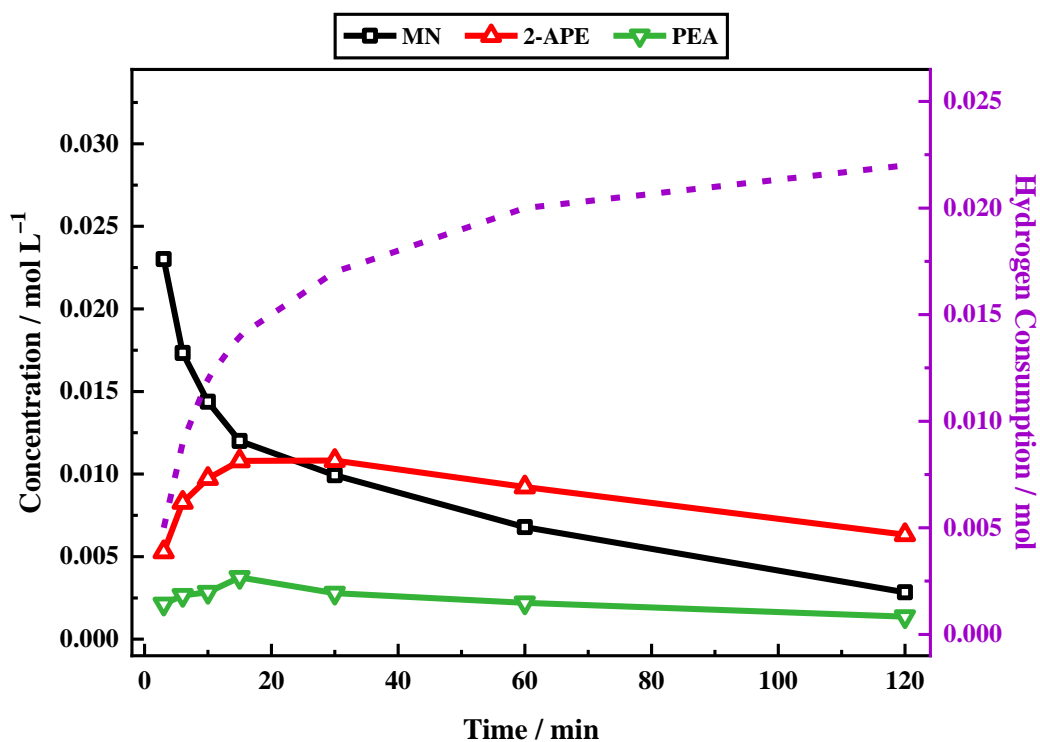


Figure 7.14. Reaction profile and hydrogen uptake curve (dashed purple line on the second y-axis) for the liquid phase hydrogenation reaction of mandelonitrile (31 mmol L^{-1}) over a 5% Pd/C catalyst (300 mg) in the presence of 2 equivalents of **phosphoric acid** in methanol. The reaction was conducted at 40°C under 6 barg hydrogen pressure with an external line pressure of 6.5 barg and an agitation speed of approximately 1050 rpm. [MN = mandelonitrile; 2-APE = 2-amino-1-phenylethanol; PEA = phenethylamine].

Figure 7.14 illustrates that in comparison to the results observed for hydrochloric and acetic acids, the conversion of mandelonitrile in the presence of a phosphoric acid additive is enhanced, reaching 91% conversion by reaction completion. Also observed in Figure 7.14 is the production of *both* phenethylamine and 2-amino-1-phenylethanol. However, whilst Route **B** is enhanced compared to the reference, Route **A** is diminished. Most notable though is the missing mass (Route **C**) which occupies 66% of the reaction mixture at reaction completion.



Figure 7.15. The Büchi stirred autoclave utilised for the hydrogenation reaction of mandelonitrile containing a solution of amines (phenethylamine and 2-amino-1-phenylethanol) in methanol post introduction of **A**, sulphuric acid and, **B**, phosphoric acid.

An important observation for the use of phosphoric acid is that, upon its addition to a solution of amines (phenethylamine and 2-amino-1-phenylethanol) in methanol, the resultant salt precipitated from the solution in quite a dramatic manner, as visualised in Figure 7.15 **B**. When the same experiment was conducted with sulphuric acid, however, no obvious salt formation was detected (Figure 7.15 **A**). It is proposed that the sulphate anion is more soluble in methanol than the phosphate anion, thus causing the phosphate salt to precipitate out of the solution. The additional presence of a solid (in the form of the phosphate salt) may hinder mixing, consequently restricting the availability of hydrogen. The outcomes of Figure 7.14 can therefore be rationalised in terms of limited hydrogen availability. Namely, that Routes **B** and **C**, which require a reduced hydrogen supply, will be enhanced under such conditions whilst the opposite is true for hydrogen demanding Route **A**.

7.6.4 The Acid Additive Function is Compared

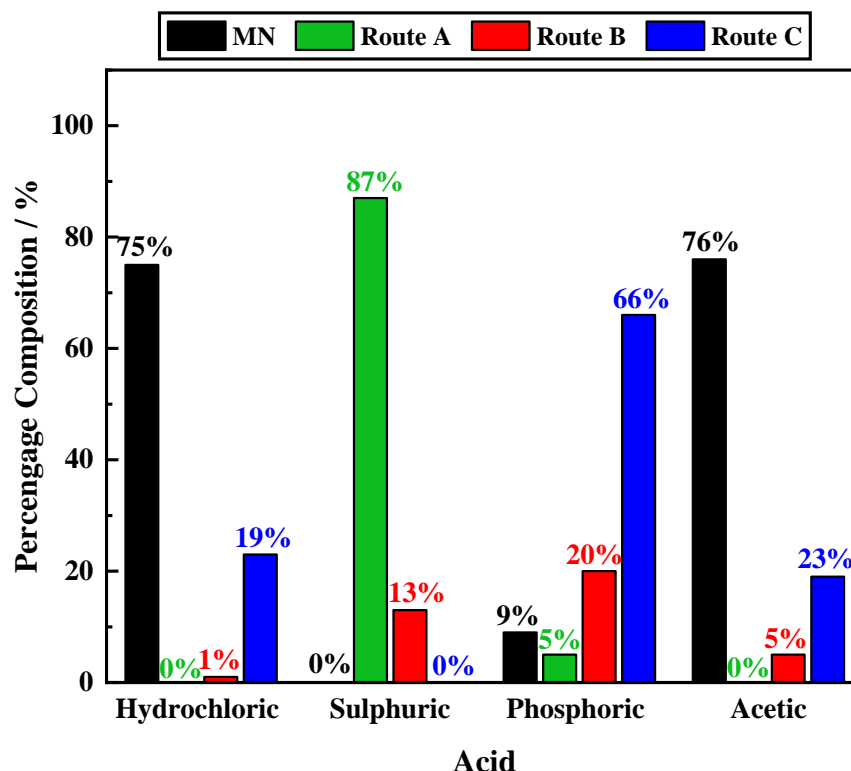


Figure 7.16. Selectivity towards each of the described Routes (A–C), calculated at reaction completion (time = 120 minutes) for the liquid phase hydrogenation reaction of mandelonitrile (35 mmol L^{-1}) over a 5% Pd/C catalyst (300 mg) in the presence of 2 equivalents of acid in methanol. The reaction was conducted at 40°C under 6 barg hydrogen pressure with an external line pressure of 6.5 barg and an agitation speed of 1050 rpm. In this instance, acid choice is compared. [MN = mandelonitrile; Route A = phenethylamine; Route B = 2-amino-1-phenylethanol; Route C = missing mass].

The selectivity towards Routes A–C, for each of the examined acids, is compared in Figure 7.16. Acids are ordered by increasing strength from left to right. Where an acid is multi-protic, $\text{pK}_{\text{a}1}$ has been used to determine the strength. When inspected, however, Figure 7.16 reveals no trends. Regarding the desired outcome, sulphuric acid is shown to be, by far, the most suitable acid for this application. Interestingly, the intermediate 2-aminoacetophenone was only observable for the reaction using sulphuric acid. Considering the outcomes of the other acids, this perhaps suggests that the release of 2-aminoacetophenone from the surface and its subsequent detection in the liquid phase is pivotal in the formation of phenethylamine.

7.6.5 Variations to the Concentration of the Sulphuric Acid Additive

The findings of Section 7.6.4 indicate that sulphuric acid is the most effective acid additive in terms of achieving favourable nitrile conversion and phenethylamine selectivity for the mandelonitrile hydrogenation reaction system. Standard operating conditions include 2 equivalents of sulphuric acid with respect to the starting nitrile concentration. It has been firmly established that the acid additive is an essential component of the reaction mixture (Section 5.2). It is, however, necessary to ascertain whether the correct concentration of acid is present in the reaction system for optimum performance.

In addition to its essential amine protonation function, the acid present in the reaction mixture also has a catalytic role. As previously described (Section 5.5), the acid catalysed tautomerisation of the hydroxy-imine intermediate leads to the formation of the ketone 2-aminoacetophenone and opens up tautomerisation derived equilibria pathways which are believed to facilitate the rapid formation of the desired primary amine. It is therefore proposed that an increase in acid concentration will improve the rate of this equilibria, thus enhancing the selectivity towards phenethylamine. It is also possible that the acid additive is able to catalyse additional reactions within the system to yield unwanted by-products, and thus, reduce the selectivity towards phenethylamine. As such, both an increase and a decrease in acid concentration, relative to the standard 2 equivalents, are investigated.

7.6.5.1 Acid Lean Conditions

Acid lean conditions in which the concentration of acid added was reduced to 1 equivalent, with respect to the initial nitrile concentration, were implemented in an attempt to minimise any potential side reactions. It is important to note that, whilst unwanted chemistry of this nature is not identified as a problem for a single batch reaction under standard conditions (Section 5.3), it may prove problematic on reaction scale-up. Thus, a single batch reaction, operating under reduced acid conditions, is used to probe how the reaction behaves when acid is limited.

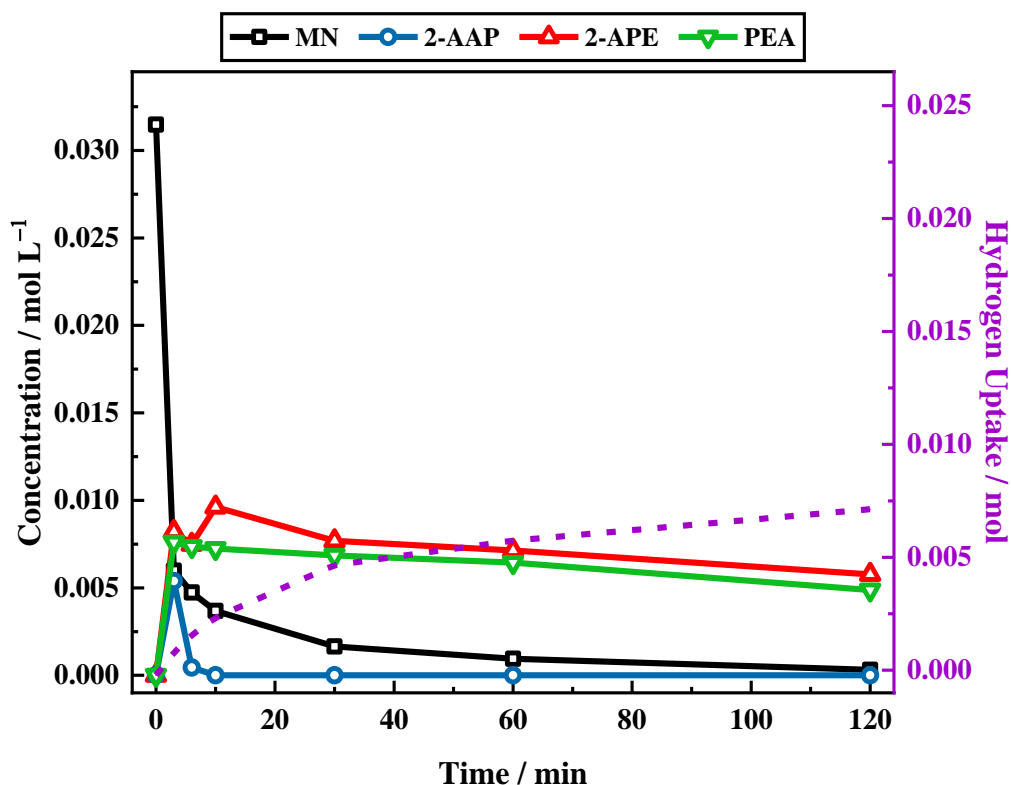


Figure 7.17. Reaction profile and hydrogen uptake curve (dashed purple line on the second y-axis) for the liquid phase hydrogenation reaction of mandelonitrile (31 mmol L^{-1}) over a 5% Pd/C catalyst (300 mg) in the presence of **1 equivalent** of sulphuric acid in methanol. The reaction was conducted at 40°C under 6 barg hydrogen pressure with an external line pressure of 6.5 barg and an agitation speed of approximately 1050 rpm. [MN = mandelonitrile; 2-AAP = 2-aminoacetophenone; 2-APE = 2-amino-1-phenylethanol; PEA = phenethylamine].

Figure 7.17 shows that whilst full conversion of mandelonitrile is achieved under acid lean conditions, the reaction takes substantially longer to reach complete conversion (approximately 120 minutes) than the standard acid conditions previously presented (approximately 20 minutes, Figure 5.4). Complete conversion of the starting material indicates a successful first step of the reaction (mandelonitrile to hydroxy-imine). Further examination of the product distribution, however, reveals a less favourable outcome. Within the first 3 minutes of the reaction, phenethylamine production is observed. Nonetheless, as reaction time is increased, no further production of the desired product is observed. Indeed, the slight decline in phenethylamine concentration observed at reaction times >3 minutes indicates that phenethylamine is consumed rather than produced. In contrast, the yield of 2-amino-1-phenylethanol is enhanced when compared to acid standard conditions at reaction completion (time = 120 minutes). These findings may be

attributed to an insufficient acid presence, thus resulting in the presence of unprotonated amines. When in their unprotonated form, the amine products are free to participate in coupling reactions and thus, it is predicted that under acid lean conditions, Route C will be enhanced. This postulate is evidenced by the detection of missing mass (65%) at reaction completion, indicating a dominance of Route C. Furthermore, a reduced uptake of hydrogen, 42% of that observed for standard conditions is detected.

7.6.5.2 Acid Rich Conditions

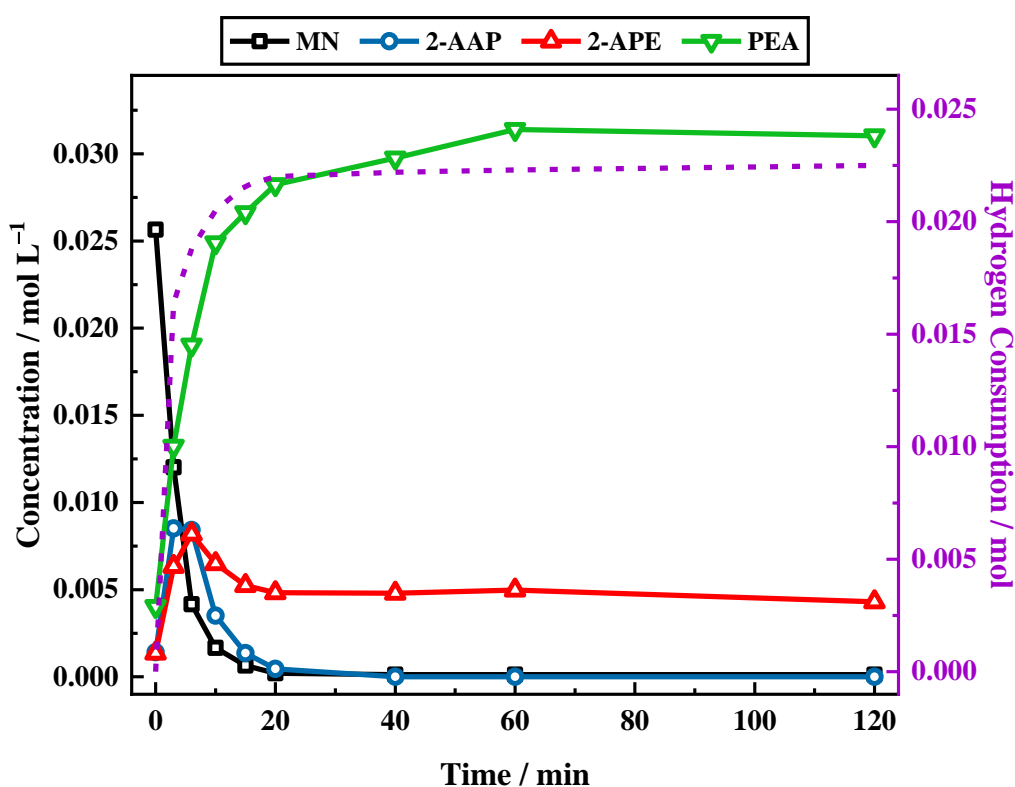


Figure 7.18. Reaction profile and hydrogen uptake curve (dashed purple line on the second y-axis) for the liquid phase hydrogenation reaction of mandelonitrile (31 mmol L^{-1}) over a 5% Pd/C catalyst (300 mg) in the presence of **4 equivalents** of sulphuric acid in methanol. The reaction was conducted at 40°C under 6 barg hydrogen pressure with an external line pressure of 6.5 barg and an agitation speed of 1050 rpm. [MN = mandelonitrile; 2-AAP = 2-aminoacetophenone; 2-APE = 2-amino-1-phenylethanol; PEA = phenethylamine].

Further, an increase in acid concentration was examined. Figure 7.18 therefore shows the reaction profile for the hydrogenation reaction of mandelonitrile in the presence of 4 equivalents of sulphuric acid. When compared directly to standard conditions (Figure 5.4), no notable differences are observed, indicating that it is likely that increasing the acid concentration from 2 to 4 equivalents does not result in any mechanistic alterations. A similar trend was documented by Kárpáti *et al.*. In this instance, it was found that once a minimum acid requirement was met, further increasing the acid concentration did not significantly enhance product yield.^[65]

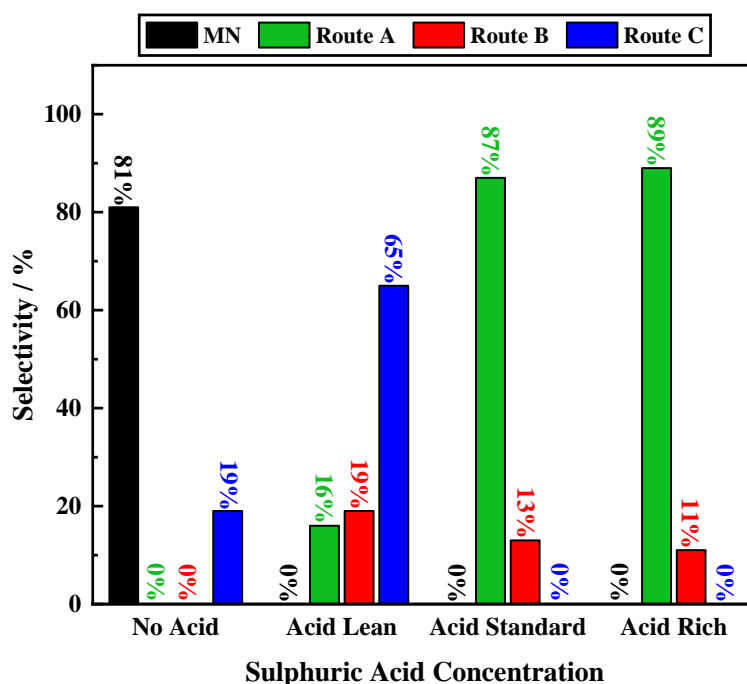


Figure 7.19. Selectivity towards each of the described Routes (A–C), calculated at reaction completion (time = 120 minutes) for the liquid phase hydrogenation reaction of mandelonitrile (35 mmol L^{-1}) over a 5% Pd/C catalyst (300 mg) in the presence and absence of sulphuric acid. The reaction was conducted at 40°C under 6 barg hydrogen pressure with an external line pressure of 6.5 barg and an agitation speed of 1050 rpm. In this instance, acid concentration is compared. [MN = mandelonitrile; Route A = phenethylamine; Route B = 2-amino-1-phenylethanol; Route C = missing mass; acid lean = 1 equivalent sulphuric acid; acid standard = 2 equivalents sulphuric acid; acid rich = 4 equivalents sulphuric acid].

Comparing the outcomes of the various acid concentrations (Figure 7.19), further deductions regarding the role of the acid may be made. Figure 7.19 reiterates the findings of Figures 7.17 and 7.19. Specifically, increasing the acid concentration from the standard value does not cause a selectivity change whereas, a decrease in acid concentration results in a markedly different product distribution. Moreover, Figure 7.19 clearly indicates that there is a minimum acid requirement necessary to afford phenethylamine in appreciable quantities (2 equivalents).

The concentration of the acid in the reaction system is likely to affect the rate of the acid catalysed tautomeric pathway, with an increasing concentration resulting in an acceleration in rate. It is therefore proposed that, above the minimum acid requirement, the relative rate of the equilibrium must be faster than the hydrogenation of 2-aminacetophenone to 2-amino-1-phenylethanol. If this was not the case, then 2-amino-1-phenylethanol would appear as the major product of the reaction.

7.7 Conclusions

Optimisation of the mandelonitrile hydrogenation reaction to afford phenethylamine with an enhanced selectivity was explored such that product scale-up could be effectively undertaken. Ideally, the production of phenethylamine would be completely selective with no by-product presence detected. Nevertheless, the standard reaction conditions utilised in Chapters 5 and 6 were found to be superior. The following conclusions based on a series of parameter changes, however, were able to be drawn:

- Expansion of the reaction scheme allowed three Routes, denoted **A–C**, each with a distinct product output, to be defined. Further, this notation allowed the observed product distribution for any specific set of reaction conditions to be used to determine hydrogen supply.
- Both an elevation and a decrease in temperature from standard conditions (40 °C) were explored. It was found that, at 40 °C, the reaction exhibited the correct balance between effective hydrogen solubility and the prevention of unwanted side reactions, such that selectivity towards phenethylamine was maximised.

- The inclusion of water as a component of the reaction solvent was found to be detrimental to phenethylamine selectivity, with the selectivity being progressively worsened with an increasing water percentage. Further, the use of water as a solvent in the absence of an acid additive, though found to enhance mandelonitrile conversion when compared to the use of methanol in neutral conditions, is determined to be an unsuitable substitute for the sulphuric acid additive.
- Whilst reported to enhance hydrogen solubility, increasing the chain length of the alcoholic solvent reduced phenethylamine selectivity. This observation was attributed to the increasing viscosity associated with increasing alcohol chain length which potentially resulted in poorer mass transport.
- The use of tetrahydrofuran as a reaction solvent was found to be incompatible with the concentration of sulphuric acid required for the mandelonitrile hydrogenation reaction and thus, was not a suitable alternative.
- Several other acid additives were also tested. However, all but sulphuric acid significantly hindered or prevented the formation of phenethylamine.
- Increasing the concentration of sulphuric acid, despite yielding no selectivity improvements, matched that obtained for acid standard conditions. In contrast, a decrease in acid concentration was found to significantly enhance the occurrence of the unwanted coupling reactions. These outcomes indicate that a minimum acid requirement must be met for the successful production of phenethylamine to be achieved.

CHAPTER 8

*Towards Sustained Product
Formation in the Liquid Phase
Hydrogenation of Mandelonitrile
over a Pd/C Catalyst*

8.1 Introduction

The previous mandelonitrile hydrogenation and deuteration studies, explored in Chapters 5–7, examined single batch reactions. Whilst these studies have been critical for the development and understanding of the reaction mechanism, the industrial relevance of the mandelonitrile hydrogenation reaction must also be considered. In relation to this statement, it is noted that the industrial process linked to this substrate system operates as a fed batch protocol. Moreover, deactivation issues associated with the cycling of the catalyst have been identified and this therefore represents an area where improvement is essential for the process to be deemed viable in an industrial setting.

Though well set-up to perform single batch reactions, the Büchi reactor at the University of Glasgow is not specifically designed as a fed batch reactor. As such, a repeat batch methodology, described in the subsequent section (Section 8.2), was developed. Specifically, this study aims to transform the mandelonitrile hydrogenation reaction from a single batch to a repeat batch process in order to address the catalyst deactivation issues experienced industrially. An optimised reaction profile is presented, representing the best possible outcome within safety and equipment constraints at the University of Glasgow. Crucially, however, the reaction mechanism, by way of the observed product distribution, can be utilised to provide an understanding for this outcome. Consequently, methods of further improvement with regard to catalyst durability and sustainability, currently outside the capability at the University of Glasgow, can be proposed. A preliminary venture into the use of a continual stirred tank reactor (CSTR) arrangement conducted at the industrial facility (Syngenta, Jealott's Hill) has also been explored.

8.2 A Repeat Batch Protocol was Implemented to Replicate the Industrial Process

A repeat batch protocol, which aims to mimic the industrial fed batch process, has been developed. However, due to equipment limitations at the University of Glasgow, slight methodology differences were necessary. The repeat batch protocol can be defined as follows. The reactor was first charged with hydrogen, as with the batch process, and the catalyst reduced for 30 minutes. The reagents, both the mandelonitrile and the sulphuric acid additive, were subsequently added and left to react for 120 minutes. Sampling of the reaction mixture at the end of this time period represented the completion of the first batch

reaction (addition 1). Following this, the next aliquot of reagent (mandelonitrile and sulphuric acid), without the inclusion of any further catalyst, was added to the reactor and left for the standardised time period of 120 minutes. Once again, a sample of the reaction mixture was taken at the end of the batch reaction (addition 2). This process was repeated for the desired number of additions (typically 6). Further experimental details can be found in Section 2.2.3.

Crucially, as reagent introduction could not be performed under pressure, each time a reagent addition was made, it was necessary for the reactor to be depressurised and subsequently re-charged to the required hydrogen pressure. For each reagent addition, a charging time was thus incurred. It is this factor which represents the major difference between repeat batch and fed batch technologies. In a fed batch process one or more of the reactants are charged batchwise (mandelonitrile and sulphuric acid), whilst a co-reactant is fed continually (hydrogen). For the repeat batch protocol employed here, *both* reactant (mandelonitrile and sulphuric acid) and co-reactant (hydrogen) are charged batchwise.

8.3 Early Investigations into the Repeat Batch Protocol for the Hydrogenation Reaction of Mandelonitrile

Preliminary repeat batch studies, conducted using the reported method (Section 8.2), were performed by McMillan^[150] and Gilpin^[151] at the University of Glasgow. These studies were carried out under a generic operational environment, found to be suitable for similar, previously studied substrate systems (4 barg hydrogen pressure, 60 °C and an agitation speed of 800 rpm).^[150–151] Initially, these conditions were thought to be under kinetic control, with the reported agitation speed corresponding to a value on the plateau region of a nitrile consumption rate *versus* agitation speed plot conducted by McMillan.^[150] The literature indicates that, where an increase in agitation speed yields no improvement in hydrogenation rate, gas-liquid diffusional constraints should be minimal.^[3, 6, 39, 154, 255] Nevertheless, this inference, combined with a successful single batch reaction (Section 5.3, Figure 5.4), was found to be misleading. Indeed, the findings of the initial repeat batch study mirrored the industrial outcome, with significant catalyst deactivation observed.

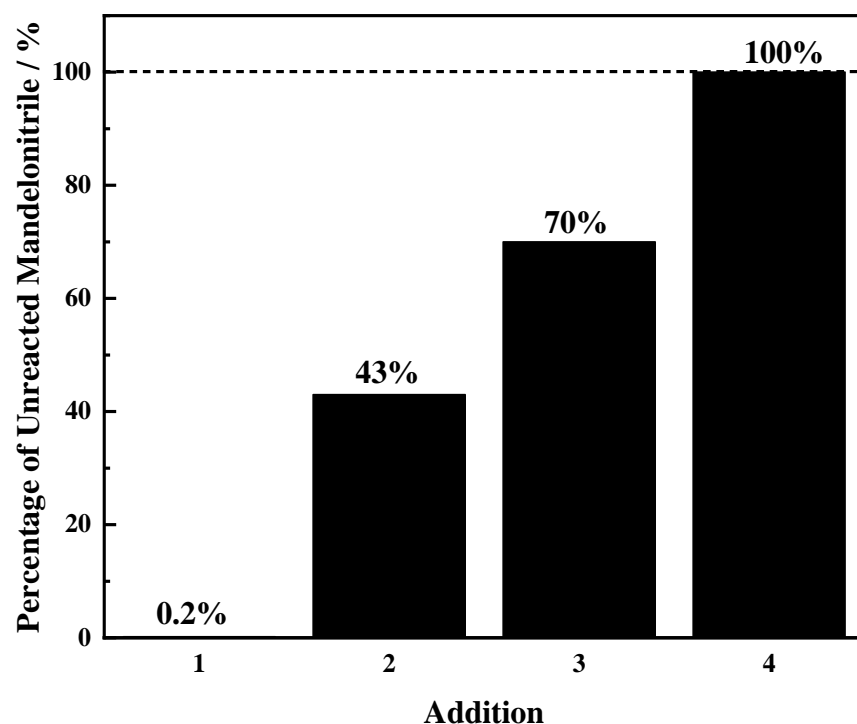


Figure 8.1. Percentage of unreacted mandelonitrile detected in the liquid phase for a 4-batch liquid phase hydrogenation reaction of mandelonitrile. Each reagent addition is comprised of mandelonitrile (11 mmol) and 2 equivalents of sulphuric acid, reacted over the same 5% Pd/C catalyst (300 mg), in methanol. The reaction was conducted at 60 °C under 4 barg hydrogen pressure with an external line pressure of 6.5 barg and an agitation speed of 800 rpm. Each addition (1–4) represents a fixed 120 minute time period. [MN = mandelonitrile]. This figure is reproduced from reference 150.

Figure 8.1 is representative of an early outcome for the repeat batch protocol and shows the percentage of unreacted mandelonitrile at the end of each 120 minute reaction. The rapid decline of the hydrogenation activity of the catalyst can be clearly seen as the number of additions is increased. Complete deactivation is observed by the 4th addition, where no conversion of the starting material was detected. Despite the implication of the rate *versus* agitation plot conducted by McMillan, the substantial deterioration of catalyst activity observed on repeat use (Figure 8.1) indicates the presence of a potential mass transfer limitation within the system. Further, the outcome of Figure 8.1 illustrates the difficulties associated with product scale-up from single batch to repeat batch. Due to the unsatisfactory outcome of Figure 8.1, further examination of the hydrodynamic features of this process was commissioned.

8.4 Improving Hydrogen Availability Improves Catalyst Durability

As described in Chapter 4, hydrogen availability and hydrodynamic improvements were implemented for the 4-hydroxybenzyl cyanide reaction system. Such improvements were initially investigated by Gilpin.^[151] A temperature reduction ($60\text{ }^{\circ}\text{C} \rightarrow 40\text{ }^{\circ}\text{C}$) was accompanied by an increase in both hydrogen pressure (4 barg \rightarrow **6 barg**) and agitation speed (800 rpm \rightarrow **1050 rpm**). The experimental parameters highlighted in bold represent hydrogen rich conditions (compared with hydrogen lean conditions). Nevertheless, whilst improvements to the durability of the catalyst were made, no connection between the observed product distribution and the reaction mechanism was made.

Whilst Figure 8.1 clearly represents an undesirable outcome, it is essential that a ‘good’ outcome is defined. With reference to the previous chapter (Chapter 7), Routes A–C can again be used, allowing catalyst activity to be monitored as it is cycled. For the single batch mandelonitrile hydrogenation reaction (Figure 5.4), both Routes A (phenethylamine production) and B (2-amino-1-phenylethanol production) are seen to be operational, with Route A dominating. Route C (missing mass) is inoperative, as evidenced by a complete mass balance (Figure 5.5). Thus, if catalyst activity is sustained through cycling, it is to be expected that, as each substrate addition is made, production of both phenethylamine and 2-amino-1-phenylethanol will be observed. Notably, the selectivity of the product mixture should remain unaltered.

Expanding on this, Scheme 7.1 (Section 7.1) also defines the hydrogen requirement for each route. As such, further predictions relating to changes in the product distribution as the experimental conditions are altered can be made. Thus, it is postulated that when hydrogen becomes limited, the route which requires the most hydrogen (Route A) will experience preferential deactivation. In contrast, routes requiring less hydrogen (Routes B and C) will be sustained for more substrate additions over the catalyst and may even be enhanced. It can be surmised that, at each of the branching points, homogeneous pathways will be favoured over heterogeneous pathways when hydrogen is limited.

It is also important that the limits of the system are fully tested. As such, it was deemed necessary to increase the number of reagent additions from 4 to 6. The elevated number of substrate additions, whilst increasing the total time required to perform the experiment, also provided a more convincing platform by which catalyst durability could be assessed. An experiment examining 6 reagent additions over the same un-regenerated catalyst,

conducted under the above-mentioned hydrogen rich conditions, was performed, the results of which can be visualised in Figure 8.2.

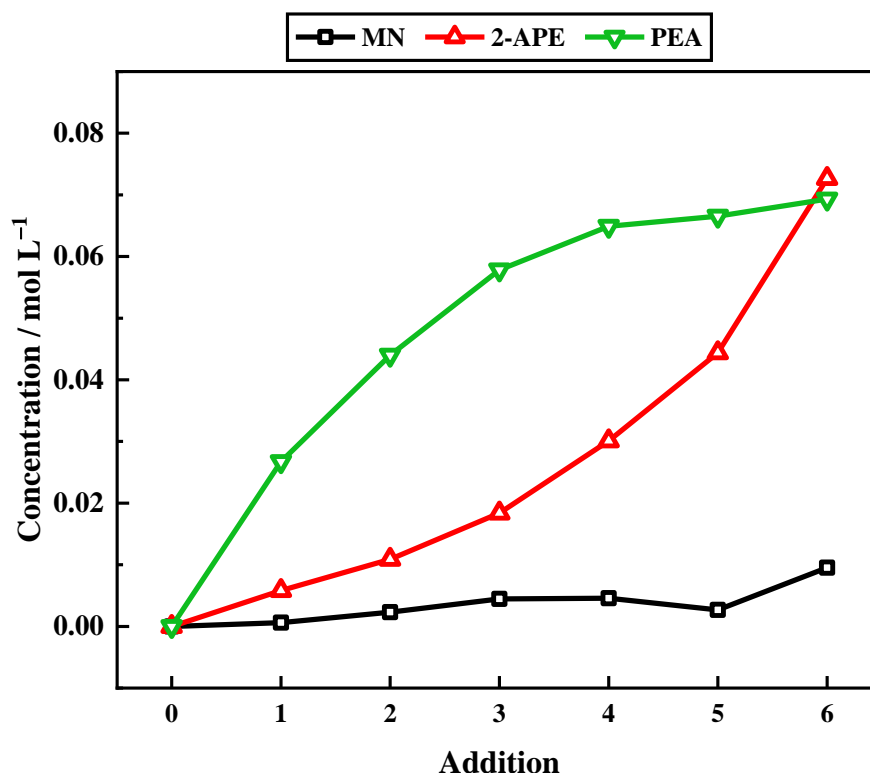


Figure 8.2. Reaction profile for a 6-batch mandelonitrile hydrogenation reaction. Each reagent addition is comprised of mandelonitrile (11 mmol) and 2 equivalents of sulphuric acid, reacted over the same 5% Pd/C catalyst (300 mg), in methanol. The reaction was conducted at 40 °C under 6 barg hydrogen pressure with an external line pressure of 6.5 barg and an agitation speed of 1050 rpm. Each addition (1–6) represents a fixed 120 minute time period. [MN = mandelonitrile; 2-APE = 2-amino-1-phenylethanol; PEA = phenethylamine].

Examination of the mandelonitrile component of Figure 8.2 showed that, for *all* 6 reagent additions, $\geq 95\%$ conversion was achieved. This illustrates a vast improvement from the initial outcome, presented in Figure 8.1, which showed complete conversion of the mandelonitrile for only 1 addition. This demonstrates that a significant enhancement to catalyst activity on cycling can be achieved by increasing the hydrogen availability.

Unfortunately, McMillan did not document any information regarding phenethylamine yield or reaction selectivity for the original reaction conditions presented in Section 8.3. As such, comparisons between the two sets of conditions, in terms of product formation,

cannot be made. Nevertheless, when production of phenethylamine is considered under hydrogen rich conditions (Figure 8.2), it can be seen that product formation has not been sustained on later additions (additions 4 to 6). After 4 reagent additions phenethylamine production begins to plateau, indicating that the catalyst has shut down Route **A**. If the 87% selectivity towards phenethylamine produced in addition 1 is taken as a 100% yield for this reaction, the phenethylamine yield for addition 6 is a mere 10%. In contrast, production of the by-product 2-amino-1-phenylethanol is enhanced as the number of reagent additions increases. Again, taking the yield of 2-amino-1-phenylethanol produced in addition 1 as 100%, the yield of the by-product by addition 6 is found to be 485%. The 2-amino-1-phenylethanol and phenethylamine yields for each of the 6 additions as a percentage of the yield associated with the first addition are tabulated in Table 8.1. Here it is shown that, unlike Route **A**, Route **B** is enhanced as the catalyst is cycled. Despite the impeded production of phenethylamine from addition 4 onwards, the continued formation of 2-amino-1-phenylethanol is indicative of a maintained catalyst functionality.

Table 8.1. Yield of 2-amino-1-phenylethanol and phenethylamine for additions 1–6 produced in the hydrogenation reaction of mandelonitrile (11 mmol) in the presence of 2 equivalents of sulphuric acid reacted over a 5% Pd/C catalyst (300 mg). The reaction was conducted at 40 °C under 6 barg hydrogen pressure with an external line pressure of 6.5 barg and an agitation speed of 1050 rpm. Each addition (1–6) represents a fixed 120 minute time period.

<i>Addition</i>	<i>2-Amino-1-phenylethanol</i>	<i>Phenethylamine</i>
1	100%	100%
2	96%	93%
3	115%	91%
4	201%	26%
5	245%	6%
6	485%	10%

Looking at the same data set, Figure 8.3 shows the selectivity towards each of the predefined reaction Routes (A–C) at the end of each 120 minute batch reaction (1–6). In all instances, unreacted mandelonitrile accounted for <4% of the reaction mixture at the end of each reagent addition and was thus considered negligible. Examining the initial 3 additions, a complete mass balance ($\pm 5\%$) was achieved, indicating the near absence of the unfavourable imine chemistry responsible for unwanted side product formation (Route C). Additionally, Figure 8.2 shows that a comparable selectivity outcome to that obtained for the single batch process (Figure 5.4) is obtained for the first 3 batch reactions (additions 1–3). The selectivity towards both phenethylamine and 2-amino-1-phenylethanol remains largely unaltered during this time, suggesting that catalyst activity was successfully maintained.

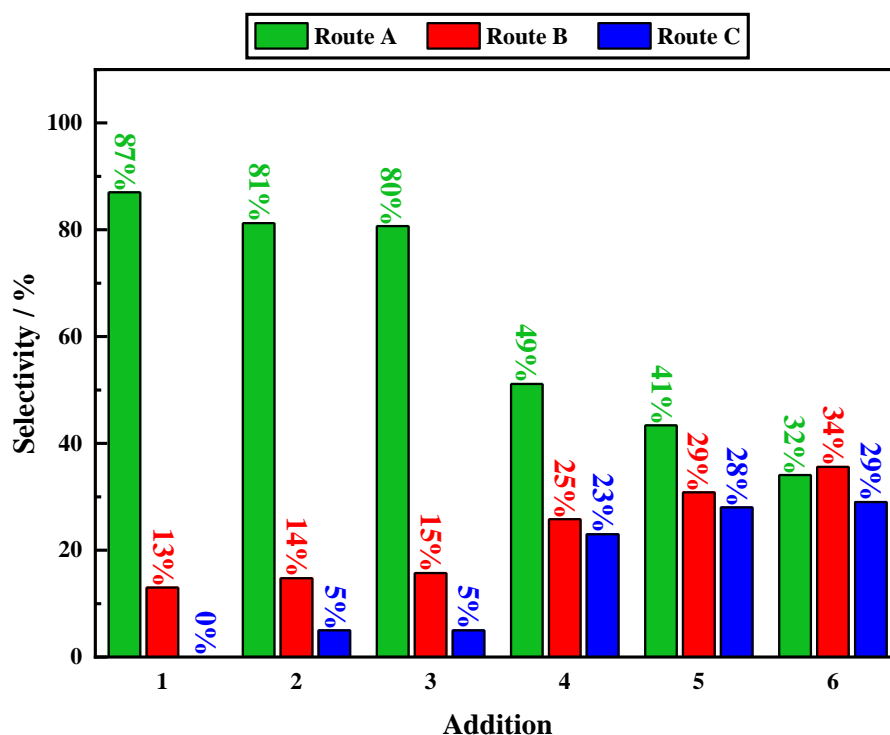


Figure 8.3. Selectivity towards each of the described Routes (A–C), calculated at the end of each addition for a 6-batch mandelonitrile hydrogenation reaction. Each reagent addition is comprised of mandelonitrile (11 mmol) and a sulphuric acid additive (2 equivalents), reacted over the same 5% Pd/C catalyst (300 mg), in methanol. The reactions were conducted at 40 °C under 6 barg hydrogen pressure with an external line pressure of 6.5 barg and an agitation speed of 1050 rpm. Each addition (1–6) represents a fixed 120 minute time period. [Route A = phenethylamine; Route B = 2-amino-1-phenylethanol; Route C = missing mass].

When more additions were made, however, the mass balance exhibited a significant drop, with Route **C** accounting for an increasingly significant portion of the reaction mixture. Figure 8.3 shows a clear trend. Specifically, as the number of reagent additions is increased above a threshold number (in this instance 3), the selectivity towards Routes **B** and **C** is enhanced but is decreased towards Route **A**. Combined, these findings provide a strong indication of a diminishing hydrogen supply as the number of reagent additions is increased.

8.5 Examination of the Hydrodynamics of the Reaction System within the Improved Experimental Domain Described in Section 8.4

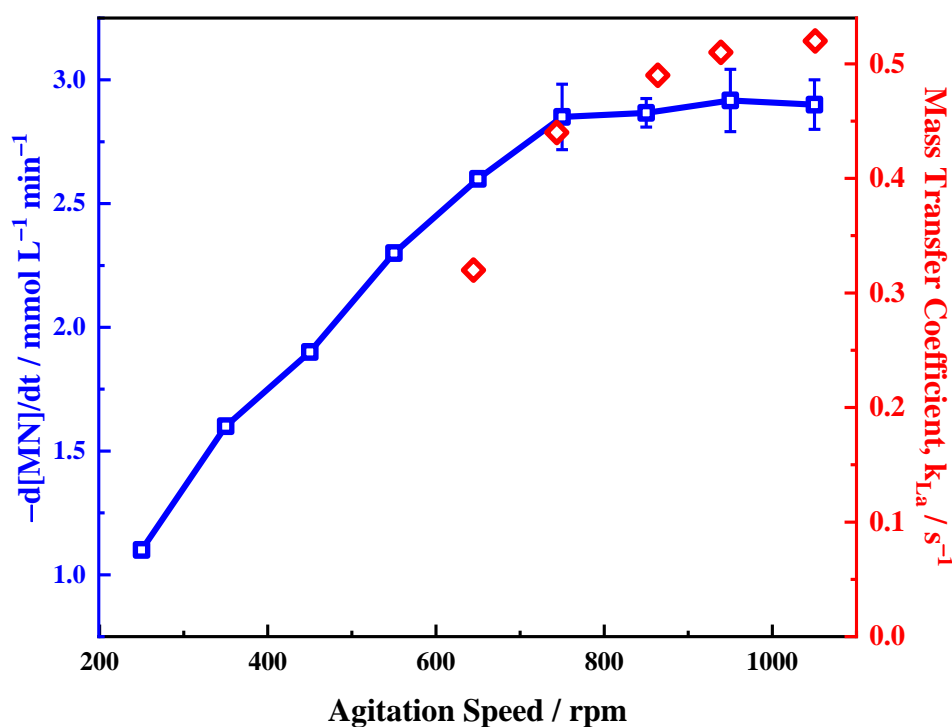


Figure 8.4. Influence of agitation speed on the rate of consumption of starting material for the liquid phase hydrogenation of mandelonitrile (35 mmol L^{-1}) over a 5% Pd/C catalyst (300 mg) in the presence of 2 equivalents of sulphuric acid in methanol (blue trace). The reaction was conducted at 40°C under 6 barg hydrogen pressure with an external line pressure of 6.5 barg and an agitation speed of 1050 rpm. The error bars represent experimental triplicates. Shown on the second y-axis (red trace) is the influence of agitation on the gas-liquid mass transfer coefficient at 40°C and 6 barg pressure. [MN = mandelonitrile].

As discussed in Section 4.4, a generic method of determining the extent to which mass transport controls a catalytic reaction is to run the reaction at several different agitation speeds and monitor the effect on the rate of reagent consumption.^[39, 255–256] With reference to the rate *versus* agitation plot for reagent consumption presented in Figure 8.4, the outcome is shown to corroborate the findings of McMillan.^[150] Here it is shown that applying an agitation speed of ≥ 750 rpm *should* ensure efficient hydrodynamics for the mandelonitrile hydrogenation reaction system. Operating at agitation speeds lower than this value will likely lead to a mass transfer limitation at the gas-liquid interface. However, the three-phase mandelonitrile hydrogenation system (solid-liquid-gas) constitutes a multi-step reaction pathway, requiring hydrogen availability throughout the full reaction coordinate.^[240] Consequently, the sole analysis of rate of reagent consumption *versus* agitation speed may not provide the most comprehensive description of hydrogen dissolution for the reaction system as a whole, potentially resulting in a misleading outcome.^[255–257]

Not considered within the mandelonitrile consumption rate/agitation speed correlation are the subsequent hydrogen requiring steps necessary to afford phenethylamine. A more rigorous experimental method of ensuring that a process operates under a maximised hydrogen supply is the determination of liquid mass transfer coefficients (k_{La}).^[257] As such, Figure 8.4 also presents k_{La} values as a function of agitation rate, and shows the rate of hydrogen dissolution to be close to a maximum value at the maximum stirring speed (1050 rpm). This outcome indicates that the dihydrogen solvation rate is optimised at elevated agitation rates, with the quantity of dissolved hydrogen in methanol ultimately limited by Henry's law.^[211–212] Thus, to ensure that the reaction vessel operates at its best possible efficiency, and to allow favourable kinetics for the $H_{2(g)} \rightarrow H_{2(soln)}$ step which is active at the gas-liquid interface, agitation of the reaction mixture at 1050 rpm is necessary.

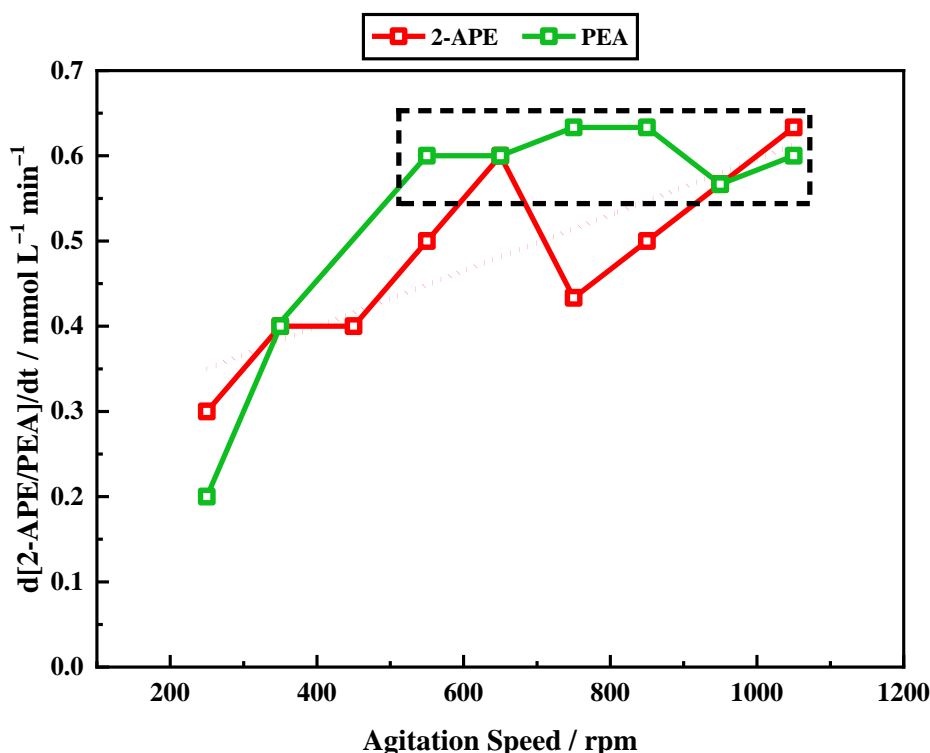


Figure 8.5. Influence of agitation speed on the rate of product formation production for the liquid phase hydrogenation of mandelonitrile (35 mmol L^{-1}) over a 5% Pd/C catalyst (300 mg) in the presence of 2 equivalents of sulphuric acid in methanol. The reaction was conducted at 40°C under 6 barg hydrogen pressure with an external line pressure of 6.5 barg and an agitation speed of 1050 rpm. The dotted red line represents a linear fit of all 2-amino-1-phenylethanol data points. [2-APE = 2-amino-1-phenylethanol; PEA = phenethylamine].

To supplement the measurements shown in Figure 8.4, rate *versus* agitation plots for product and by-product formation were also conducted (Figure 8.5). As illustrated in Figure 8.5, the plateaus in the rate of product formation for both desired product and by-product are found to be in different ranges from that obtained for the rate of mandelonitrile consumption (Figure 8.4). Indeed, the plateau for the production of phenethylamine is found to be within the 550–1050 rpm range. This region has been highlighted in Figure 8.5 by a dashed black box. The by-product (2-amino-1-phenylethanol) does not, however, appear to reach a plateau, indicating that a kinetic regime is not achieved. The dotted red line in Figure 8.5 represents a linear fit of all the data points corresponding to 2-amino-1-phenylethanol production rate. However, a degree of caution must be exercised when analysing the 2-amino-1-phenylethanol data due to its unusual trajectory in the reaction profile (Figure 5.4).

8.6 Methods of Improving the Catalyst Lifetime (Acid Considerations)

Following examination of hydrogen supply and reaction hydrodynamics, alternative methods of improving the catalyst lifetime were explored. Various aspects relating to the acid additive were discussed in the reaction optimisation exercise conducted for the single batch reaction reported in Chapter 7. It was found that, for the hydrogenation reaction of mandelonitrile, sulphuric acid was the most effective acid additive, and thus, focus was centred here.

Both acid rich (4 equivalents of sulphuric acid) and acid lean (1 equivalent of sulphuric acid) conditions were examined and compared to acid standard conditions (2 equivalents of sulphuric acid). Section 7.6.5 has previously highlighted that, whilst the increase in acid concentration did not have a noticeable selectivity effect on a single batch mandelonitrile hydrogenation reaction (Figures 5.4 and 7.18), acid lean conditions were far from favourable (Figure 7.17). Acid lean reaction conditions have, however, been selected for further exploration to further illustrate this observation. A 6 batch study using acid lean conditions is thus undertaken to further illustrate the necessity of an adequate acid presence.

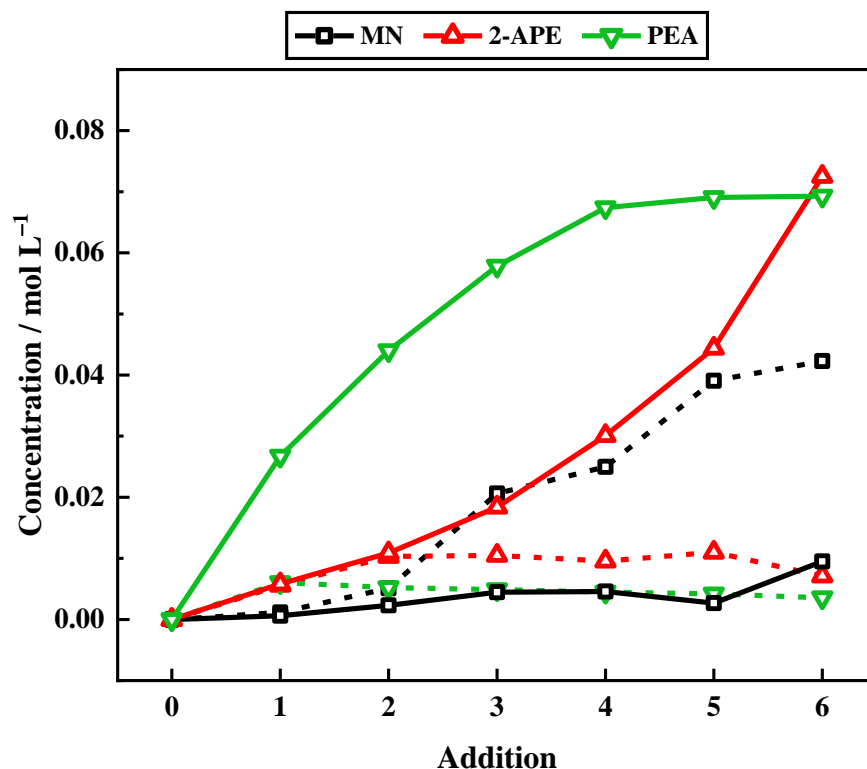


Figure 8.6. Reaction profile for a 6-batch mandelonitrile hydrogenation reaction. Each reagent addition is comprised of mandelonitrile (11 mmol) and either 1 equivalent (dashed lines), or 2 equivalents (solid lines), of sulphuric acid, reacted over the same 5% Pd/C catalyst (300 mg) in methanol. The reaction was conducted at 60 °C under 4 barg hydrogen pressure with an external line pressure of 6.5 barg and an agitation speed of 1050 rpm. Each addition (1–6) represents a fixed 120 minute time period. [MN = mandelonitrile; 2-APE = 2-amino-1-phenylethanol; PEA = phenethylamine].

As discussed in Section 7.6.5.1, it was initially proposed that the acid additive has a supplementary role in catalysing additional unwanted side reactions within the mandelonitrile hydrogenation reaction system. Figure 8.6 compares the 6 batch processes conducted under acid lean (dashed lines) and acid standard (solid lines) conditions, illustrating a stark contrast between the two profiles.

As described in Section 8.4, complete conversion is achieved for all 6 reagent additions under acid standard conditions. Contrastingly, Figure 8.6 shows that complete consumption of the starting material is only observed for addition 1 in an acid lean environment. Conversion of the starting material is thus hindered, resulting in a build-up of unreacted mandelonitrile in the system. The average conversion of mandelonitrile, over the 6 addition process, is found to be 77% (cf. 98% under acid standard conditions). In

line with the reduced conversion, product formation was also stilted. The selectivity of phenethylamine for addition 1 was found to be 16%, representing only 18% of the value obtained under acid standard conditions. As more reagent additions were made, no further phenethylamine production was observed. Incidentally, there was slight consumption of the desired product such that, by addition 6, a selectivity of only 11% was determined. The formation of the by-product 2-amino-1-phenylethanol fairs marginally better, maintaining standard production levels for 2 additions before a plateau is reached. This therefore indicates that Route **B** is more favourable than Route **A** when the acid presence is compromised.

Both Routes **A** and **B** involve the use of an acid catalysed tautomeric pathway to afford their designated products. The reduced acid content will therefore not favour one route over the other on the grounds of kinetic reasoning as the result of decelerated acid catalysed chemistry. It is therefore proposed that the major differences observed for the acid lean and acid standard conditions, as illustrated in Figure 8.6, relates to Route **C**. By addition 6, Route **C** accounted for 92% of the reaction mixture under acid lean conditions (*cf.* 20% missing mass was observed under acid standard conditions by the end of addition 6). Thus, the occurrence of coupling reactions is shown to be more prevalent under acid lean conditions. It is clear that a minimum acid requirement in the reaction system is necessary to hinder Route **C** when the catalyst is cycled. The outcome of Figure 7.17 (Section 7.6.5.1) is therefore endorsed, further highlighting that an acid presence alone is not sufficient to allow the sustained production of phenethylamine.

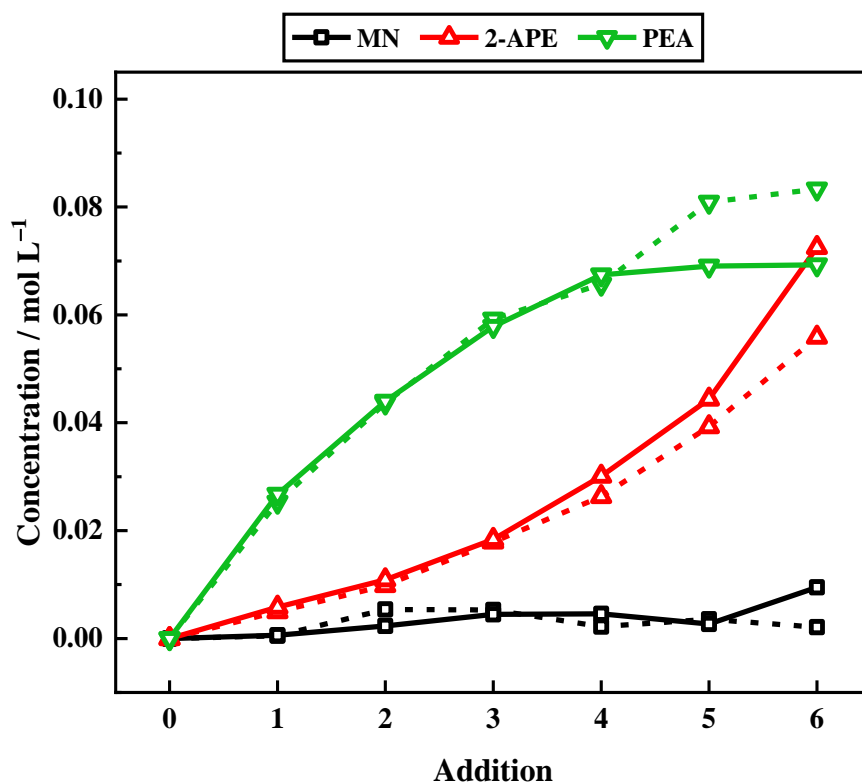


Figure 8.7. Reaction profile for a 6-batch mandelonitrile hydrogenation reaction. Each reagent addition is comprised of mandelonitrile (11 mmol) and either 2 equivalents (solid lines), or 4 equivalents (dashed lines) of sulphuric acid, reacted over the same 5% Pd/C catalyst (300 mg) in methanol. The reaction was conducted at 60 °C under 4 barg hydrogen pressure with an external line pressure of 6.5 barg and an agitation speed of 1050 rpm. Each addition (1–6) represents a fixed 120 minute time period. [MN = mandelonitrile; 2-APE = 2-amino-1-phenylethanol; PEA = phenethylamine].

The sulphuric acid concentration was then increased from 2 to 4 molar equivalents (with respect to starting nitrile concentration), thus rendering the reaction system to be under acid rich conditions. A comparison profile for a 6 batch reaction is presented in Figure 8.7 where the resultant profiles are shown to be similar. Under both regimes, $\geq 95\%$ conversion of the starting material was achieved for all 6 additions. Within experimental error, the first 3 additions showed an identical outcome. It is not until addition 4 that deviations, as the result of differing acid concentration, are observed. Figure 8.7 highlights that the increased acid enhances phenethylamine production but hinders 2-amino-1-phenylethanol formation. Thus, it is revealed that the final phenethylamine selectivity is improved by 6% through the application of acid rich conditions.

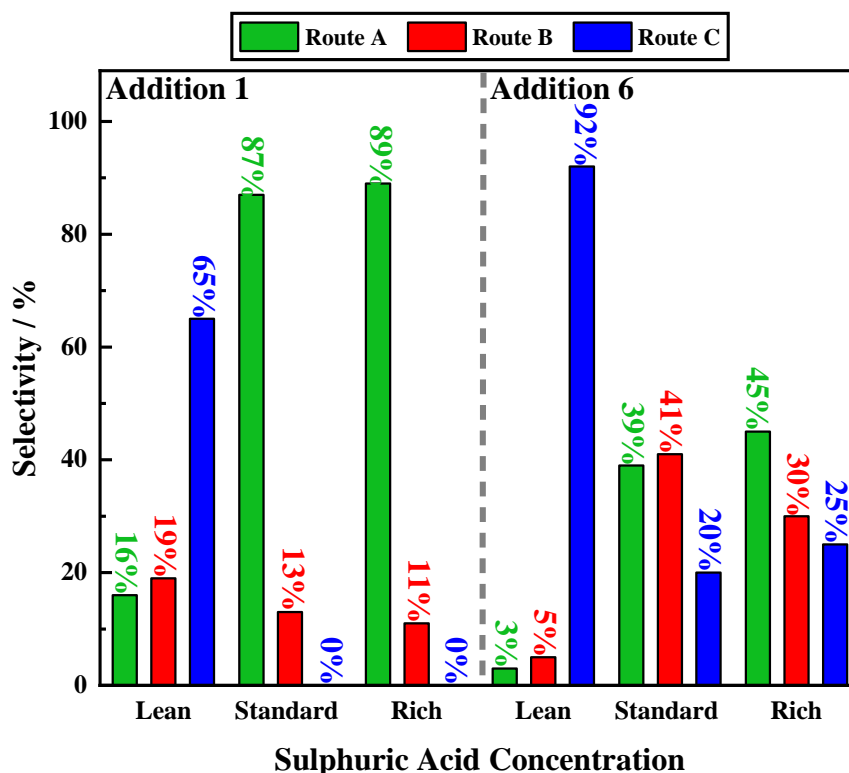


Figure 8.8. Selectivity towards each of the described Routes (A–C), calculated at the end of addition 1 and addition 6 for 6-batch mandelonitrile hydrogenation reactions. Each reagent addition is comprised of mandelonitrile (11 mmol) and a sulphuric acid additive (various concentrations), reacted over the same 5% Pd/C catalyst (300 mg) in methanol. The reactions were conducted at 40 °C under 6 barg hydrogen pressure with an external line pressure of 6.5 barg and an agitation speed of 1050 rpm. In this instance, acid concentration is compared. [Route A = phenethylamine; Route B = 2-amino-1-phenylethanol; Route C = missing mass; acid lean = 1 equivalent sulphuric acid; acid standard = 2 equivalents sulphuric acid; acid rich = 4 equivalents sulphuric acid].

The selectivity outcomes of all three acid conditions at the end of addition 1 and addition 6 are compared in Figure 8.8. For all considered acid concentrations, an enhancement of Routes B and C, but a decline in Route A, is observed when the catalyst is cycled (compare the outcome of addition 1 with the outcome of addition 6). Further, despite the improvement in phenethylamine selectivity experienced when acid concentration was increased, the prevalence of Route C cannot be ignored. Acid rich conditions were found to slightly enhance the occurrence of this route. Moreover, Figure 8.8 illustrates that, when the acid concentration is doubled from standard to rich conditions, only minor improvements to catalyst longevity, in relation to the selective production of phenethylamine, were incurred.

Against these observations, it was initially postulated that a concentration dependence, relating to the ammonium salts (both phenethylamine and 2-amino-1-phenylethanol), was impeding catalyst turnover. Consequently, it was proposed that, in order to prevent catalyst deactivation, it is essential that the concentration of the ammonium salts is kept below a threshold value. The use of an alternative reactor design/set-up is a potential solution. This possibility is considered further in Section 8.10 where the mandelonitrile hydrogenation reaction is performed in a continuous stirred tank reactor (CSTR) set-up.

If this postulate was to stand, the production of *both* phenethylamine and 2-amino-1-phenylethanol would be negatively affected. Examination of Figure 8.2, however, reveals that, although phenethylamine formation is hindered, 2-amino-1-phenylethanol production is conversely enhanced. This does not fit with the concentration dependence theory. Further investigation into the true nature of the observed catalyst deactivation is thus necessary.

8.7 The Repeat Batch Experiments were Revisited to Test the Concentration Dependence Theory

After essential lab refurbishment and gas manifold maintenance (2018), the repeat addition experiments were re-examined with the aim of further exploring the proposed concentration dependence theory detailed in Section 8.6. As shown in Figure 8.2, deactivation was primarily observed from the 4th consecutive batch reaction onwards. Therefore, a proposed benchmark reaction, focusing on additions 4–6, was initially conducted (Figure 8.9). To do this, the composition of the reaction mixture at the end of addition 3, as determined from Figure 8.2, was reproduced. As such, a solution containing 58 mmol L⁻¹ phenethylamine and 18 mmol L⁻¹ 2-amino-1-phenylethanol in methanol was prepared. Three aliquots (one for each batch reaction that would have occurred if the repeat batch methodology was employed) of two equivalents of sulphuric acid were also added. It is important to note that the amines and the acid were added to the reactor separately, with a methanol flush between them, to prevent salt formation in the injection port. No mandelonitrile was included as it was shown to be completely consumed (Figure 8.2). Once the starting conditions were applied, 3 reagent additions were made using the repeat batch methodology described in Section 8.2. These 3 mandelonitrile and sulphuric

acid additions should, in theory, be analogous to additions 4–6, presented in Figure 8.2. However, with reference to Figure 8.9, this was not found to be the case.

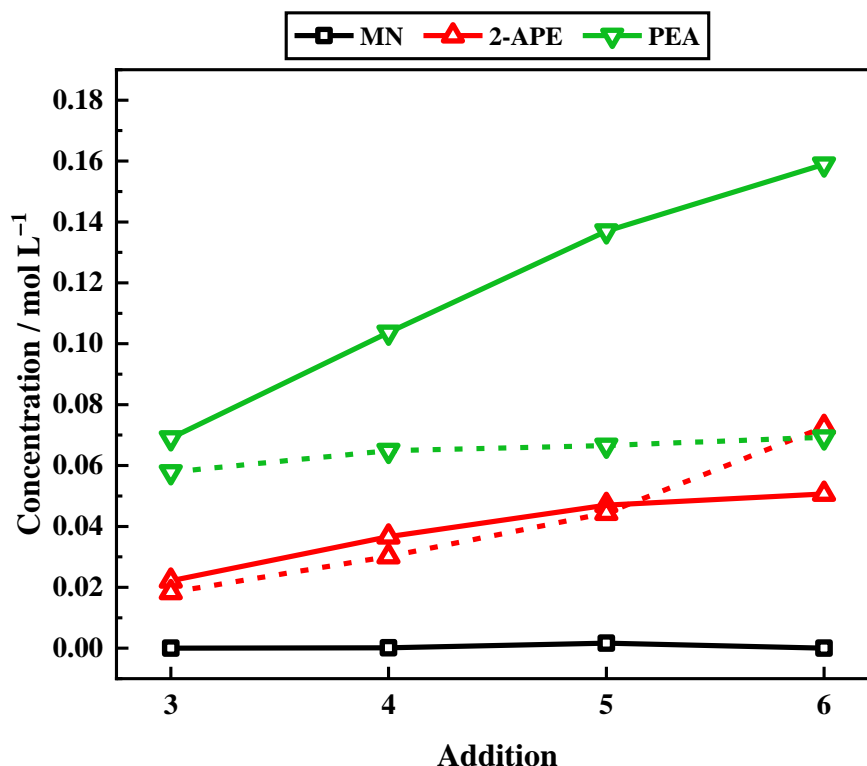


Figure 8.9. Reaction profile for a 3-batch mandelonitrile hydrogenation reaction (additions 4–6). Each reagent addition is comprised of mandelonitrile (11 mmol) and 2 equivalents of sulphuric acid, reacted over the same 5% Pd/C catalyst (300 mg), in methanol. The reaction was conducted at 40 °C under 6 barg hydrogen pressure with an external line pressure of 8 barg and an agitation speed of 1050 rpm. Each addition (3–6) represents a fixed 120 minute time period. The aforementioned conditions are represented by the solid lines. The dashed lines correspond to the outcomes of additions 3–6 as reported in Figure 8.2. [MN = mandelonitrile; 2-APE = 2-amino-1-phenylethanol; PEA = phenethylamine].

Instead, the outcome of additions 4–6 (Figure 8.9) more closely matches the findings of the first 3 batches (Figure 8.2). Figure 8.9 (solid lines) illustrates the continuous formation of both phenethylamine and 2-amino-1-phenylethanol. This is in stark contrast to the previous result, shown initially in Figure 8.2, but reproduced in Figure 8.9 (dashed lines) for ease of comparison. The continued production of phenethylamine in the presence of a highly concentrated amine solution, whilst favourable, was somewhat surprising. Therefore, the outcome of Figure 8.9 suggests that there is *not* a concentration dependence

on the amine hydrogen sulphate salts which impedes catalyst turnover. An alternative hypothesis was thus proposed. Namely, that oligomeric produce from a critical number of reagent additions (in this case 3) over the same catalyst blocks a sufficient number of active sites such that the catalyst is deactivated. This would consequently imply that the last 3 additions (4–6), presented in Figure 8.2, are not sufficient to deactivate the catalyst, thus rationalising the favourable outcome of Figure 8.9. The number of reagent additions was consequently extended from 3 (additions 4–6) to 6 (additions 4–9) to test this postulate. Note that amine concentration conditions observed at the end of addition 3 were again replicated prior to the commencement of the repeat batch process for additions 4–9. The resultant profile is presented in Figure 8.10.

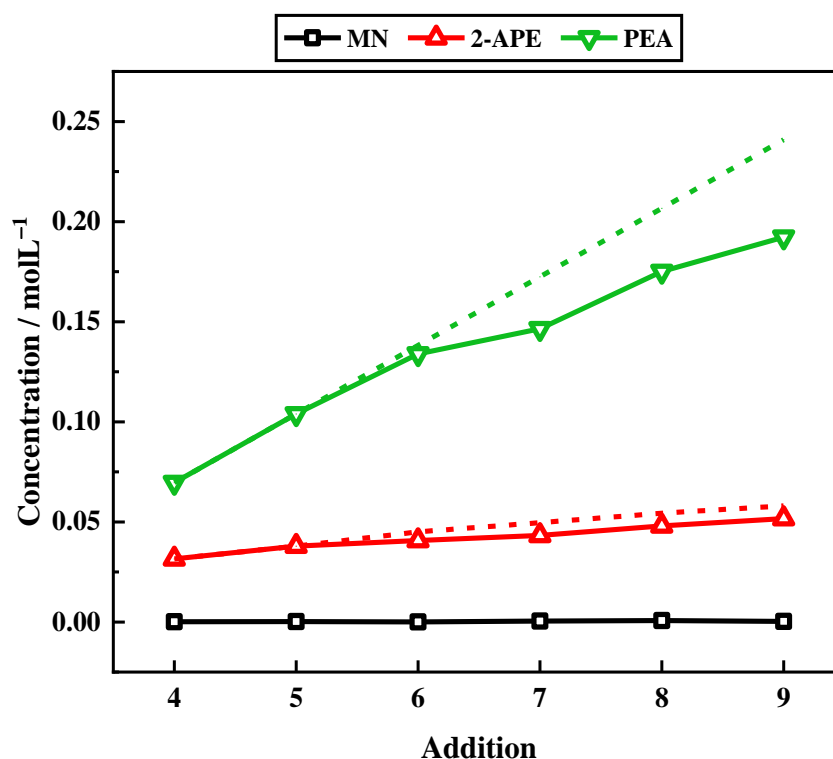


Figure 8.10. Reaction profile for a 6-batch mandelonitrile hydrogenation reaction (additions 4–9). Each reagent addition is comprised of mandelonitrile (11 mmol) and 2 equivalents of sulphuric acid, reacted over the same 5% Pd/C catalyst (300 mg) in methanol. The reaction was conducted at 40 °C under 6 barg hydrogen pressure with an external line pressure of 8 barg and an agitation speed of 1050 rpm. Each addition (4–9) represents a fixed 120 minute time period. The aforementioned conditions are represented by the solid lines. The dashed lines associated with the 2-amino-1-phenylethanol and phenethylamine data points are representative of predicted continuous product formation based on the product formation observed for the first batch reaction in the process (addition 4). [MN = mandelonitrile; 2-APE = 2-amino-1-phenylethanol; PEA = phenethylamine].

Again, the outcome of Figure 8.10 is found to be surprising. As before (Figure 8.9), additions 4–6 exhibit the favourable outcome observed for additions 1–3 as shown in Figure 8.2. It was predicted that additions 7–9 would follow the same trend as additions 4–6 of Figure 8.2. This, however, was shown not to be the case. Whilst phenethylamine production is revealed to decline on later additions (4–9), with the experimentally determined concentrations (solid line) deviating from the predicted concentration (dashed line), continuous formation is observed for all monitored additions. The predicted concentrations of phenethylamine and 2-amino-1-phenylethanol are represented by dashed lines and are calculated as an extrapolated yield, based on the assumption that the yield for the first addition will be maintained for all subsequent additions.

The outcome of Figure 8.10 hence suggests that the catalyst, showing sustained product formation for 6 additions, had not been significantly poisoned by the elevated amine concentration present in the reaction mixture. Therefore, it is not a concentration dependence or a detrimental build-up of oligomeric material occurring on the first 3 additions under the reported conditions which causes the deactivation observed in Figure 8.2. Thus, an additional source, allowing the improvement observed in Figures 8.9 and 8.10 to be rationalised, must be identified. Accordingly, it was proposed that the original 6 batch experiment (examination of additions 1–6 without an elevated initial amine concentration) was reconducted to ascertain whether the initial figure (Figure 8.2) could be replicated.

8.8 Hydrogen Line Pressure, Relating to Reactor Charging Time, was Identified as a Key Contributor to Sustained Product Formation

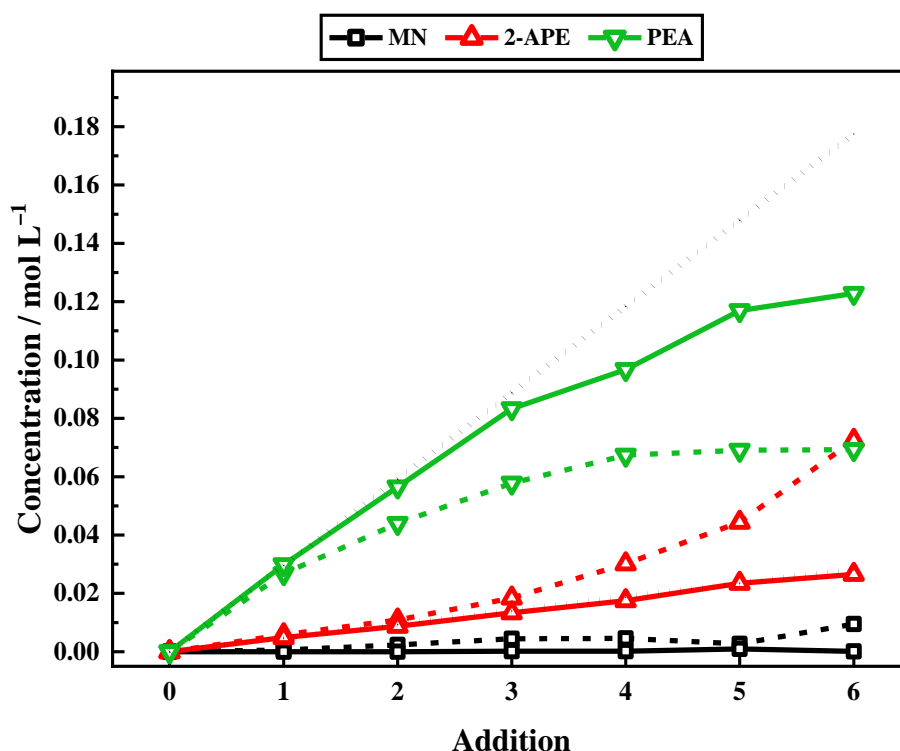


Figure 8.11. Reaction profile for a 6-batch run for the hydrogenation reaction of mandelonitrile. Each reagent addition is comprised of mandelonitrile (11 mmol) and 2 equivalents of sulphuric acid, reacted over the same 5% Pd/C catalyst (300 mg) in methanol. The reaction was conducted at 40 °C under 6 barg hydrogen pressure with an external line pressure of 8 barg (solid lines) and 6.5 barg (dashed lines), and an agitation speed of 1050 rpm. Each addition (1–6) represents a fixed 120 minute time period. The dotted black lines associated with the 2-amino-1-phenylethanol and phenethylamine data points are representative of predicted continuous product formation based on the product formation observed for addition 1. [MN = mandelonitrile; 2-APE = 2-amino-1-phenylethanol; PEA = phenethylamine].

The outcome of the repeated 6-batch reaction is shown in Figure 8.11 (solid lines) and compared to the original outcome originally visualised in Figure 8.2 (dashed lines). The two profiles, conducted under identical experimental conditions, are shown to be vastly different. Further investigation, however, revealed a difference between the two reactions. During gas manifold maintenance the hydrogen line pressure had been increased from 6.5 barg to 8 barg.

As discussed in Section 8.2, by nature of the reactor design, the set-up at the University of Glasgow incurs a hydrogen charging period once reagent addition has been conducted at ambient pressure. It has been identified that the external line pressure has a significant effect on the time taken to charge the reactor from ambient conditions to the 6 barg required for the mandelonitrile hydrogenation reaction. For comparative purposes, the time taken to reach 6 barg with an external line pressure of 6.5 barg is 7.5 minutes, whereas a 3 minute charging time corresponds to an external line pressure of 8 barg. During the charging time, a hydrogen ‘super lean’ environment is created as the result of the reduced agitation speed and pressure experienced as the reactor is brought to optimal conditions. Further, during this protocol, there is a period of time when the gaseous headspace contains no hydrogen. A constant supply of hydrogen is required to for an active catalyst surface to be maintained.

It is consequently the effect of external line pressure, and therefore charging time, on the reaction profile which is illustrated in Figure 8.11. Production of both phenethylamine and 2-amino-1-phenylethanol is shown to be sustained throughout the repeat batch sequence for at least 4 additions under both sets of charging conditions. However, from Figure 8.11, a reduced charging time (solid lines compared to dashed lines) dramatically improves the production of phenethylamine and diminishes the production of 2-amino-1-phenylethanol. Whilst 2-amino-1-phenylethanol is shown to be produced at a consistent quantity for each addition, closely following the projected rate (black dotted lines), phenethylamine formation is shown to drop-off on later additions (\geq addition 4). The concentration of reagent and products are only monitored at the end of each 120 minute batch process, and thus, accurate rate data cannot be obtained. Nonetheless, it is clear from Figure 8.11 that reduced phenethylamine yields are observed on repeated cycling.

The reaction scheme presented in Section 7.2 (Scheme 7.1) highlights that, regardless of the route the reaction takes, hydrogenation of mandelonitrile to the hydroxy-imine is always the first step. Hence, despite the hydrogen ‘super lean’ conditions of the charging period, formation of the hydroxy-imine will always be favoured. Supporting this postulate is the observation of complete nitrile consumption for all 6 additions under both charging scenarios (Figure 8.11). Therefore, reaction processes further through the reaction scheme become hindered when charging time is increased. It is thought that as charging time increases, the longer the catalyst is starved of an adequate hydrogen supply. Thus, it is

likely that this process incurs a progressive loss in active sites *via* oligomer formation that is not readily reversible under standard reaction conditions.

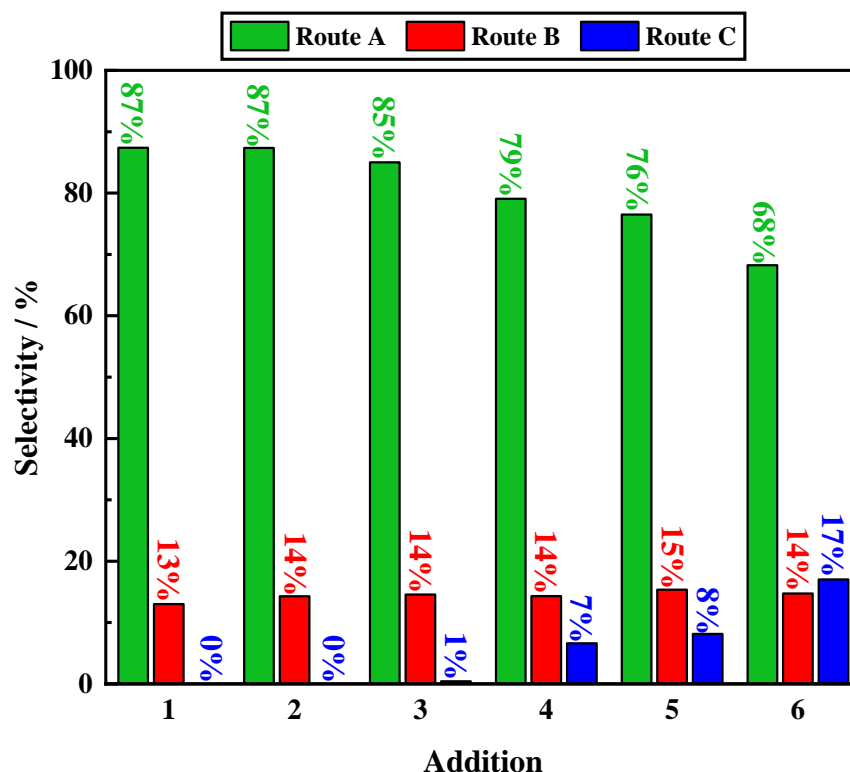


Figure 8.12. Selectivity towards each of the described Routes (A–C) for a 6-batch run for the hydrogenation reaction of mandelonitrile. Each reagent addition is comprised of mandelonitrile (11 mmol) and 2 equivalents of sulphuric acid, reacted over the same 5% Pd/C catalyst (300 mg) in methanol. The reaction was conducted at 40 °C under 6 barg hydrogen pressure with an external line pressure of 8 barg and an agitation speed of 1050 rpm. Each addition (1–6) represents a fixed 120 minute time period. [Route A = phenethylamine; Route B = 2-amino-1-phenylethanol; Route C = missing mass].

Figure 8.12 shows the selectivity of the reaction mixture, at the end of each of the 6 reported additions, towards the predefined Routes (A–C). Complete consumption of the nitrile is observed for all 6 additions. A further consistency for each addition is the Route B product which is shown to occupy approximately 14% of the reaction mixture for all additions. In contrast, the Route A product is shown to be less consistent, occupying between 85% and 87% of the product distribution for additions 1–3 before a drop in selectivity is observed. A closed mass balance, indicated by the absence of Route C, is therefore returned for additions 1–3, indicating that all of the chemistry associated with the first 3 additions is accounted for. After addition 3, however, phenethylamine

selectivity declines, resulting in an increasingly incomplete mass balance. By addition 6, the missing mass accounts for approximately 17% of the reaction mixture. The phasing of the mass imbalance (additions 4–6 as shown in Figure 8.12) suggests that a portion of these oligomeric entities are surface bound species.

When hydrogen is limited, *i.e.* during reactor charging and re-charging, there will be competition for $H_{(ads)}$ at the branching points in the reaction. Thus, the homogeneous reactions which do not require a hydrogen supply will be favoured at **BP1** and **BP2**. Nonetheless, as the reaction is not completely starved of hydrogen, Route **A**, which possesses the highest hydrogen demand will still be able to occur, but crucially, at a slower rate. As more substrate additions are made, each with its own charging period, increasingly more of the catalyst active sites will become blocked, thus progressively hindering production of the desired product. Figure 8.12 therefore highlights that a reduced charging time (solid lines) significantly enhances formation of phenethylamine (Route **A**) but reduces 2-amino-1-phenylethanol formation (Route **B**). Route **C**, however, is largely unaffected. A reduced charging time therefore results in a more favourable product outcome.

In order to ensure sustained phenethylamine formation and prevent the build-up of the major by-product and oligomeric products, the hydrogen ‘super lean’ conditions incurred during the charging protocol must be avoided. This may be achieved in an industrial environment by an alternative reagent addition method where reagents are introduced under pressurised conditions thus avoiding the charging process adopted in this work. Specifically, this may be achieved by application of a fed batch arrangement where hydrogen over-pressure is continually maintained or, alternatively, *via* the implementation of a CSTR. Preliminary studies into the use of a CSTR arrangement for the hydrogenation reaction of mandelonitrile are described in Section 8.10.

8.9 The Optimised Repeat Batch Reaction Profile: Towards an Improved Understanding

The reaction profile presented in Section 8.8 (Figure 8.11, solid lines) represents the best outcome possible at the University of Glasgow for the repeat batch mandelonitrile hydrogenation reaction when safety and equipment considerations are accounted for. Further, it has been identified in Section 8.8 that external hydrogen line pressure is identified as a major contributor to the improved 6 batch reaction profile. Nevertheless, there are additional, more subtle, factors which also contribute to this outcome. Focus is now brought to some of the intricacies associated with the sustained production of the desired material. To fully understand the outcome of Figure 8.11 (solid lines) it is necessary to acknowledge that there are a number of factors which are important. Accordingly, the roles of the acid additive, the hydrogen supply during reaction, and catalyst mass are examined.

8.9.1 The Role of the Acid Additive in the Optimised Regime

The role of the acid additive in the repeat batch hydrogenation reaction experiments has previously been discussed (Section 8.6), in line with the previous operational regime (relating to a reduced external hydrogen line pressure). Here it was identified that there was a minimum acid requirement for Route **A** to continually afford appreciable quantities of phenethylamine. However, an elevation in acid concentration, whilst showing a favourable outcome for Route **A**, was also found to enhance Route **C**. Investigation has revealed that the minimisation of Route **C** is crucial in the prevention of catalyst deactivation. It is thus established that achieving an appropriate balance with regard to acid concentration is critical.

8.9.2 The Role of Hydrogen Supply and Hydrodynamics During the Reaction in the Optimised Regime

The complex nature of the mandelonitrile hydrogenation reaction system has been described in detail prior, with the findings summarised in (Section 7.2). It is highlighted in Scheme 7.1 that, in order to afford the desired product, there is a significant hydrogen requirement. Consequently, once the previously discussed acid requirement has been satisfied, it is essential that the hydrogen supply is considered.

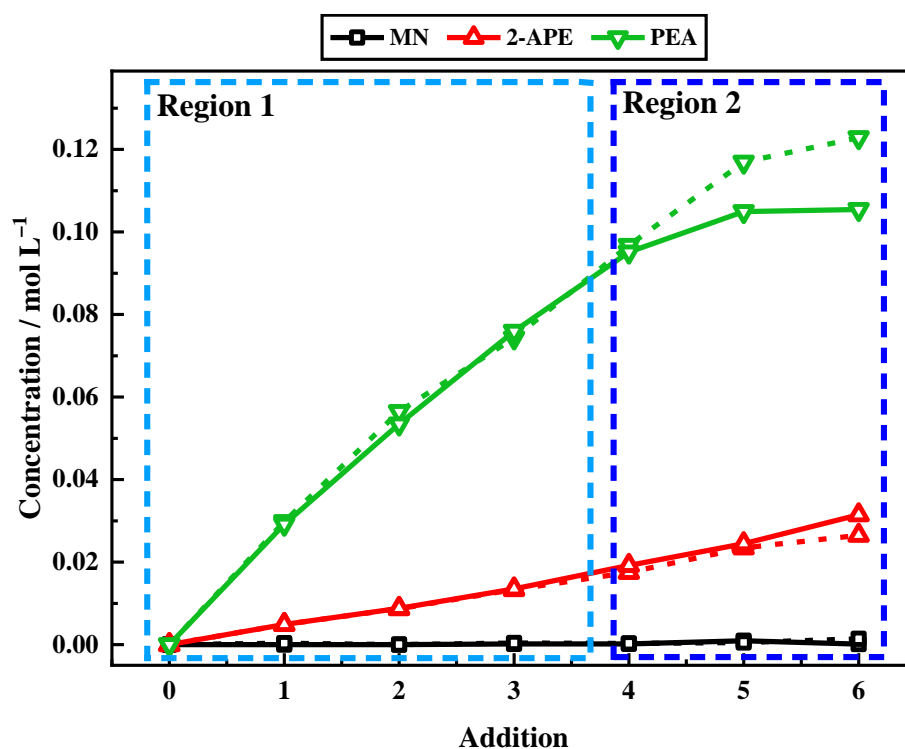


Figure 8.13. Reaction profile for a 6-batch run for the hydrogenation reaction of mandelonitrile. Each reagent addition is comprised of mandelonitrile (11 mmol) and 2 equivalents of sulphuric acid, reacted over the same 5% Pd/C catalyst (300 mg) in methanol. The reaction was conducted under two different experimental regimes. The solid lines represent 'hydrogen lean' conditions (40 °C under 4 barg hydrogen pressure with an agitation speed of 600 rpm) whilst the dashed lines represent 'hydrogen rich' conditions (40 °C under 6 barg hydrogen pressure with an agitation speed of 1050 rpm). Both reactions were conducted at an external line pressure of 8 barg. Each addition (1–6) represents a fixed 120 minute time period. [MN = mandelonitrile; 2-APE = 2-amino-1-phenylethanol; PEA = phenethylamine].

The effects of hydrogen supply can be visualised in Figure 8.13, where the optimised reaction conditions (dashed lines) are compared to conditions which represent a reduced hydrogen supply (solid lines). In the latter instance, both hydrogen pressure and agitation speed have been reduced. Interestingly, under both sets of experimental conditions, the reaction profile is effectively identical for additions 1–4, with differences only becoming observable on additions 5 and 6. As such, Figure 8.13 can be described as being composed of two well defined regimes. The two regimes are highlighted by coloured boxes in Figure 8.13. Region 1 encompasses additions 1–4 and shows an identical output to that observed under the richer hydrogen conditions. Differences in the product distribution, however, become apparent in Region 2, which is representative of additions 5 and 6. Whilst full conversion of the nitrile functionality is still observed, there is a slight enhancement towards the production of 2-amino-1-phenylethanol and a decline in phenethylamine formation. The enhancement of Route **B** and deterioration of Route **A** observed from addition 5 onwards is therefore deduced to be an indicator of a hydrogen supply issue.

Under the reduced hydrogen supply (Figure 8.13, solid lines) Route **C** occupies 26% of the reaction mixture by addition 6 (*cf.* 17% for optimised conditions, Figure 8.13, dashed lines). It therefore appears that under conditions of a reduced hydrogen availability, there is a small increase in the number of sites blocked *via* an accumulation of retained oligomeric species, making it harder for the Route **A** hydrogen requirement (3 molar equivalents of hydrogen) to be satiated. Hence, at a certain surface coverage of oligomeric product, Route **B**, which has a lower hydrogen requirement (2 molar equivalents of hydrogen), will begin to be favoured, as observed on later additions (5 and 6). The findings of Figure 8.13 relate directly to the effects of external hydrogen line pressure, discussed in Section 8.8. External line pressure is shown to have a more dramatic effect on product distribution than the hydrogen supply during the reaction. Nevertheless, when combined, Figures 8.11 and 8.13 illustrate the same outcome and highlight the essential nature of a sufficient supply of hydrogen.

8.9.3 The Role of Catalyst Mass in the Optimised Regime

It was deduced in Section 8.5 that the reactor was operating close to its maximum capacity with regard to the provision of hydrogen gas to the liquid phase. As agitation has a more profound effect on gas-liquid transport than liquid-solid transport, the agitation test does not fully evaluate all diffusion limitations within a reaction system.^[255] Therefore, the catalyst mass dependence can be utilised to evaluate liquid-solid limitations within the reaction system.^[255]

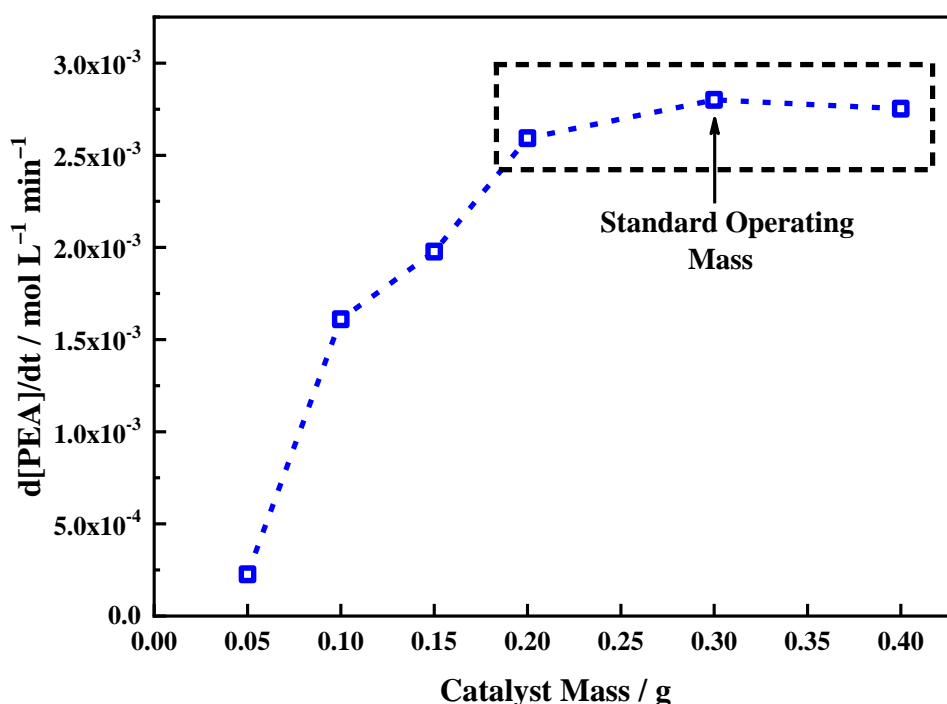


Figure 8.14. Effect of catalyst mass on the rate of formation of phenethylamine for the *single batch* liquid phase hydrogenation reaction of mandelonitrile (35 mmol L^{-1}) over a 5% Pd/C catalyst (varied mass) in the presence of 2 equivalents of sulphuric acid in methanol. The reaction is conducted at 40°C under 6 barg hydrogen pressure with an external line pressure of 6.5 barg and an agitation speed of approximately 1050 rpm. The dashed black box provides an indication as to where the graph reaches a plateau indicating 0^{th} order in catalyst mass.

Figure 8.14 shows the effect of catalyst mass on the rate of phenethylamine formation for a single batch process. Here it is revealed that the rate of product formation increases linearly with increasing catalyst mass until a saturation point is reached, where further increases to the catalyst mass no longer enhance the rate. The standard operational

catalyst mass of 300 mg (Section 5.3) appears on the plateau region of the graph, as indicated in Figure 8.14. The origins of the plateau region are attributed to a mass transport limitation. At low catalyst mass, the rate of phenethylamine production is directly proportional to catalyst mass, implying that the production of adsorbed hydrogen atoms ($H_{(ads)}$, formed *via* the dissociative adsorption of $H_{2(solv)}$ at the palladium crystallites) is unimpeded by the availability of solvated dihydrogen, $H_{2(solv)}$. Increasing catalyst mass, above approximately 200 mg, nudges the $H_{(ads)}$ demand above the dihydrogen solvation rate, leading to saturation of product formation.

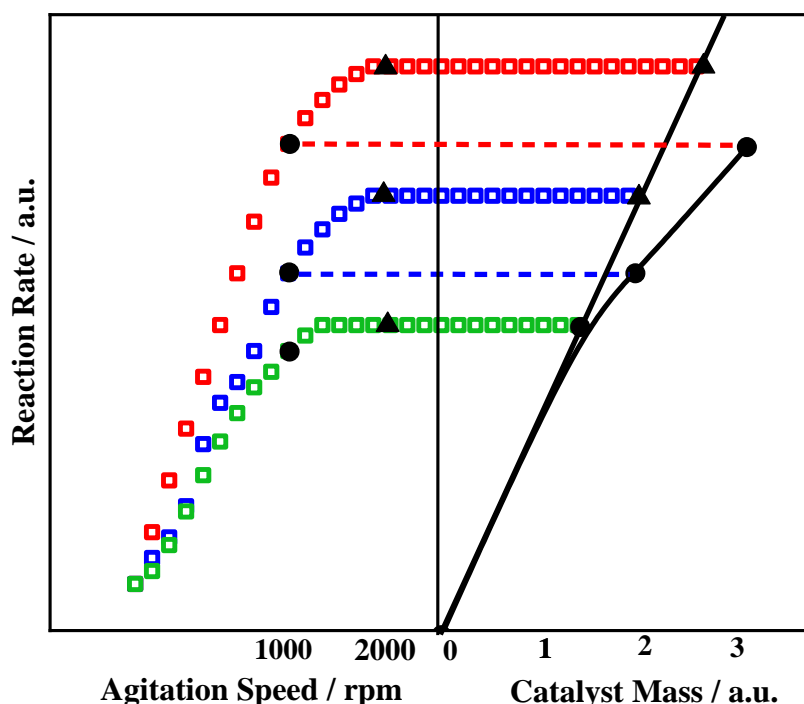


Figure 8.15. Generic example showing the relationship between agitation speed and catalyst mass. Figure reproduced from reference 258.

Typically, as demonstrated for a generic example in Figure 8.15, an increase in agitation speed is required to overcome the mass transport limitations incurred with the use of high masses of catalyst. At 1050 rpm, however, the maximum limit for the Büchi autoclave has been reached. As an alternative method of alleviating these mass transport limitations a 6-batch hydrogenation reaction sequence using a reduced catalyst mass (100 mg) is examined. In this instance the reduced quantity of catalyst should be able to sustain a $H_{2(solv)} \rightarrow 2H_{(ads)}$ formation rate below that limited by the $H_{2(g)} \rightarrow H_{2(solv)}$ solvation limit

that is restricted by Henry's Law constraints. The results of the repeat batch experiment using a reduced catalyst mass presented in Figure 8.16.

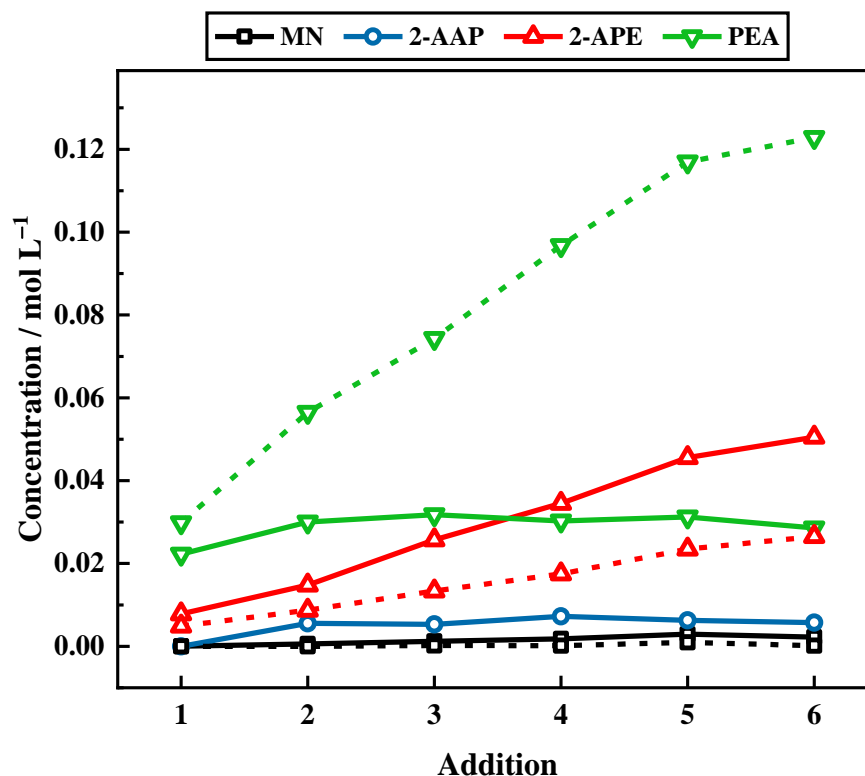


Figure 8.16. Reaction profile for a 6-batch run for the hydrogenation reaction of mandelonitrile. Each reagent addition comprised mandelonitrile (11 mmol) and 2 equivalents of sulphuric acid, reacted over the same 5% Pd/C catalyst in methanol. The solid lines represent low catalyst mass (100 mg) whereas the dashed lines represent standard catalyst mass (300 mg). The reaction was conducted at 60 °C under 4 barg hydrogen pressure with an external line pressure of 6.5 barg and an agitation speed of 1050 rpm. Each addition (1–6) represents a fixed 120 minute time period. [MN = mandelonitrile; 2-AAP = 2-aminoacetophenone; 2-APE = 2-amino-1-phenylethanol; PEA = phenethylamine].

The two profiles shown in Figure 8.16 (catalyst mass = 300 mg compared with catalyst mass = 100 mg) show vastly different outcomes. Firstly, the reduced catalyst mass profile (100 mg sample, Figure 8.16 solid lines) is considered. It is observed that from addition 2 onwards, there is no further production of phenethylamine, indicating that Route **A** has been obstructed by the reduced quantity of catalyst mass. The production of 2-amino-1-phenylethanol, however, is enhanced, highlighting that Route **B** is favoured when the catalyst mass is lowered; in Section 8.9.2 this attribute was associated with a reduced

hydrogen supply. A slight build-up of the intermediate species 2-aminoacetophenone can also be observed. This observation is not seen for the 300 mg sample (Figure 8.16, dashed lines). Previous work, detailed in Section 5.8, has shown the conversion of 2-aminoacetophenone to 2-amino-1-phenylethanol to be kinetically fast.^[217] With reference to Scheme 7.1, the hydrogenation of 2-aminoacetophenone represents the second hydrogen requiring step in the production of 2-amino-1-phenylethanol (Route **B**). The detection of 2-aminoacetophenone from addition 2 onwards implies that this facile reaction has become kinetically hindered. This is presumably due a restricted supply of $H_{(ads)}$ as a result of the reduced palladium surface area.

The matter of hydrogen supply at the catalyst surface and product selectivity can be further rationalised with reference to Scheme 7.1. In order to successfully obtain phenethylamine, Scheme 7.1 indicates that two branching points must be passed (**BP1** and **BP2**), each requiring an unhindered supply of adsorbed hydrogen atoms. When the mass of catalyst is reduced there are fewer active sites for the generation of adsorbed hydrogen, therefore reducing surface hydrogen availability. When $H_{(ads)}$ is limited, homogeneous routes (Route **B** and **C**) are favoured over the heterogeneous route (Route **A**) at each of the branching points. Thus, the predominance of Routes **B** and **C** (53% missing mass detected by addition 6) and the deactivation of Route **A** can be effectively rationalised.

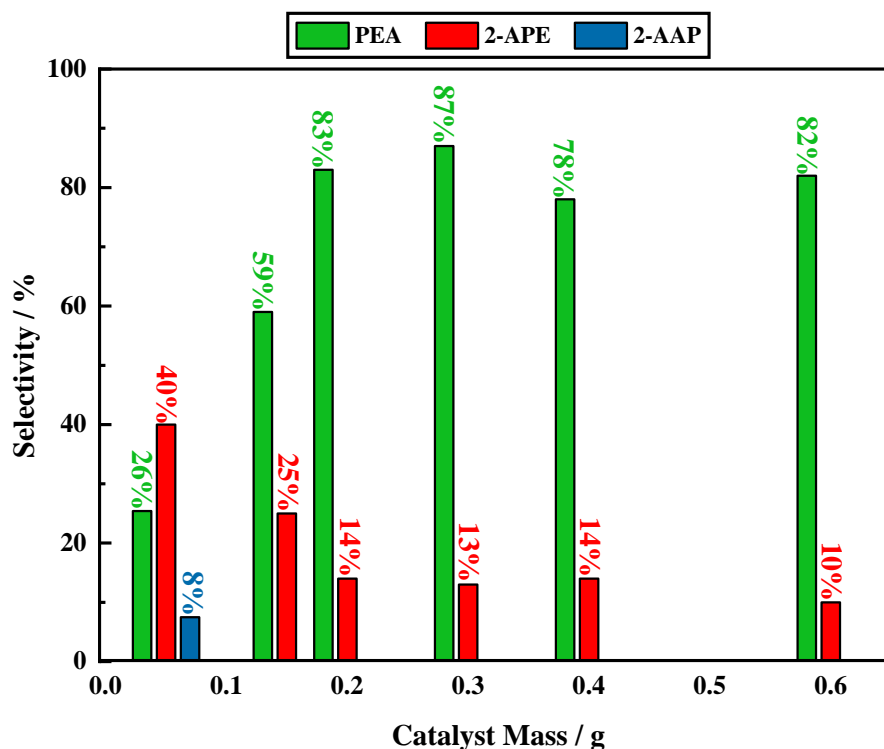


Figure 8.17. Effect of catalyst mass on selectivity for a **single batch** process for the hydrogenation reaction of mandelonitrile. Each reagent addition is comprised of mandelonitrile (31 mmol L^{-1}) and 2 equivalents of sulphuric acid, reacted over the same 5% Pd/C catalyst in methanol. The reaction was conducted at 60°C under 4 barg hydrogen pressure with an external line pressure of 6.5 barg and an agitation speed of 1050 rpm. Each addition (1–6) represents a fixed 120 minute time period. [2-AAP = 2-aminoacetophenone; 2-APE = 2-amino-1-phenylethanol; PEA = phenethylamine].

If a range of catalyst masses are considered, it becomes clear that the mass of catalyst used is critical in maximising selectivity towards phenethylamine. Figure 8.17 illustrates the effect of catalyst mass on selectivity, at reaction completion, for a single batch reaction. The selectivity towards by-product 2-amino-1-phenylethanol is shown here to decrease as catalyst mass increases, and plateaus upon reaching the critical mass. Selectivity towards the desired product, however, appears to increase. The approximate plateau is reached at 200 mg of catalyst in both instances.

Figure 8.17 indicates that catalyst mass, within the 200–300 mg range, represents a balance between the rate of product formation and the delivery of surface hydrogen, $\text{H}_{(\text{ads})}$. Lower catalyst masses (<200 mg) can be linked to a regime of insufficient $\text{H}_{(\text{ads})}$, whereas, at higher catalyst masses (>300 mg), the reaction is impeded due to a limited solubilisation rate of $\text{H}_{2(\text{g})}$. Crucially, at higher catalyst masses, a limitation at the gas-

liquid interface impedes the reaction. Thus, for sustained production of phenethylamine to be achieved, the correct balance needs to be sought. There must be efficient replenishment of solvated dihydrogen within the Henry's law solubilisation limit (accomplished by agitating at speeds ≥ 750 rpm) and, production of $H_{(ads)}$ at a rate that is greater than the kinetic requirement of the mandelonitrile \rightarrow phenethylamine transformation rate.

Against this heightened awareness of parameters contributing to sustained phenethylamine yield, it is informative to re-examine Figures 8.11 and 8.12 to summarise why the product formation rate retards from addition 4 onwards. One possibility is that, despite relatively favourable conditions, a small but undetectable amount of oligomer formation occurs during the course of additions 1–3. This formation is progressive until it becomes indirectly observable in the form of a mass imbalance from addition 4 onwards. As considered above, oligomerisation reduces active surface area, reducing the availability of chemisorbed hydrogen atoms for reaction, leading to decreasing product yields.

8.10 A Continuously Stirred Tank Reactor Arrangement was Proposed as a Means of Extending Catalyst Lifetime (Syngenta)

As discussed in Section 8.6, alternative reactor configurations for the mandelonitrile hydrogenation reaction were proposed in order to prevent catalyst fouling, such that desired product formation could be sustained. The mandelonitrile hydrogenation reaction was therefore explored as a continuous stirred tank reactor (CSTR) arrangement at the industrial facility (Syngenta, Jealott's Hill). It was proposed that this reactor arrangement would allow sustained phenethylamine production to be achieved. In order to ascertain whether this was a superior methodology to the repeat batch set-up, the reaction must be run at steady state for a period of time greater than the equivalent of 6 consecutive batch reactions.

The CSTR set-up, described in Section 2.3.2, can also be operated as a batch reactor. As such, the mandelonitrile hydrogenation reaction was first run as a batch reaction, allowing the hydrodynamics of the Syngenta reactor to be compared with the Büchi reactor at the University of Glasgow. The resultant batch reaction profile is presented in Figure 8.18.

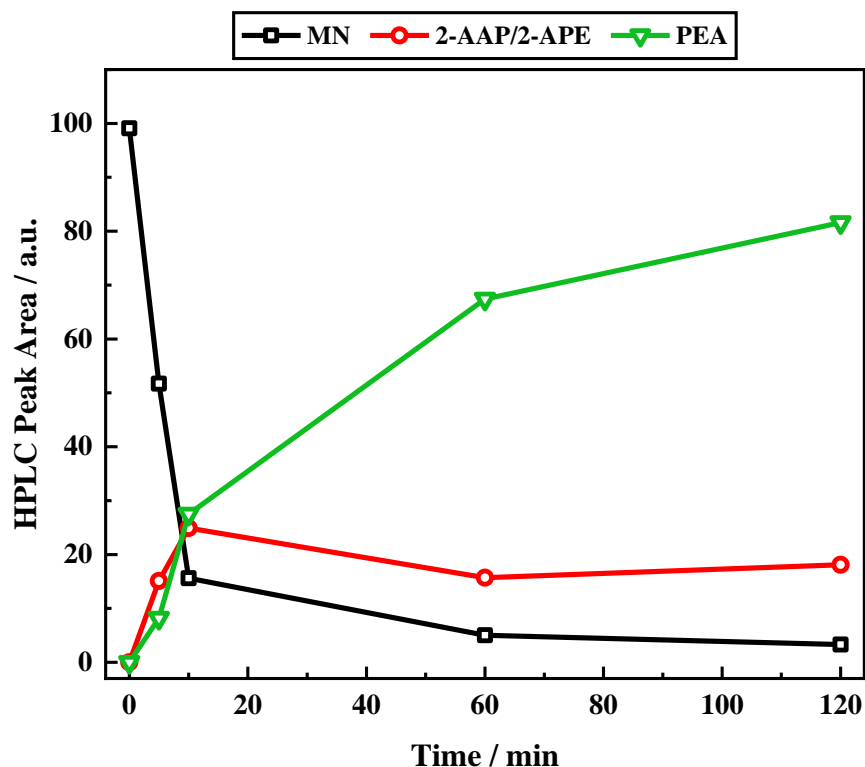


Figure 8.18. Reaction profile for the liquid phase hydrogenation reaction of mandelonitrile (35 mmol L^{-1}) over a 5% Pd/C catalyst (300 mg) in the presence of 2 equivalents of sulphuric acid in methanol. The reaction was conducted at 40°C under 6 barg hydrogen pressure and an agitation speed of 1000 rpm. The reaction was performed as a batch reaction in the CSTR set-up at Syngenta. [MN = mandelonitrile; 2-AAP = 2-aminoacetophenone; 2-APE = 2-amino-1-phenylethanol; PEA = phenethylamine].

It is shown in Figure 8.18 that the outcome of the mandelonitrile hydrogenation reaction conducted in the Syngenta reactor is largely comparable to the profile obtained at the University of Glasgow (Figure 5.4). The rate of phenethylamine production does, however, appear to be slightly slower in the Syngenta reactor which suggests that the hydrodynamics are inferior compared to the Glasgow reactor. Due to their being limited time at Syngenta, calibration protocols were not conducted. Thus, no quantification was achieved, and therefore, HPLC peak area is plotted on the y-axis rather than concentration. Moreover, poor resolution was found between the chromatographic peaks associated with 2-aminoacetophenone and 2-amino-1-phenylethanol using the Syngenta HPLC. The peaks were consequently integrated together and plotted as a single trace in Figure 8.18. This poor resolution is likely a result of varying performance capabilities between HPLC instruments.

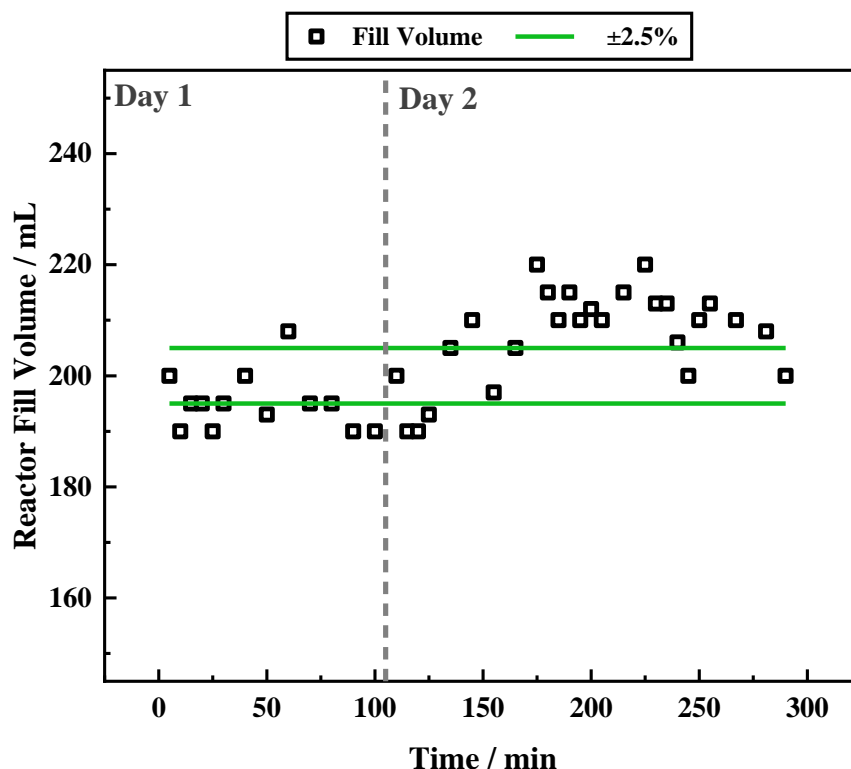


Figure 8.19. Representative volume tracker for the mandelonitrile hydrogenation reaction run in a CSTR. The green lines are representative of $\pm 2.5\%$ of the target volume (200 mL) and the black squares represent the experimentally obtained fill volume data. The dashed grey line denotes Day 1 and Day 2 of the experiment.

In a CSTR, the substrate stream is continually pumped into the reactor while the product stream is removed. The cumulative in-feed and the total out-feed should occur at the same rate such that the volume inside the reactor remains constant. As described in Section 2.3.2, the CSTR at Syngenta has three feeds (two in and one out), each controlled by a HPLC pump. The reactor volume was monitored at regular intervals throughout the course of the reaction, with alterations to the flow rates made to ensure that a volume of 200 mL was maintained. A representative volume tracker for a mandelonitrile hydrogenation reaction conducted in a CSTR is shown in Figure 8.19. Here, the green lines represent $\pm 2.5\%$ of the target volume (200 mL) and the black squares represent the experimentally determined volume data. Ideally the reactor volume will be kept within $\pm 2.5\%$ of 200 mL. Overall, Figure 8.19 illustrates that the volume in the reactor was kept reasonably close to the target volume.

In continuous flow systems, residence time is defined as the average time a molecule spends in the reaction vessel. For steady state systems, residence time is equal to the reactor volume divided by the flow rate. For a reactor volume of 200 mL and a flow rate of 4 mL min⁻¹, as presented here, the residence time is 50 minutes. Typically, five residence times are required for the reaction to reach steady state (250 minutes).^[154] Taking into consideration reaction set-up time and the catalyst reduction process, a 250 minute lag at the beginning of the CSTR reaction means that reaction time becomes quite extensive. It was thus proposed that the initial use of a batch reaction, to rapidly achieve steady state at approximately 90% conversion, represents a potential means of accelerating this process. Thus, a batch mandelonitrile hydrogenation reaction was run to 90% mandelonitrile conversion (approximately 40 minutes, as extrapolated from Figure 8.18) before the CSTR reaction was initiated. This, however, was unsuccessful with high concentrations of mandelonitrile maintained throughout the course of the reaction. Further method development, out with the time available on the industrial placement, would be required to execute this more effectively.

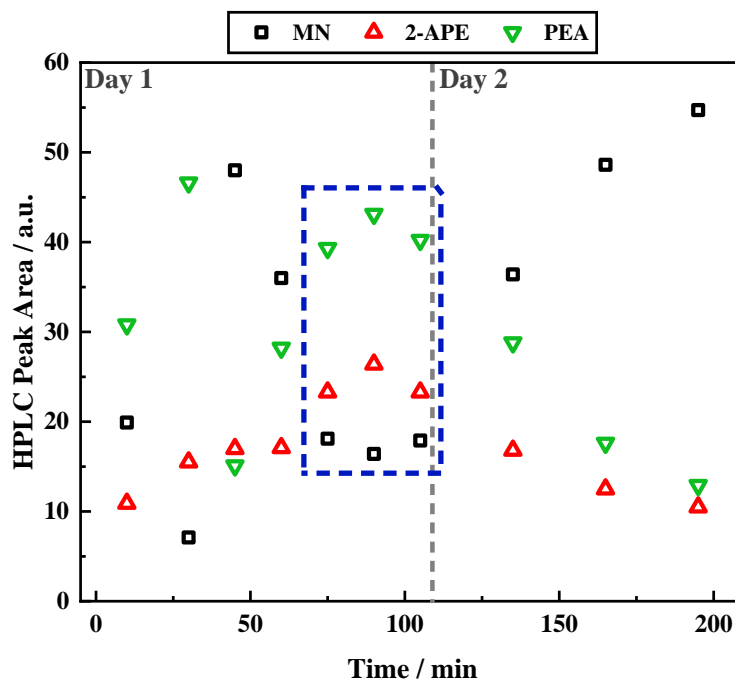


Figure 8.20. The liquid phase hydrogenation reaction of mandelonitrile over a 5% Pd/C catalyst (171 mg) in methanol run as a CSTR reaction. Reagent feeds: mandelonitrile (31 mmol L^{-1}) and sulphuric acid (2 equivalents) were pumped in at a rate which matched the product outfeed (4 mL min^{-1}). The reaction was performed over 2 days, with the dashed grey vertical line indicating each day. The reaction was conducted at 40°C under 8 barg hydrogen pressure and an agitation speed of 1000 rpm. [MN = mandelonitrile; 2-APE = 2-amino-1-phenylethanol; PEA = phenethylamine].

Instead, the CSTR arrangement was used from the initiation of the reaction. The results of this reaction are presented in Figure 8.20. On Day 1, the reaction was run for a total of 105 minutes. The data collected for the initial 75 minutes of the reaction is shown to be, as expected, quite varied in concentration. This therefore indicates that the reaction had not yet reached steady state. Following this, at reaction times of 75–105 minutes, highlighted by the dark blue dashed box in Figure 8.20, the concentration of the reaction species is shown to stabilise. It is thus proposed that, by a reaction time of approximately 75 minutes, a state close to steady state is achieved. By 75 minutes, the approximate mandelonitrile conversion is 83%. At this conversion the selectivity towards 2-amino-1-phenylethanol and phenethylamine is 25% and 42%, respectively. The reaction was then stopped, the reactor vented of hydrogen, purged with nitrogen and left at ambient pressure overnight. The reaction was then recommenced the next day (Day 2) by purging the

reactor vessel with hydrogen and reinitiating the hydrogen supply and the CSTR reaction. Unfortunately, the results from Day 2 indicate that the catalyst had been poisoned. As shown in Figure 8.20, significant build-up of mandelonitrile was observed, illustrating that the catalyst was no longer able to convert the reagent. Moreover, the concentration of both phenethylamine and 2-amino-1-phenylethanol are shown to diminish indicating the cessation of their continued production. It is proposed that the removal of the hydrogen supply to allow the experiment to be safely left overnight was the source of the catalyst deactivation observed. Indeed, it is thought that a constant flow of hydrogen is required in order to preserve the active surface of the catalyst. Moreover, it is likely that this outcome relates directly to the negative affects of the charging protocol described in Section 8.8.

Ideally, this reaction would be conducted in one day to prevent the observed catalyst deactivation. Time, however, did not permit further investigation. Enhanced exploration of the mandelonitrile hydrogenation reaction in a CSTR therefore represents an area where further investigation is required. Methods of reducing the time required to complete this test must therefore be considered. Firstly, a reduced residence time could be implemented by decreasing the reactor volume. Alternatively, multiple CSTR's may be applied in series, thus reducing the required level of conversion in each CSTR. Such investigations are currently being undertaken at the industrial site. It is hoped that the extended reaction times will afford a favourable outcome with regards to longevity of the catalyst for phenethylamine production.

8.11 Conclusions

The single batch liquid phase hydrogenation reaction of mandelonitrile over a 5% Pd/C catalyst has been developed, such that production of the desired primary amine product (phenethylamine) can be maximised. Thus, this study aims to allow a process of commercial viability to be established. To achieve this, repeat batch technology was employed, and a series of 6 substrate additions over the same catalyst were monitored for different experimental conditions. The following conclusions were drawn:

- The initial outcome observed by McMillan and Gilpin replicated the industrial finding and showed significant catalyst deactivation after a single batch process.

- Improvements to the hydrogen availability, implemented through several experimental parameter changes, improved the durability of the catalyst. Nevertheless, whilst phenethylamine production was sustained for 4 additions, product formation plateaued after this point.
- Reaction hydrodynamics within the improved experimental domain were examined. It was found that the maximum available agitation speed (1050 rpm) was required in order to minimise a diffusion constraint at the gas-liquid interface. Further, it was determined that the reactor was operating at maximum possible efficiency within the limitations of the equipment and safety considerations.
- Acid concentration was varied as a potential means of improving catalyst lifetime. It was identified that, in order for sustained phenethylamine production to be achieved, there is a minimum acid requirement (two molar equivalents), necessary to prevent the occurrence of coupling reactions (Route C). When the acid concentration is increased, phenethylamine production is enhanced. Nevertheless, the undesirable enhancement of Route C reactions also accompanies this, rendering this an overall ineffective method of improving the selectivity towards phenethylamine.
- Following the investigation into the concentration of the acid additive, it was proposed that, above a specific concentration of amine product, the catalyst was no longer able to function despite the presence of adequate acid additive. This theory was tested by re-examining the repeat batch experiments at higher amine concentrations. It was consequently identified that the amine concentration was not responsible for the observed deactivation of the catalyst. Instead, external line pressure, relating directly to the hydrogen charging period, was found to afford a dramatic improvement.
- It is identified that sustained phenethylamine production requires a significant acid presence (2 equivalents) as well as maintenance of hydrogen availability, at both the gas-liquid and liquid-solid interfaces, throughout the reaction. Catalyst mass dictates the availability of chemisorbed hydrogen atoms within the

limitations of hydrogen solubility in the reaction solvent. It is essential that sufficient catalyst (>200 mg) is employed to ensure adequate $H_{(ads)}$ throughout the full reaction coordinate. Care, however, must be taken to ensure that the quantity of catalyst used does not exceed a critical level, and thus, induce diffusional constraints.

- Within the limitations of the present set-up, phenethylamine is continuously produced for 6 substrate additions, with moderate deactivation observed only after addition 4.
- It is proposed that further improvements to the process could be made if alternative reactor configurations are explored. The application of a CSTR arrangement for the hydrogenation reaction of mandelonitrile was preliminarily tested. Further work, out-with the scope of this project is, however, required to fully explore the effectiveness of this method.

CHAPTER 9

Concluding Remarks and Future Work

The liquid phase hydrogenation reactions of various aromatic nitriles over a generic 5% Pd/C catalyst have been explored within the remit of this study; the overall aim being to understand the complexity of the interconnecting reactions involved in the process. Analysis of the resultant product distribution was primarily achieved by HPLC, however, multinuclear NMR spectroscopy and mass spectrometry were also utilised. Initially, single batch studies were used to gain a detailed mechanistic understanding. A repeat batch methodology was subsequently employed to achieve an outcome of greater industrial relevance. The following concluding remarks aim to succinctly summarise the findings:

- Alongside the 5% Pd/C catalyst used throughout this study, a 5% Pd/ γ -Al₂O₃ reference catalyst, was characterised by a number of techniques. Whilst the latter catalyst has only been briefly studied, its amenability to investigation by infrared spectroscopy (Section 3.10) provides a springboard for morphological studies to be explored in the future.
- Following the preliminary nitrile hydrogenation studies (conducted by McMillan and Gilpin), the hydrogenation of 4-hydroxybenzyl cyanide was examined. The adjustment of various experimental parameters was effectively explored such that the desired product, tyramine, was produced in quantitative yield. In this instance, whilst both hydrogenation and condensation reactions were observed, no hydrogenolysis reaction occurred. It was therefore proposed that it was the molecular framework of tyramine which prevented this reaction. Thus, it was found necessary for there to only be a single methylene unit between the aromatic ring and the leaving group for hydrogenolysis to be supported.
- Investigative efforts then progressed to the cyanohydrin mandelonitrile, where a significant portion of this study was focused. Primarily, the mechanism for a single batch hydrogenation reaction was considered. As a result, the inclusion of an acid additive was found to be critical for the production of the desired product, phenethylamine. The acid additive was shown to facilitate an acid catalysed tautomeric pathway, resulting in the formation of ketone intermediate 2-aminoacetophenone. The hydrogenation reaction of 2-aminoacetophenone was rapid and afforded 2-amino-1-phenylethanol. In contrast, the subsequent

hydrogenation reaction of 2-amino-1-phenylethanol to afford phenethylamine was found to be kinetically hindered, resulting in the build-up of this molecule as a by-product of the reaction. It was thus proposed, by process of elimination, that the hydrogenolytic cleavage necessary to afford phenethylamine occurred at either the hydroxy-imine or the hydroxy-enamine intermediates.

- Adequate differentiation between these two pathways (defined as Pathways **I** and **II**) could not be achieved by chromatographic means. Therefore, the use of a deuteration reaction was proposed to supplement the mechanistic insight previously gleaned. The use of deuterium, to probe the progress of the reaction, revealed a mechanism of significant complexity. The use of ^{13}C NMR spectroscopy and mass spectrometry revealed the isotopologue distribution for the mandelonitrile deuteration reaction. It was identified that, in order to yield phenethylamine, three hydrogen requiring steps were necessary: two hydrogenation reactions and a hydrogenolysis reaction. Moreover, these processes were found to occur in a specified order.
- Following the mechanistic studies, optimisation of the mandelonitrile hydrogenation reaction to afford phenethylamine with an enhanced selectivity was explored, such that, product scale-up could effectively be undertaken. In order to compare the outcomes, it was necessary for the reaction scheme to be expanded to include potential routes for deactivation. Consequently, Routes **A**, **B** and **C**, which respectively represent, the production of phenethylamine, 2-amino-1-phenylethanol, and higher amines. Temperature, alcohol chain length, the nature of the acid additive, and the concentration of sulphuric acid were examined. Nonetheless, it was identified that no significant improvements could be made to the selectivity of phenethylamine by any of the parameters explored here. It was thus suggested that optimal reaction conditions had already been identified.
- Having established optimal reaction conditions for a single batch process, the mandelonitrile hydrogenation reaction subsequently underwent product scale-up development, such that, the industrial process could be more effectively mimicked. To achieve this, a repeat batch technology was developed. Typically, 6 substrate additions over the same un-regenerated catalyst were examined to provide an indication of the catalyst's durability. Previously, the outcome

achieved by McMillan was poor, with significant catalyst deactivation observed after only 1 reagent addition. Improvements to the hydrogen availability afforded a more favourable outcome, with phenethylamine production sustained for 4 substrate additions before a product formation plateau was observed. In line with this finding, it was initially proposed that it was a concentration dependence of the amine salts which caused the observed deactivation. This theory, however, was disproven. Instead, it was identified that adequate hydrogen availability throughout the process was of critical importance for catalyst sustainability. Moreover, it was essential that a number of reaction parameters, including the acid additive, catalyst mass, external hydrogen line pressure, temperature, hydrogen pressure during reaction, and agitation speed were all fine-tuned to achieve optimal performance. The optimised repeat batch profile presented represents the best possible performance within equipment and safety limitations at the University of Glasgow.

With regard to future work, collaborative projects are already in place. It is proposed that DFT can be used to provide some illumination on the energetics of the hydrogenolysis step. It is hoped that insight regarding the favourability of Pathway **I** or Pathway **II** will be achieved, allowing further detail for this area of the reaction mechanism to be elucidated. These calculations are currently being explored externally in collaboration with Cardiff University. It is also deemed prudent to further explore the use of a CSTR arrangement for the hydrogenation reaction of mandelonitrile. Extended reaction times for this reaction as a CSTR arrangement are being investigated at Syngenta.

Regarding the next phase of the University of Glasgow/Syngenta collaboration, the hydrogenation reaction of 1,2-dicyanobenzene is considered. Progressing from the mandelonitrile investigation, the use of a dinitrile hydrogenation reaction as a chemical probe for hydrogen availability is proposed. In preparation, a preliminary study into this substrate system was conducted and the findings presented in the appendix as Chapter 12.

CHAPTER 10

Associated Publications

The following publications are associated with this thesis. Where applicable, the relevant chapter or chapters have been specified:

- M.I. McAllister, C. Boulho, L. McMillan, L.F. Gilpin, S. Wiedbrauk, C. Brennan and D. Lennon, The production of tyramine *via* the selective hydrogenation of 4-hydroxybenzyl cyanide over a carbon supported catalyst. *RSC Adv.* 2018, **8**, 29392–29399. [**Chapter 4**]
- M.I. McAllister, C. Boulho, L.F. Gilpin, L. McMillan, C. Brennan and D. Lennon, Hydrogenation of benzonitrile over supported Pd catalysts: Kinetic and mechanistic insight. *Org. Process Res. Dev.*, 2019, **23**, 977–989. [**Not Included**]
- M.I. McAllister, C. Boulho, L. McMillan, L.F. Gilpin, C. Brennan and D. Lennon, The hydrogenation of mandelonitrile over a Pd/C catalyst: Towards a mechanistic understanding. *RSC Adv.* 2019, **9**, 26116–26125. [**Chapters 3 and 5**]
- M.I. McAllister, C. Boulho, C. Brennan, P.J. Sidebottom and D. Lennon, Isotopic substitution experiments in the hydrogenation of mandelonitrile over a carbon supported Pd catalyst: A nuclear magnetic resonance study. *Molecular Catalysis*, 2020, **484**, 110720. [**Chapter 6**]
- M.I. McAllister, C. Boulho, C. Brennan, S.F. Parker and D. Lennon, Towards sustained product formation in the liquid phase hydrogenation of mandelonitrile over a Pd/C catalyst. *Org. Process Res. Dev.*, 2020, **4**, 1112–1123. [**Chapter 8**]

CHAPTER 11

References

- [1] D.B. Bagal and B. M. Bhanage, *Adv. Synth. Catal.*, 2015, **357**(5), 883–900.
- [2] J.J.W. Bakker, A. Geert van der Neut, M.T. Kreutzer, J.A. Moulijn and F. Kapteijn, *J. Catal.*, 2010, **274**, 176–191.
- [3] L. Hegedűs and T. Máthé, *Appl. Catal. A:Gen.*, 2005, **296**, 209–215.
- [4] S. Chakraborty, G. Leitus and D. Milstein, *Chem. Commun.*, 2016, **52**, 1812–1815.
- [5] S.A. Lawrence, *Amines: Synthesis, Properties and Application*, Cambridge University Press (Cambridge), 2004.
- [6] S.P. Bawane and S.B. Sawant, *Chem. Eng. J.*, 2004, **103**, 13–29.
- [7] B. Miriyala, S. Bhattacharyya and J.S. Williamson, *Tetrahedron*, 2004, **60**, 1463–1471.
- [8] R.A. Sheldon and H. van Bekkum, *Fine Chemicals Through Heterogeneous Catalysis*, Wiley-VCH (Weinheim), 2001.
- [9] P. Roose, K. Eller, F. Henkes, R. Rossbacher, H. Höke, *Ullmann's Encyclopedia of Industrial Chemistry* 7th Edition, Wiley-Verlag GmbH & Co KGaA (Weinheim), 2015.
- [10] K. Weissermel, H.-J. Arpe, *Industrial Organic Chemistry* 3rd Edition, VCH (Weinheim), 1997.
- [11] J. Neumann, C. Bornschein, H. Jiao, K. Junge and M. Beller, *Eur. J. Org. Chem.*, 2015, **27**, 5944–5948.
- [12] A. Agrawal and P.G. Tratnyek, *Environ. Sci. Technol.*, 1995, **30**, 153–160.
- [13] S. Laval, W. Dayoub, L. Pehlivan, E. Maetay, A. Favre-Reguillion, D. Delbrayelle, G. Mignani and M. Lenaire, *Tet. Lett.*, 2011, **52**(32), 4072–4075.
- [14] E.M. Dangerfield, C.H. Plunkett, A.L. Win-Mason, B.L. Stoker and M.S.M. Timmer, *J. Org. Chem.*, 2010, **75**, 5470–5477.
- [15] K. Lévy and L. Hegedűs, *Period. Polytech. Chem. Eng.*, 2018, **62**(4), 476–488.
- [16] C. de Bellefon and P. Fouilloux, *Catal. Rev. Sci. Eng.*, 1994, **36**(3), 459–506.
- [17] P.N. Rylander, *Catalytic Hydrogenation over Platinum Metals*, Academic Press (New York), 1967.
- [18] M. Freifelder, *Practical Catalytic Hydrogenation: Techniques and Applications*, Wiley (New York), 1971.
- [19] C.V. Rode, M. Arai, M. Shirai and Y. Nishiyama, *App. Catal. A:Gen.*, 1997, **148**, 405–413.
- [20] P. Sabatier and J.B. Senderns, *C. R. Acad. Sci.*, 1905, **140**, 482.
- [21] J. Volf and J. Pašek, *Stud. Surf. Sci. Catal.*, 1986, **27**, 105–144.
- [22] I. Ortiz-Hernandez and C. T. Williams, *Langmuir*, 2007, **23**, 3172–3178.
- [23] A. Chojecki, M. Veprek-Heijman, T.E. Müller, P. Schäringer, S. Vepreck and J.A. Lercher, *J. Catal.*, 2007, **245**(1), 237–248.

- [24] J. Braun, G. Blessing and F. Zobel, *Ber.* **1923**, 36, 283–290.
- [25] G. Mignonac, *Comptes Rendus*, 1920, **171**, 114–117.
- [26] C.F. Windana and H. Adkins, *J. Am. Chem. Soc.*, 1932, **54**(1), 306–312.
- [27] R. Juday and H. Adkins, *J. Am. Chem. Soc.*, 1955, **77**(17), 4559–4564.
- [28] J. Barrault and Y. Pouilloux, *Catal. Today*, 1997, **37**, 137–153.
- [29] K. Kindler and F. Hesse, *Arch. Pharm.*, 1933, **27**, 439.
- [30] H. Greenfield, *Ind. Eng. Chem. Prod. Res.*, 1967, **6**(2), 142–144.
- [31] M. Arai, Y. Takada and Y. Nishiyama, *J. Phys. Chem. B*, 1998, **102**(11), 1968–1973.
- [32] A.J. Yap, B. Chan, A.K.L. Yuen, A.J. Ward, A.F. Masters and T. Maschmeyer, *ChemCatChem*, 2011, **3**, 1496–1502.
- [33] A.J. Yap, A.F. Masters and T. Maschmeyer, *ChemCatChem*, 2012, **4**, 4839–4849.
- [34] D.J. Segobia, A.F. Trasarti and C.R. Apesteguía, *Appl. Catal. A:Gen.*, 2012, **445**, 69–75.
- [35] L. McMillan, L.F. Gilpin, J. Baker, C. Brennan, A. Hall, D.T. Lundie and D. Lennon, *J. Mol. Catal. A:Chem.*, 2016, **411**, 239–246.
- [36] M.I. McAllister, C. Boulho, L.F. Gilpin, L. McMillan, C. Brennan and D. Lennon, *Org. Process Res. Dev.*, 2019, **23**, 977–989.
- [37] M.I. McAllister, C. Boulho, L. McMillan, L.F. Gilpin, S. Wiedbrauk, C. Brennan and D. Lennon, *RSC Adv.* 2018, **8**, 29392–29399.
- [38] Y. Huang and W.M.H. Sachtler, *Appl. Catal. A:Gen.*, 2000, **191**, 35–44.
- [39] R.L. Augustine, *Heterogeneous Catalysis for the Synthetic Chemist*, Marcell Dekker Inc. (New York), 1996.
- [40] M. Chatterjee, H. Kawanami, M. Sato, T. Ishizaka, T. Yokoyama and T. Suzuki, *Green Chem.*, 2010, **12**, 87–93.
- [41] M.W. Duch and A.M. Allgeier, *Appl. Catal. A:Gen.*, 2007, **318**, 190–198.
- [42] J. Karupka and J. Pašek, *Curr. Org. Chem.*, 2012, **16**(8), 988–1004.
- [43] O.G. Degischer and F. Roessler, *P. Rhys. Chem. Ind.: Catal. Org. React.*, 2001, **82**, 241–254.
- [44] W. Huber, *J. Am. Chem. Soc.*, 1944, **66**(6), 876–879.
- [45] S. Gomez, J.A. Peters and T. Maschmeyer, *Adv. Synth. Catal.*, 2002, **344**(10), 1037–1057.
- [46] P. Kukula, M. Studer and H.-U. Blaser, *Adv. Synth. Catal.*, 2004, **346**(12), 1487–1793.
- [47] T.A. Johnson and D.P. Freyberger, *Lithium Hydroxide Modified Sponge Catalysts for Control of Primary Amine Selectivity in Nitrile Hydrogenation*, Marcel Dekker (New York), 2001.

- [48] F. Gould, G. Johnson and G. Ferris, *J. Org. Chem.*, 1960, **25**(9), 1658–1660.
- [49] B.W. Hoffer and J.A. Moulijn, *Appl. Catal. A:Gen.*, 2009, **352**(1-2), 193–201.
- [50] P. Zhang, Q. Zhang and X. Li, *Ind. Catal.*, 2012, **7**, 71–75.
- [51] D.J. Segobia, C.R. Trasarti and C.R. Apesteguía, *J. Braz. Chem. Soc.*, 2014, **25**(12), 2272–2279.
- [52] D.J. Segobia, C.R. Trasarti and C.R. Apesteguía, *Appl. Catal. A:Gen.*, 2015, **494**, 41–47.
- [53] Z. Jia, B. Zhen, M. Han and C. Wang, *Catal. Commun.*, 2016, **73**, 80–83.
- [54] C. Liu and T. Wang, *RSC Adv.*, 2014, **4**(109), 63725–63733.
- [55] C. Liu and T. Wang, *RSC Adv.*, 2015, **5**(34), 26465–26474.
- [56] C. Liu and T. Wang, *RSC Adv.*, 2015, **5**(71), 57277–57285.
- [57] H. Cheng, X. Meng, C. Wu, X. Shan, Y. Yu and F. Zhao, *J. Mol. Catal. A:Chem.*, 2013, **379**, 72–79.
- [58] Y. Lv, F. Hao, P. Liu, S. Xiong and H. Luo, *React. Kin. Mech. Catal.*, 2016, **119**(2), 555–568.
- [59] Y. Cao, L. Niu, X. Wen, W. Feng, L. Huo and G. Bai, *J. Catal.*, 2016, **339**, 9–13.
- [60] V.M. Mokhov, Y.V. Popov and K.V. Shcherbakova, *Rus. J. Gen. Chem.*, 2016, **86**(2), 273–280.
- [61] H. Konnerth and M.H.G. Precht, *New. J. Chem.*, 2017, **41**(18), 9594–9597.
- [62] A. Ansmann, C. Benisch, *Supported Cobalt Catalysts for Nitrile Hydrogenations*, 2004, United States Patent: US 6 790 996 B2.
- [63] J. Long, K. Shen, Y. Li, *ACS Catal.*, 2017, **7**(1), 275–284.
- [64] F. Chen, C. Topf, J. Radnik, C. Kreyenschulte, H. Lund, M. Schneider, A.-E. Surkus, L. He, K. Junge, M. Beller, *J. Am. Chem. Soc.*, 2016, **138**(28), 8781–8788.
- [65] L. Hegedűs, T. Mathé and T. Kárpáto, *Appl. Catal. A:Gen.*, 2008, **349**(1-2), 40–45.
- [66] M. Vilches-Herrera, S. Weárkmeister, K. Junge, A. Börner and M. Beller, *Catal. Sci. Technol.*, 2014, **4**, 629–632.
- [67] Y. Hao, X. Wang, N. Perret, F. Cárdenas-Lizana and M.A. Keane, *Catal. Struct. React.*, 2015, **1**(1), 4–10.
- [68] Y. Hao, M. Li, F. Cárdenas-Lizana and M.A. Keane, *Catal. Lett.*, 2016, **146**(1), 109–116.
- [69] H. Yoshida, Y. Wang, S. Narisawa, S. Fujita, R. Liu and M. Arai, *Appl. Catal. A Gen.*, 2013, **456**, 215–222.
- [70] A. Sale, H. Yoshida, S. Fujita and M. Arai, *J. CO₂ Utilization*, 2016, **16**, 371–374.
- [71] A. Bhosale, H. Yoshida, S. Fujita and M. Arai, *Green Chem.*, 2015, **17**(2), 1299–1307.

- [72] C. Dai, F. Lui, W. Zhang, Y. Li, C. Ning, X. Wang and C. Zhang, *Appl. Catal. A:Gen.*, 2017, **538**, 199–206.
- [73] C. Dai, S. Zhu, X. Wang, C. Zhang, W. Zhang, Y. Li and C. Ning, *New J Chem.*, 2017, **41(10)**, 3758–3765.
- [74] C. Dai, Y. Li, C. Ning, W. Zhang, X. Wang and C. Zhang, *Appl. Catal. A:Gen.*, 2017, **545**, 97–103.
- [75] M. Yoshimura, A. Komatsu, M. Niimura, Y. Takagi, T. Takahashi, S. Ueda, T. Ichikawa, Y. Kobayashi, H. Okami, T. Hattori, Y. Sawama, Y. Monguchi and H. Sajiki, *Adv. Synth. Catal.*, 2019, **360(8)**, 1726–1732.
- [76] C. Lin, B. Wang, H. Guo, L. Chen and X. Yan, *Bull. Kor. Chem. Soc.*, 2018, **38(3)**, 391–396.
- [77] Y. Hao, M. Li, F. Cárdenas-Lizana and M.A. Keane, *Catal. Struct. React.*, 2015, **1(3)**, 43–51.
- [78] R.K. Marella, K.S. Koppadi, Y. Jyothi, K.S.R. Rao and D.R. Burri, *New J. Chem.*, 2013, **37**, 3229–3235.
- [79] S.K. Sharma, J. Lynch, A.M. Sobolewska, P. Plucinski, R.J. Watson, J.M.J. Williams, *Catal. Sci. Technol.*, 2013, **3(1)**, 85–88.
- [80] S. Göbölös, N. Mahata, I. Borbáth, M. Hegedüs, J.L. Margitfalvi, *Reaction Kinetics and Catalysis Letters*, 2001, **74(2)**, 345–352.
- [81] M. Arai, Y. Takada, T. Ebina, M. Shirai, *Appl. Catal. A:Gen.*, 1999, **183(2)**, 365–376.
- [82] C. Poupin, R. Maache, L. Pirault-Roy, R. Brahmi, C.T. Williams, *Appl. Catal. A:Gen.*, 2014, **475**, 363–370.
- [83] F. Saad, J.D. Comparot, R. Brahmi, M. Bensitel, L. Pirault-Roy, *Appl. Catal. A:Gen.*, 2017, **544**, 1–9.
- [84] C. Lin, J. Li, H. Guo, X. Wu, B. Wang, X. Yan, *Catal. Commun.*, 2018, **111**, 64–69.
- [85] Armour and Co., *British Patent*, 773 432, 1955.
- [86] K. Obert, D. Roth, M. Ehrig, A. Schönweiz, D. Assenbaum, H. Lange, P. Wasserscheid, *Appl. Catal. A: Gen.*, 2009, **356(1)**, 43–51.
- [87] D.J. Segobia, A.F. Trasarti, C.R. Apesteguía, *Catal. Sci. Technol.*, 2014, **4(11)**, 4075–4083.
- [88] S. Muratsugu, S. Kityakarn, F. Wang, N. Ishiguro, T. Kamachi, K. Yoshizawa, O. Sekizawa, T. Urgua, M. Tada, *Phys. Chem. Chem. Phys.*, 2015, **17(38)**, 24791–24802.
- [89] C. Ortiz-Cervantes, I. Iyanes, J.J. Garcia, *J. Phys. Org. Chem.*, 2012, **25(11)**, 2394–2398.
- [90] M. Freifelder, *J. A. Chem. Soc.*, 1960, **82(9)**, 2386–2389.
- [91] M. Chatterjee, M. Sato, H. Kawanami, T. Yokoyama, T. Suzuki, T. Ishizaka, *Adv. Synth. Catal.*, 2010, **352(14-15)**, 2394–2398.
- [92] Y.M. López-De Jesus, C.E. Johnson, J.R. Monnier, C.T. Williams, *Topics in Catalysis*, 2010, **53(15-18)**, 1132–1137.

- [93] M. Morák, F. Kršňák and H. Hrdličková, *J. Am. Chem. Soc.*, 1939, **61**, 3499–3502.
- [94] N. Waddleton, British Patent, 1 321 981, 1973.
- [95] H. Greenfield, *Ind. Eng. Chem. Prod. Res. Develop.*, 1976, **15**, 156–158.
- [96] W.H. Hartung, *J. Am. Chem. Soc.*, 1928, **50(12)**, 3370–3374.
- [97] E. Miller, J.M. Sprague, L.W. Kissenger, L.F. McBurney, *J. Am. Chem. Soc.*, 1940, **62(8)**, 2099–2103.
- [98] M.A. Schwartz, M. Zoda, B. Vishnuvajjala, I. Mama, *J. Org. Chem.*, 1976, **41(14)**, 2502–2503.
- [99] W.H. Carothers, G.A. Jones, *J. Am. Chem. Soc.*, 1925, **47(12)**, 3051–3057.
- [100] C.G. Overberger, J.E. Mulvaney, *J. Am. Chem. Soc.*, 1959, **81(17)**, 4697–4701.
- [101] M.J.F.M. Verhaak, A.J. van Dillen and J.W. Geus, *Catal. Lett.*, 1994, **26(1-2)**, 37–53.
- [102] B. Coq, D. Tichit and S. Ribet, *J. Catal.*, 2000, **189**, 117–128.
- [103] A.J. Lazaris, E.N. Zilberman, E.V. Lumitcheva and A.M. Vedin, *Zh. Prikl. Khim.*, 1965, **38**, 1097–1101.
- [104] J. Pašek, P. Richter, L. Rusek, L. Jarkovský and V. Růžicka, *Czech. Pat.*, 131 353, 1969.
- [105] Sh.A. Zelenaya, A.S. Basov, A.A. Pavlov, N.K. Petryakva and N.V. Gushin, *Khim. Prom. Moscow*, 1970, **46**, 11–12.
- [106] M.I. Yakushin, M.V. Blinova and P.V. Bazyleva, *Khim. Prom. Moscow*, 1968, **44**, 265–267.
- [107] J. Pašek, P. Kondelík and P. Richter, *Ind. Eng. Chem. Prod. Res. Develop.*, 1972, **11**, 333–337.
- [108] P.N. Rylander and L. Hasbrouck, *Engelhard. Ind. Tech. Bull.*, 1970, **11**, 19–24.
- [109] J. Clayden, N. Greeves and S. Warren, *Organic Chemistry*, 2nd Edition, Oxford University Press Inc. (New York), 2012.
- [110] R.J.H. Gregory, *Chem. Rev.*, 1999, **99**, 3649–3682.
- [111] P. Clapés, *Organic Synthesis using Biocatalysis*, Elsevier (Amsterdam), 2016.
- [112] H. Kunz and H. Waldmann, *Comprehensive Organic Synthesis; Protecting Groups*, Elsevier (Amsterdam), 1991.
- [113] W.F. Willeman, U. Handefeld, A.J.J. Straathod and J.J. Heijnen, *Enz. Microb. Technol.*, 2000, **27**, 423–433.
- [114] M. Asif and T. C. Bhalla, *Catal. Lett.*, 2017, **147**, 1592–1597.
- [115] D. Alagöz, S. S. Tükel and D. Yildirim, *Appl. Biochem. Biotechnol.*, 2015, **177**, 1348–1363.
- [116] K. Kindler, *Arch. Pharm.*, 1927, **265**, 389–415.

- [117] J.S. Buck, *J. Am. Chem. Soc.*, 1933, **55**(6), 2593–2597.
- [118] P. Tinapp, *Chem. Ber.*, 1971, **104**(7), 2266–2272.
- [119] M. North, *Tetrahedron: Asymmetry*, 2003, **14**, 147–176.
- [120] K. Tanaka, A. Mori and S. Inoue, *J. Org. Chem.*, 1990, **55**, 181–185.
- [121] T. Ooi, M. Kamdea, J. Fujii and K. Mrnoka, *Org. Lett.*, 2004, **6**(14), 2397–2399.
- [122] L. Veum, S.R.M. Pereira, J.C. van der Waal and U. Hanefeld, *Eur. J. Org. Chem.*, **7**, 2006, 1664–1671.
- [123] D.A. Skoog, F.J. Holler and T.A. Nieman, *Principles of Instrumental Analysis*, Philadelphia Saunders College Publishers (Orlando), 1998.
- [124] P. Atkins, J. de Paula and J. Keeler, *Atkin's Physical Chemistry* 11th Edition, Oxford University Press (Oxford), 2009.
- [125] M. Thommes, *Chemie Ingenier Technik*, 2010, **82**(7), 1059–1073.
- [126] P.K. Chu and L. Li, *Mat. Chem. Phys.*, 2006, **96**, 553–277.
- [127] D. Mullan, *Scanning*, 2006, **17**(3), 175–185.
- [128] D.H. Williams and C. B. Carter, *Transmission Electron Microscopy: A Textbook for Materials Science*, Springer (USA), 1996.
- [129] P.A. Webb, *MIC Tech. Pubs.*, 2003, 1–12.
- [130] P. Canton, G. Fagherazzi, M. Battagliarin, F. Mengazzo, F. Pinna and N. Pernicone, *Langmuir*, 2002, **8**, 653–3535.
- [131] N. Mahata, *Surf. Interfaces*, 2016, **4**, 51–54.
- [132] A. Cooper, *Biophysical Chemistry* 2nd Edition, Royal Society of Chemistry Publishers (Cambridge), 2011.
- [133] S.E. Dann, *Reactions and Characterization of SOLIDS*, Royal Society of Chemistry Publishers (USA), 2002.
- [134] D.A. Skoog, F.J. Holler and S.R. Crouch, *Principles of Instrumental Analysis* 6th Edition, Thomson Brooks/Cole (USA), 2007.
- [135] D.J. Gardiner, *Practical Raman Spectroscopy*, Springer-Verlag (Berlin), 1989.
- [136] G.A. Somorjai and J.Y. Park, *Angew. Chem. Int. Ed.*, 2008, **47**, 9212–9228.
- [137] J. Rouquerol, F. Rouquerol, P. Llewellyn, G. Mauria and K. Sing, *Adsorption by Powder and Porous Solids*, Academic Press (London), 1999.
- [138] W. Wang, P. Liu, M. Zhang, J. Hu and F. Xing, *Open J. Comp. Mat.*, 2012, **2**(3), 104–112.
- [139] S. Storck, H. Bretinger and W.H. Maier, *Appl. Catal. A:Gen.*, 1998, **174**, 137–146.

- [140] P. Jacobs and R. van Santen, *Zeolites: Facts, Figures, Future*, Elsevier (Amsterdam), 1989.
- [141] D. Shaw, *Introduction to Colloid and Surface Chemistry* 3rd Edition, Butterworths (London), 1983.
- [142] A.W. Coats and J.P. Redfern, *Analyst*, 1963, **88**, 906–924.
- [143] L.R. Snyder, J.J. Kirkland and J.W. Dolan, *Introduction to Modern Liquid Chromatography* 8th Edition, Thomson Brooks/Cole (London), 2004.
- [144] T. Kupiec, *Int. J. Pharm. Compd.*, 2004, **8(3)**, 223–227.
- [145] J. Sherma, *High Performance Liquid Chromatography in Photochemical Analysis*, CRC Press, Taylor and Francis Group (Florida), 2010.
- [146] P.J. Hore, *Nuclear Magnetic Resonance*, Oxford University Press Inc. (New York), 2004.
- [147] J.A. Iggo, *NMR Spectroscopy in Inorganic Chemistry*, Oxford University Press Inc. (New York), 1999.
- [148] D.H. Williams and I. Fleming, *Spectroscopic Methods in Organic Chemistry* 5th Edition, McGraw Hill (New York), 1995.
- [149] H. Günther, *NMR Spectroscopy*, John Wiley and Sons, Ltd. (Chichester), 1980.
- [150] L. McMillan, *The palladium catalysed hydrogenation of multi-functional aromatic nitriles*, PhD in Chemistry Thesis, University of Glasgow, 2012.
- [151] L. Gilpin, *The liquid phase hydrogenation of aromatic nitriles over supported palladium catalysts*, PhD in Chemistry Thesis, University of Glasgow, 2015.
- [152] D. Lennon, R. Waringham, T. Guidi and S.F. Parker, *Chem. Phys.*, 2013, **427**, 49–53.
- [153] R. Waringham, D. Bellaire, S.F. Parker, J. Taylor, R. Ewing, C.M. Goodway, M. Kibble, R.M. Wakefield, M. Jura, M.P. Dudman, R.P. Toose, P.B. Webb and D. Lennon, *J. Phys. Conf. Series*, 2014, **554**, 012005.
- [154] J.H. Atherton and K.J. Carpenter, *Process Development: Physiochemical Concepts*, Oxford Chemistry Primers, Oxford University Press Inc. (New York), 1999.
- [155] A. Tamas, R. Martagu and R. Minea, *Chem. Bull.*, 2007, **52(66)**, 133–138.
- [156] W.J.N. Fernando, M.R. Othman and D.G.G.P. Karunarathe, *Int. J. Eng. Tech.*, 2011, **11(1)**, 71–79.
- [157] E. Dietrich, C. Mathieu, H. Delmas and J. Jenck, *Chem. Eng. Sci.*, 1992, **47**, 3597–3604.
- [158] K. Nasirzadeh, D. Zimin, R. Neueder and W. Kunz, *J. Chem. Eng. Data*, 2004, **49**, 607–612.
- [159] B. Vitorge, S. Bieri, M. Humam, P. Christen, K. Hostermann, O. Muñoz, S. Loss and D. Jeannerat, *Chem. Commun.*, 2009, 950–952.
- [160] T. Lear, R. Marshall, J.A. Lopez-Sanchez, S.D. Jackson, T.M. Klapotke, M. Baumer, G. Rupprechter, H.J. Freund and D. Lennon, *J. Chem. Phys.*, 2005, **123**, 174706.

- [161] D. Lennon, D.R. Kennedy, G. Webb and S.D. Jackson, *Stud. Surf. Sci. Catal.*, 2000, **130**, 245–250.
- [162] J.L. Lemaitre, P.G. Menon and F. Delanny, *Characterisation of Heterogeneous Catalysts* Marcel Dekker, (New York), 1984.
- [163] M.A. Vanice and R.L. Garten, *J. Catal.*, 1979, **56**, 236–248.
- [164] M.A.S. Garcia, D.M. Silvestre, C.S. Nomura and L.M. Rossi, *J. Braz Chem Soc.*, 2015, 26(2), 359–364.
- [165] G. Fagherazzi, P. Canton, P. Riello, N. Pernicone, F. Pinna and M. Battagliarin, *Langmuir*, 2000, **16**, 4539–4546.
- [166] N. Pernicone, M. Cerboni, G. Prelazzi, F. Pinna and G. Fagherazzi, *Catal. Today*, 1998, **44**, 129–135.
- [167] G. Fagherazzi, P. Canton, P. Riello, F. Pinna, N. Pernicone, *Catal. Lett.*, 2000, **64**, 119–124.
- [168] L. Samain, A. Jaworski, M. Edén, D.M. Ladd, D.-K. Seo, F.J. Garcia-Garcia, U. Häussermann, *J. Solid State Chem.*, 2014, **217**, 1–8.
- [169] J.A. Wang, X. Bokhimi, A. Morales, O. Novaro, T. Lopes, R. Gomes, *J. Phys. Chem. B*, 1999, **103**, 299–303.
- [170] J.A. Creighton and R. Withnall, *Chem. Phys. Lett.*, 2000, **326**, 311–313.
- [171] A. Sadezky, H. Muckenhuber, H. Grothe, R. Niessner and U. Pschl, *Carbon*, 2005, **43**, 1731–1742.
- [172] T. Tuinstra and J.L. Koenig, *J. Chem. Phys.*, 1970, **53**, 1126–1130.
- [173] M.A. Pimenta, G. Dresselhaus, M.S. Dresselhaus, L.G. Cancado, A. Jorio and R. Saito, *Phys. Chem. Chem. Phys.*, 2007, **9**, 1276–1291.
- [174] Y. Wang, D.C. Alsmeyer and R.L. McCreary, *Chem. Mat.*, **2**, 1990, 557–563.
- [175] R.Al Jishi and G. Dresselhaus, *Phys. Rev. B*, 1982, **26**, 4514–4522.
- [176] R.J. Nemanich and S.A. Solin, *Phys. Rev. B*, 1979, **20**, 392–401.
- [177] E. Sanchez-Cortezon, M. Dieterle, Y. Uchida, G. Mestl, M. Schur and R. Schlögl, *EuroCarbon*, 2000, **7**, 9–13.
- [178] J. McGregor, Z. Huang, E.P.J. Parrott, J.A. Zeitler, K.L. Nguyen, J.M. Rawson, A. Carley, T.W. Hansen, J.-P. Tessonier and D.S. Su, *J. Catal.*, 2010, **269**, 329–339.
- [179] M.A. Vuurman and I.E. Wachs, *J. Phys. Chem.*, 1992, **96**, 5008–5016.
- [180] R.S. Krishnan, *Nature*, 1947, **160**, 26.
- [181] A. Mortensen, D.H. Christensen, O. Faurskov, E. Nielsen and J. Pearsen, *Raman Spectrosc.*, 1991, **22(1)**, 47–49.
- [182] Y. Chen, J. Hyvdotoft, C.J.H. Jacobsen, O. Faurskov and E. Nielsen, *Spectrochimica Acta (A)*, 1995, **51**, 2161–2169.

- [183] S.P.S. Porto, R. S. Krishnan, *J. Chem. Phys.*, 1967, **47**, 1009.
- [184] A. Aminzaden and H. Saikhani-Fard, *Spectrochimica Acta (A)*, 1999, **55**, 1421–1425.
- [185] A. Mortensen, D.H. Christensen, O. Faurskov, E. Nielsen and J. Pedersen, *Raman Spectroscopy*, 1993, **24**, 667–673.
- [186] W.R. Smith, F.S. Thornhill and R.I. Bray, *Rubber Chem. Technol.*, 1942, **15**(1), 206–215.
- [187] O. Boujibar, F. Ghamouss, A. Ghosh, O. Achak and T. Chafik, *J. Power Sources*, 2019, **436**, 226882.
- [188] L. Zhang, Y. Wu, L. Zhang, Y. Wang and M. Li, *Vacuum*, 2016, **133**, 1–6.
- [189] S. Brunauer, L.S. Deming, W.E. Deming and E. Teller, *J. Am. Chem. Soc.*, 1940, **62**, 1723.
- [190] K. Sing, *Colloids and Surfaces A*, 2001, **187-188**, 3–9.
- [191] K.S.W. Sing and R.T. Williams, *Adsorpt. Sci. Technol.*, 2004, **22**(10), 773–782.
- [192] T. Lear, R. Marshall, E.K. Gobson, T. Schütt, T.M. Klopötke, G. Rupprechter, H.-J. Freund, J.M. Winfield and D. Lennon, *Phys. Chem. Chem. Phys.*, 2005, **7**, 565–567.
- [193] N. Sheppard and C. de la Cruz, *Adv. Catal.* 1996, **41**, 1–112.
- [194] T. Dellwig, G. Rupprechter, H. Unterhalt and H.-J. Freund, *Phys Rev Lett*, 2000, **85**, 776–779.
- [195] S. Sumner, M. Sock, M.G. Ramsey, F.P. Netzer, M. Wiklund, M. Borg and J.N. Andersen, *Surf. Sci.*, 2000, **470**, 171–185.
- [196] I. V. Yudanor, R. Sahnoun, K.M. Neyman, N. Rösch, J. Hoffmann, S. Schauerermann, V. Johánek, H. Unterhalt, G. Rupprechter, L. Libunda and H.-J. Freund, *J. Phys. Chem. B*, 2003, **107**, 255–264.
- [197] A.A. Nechitailor, N.V. Glebova, Yu.A. Kukushkina and V.V. Sokolov, *Russian J. Appl. Chem.*, 2011, **84**(10), 1710–1715.
- [198] S. Jun, W. Li and S. Gang, *Appl. Sci. Eng. Innov.*, 2014, **1**(1), 2331–9062.
- [199] M. Trueba, S.P. Trasatti, *Eur. J. Inorg. Chem.*, 2005, **17**, 3393–3403.
- [200] J.H. Kang, L.D. Menard and R.G. Frenkel, *J. Am. Chem. Soc.*, 2006, **128**, 12068–12069.
- [201] F. Rason, R. Wischert and C. Coperet, *Chem. Sci.*, 2011, **2**, 1149–1156.
- [202] X. Yang, L. Quing, L. Erjum, Z. Wang, X. Gong, Z. Yu, Y. Guo, L. Wang, W. Zhan, J. Zhang and S. Dai, *Nat. Comm.*, 2019, **10**, 1611.
- [203] A. Boumaza, L. Favaro, J. Leaion, G. Sattonnay, J.B. Brubach, P. Berthet, A.M. Huntz, R. Roy and R. Tetot, *J Solid State Chem*, 2009, **182**, 1171–1176.
- [204] S. Lamouri, M. Hamidouche, N. Bouaouadja, H. Belhouchet, V. Garnier, G. Fantozzi and J.F. Trelkat, *Boletin de la Sociedad Espanola Ceraminca y vidrio*, 2017, **56**, 47–54.
- [205] M. Kohno and S.S.S.-I. Murahashi, *Bull. Chem. Soc. Jpn.*, 1990, **63**, 1252–1254.

- [206] K.J. Broadley, *Pharmacol. Ther.*, 2010, **125**, 363–375.
- [207] E. Ouellet and D. Poirier, *Synlett*, 2011, **14**, 2025–2028.
- [208] T.S. Work, *J. Chem. Soc.*, 1942, **79**, 426–429.
- [209] M. Freifelder and Y. H. Ng, *J. Pharm. Sci.*, 1965, **54**, 1204.
- [210] H.-U. Blaser, *Catal. Today*, 2000, **60**, 161–165.
- [211] P.G.T. Fogg and W. Gerrard, *Solubility of Gases in Liquids*, John Wiley and Son (New York), 1991.
- [212] C. Descamps, C. Coquelet, C. Boullou and D. Richon, *Thermochimica Acta*, 2005, **430**, 1–7.
- [213] G.R. Fuller, A.J.M. Miller, N.H. Sherden, H.E. Gottlieb, A. Nudelman, B.M. Stoltz, J.E. Bercaw and K.I. Goldberg, *Organometallics*, 2010, **29(9)**, 2176–2179.
- [214] A.P.G. Kieboom, J.F. de Kreuk and H. van Bekkum, *J. Catal.*, 1971, **20**, 58–66.
- [215] S. Rustler, V. Windeisen, A. Chmura, B.C.M. Fernandes, C. Kiziak and A. Stolz, *Enzy. Microb. Technol.*, 2007, **40**, 598–606.
- [216] F. Pinna, F. Menegazzo, M. Signoretto, P. Canton, G. Fagherazzi and N. Pernicone, *Appl. Catal. A:Gen.*, 2001, **219**, 195–200.
- [217] M.I. McAllister, C. Boulho, L. McMillan, L.F. Gilpin, C. Brennan and D. Lennon, *RSC Adv.*, 2019, **9**, 26116–26125.
- [218] V. Kogan, Z. Aizenshtat and R. Neumann, *Angew. Chem. Int. Ed.*, 1999, **38(22)**, 3331–3334.
- [219] D. Procházková, P. Zámotný, M. Bejblová, L. Červený and J. Čejka, *Appl. Catal. A:Gen.*, 2007, **332**, 56–64.
- [220] R. Abu-Reziq, D. Avnir and J. Blum, *J. Mol. Catal A: Chem.*, 2002, **187**, 277–281.
- [221] Y. Huang and W.M.H. Sachtler, *J. Catal.*, 1999, **188**, 215–225.
- [222] M. Bejlová, L. Zámotný, L. Čeverný and J. Čejka, *Appl. Catal. A:Gen.*, 2005, **296**, 169–175.
- [223] K. Morkawa, W.S. Benedict, H.S. Taylor, *J. Am. Chem. Soc.*, 1935, **57**, 592–593.
- [224] N. Thakar, N.F. Polder, K. Djanashvili, H. van Bekkum, F. Kapteijn, J.A. Moulijn, *J. Catal.*, 2007, **246**, 344–350.
- [225] R.L. Burwell, *Accounts Chem. Res.*, 1969, **2(10)**, 289–296.
- [226] V.S. Ranade and R. Prins, *Chem. Eur. J.*, 2000, **6(2)**, 313–320.
- [227] J. Horiuti and M. Polanyi, *Nature*, 1933, **132**, 819.
- [228] J. Horiuti and M. Polanyi, *Nature*, 1934, **134**, 847.
- [229] R. Brown, *J. Chem. Soc. Faraday Trans.*, 1993, **89(14)**, 2519–2526.

- [230] L.N. Kauder and T.I. Taylor, *Science*, 1951, **113**, 238–241.
- [231] R. Brown and C. Kemball, *J. Chem. Soc. Faraday Trans.*, 1993, **89(14)**, 2519–2526.
- [232] G.C. Levy, R.L. Lichter and G.L. Nelson, *Carbon-13 Nuclear Magnetic Resonance Spectroscopy* 2nd Ed, John Wiley and Sons (New York), 1980.
- [233] J.P. Guzowski, E.J. Delaney, M.J. Humora, E. Irdam, W.F. Kiesman, A. Kwok and A.D. Moran, *Org. Process Res. Dev.*, 2012, **16(2)**, 232–239.
- [234] Syngenta Technical Report, Co Brennan Personal Communication, Received April 2018.
- [235] H.M. Mantsch, H. Saito and I.C.P. Smith, *Prog. NMR Spectrosc.*, 1977, **11(4)**, 211–272.
- [236] P.E. Hansen, *Prog. NMR Spectrosc.*, 1988, **20**, 207–255.
- [237] P.E. Hansen, *Annu. Rep. NMR Spectrosc.*, 1983, **15**, 105–234.
- [238] B. Vitorge, M. Humam, P. Christen, K. Hostettmann, O. Muñoz, S. Loss and D. Jeannerat, *Chem. Commun.*, 2009, 950–952.
- [239] D.A.L. Otte, D.E. Borchmann, C. Lin, M. Weck and K.A. Woerpel, *Org. Lett.*, 2014, **16**, 1566–1569.
- [240] M.I. McAllister, C. Boulho, C. Brennan, P.J. Sidebottom and D. Lennon, *Mol. Catal.*, **484**, 110720.
- [241] C. Morisse, *The structure/activity relationship of nitrobenzene hydrogenation over Pd/alumina catalysts*, PhD in Chemistry Thesis, University of Glasgow, 2015.
- [242] J.W. Campbell, *The selective hydrogenation of nitrobenzene at elevated temperatures over alumina-supported palladium catalysts*, PhD in Chemistry Thesis, University of Glasgow, 2019.
- [243] P.J. Dyson and P.G. Jessop, *Catal. Sci. Technol.*, 2016, **6**, 3302–3316.
- [244] H.P. Young and C.W. Christensen, US Patent 2,287,219, 1942.
- [245] R. Sander, *Atmos. Chem. Phys.*, 2015, **15(8)**, 4399–4381.
- [246] R.S. Downing, P.J. Kunkeler and H. van Bekkum, *Catal. Today*, 1997, **37**, 121–136.
- [247] R.A. Rajadhyaksha and S.L. Karwa, *Chem. Eng. Sci.*, 1986, **41(7)**, 1765–1770.
- [248] M. Munz, C.E. Giusca, R.L. Myers-Ward, D.K. Gaskill and O. Kazakova, *CS Nano*, 2015, **9(8)**, 8401–8411.
- [249] J.V.H. d'Angelo and A.Z. Francesconi, *J. Chem. Eng. Data*, 2001, **46**, 671–674.
- [250] H. Beckhaus, E. Waldau and H. Witt, Ger. Offen. DE 3611677, 1987.
- [251] K. Sakata and M. Hashimoto, *J. Heterocyclic Chem.*, 2000, **37**, 1351–1353.
- [252] A. Tungler and E. Szabados, *Org. Process. Res. Dev.*, 2016, **20(7)**, 1246–1251.
- [253] G. Joseph, J. Kushy and P.M. Kallanickal, *Int. J. Eng. Si. Inov. Tech*, 2013, **2(2)**, 106–113.
- [254] P.N. Bruce, *West Indian J. Eng.*, 1973, **4(2)**, 57–80.

- [255] C. Perego and S. Pertello, *Catal. Today*, 1999, **52**, 133–145.
- [256] I.K. Stamatou and F.L. Muller, *AIChEJ.*, 2017, **63**, 273–282.
- [257] R.M. Machado, *ARL Application Note*, 2007, **1**, 1–13.
- [258] G.C. Bond, *Heterogeneous Catalysis Principles and Applications*. Oxford Chemistry Series. Clarendon Press (Oxford), 1974.

Appendix

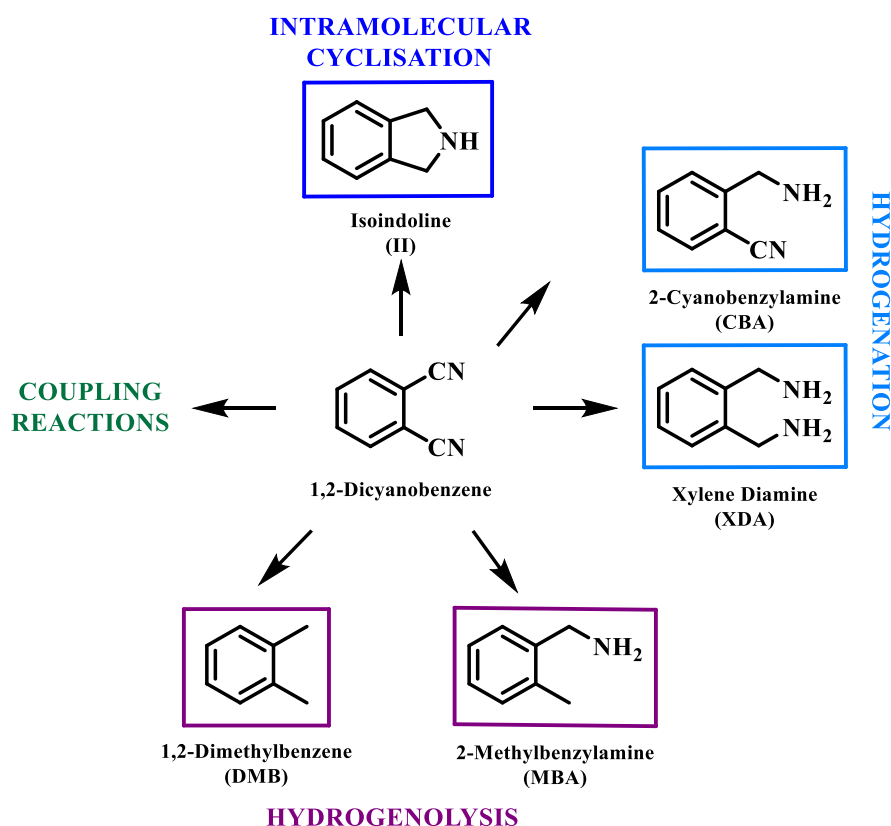
CHAPTER 12

The Liquid Phase Hydrogenation Reaction of 1,2-Dicyanobenzene

The work documented in this section relates to the future of this collaborative project between Syngenta and the University of Glasgow.

12.1 Introduction

Expanding on the work described in previous chapters, the hydrogenation of a dinitrile, specifically, 1,2-dicyanobenzene, is explored. Following on from the previous substrates, this study adds a degree of complexity regarding the potential product distribution. However, it is essential to note at this juncture that the investigation into the hydrogenation reaction of 1,2-dicyanobenzene is preliminary. This study aims to provide only a basic understanding of the reaction system, such that the associated chemistry may be explored in the next phase of the academic/industrial partnership investigating the application of heterogeneous catalysis in the formation of primary amines. Consequently, this represents a method development and trouble-shooting exercise, rather than a detailed mechanistic study, as was conducted for the hydrogenation reaction of mandelonitrile.



Scheme 12.1. Postulated pathways for the liquid phase hydrogenation reaction of 1,2-dicyanobenzene showing the proposed products for each route.

The postulated chemistry associated with the hydrogenation reaction of 1,2-dicyanobenzene is illustrated in Scheme 12.1. Four major routes are proposed, three of which have been observed for the previously examined nitrile systems. The hydrogenation pathway may afford either 2-cyanobenzylamine or xylene diamine, depending on whether only one or both nitrile groups are hydrogenated. A study conducted by Chatterjee *et al.*, examined the hydrogenation reaction of adiponitrile, amongst other nitriles, over a Rh/Al₂O₃ catalyst and in the presence of supercritical carbon dioxide. The selective production of the aminonitrile in this instance suggested that only one nitrile group adsorbed onto the surface.^[1] Nevertheless, over Raney nickel, it was the diamine product which was reported in the hydrogenation reactions of various aliphatic dinitriles, ranging in chain length from two carbons (succinonitrile) to five carbons (pimelonitrile).^[2] It is therefore clear that the product distribution is highly dependent on the catalyst and reaction conditions which are employed, making an accurate prediction of product distribution difficult.

In addition to the hydrogenation pathway is a hydrogenolysis route which affords either, or both, 2-methylbenzylamine and 1,2-dimethylbenzene. It is noted that, whilst Scheme 12.1 indicates that these hydrogenolysis products are produced directly from the starting material, it is in fact more likely that they will form as the result of cleavage of the amine groups of the hydrogenation products. Further, the occurrence of coupling reactions of the imine intermediates and the amine products is also a possibility. However, as the resultant products of these coupling reactions are not commercially available, quantification may prove problematic if this pathway is found to be operational.

A further pathway, not available to either the 4-hydroxybenzylcyanide or mandelonitrile reaction systems, is shown in Scheme 12.1. Intramolecular cyclisation is exclusive to dinitrile systems and is a process governed predominantly by hydrocarbon chain length and rigidity, as the resultant ring system must be stable.^[3–4] As such, short chain dinitriles ($n = 2$) afford the intramolecular C-N cyclisation product in high yields. For medium chain lengths ($n = 3, 4$), a mixture of cyclic and straight chain amines are produced, whereas dinitriles having longer chains ($n \geq 5$), afford no cyclisation products.^[3] The introduction of an aromatic ring within the chain, as is the case for 1,2-dicyanobenzene, is additionally shown to enhance the cyclisation process. It is, however, essential that the nitrile moieties are on adjacent carbon atoms for this reaction to be feasible. The ability

of a dinitrile to undergo cyclisation is therefore drastically important in terms of the selectivity of the reaction.^[2]

Against this background, it is proposed that, as the hydrogenation reaction to form xylene diamine and the intramolecular cyclisation reaction to yield isoindoline are likely to proceed by different means and having differing hydrogen requirements, the product distribution may be used as a probe of hydrogen availability. Consequently, it is essential that appropriate reaction conditions for the aforementioned application are determined. The apparent simplicity of Scheme 12.1 may, however, prove misleading. The presented scheme does not include intermediate species which may or may not also be detectable. Further, additional intricacies may also have been overlooked and thus, a degree of caution must be exercised at this time.

12.2 Analytical Method Development

As a new and previously untested substrate system, there was no analytical method in place to analyse the progress of the 1,2-dicyanobenzene hydrogenation reaction. However, as similarities existed between the expected product range for the 1,2-dicyanobenzene system and the previously explored nitrile systems, the HPLC methodology employed prior (Section 2.4.1) was tested for suitability. It was identified that this method was appropriate for the reagent and the majority of the predicted products, with all species eluting from the column within the first 15 minutes of the program with good separation. The exception to this being the hydrogenolysis product, 1,2-dimethylbenzene. As such, development of an alternative method was deemed appropriate. 1,2-Dimethylbenzene is reported to be insoluble in water, but to have good solubility in acetonitrile. An eluent stream composed solely of acetonitrile afforded a clear peak for the 1,2-dimethylbenzene. Nonetheless, these chromatographic conditions were found to be of detriment to the other molecules which could no longer be distinguished.

Following this was the development of a new method where the acetonitrile content was increased after the first 15 minutes of analysis time. This allowed all proposed components of the reaction mixture to be effectively separated, with the next step being calibration. The calculation of response factors for each of the products afforded linear plots. Unfortunately, despite the detection of the 1,2-dicyanobenzene using this method,

a linear calibration for this molecule was not easily achieved, thus resulting in issues associated with the effective quantification of the starting material. Further work is required to establish the solubility of 1,2-dicyanobenzene in a range of solvents and/or solvent mixtures.

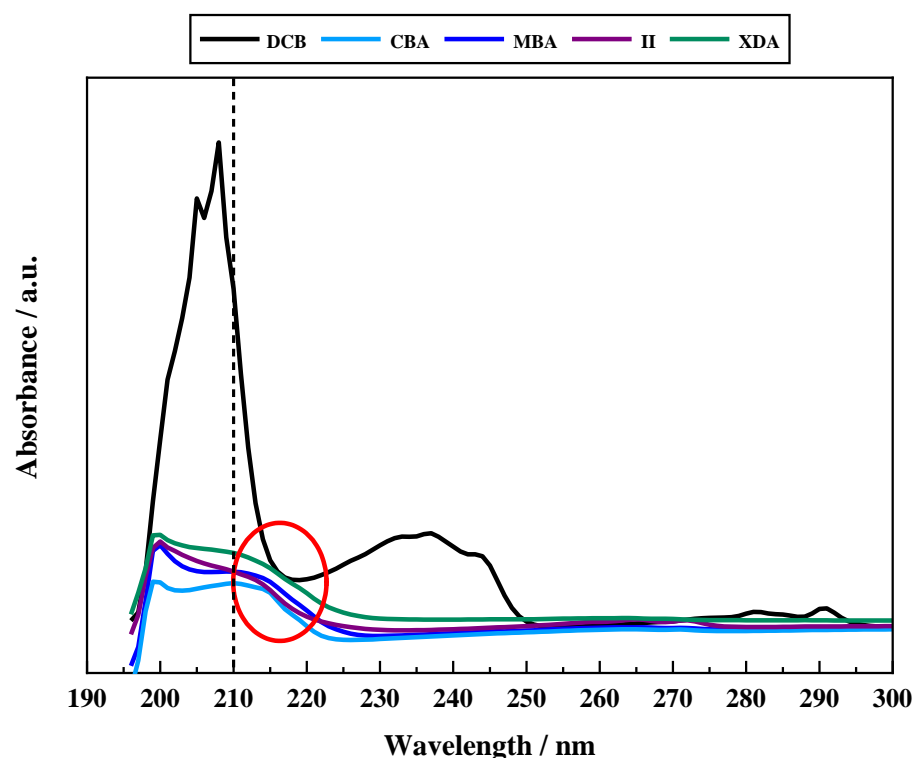


Figure 12.1. Ultraviolet-visible spectra for molecules relating to the hydrogenation reaction of 1,2-dicyanobenzene. All measurements were conducted on 0.01 mmol L^{-1} solutions of the individual compounds in ethanol. [DCB = 1,2-dicyanobenzene; CBA = 2-cyanobenzylamine; MBA = 2-methylbenzylamine; II = isoindoline; XDA = xylene diamine].

Ultraviolet-visible spectroscopy conducted on each of the relevant reagent and product molecules, each at a concentration of 0.01 mmol L^{-1} , showed that at the detector wavelength employed in the HPLC analysis (210 nm), there was a large absorbance difference between the 1,2-dicyanobenzene and the postulated products (Figure 12.1). It was thus suggested that, at 210 nm, 1,2-dicyanobenzene absorbs too strongly and, therefore, saturation of the detector at higher concentrations causes the loss in linearity observed. With reference to Figure 12.1, at 215 nm (highlighted by a red circle), the

absorbance of each of the molecules is shown to be more uniform. Alteration of the detector wavelength analysed by HPLC to 215 nm was hence implemented. A comparison of the calibration curves obtained at detector wavelengths 210 nm and 215 nm is presented in Figure 12.2.

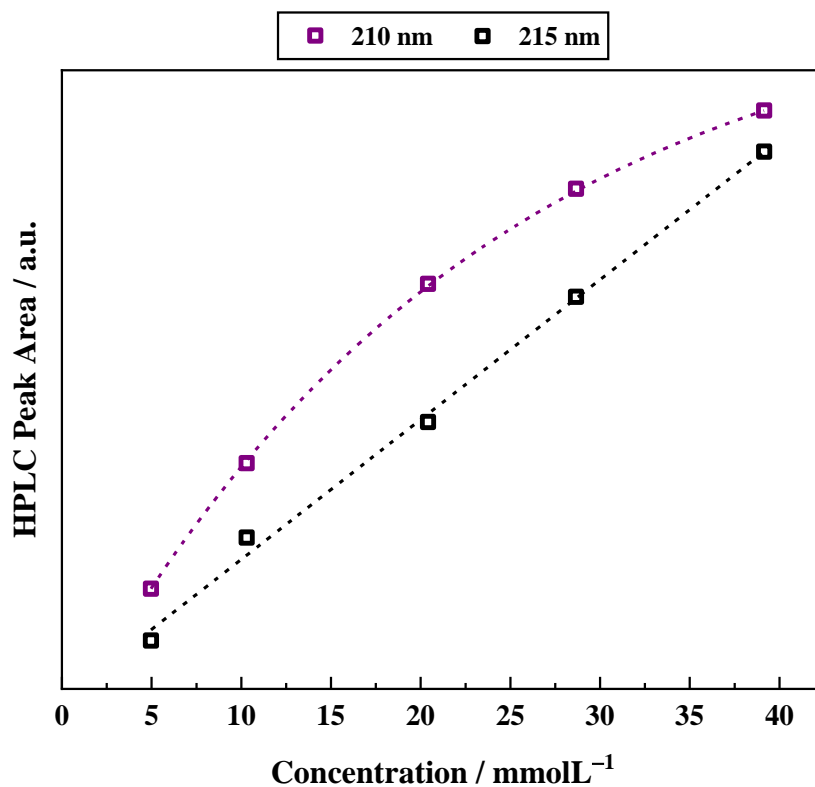


Figure 12.2. Calibration curves associated with 1,2-dicyanobenzene conducted at detector wavelengths of 210 nm and 215 nm.

12.3 The Hydrogenation Reaction of 1,2-Dicyanobenzene: Neutral Conditions

Once an appropriate analytical approach had been established, a generic 1,2-dicyanobenzene hydrogenation test reaction was conducted. This was undertaken in a neutral environment, at 40 °C under 4 barg hydrogen pressure with an agitation speed of 850 rpm over the 5% Pd/C catalyst described prior [GU-1] (Chapter 3). This test reaction allowed a baseline to be established and provided an opportunity for any necessary procedural alterations to be identified.

Following this, it was recognised that slight alterations were necessary. It is reported that 1,2-dicyanobenzene is soluble in hot alcohol.^[5] Moderate heating and stirring (using a hot plate) were therefore found to be essential in dissolving the reagent for facile addition to the reactor. Moreover, reagent injection, as was employed for all other substrates, was not possible. It was postulated that the warmed solution of 1,2-dicyanobenzene and ethanol precipitated out of solution in the cold Swagelok pipes, leading from the injection port to the reaction vessel. As there was no method of heating the pipes, reagent addition was conducted *via* a funnel at the main charging port. It is proposed that the reported solubility issues associated with 1,2-dicyanobenzene are due to the presence of two large electron withdrawing groups on the same side of the molecule. The symmetry of 1,2-dicyanobenzene unfortunately means there is no overall dipole moment. It is this absence of a dipole moment which makes this molecule difficult to solvate in polar solvents, ethanol in this particular instance.^[6]

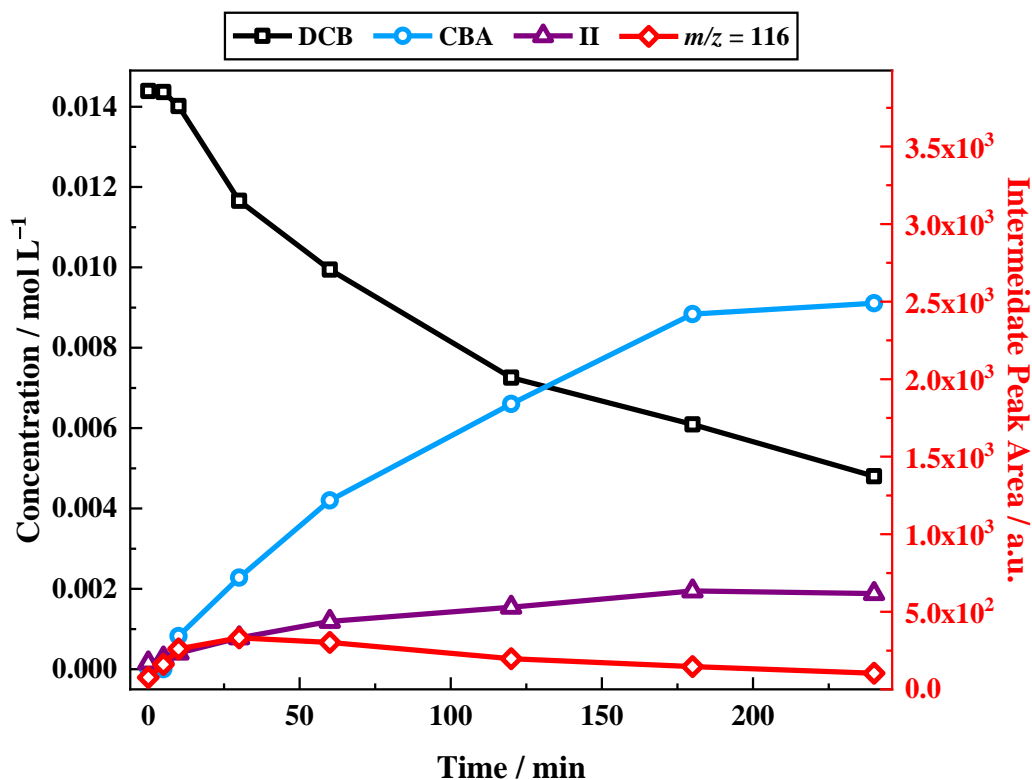
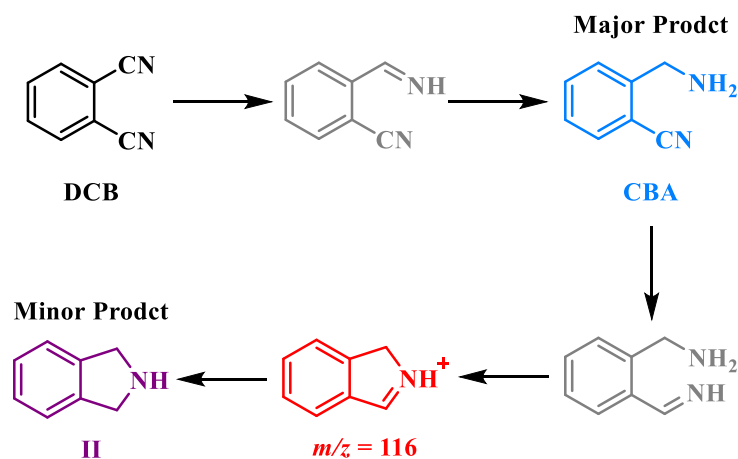


Figure 12.3. Reaction profile for the liquid phase hydrogenation reaction of 1,2-dicyanobenzene (15 mmol L^{-1}) over a 5% Pd/C catalyst (150 mg) in the absence of a sulphuric acid additive in ethanol. The reaction was conducted at 40°C under 4 barg hydrogen pressure with an external line pressure of 8 barg and an agitation speed of approximately 850 rpm. Peak area for the $m/z = 116$ intermediate is plotted separately on the second y-axis [DCB = 1,2-dicyanobenzene; CBA = 2-cyanobenzylamine; II = isoindoline].

The resultant reaction profile, achieved using the aforementioned neutral conditions, is presented in Figure 12.3. Here it is shown that consumption of the nitrile reagent is slow, with incomplete conversion achieved within 4 hours (68%). Further, it is observed that there are two products: one major, one minor; and an intermediate. Analysis by GC-MS and HPLC was employed for the identification of these species. Unfortunately, due to the lack of commercial availability of the intermediate, quantification of this species was not possible. As such, peak area obtained by HPLC for the intermediate is plotted on the second y-axis (Figure 12.3). Quantification of both the major product (2-cyanobenzylamine) and the minor product (isoindoline), however, was possible.



Scheme 12.2. Reaction scheme showing the observable chemistry associated with the liquid phase hydrogenation reaction of 1,2-dicyanobenzene (15 mmol L^{-1}) over a 5% Pd/C catalyst (150 mg) in the absence of 2 equivalents of sulphuric acid in ethanol. The reaction was conducted at 40°C under 4 barg hydrogen pressure with an external line pressure of 8 barg and an agitation speed of approximately 850 rpm. Molecules depicted in grey represent proposed intermediate species which are not detectable in the liquid phase by either GC-MS or HPLC. [DCB = 1,2-dicyanobenzene; CBA = 2-cyanobenzylamine; MBA = 2-methylbenzylamine; II = isoindoline; XDA = xylene diamine].

The observed chemistry for the hydrogenation reaction of 1,2-dicyanobenzene under neutral conditions is depicted schematically (Scheme 12.2). Somewhat interestingly, there is found to be an absence of hydrogenolysis. In their unprotonated form, the amine products are free to bind to the surface *via* the lone pair of electrons on the nitrogen atom and participate in such reactions. Nevertheless, 2-cyanobenzylamine, the molecular structure of which is ideally set up for hydrogenolytic cleavage of the amine functionality, as discussed in Section 12.1, is shown instead to favour hydrogenation of the second nitrile functionality. Inspection of Scheme 12.2 indicates that there is no branching point by which the observed product distribution could act as an indicator of hydrogen availability, thus rendering neutral conditions unsuitable for the desired application.

12.4 Inclusion of an Acid Additive Afforded a Drastically Different Reaction Profile

Being known poisons to palladium-based catalysts, the presence of unprotonated amines can be problematic for nitrile hydrogenation reactions.^[7–9] Indeed, for the hydrogenation reaction of mandelonitrile, there was no observable product without the inclusion of an acid additive (Section 5.4). This, however, has been shown not to be the case for the 1,2-dicyanobenzene substrate, as shown in Section 12.3. As such, it is hoped that the inclusion of an acid additive will enhance the observed chemistry for this substrate system, such that the product distribution may be used as a suitable probe for hydrogen supply.

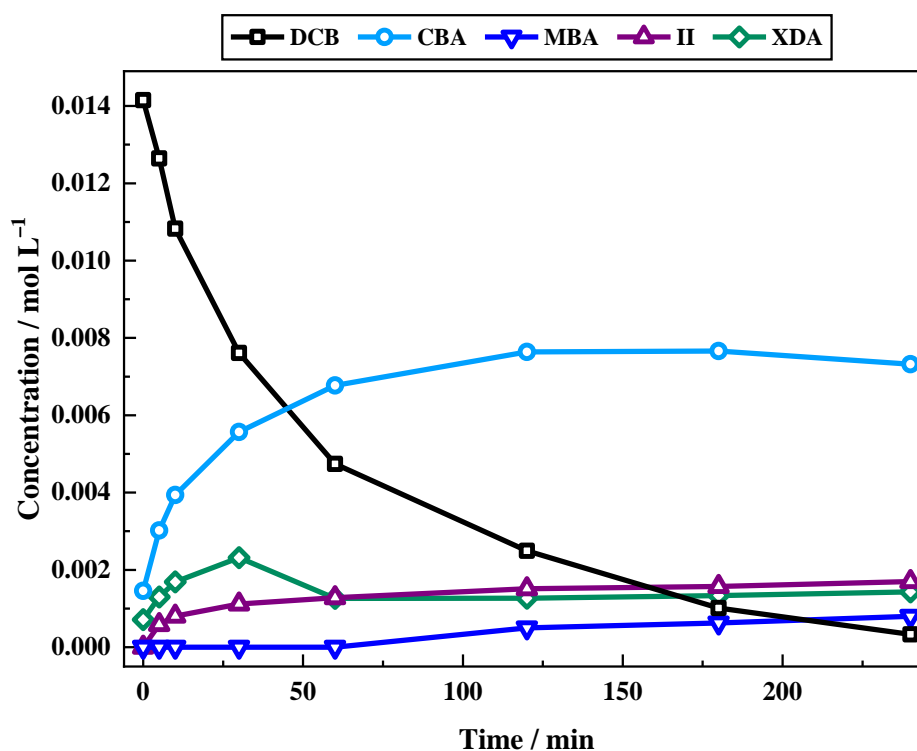
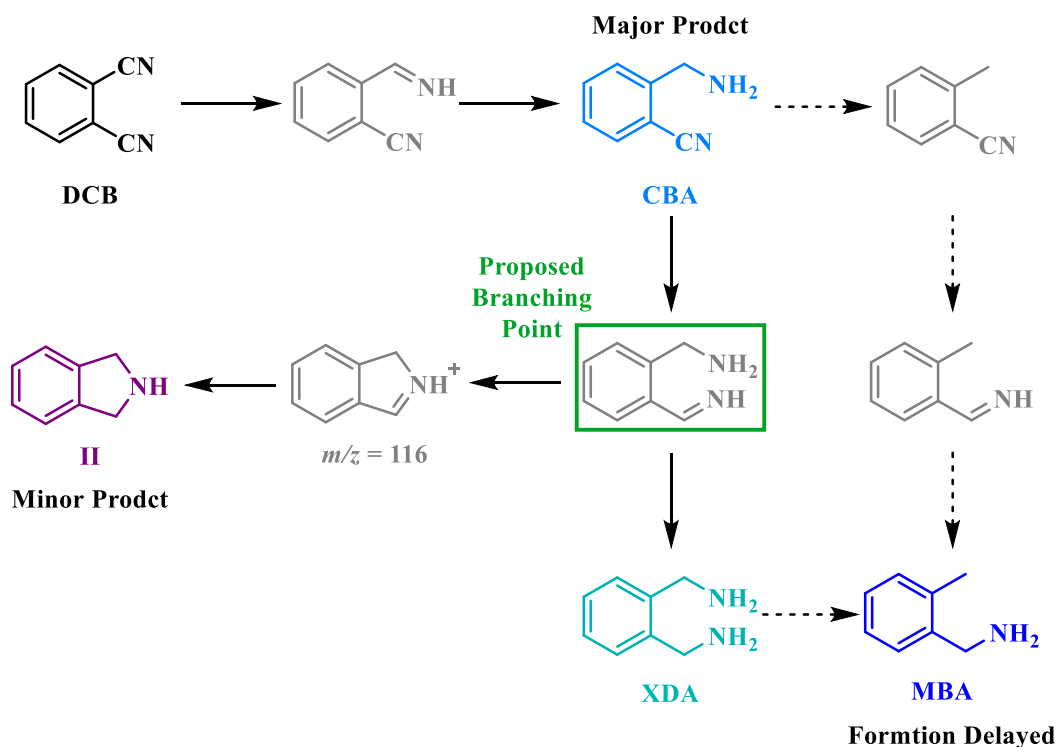


Figure 12.4. Reaction profile for the liquid phase hydrogenation reaction of 1,2-dicyanobenzene (15 mmol L^{-1}) over a 5% Pd/C catalyst (150 mg) in the presence of 2 equivalents of sulphuric acid in ethanol. The reaction was conducted at 40°C under 4 barg hydrogen pressure with an external line pressure of 8 barg and an agitation speed of approximately 850 rpm. [DCB = 1,2-dicyanobenzene; CBA = 2-cyanobenzylamine; MBA = 2-methylbenzylamine; II = isoindoline; XDA = xylene diamine].

Figure 12.4 shows that the inclusion of 2 equivalents of sulphuric acid, with respect to nitrile concentration, affords a vastly different reaction profile to that yielded in the absence of acid (Figure 12.3). In contrast to Figure 12.3, full product identification and quantification has been documented. This outcome was achieved by calibrating the commercially available reference compounds which correspond to the observed product distribution for the hydrogenation reaction of 1,2-dicyanobenzene under acidic conditions.

It is indicated in Figure 12.4 that consumption of the nitrile moiety is significantly more rapid in the presence of acid, with complete conversion now achieved within a 240 minute period (*cf.* 68% under neutral conditions). Moreover, the product distribution was also altered. At reaction termination, four products were observed under acidic conditions.

As with the neutral reaction, 2-cyanobenzylamine, identified as the product of the complete hydrogenation of one of the two nitrile groups of 1,2-dicyanobenzene, was detectable as the major product. Also detected in the liquid phase was xylene diamine, reaching a maximum at 30 minutes where it then exhibited a slight dip in consumption, before it again gradually increased for the remainder of the reaction. The second phase of xylene diamine production was observed to be a much slower rate than that experienced for the initial 30 minutes of the reaction. The decline in xylene diamine concentration was found to coincide with the production of the hydrogenolysis product 2-methylbenzylamine. The formation of 2-methylbenzylamine is shown to be delayed, being undetectable until a reaction time of 60 minutes. This finding may suggest that 2-methylbenzylamine is produced as the result of xylene diamine hydrogenolysis. The final product was identified as isoindoline, produced *via* intramolecular cyclisation.



Scheme 12.3. Reaction scheme showing the observable chemistry associated with the liquid phase hydrogenation reaction of 1,2-dicyanobenzene (15 mmol L^{-1}) over a 5% Pd/C catalyst (150 mg) in the presence of 2 equivalents of sulphuric acid in ethanol. The reaction was conducted at 40°C under 4 barg hydrogen pressure with an external line pressure of 8 barg and an agitation speed of approximately 850 rpm. Molecules depicted in grey represent proposed intermediate species which are not detectable in the liquid phase. [DCB = 1,2-dicyanobenzene; CBA = 2-cyanobenzylamine; MBA = 2-methylbenzylamine; II = isoindoline; XDA = xylene diamine].

The outcomes of Figure 12.4 can forthwith be used in the development of the reaction scheme such that it accurately represents the active chemistry associated with the hydrogenation reaction of 1,2-dicyanobenzene in the presence of an acid additive (Scheme 12.3). Scheme 12.3 shows that the chemistry associated with an acidic environment is more complex than the chemistry observed under neutral conditions (Scheme 12.2). Further, Scheme 12.3 highlights a branching point, designated by a green box. This branching point represents a point in the reaction where one of two paths will be taken, affording either isoindoline or xylene diamine. As the two possible routes are postulated to have a different hydrogen requirement, it is proposed that the availability of hydrogen in the system will dictate the observed product ratio. As the intramolecular cyclisation process to form isoindoline should have a significantly lower hydrogen

requirement than the production of xylene diamine, it is proposed that the production of isoindoline will become favoured when the hydrogen supply is limited.

Ideally, this outcome would imply that the product ratio of isoindoline to xylene diamine could be used to determine hydrogen availability. Unfortunately, hydrogenolysis is also observed. It is therefore possible that some of the xylene diamine produced *via* the hydrogenation pathway is consumed by undergoing hydrogenolysis to form 2-methylbenzylamine. This proposed pathway is indicated by a dashed arrow in Scheme 12.3. However, further mechanistic studies, determining whether the hydrogenolysis of xylene diamine to form 2-methylbenzylamine is possible, are necessary to fully resolve this issue.

12.5 Significant Sample Discolouration After Catalyst Removal in the Presence of Acid Suggests the Occurrence of Homogeneous Chemistry

It was observed that, once the sample was removed from the reactor and separated from the catalyst (in the presence of acid) there was a significant colour change. This was also found in the absence of acid, however, to a much lesser extent, with the acid appearing to accelerate this process. A sample colour change, designated as the occurrence of homogeneous chemistry, was also observed for the 4-hydroxybenzyl cyanide system (Section 4.10).

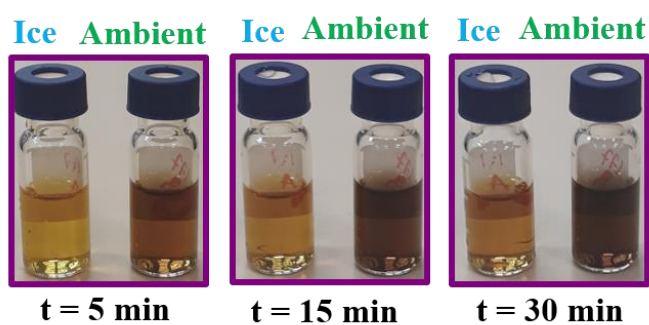


Figure 12.5. Sample vials containing a portion of the reaction mixture obtained 30 minutes into the hydrogenation reaction of 1,2-dicyanobenzene in an acidic environment. Post extraction from the reaction vessel, residual catalyst was removed by filtration. The time noted below each frame indicates the time post extraction and not reaction time. Two samples were monitored, with one stored under ambient conditions and the other stored in ice.

These findings are illustrated in Figure 12.5. At a reaction time of 30 minutes, an aliquot of the reaction mixture was extracted from the reaction vessel, the catalyst was removed, and the sample divided into two separate vials. The first vial was sealed under nitrogen and placed in ice in order to quench the reaction, whereas the second was stored under ambient conditions. Figure 12.5 shows the observed colour changes as time post extraction increased.

On sampling, after catalyst removal by filtration, the solution appeared pale yellow/orange. By 5 minutes, however, Figure 12.5 shows that a notable colour change from this reference is apparent for the sample stored in ambient conditions. As time increases the colour darkens such that, by 30 minutes post extraction, the ambiently stored sample was an opaque dark brown colour. Figure 12.5 also highlights that the samples stored in ice did not exhibit such a drastic colour change indicating that quenching the vials in ice was reasonably successful in the prevention of this chemistry. Moreover, as the reaction progressed, samples extracted from the reaction vessel were found to be increasingly coloured. This demonstrates that, whilst this chemistry is observed in the reactor, it is a homogeneous process, as evidenced by its occurrence in the absence of the catalyst. The origin of the distinctive colour observed in the sample vials is thought to be the isoindoline product. Isoindoline units occur in phthalocyanines, an important family of pigments, which are used in the creation of colour shades from yellow to brown.^[10] An alternative source of the colour change is the proposed occurrence of polymerisation reactions between the imine intermediates and the amine products. It is suggested that these issues may be alleviated by diluting the reaction components. Investigation into this is currently underway at the industrial complex.

12.6 Consideration of the Effect of Reduced Hydrogen Availability on Product Distribution

The basis for a product distribution probe for hydrogen availability within the 1,2-dicyanobenzene reaction system has been established in Section 12.1. Following on from this, alteration of the hydrogen availability through the modification of experimental parameters from those reported in Section 12.4 is implemented, and the effects monitored. As a point of reference, and as discussed in Chapter 8, hydrogen availability is shown to have a dramatic effect on product distribution in the mandelonitrile reaction system. As

such, experimental parameters, known to have an influence over hydrogen supply, were altered. While maintaining the 40 °C reaction temperature, both hydrogen pressure and agitation speed were reduced in order to obtain a ‘hydrogen lean’ environment. The reaction was subsequently probed, as before, to ascertain whether the adjusted hydrogen availability influenced the observed product distribution.

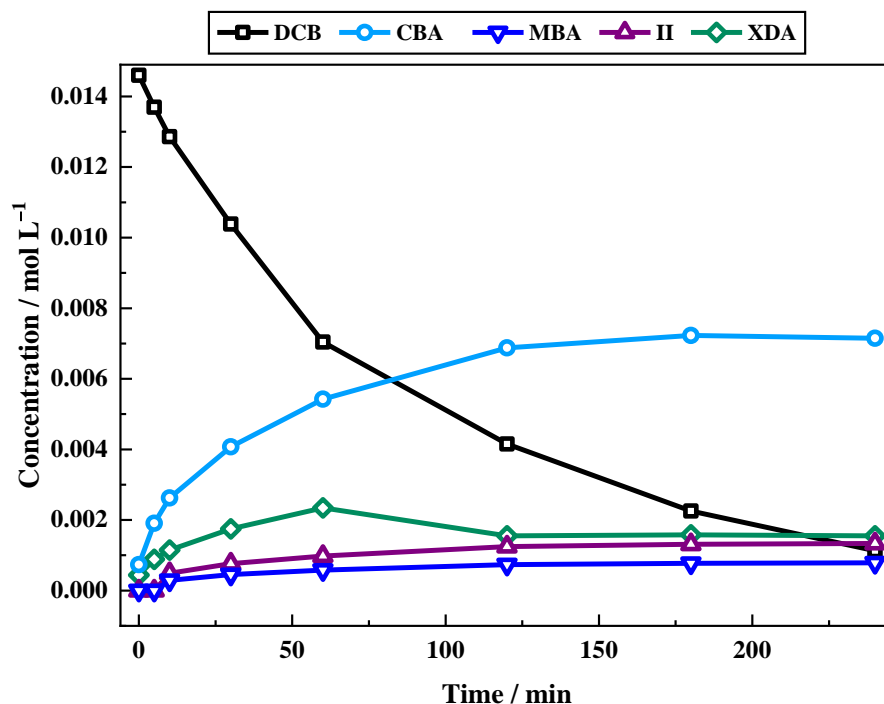


Figure 12.6. Reaction profile for the liquid phase hydrogenation reaction of 1,2-dicyanobenzene (15 mmol L^{-1}) over a 5% Pd/C catalyst (150 mg) in the presence of 2 equivalents of sulphuric acid in ethanol. The reaction was conducted at 40 °C under 2 **barg** hydrogen pressure with an external line pressure of 8 barg and an agitation speed of approximately 450 rpm. [DCB = 1,2-dicyanobenzene; CBA = 2-cyanobenzylamine; MBA = 2-methylbenzylamine; II = isoindoline; XDA = xylene diamine].

As shown in Figure 12.6, the resultant reaction profile under the reduced hydrogen conditions is very similar to Figure 12.4, which was performed at higher pressure and agitation speed. In this instance, alteration of the hydrogen availability by these means has had a very minimal effect on the product distribution. Echoing this observation, Figure 12.9 directly compares the selectivity for these conditions at reaction termination (time = 240 minutes).

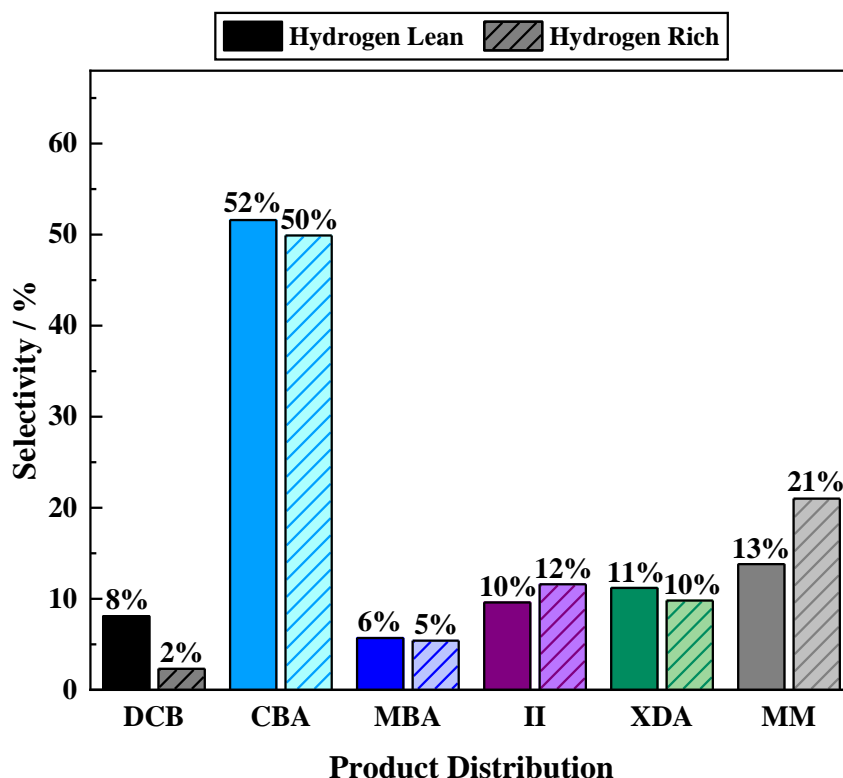


Figure 12.7. Reaction selectivity observed at reaction termination (time = 240 minutes), comparing the outcomes of the hydrogenation reaction of 1,2-dicyanobenzene under ‘hydrogen lean’ (solid bars) and ‘hydrogen rich’ (hashed bars) conditions, as described in Figures 12.6 and 12.4, respectively. [DCB = 1,2-dicyanobenzene; CBA = 2-cyanobenzylamine; MBA = 2-methylbenzylamine; II = isoindoline; XDA = xylene diamine; MM = missing mass].

Further comparing the outcomes of the two experiments, the major differences are found to relate to the conversion of the 1,2-dicyanobenzene and the selectivity towards missing mass. Under hydrogen lean conditions, a slight increase in unreacted 1,2-dicyanobenzene is observed, indicating a slight slowing in reaction rate. This observation can easily be rationalised by the alteration in hydrogen supply. For the selectivity towards the missing mass, however, the opposite trend is identified, with missing mass being more dominant when the hydrogen supply is enhanced. This indicates a slight selectivity issue relating to currently unidentified chemistry. Nonetheless, there is a strong indication here that these side reactions require hydrogen.

12.7 Consideration of the Effect of Temperature on the Product Distribution

As previously discussed, temperature can affect various aspects of a reaction (Section 7.4). This includes, but is not limited to, the rate of reaction and selectivity.^[11–12] For the 1,2-dicyanobenzene system under investigation, several potential pathways have been defined (Scheme 12.1), all of which may be subject to the effects of temperature. Thus, a degree of complexity is added to this reaction system. The role of temperature in the hydrogenation reaction of 1,2-dicyanobenzene is examined in Figure 12.8.

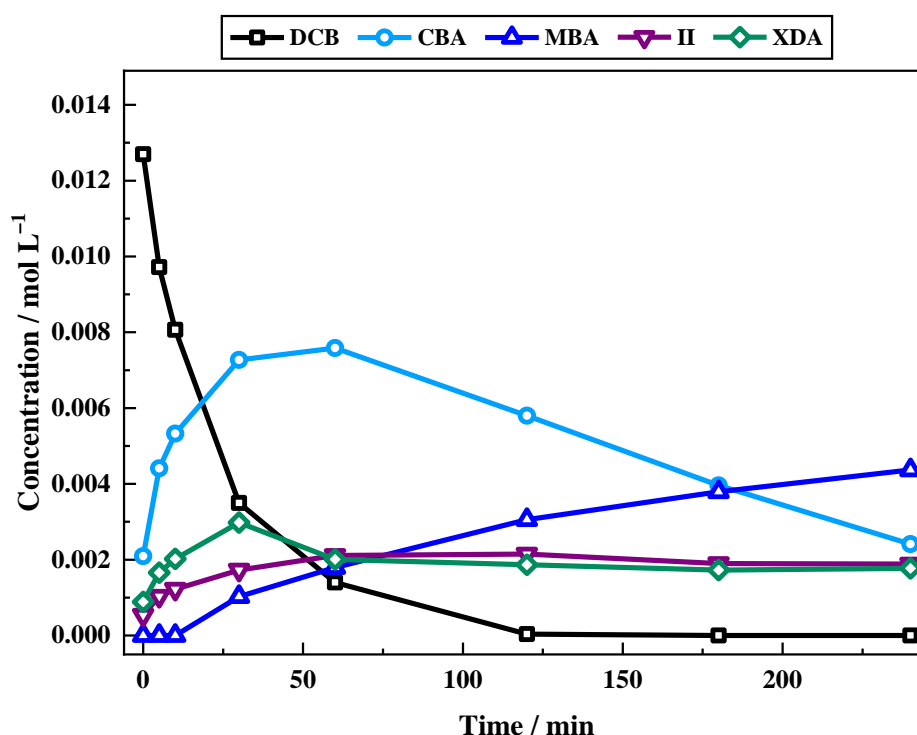


Figure 12.8. Reaction profile for the liquid phase hydrogenation reaction of 1,2-dicyanobenzene (15 mmol L^{-1}) over a 5% Pd/C catalyst (150 mg) in the presence of 2 equivalents of sulphuric acid in ethanol. The reaction was conducted at 60°C under 4 barg hydrogen pressure with an external line pressure of 8 barg and an agitation speed of approximately 850 rpm. [DCB = 1,2-dicyanobenzene; CBA = 2-cyanobenzylamine; MBA = 2-methylbenzylamine; II = isoindoline; XDA = xylene diamine].

Figure 12.8 shows the resultant profile for the hydrogenation reaction of 1,2-dicyanobenzene at an elevated temperature (60°C , cf. standard reactions are run at 40°C). To allow effective comparisons to be made, the increased temperature reaction was

conducted under otherwise identical conditions to those presented in Figure 12.4 (4 barg hydrogen pressure and an agitation speed of 850 rpm). When compared to the low temperature (40 °C) reaction (Figure 12.4), the temperature increase is shown (in Figure 12.8) to exhibit a vastly different profile.

Immediately noticeable is the accelerated consumption of the starting material, which reached full conversion at approximately 120 minutes (*cf.* 40 °C reaction where 240 minutes was required to achieve this outcome). Secondly, 2-cyanobenzylamine, shown to be the major product in Figure 12.4, appears as an intermediate at an elevated temperature (60 °C).

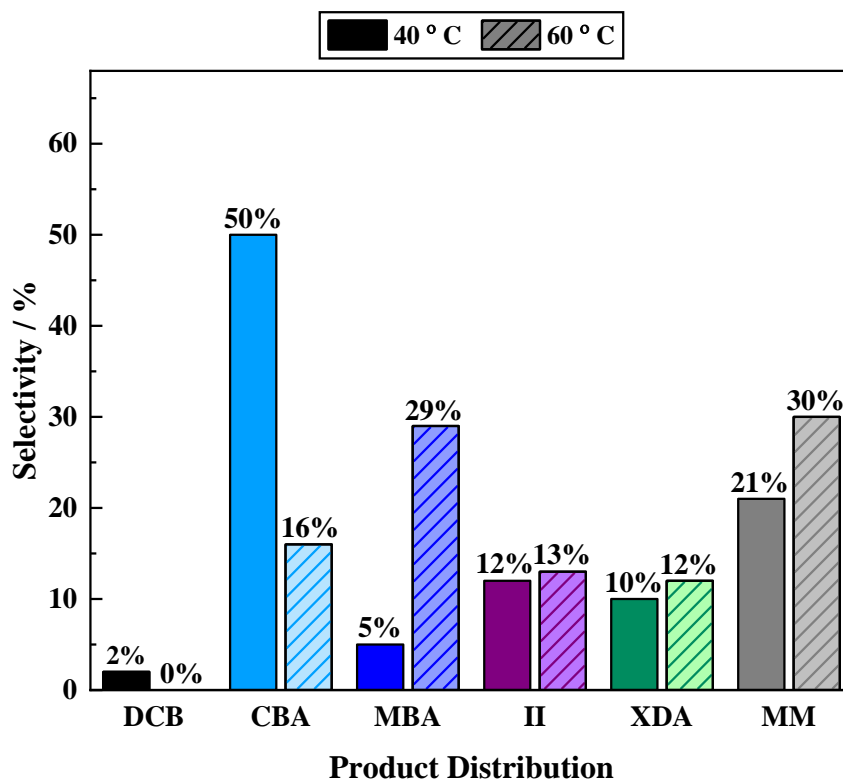
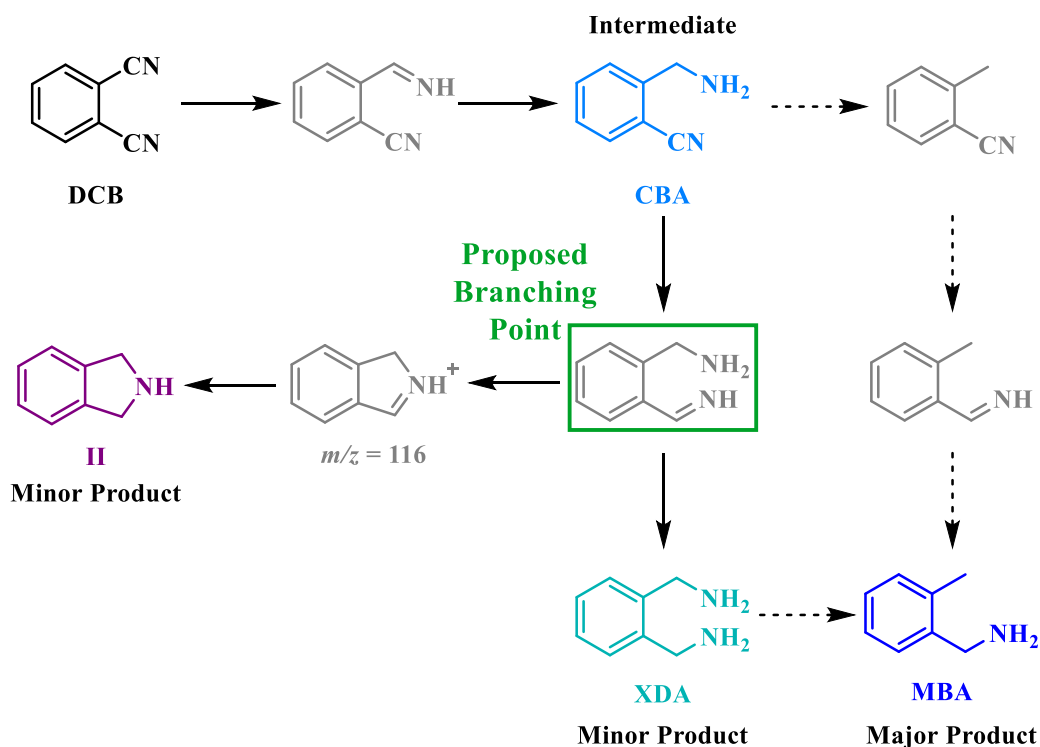


Figure 12.9. Reaction selectivity observed at reaction termination (time = 240 minutes), comparing the outcomes of the hydrogenation reaction of 1,2-dicyanobenzene at 40 °C (solid bars) and 60 °C (hashed bars), utilising the conditions described in Figures 12.4 and 12.8, respectively. [DCB = 1,2-dicyanobenzene; CBA = 2-cyanobenzylamine; MBA = 2-methylbenzylamine; II = isoindoline; XDA = xylene diamine; MM = missing mass].

Comparing the product distribution for the two temperatures in further detail Figure 12.9 shows the selectivity at reaction termination (time = 240 minutes). In addition to the previous observations, Figure 12.9 shows that the production of both isoindoline and xylene diamine is largely unaffected by the change in temperature. With reference to the reaction scheme (Scheme 12.3), it is noted that, in order to achieve both products, hydrogenation of the second nitrile group of 2-cyanobenzylamine must be favoured over hydrogenolysis. This process is therefore shown to be temperature independent.

At the end of the reaction monitoring period (time = 240 minutes), it was 2-methylbenzylamine instead of 2-cyanobenzylamine which was observed as the major product for the hydrogenation reaction of 1,2-dicyanobenzene at 60 °C. Indeed, Figure 12.9 highlights that 2-cyanobenzylamine is in fact an intermediate of the reaction. Further exploration into the 40 °C hydrogenation reaction to determine whether the same trend is observable, but at a lower rate, is an area which represents future work.



Scheme 12.4. Reaction scheme showing the observable chemistry associated with the liquid phase hydrogenation reaction of 1,2-dicyanobenzene (15 mmol L^{-1}) over a 5% Pd/C catalyst (150 mg) in the presence of 2 equivalents of sulphuric acid in ethanol. The reaction was conducted at 60°C under 4 barg hydrogen pressure with an external line pressure of 8 barg and an agitation speed of 850 rpm. Molecules depicted in grey represent proposed intermediate species which are not detectable in the liquid phase. [DCB = 1,2-dicyanobenzene; CBA = 2-cyanobenzylamine; MBA = 2-methylbenzylamine; II = isoindoline; XDA = xylene diamine].

The key findings of Figure 12.8 have been added to the reaction scheme, thus allowing the chemistry associated with the high temperature reaction to be schematically illustrated (Scheme 12.4). Based on its positioning, relative to the minor and major products of the reaction (isoindoline, xylene diamine and 2-methylbenzylamine), it is unsurprising that Figure 12.8 reveals 2-cyanobenzylamine to be an intermediate of the reaction. Nonetheless, significant mechanistic details for this reaction system are missing, particularly regarding the formation of the hydrogenolysis product, 2-methylbenzylamine. This aspect of the nascent investigation, however, represents future work.

12.8 The Durability of the Catalyst was Tested with a Repeat Batch Experiment

As this remains a relatively unknown reaction system, at least within the Lennon Group, it was necessary to determine if any of the products acted as catalyst poisons. Consequently, a primitive repeat batch study, similar to that employed in Chapter 8 for the mandelonitrile hydrogenation reaction system, was conducted. In this instance, a 2-batch reaction was performed using the procedure documented in Section 8.2. Based on the aforementioned findings, the reaction was conducted at 60 °C to ensure the rapid conversion of the starting material (Section 12.7). Each batch was run for only 120 minutes (*cf.* the standard duration for all the single batch 1,2-dicyanobenzene hydrogenation reaction studies was 240 minutes).

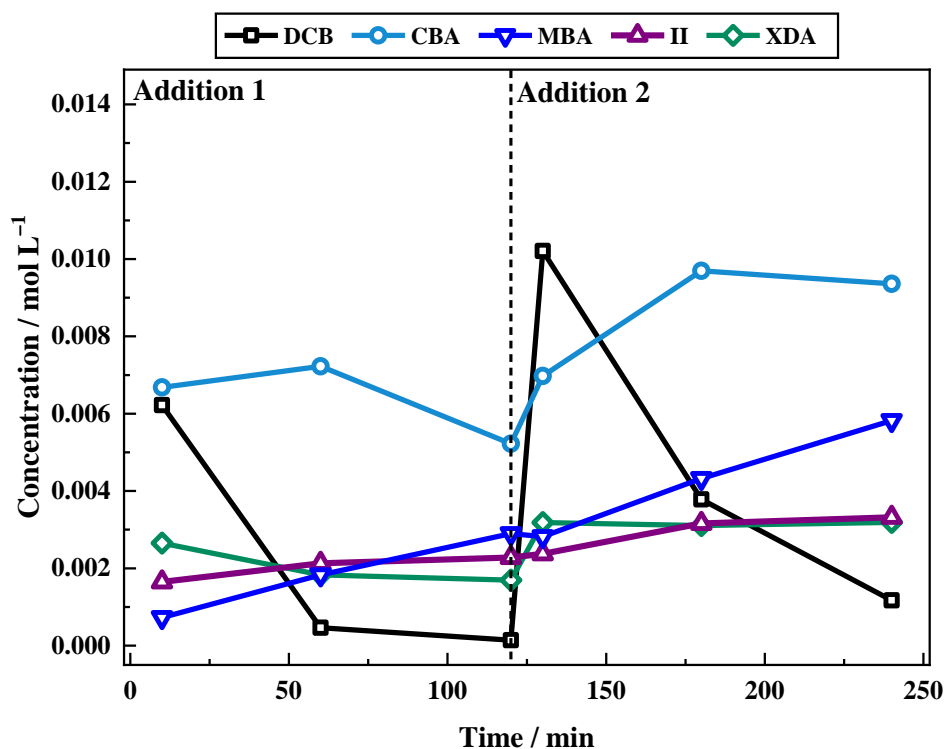


Figure 12.10. Reaction profile for a 2-batch liquid phase hydrogenation reaction of 1,2-dicyanobenzene. Each reagent addition comprised 1,2-dicyanobenzene (5.4 mmol) and 2 equivalents of sulphuric acid, reacted over the same 5% Pd/C catalyst (150 mg) in ethanol. The reaction was conducted at 60 °C under 4 barg hydrogen pressure with an external line pressure of 8 barg and an agitation speed of approximately 850 rpm. Each addition (1–2) represents a fixed 120 minute time period. [DCB = 1,2-dicyanobenzene; CBA = 2-cyanobenzylamine; MBA = 2-methylbenzylamine; II = isoindoline; XDA = xylene diamine].

These test outcomes can be visualised in Figure 12.10. It is important to acknowledge that the experiment conducted here was not performed with the same rigour as those performed for the hydrogenation reaction of mandelonitrile. Therefore, Figure 12.10 only affords a preliminary insight, and does not provide comprehensive detail on catalytic stability for this reaction system.

Following the consumption of the 1,2-dicyanobenzene in Figure 12.10, as expected from the outcome of Figure 12.8, the starting material has been completely consumed within the 120 minutes assigned to each batch reaction, reaching completion by approximately 60 minutes. As the second reagent addition is made, a spike in 1,2-dicyanobenzene concentration is observed before it declines again as the 1,2-dicyanobenzene is converted. It should be noted, however, that the rate of nitrile consumption is somewhat retarded for the second batch reaction. Although there are insufficient data points to accurately quantify this change, the time taken to achieve complete conversion is roughly doubled on the second batch. Nonetheless, by 120 minutes into the second batch reaction, near complete conversion of 1,2-dicyanobenzene is observed suggesting that the functionality of the catalyst has been maintained.

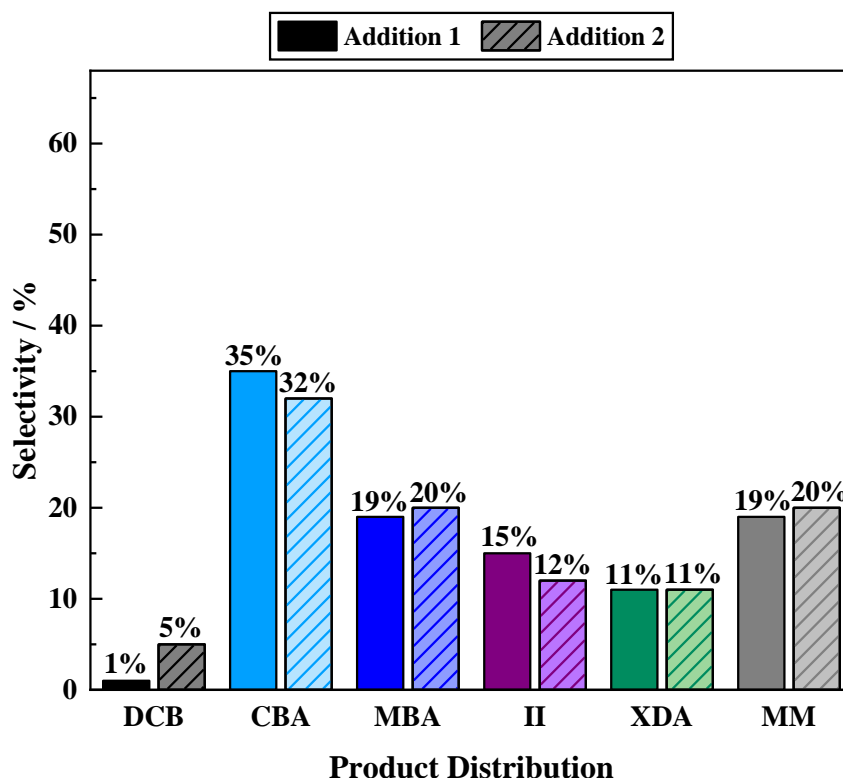


Figure 12.11. Reaction selectivity for the liquid phase hydrogenation reaction of 1,2-dicyanobenzene at reaction termination (time = 120 minutes) for each of the reagent additions. Each reagent addition comprised 1,2-dicyanobenzene (5.4 mmol) and 2 equivalents of sulphuric acid, reacted over the same 5% Pd/C catalyst (150 mg) in ethanol. The reaction was conducted at 60 °C under 4 barg hydrogen pressure with an external line pressure of 8 barg and an agitation speed of approximately 850 rpm. [DCB = 1,2-dicyanobenzene; CBA = 2-cyanobenzylamine; MBA = 2-methylbenzylamine; II = isoindoline; XDA = xylene diamine; MM = missing mass].

Considering the resultant reaction selectivity at the end of each batch reaction (time = 120 and 240 minutes for additions 1 and 2, respectively), no significant changes from the first to the second addition were observed. This indicates that, whilst the reaction rate is significantly slowed upon cycling of the catalyst, the functionality of the catalyst has largely been retained.

12.9 A Systematic Mass Balance was Detected for all Reaction Conditions

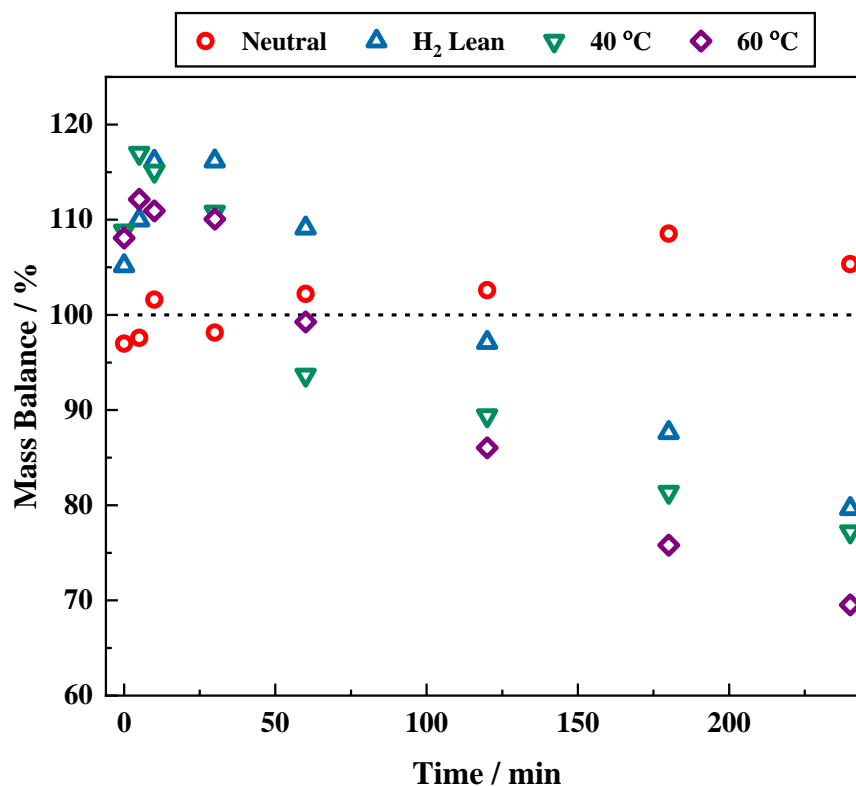


Figure 12.12. Mass balance plots for the liquid phase hydrogenation reaction of 1,2-dicyanobenzene conducted under various reaction conditions over a 5% Pd/C catalyst (150 mg). [neutral = Figure 12.3; H₂ lean = Figure 12.6; 40 °C = Figure 12.4; 60 °C = Figure 12.8). A closed mass balance (100%) is used as a reference point and is denoted by a dashed black line.

Considering the mass balances associated with each of the discussed reaction conditions, systematic trends become apparent (Figure 12.12). To a first approximation, significant issues relating to the mass balance are observed. In a neutral environment (Figure 12.12, red circles) the mass balance is shown to remain reasonably close to the reference line for a complete mass balance, deviating by approximately $\pm 8\%$. Conversely, under acidic conditions (Figure 12.12, all other data points), this is found not to be the case. Instead, a mass excess (reaching a maximum of $+20\%$) is observed for the first 60 minutes of the reaction. As reaction time increases, however, an increasing missing mass is observed.

By reaction termination (time = 240 minutes) the mass balance reaches a minimum of approximately -30%, a value which is dependent on the reaction conditions employed.

The absence of missing mass under neutral conditions suggests that the unknown reaction pathways, designated as responsible for the missing mass, are potentially acid mediated or acid enhanced. Further, this finding may be linked to the greater degree of sample discolouration observed for samples taken from reactions conducted in acidic environments, as discussed in Section 12.5. Moreover, it is postulated that the increasing mass imbalance observed on the latter half of the reaction is additionally linked to hydrogen availability. With reference to Figure 12.12, it is shown that, as hydrogen availability is increased through various parameter changes (agitation speed, hydrogen pressure and temperature), missing mass is also increased. This suggests that an enhanced hydrogen supply accelerates the rate of the undesirable side reactions.

An alternative postulate, however, is that the mass balance issues are linked to the analytical protocol. It is proposed that the HPLC method is unsuitable for the resultant amine salts formed in the presence of the acid additive. It is likely that the interactions of the ionic species with the organic HPLC medium result in the observed quantification issues shown in Figure 12.12. This proposal is further rationalised by the lack of quantification issues under neutral conditions. It is thus deduced that HPLC may not be the most suitable method of quantification for this reaction system. Despite this, the conclusions regarding the reaction scheme hold true. It is proposed that when this system is investigated further a more reliable quantification method may be required.

12.10 Syngenta Mettler Toledo Batch Reactor Studies

Separate from the work conducted on the 1,2-dicyanobenzene hydrogenation reaction system at the University of Glasgow, a parallel study was undertaken at the industrial site (Syngenta, Jealott's Hill). The primary aim of the industrial visit was to gain experience of different reactor set-ups. It is essential to note, however, that the University of Glasgow and Syngenta measurements represent discrete bodies of work.

The Syngenta studies focused on:

- (a) the hydrogenation reaction of 1,2-dicyanobenzene with an increased acid presence (4 equivalents); and
- (b) the hydrogenation reaction of the intermediate 2-cyanobenzylamine.

Measurements conducted in this section were performed in a 120 mL EasyMax reactor (Mettler Toledo), details of which can be found in Section 2.3.1. As such, the reagent quantities used in the 350 mL Büchi stirred autoclave employed at the University of Glasgow were scaled down for this reactor.

In the first instance, the hydrogenation reaction of 1,2-dicyanobenzene was examined. Experimental conditions were matched to those presented in Figure 12.4, which represent the ‘hydrogen lean’ parameters. It was proposed that, as a dinitrile, 1,2-dicyanobenzene would have a more significant acid requirement than mandelonitrile. Thus, it was suggested that 2 equivalents of the sulphuric acid additive were not sufficient to fully protonate the full complement of amine products. The notable difference between the Syngenta study and the measurements conducted at the University of Glasgow, therefore, relates to the concentration of the sulphuric acid additive. This was increased, from the standard 2 equivalents used at the University of Glasgow, to 4 equivalents.

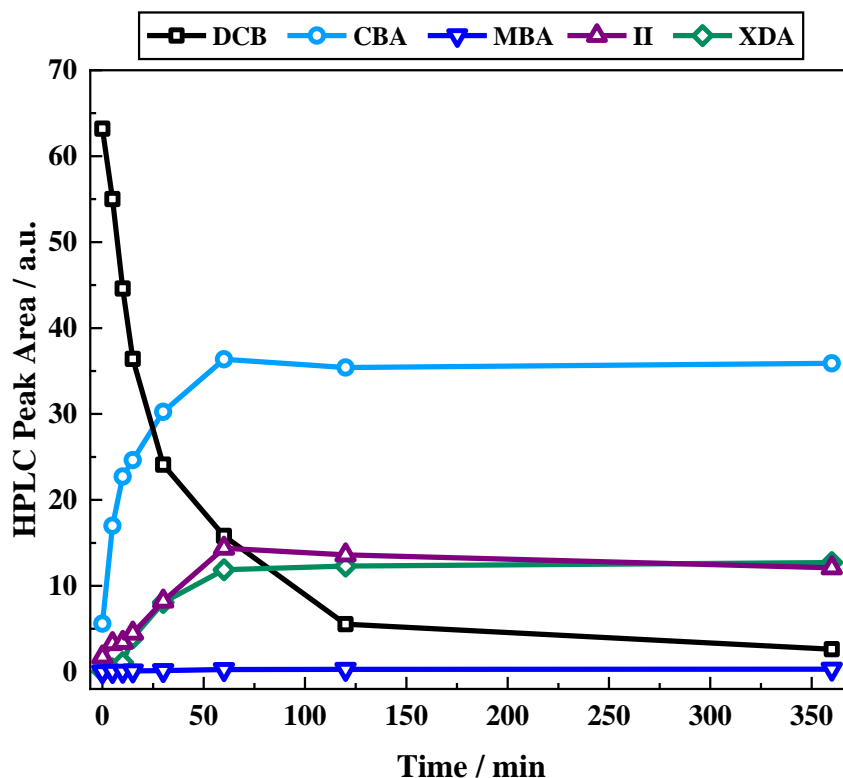


Figure 12.13. Reaction profile for the liquid phase hydrogenation reaction of 1,2-dicyanobenzene (15 mmol L^{-1}) over a 5% Pd/C catalyst (102 mg) in the presence of 4 equivalents of sulphuric acid in ethanol. The reaction conducted at 40°C under 2 barg hydrogen pressure with an external line pressure of 8 barg and an agitation speed of approximately 850 rpm. [DCB = 1,2-dicyanobenzene; CBA = 2-cyanobenzylamine; MBA = 2-methylbenzylamine; II = isoindoline; XDA = xylene diamine]. Measurement conducted at Syngenta (Jealott's Hill).

Figure 12.13 shows the resultant reaction profile for the hydrogenation reaction of 1,2-dicyanobenzene in the presence of 4 equivalents of sulphuric acid. It is noted that, due to time constraints, calibrations for each of the reaction components were not conducted. Therefore, instead of concentration, it is the HPLC peak area which is plotted on the y-axis. When the outcomes of Figures 12.4 and 12.13 are compared, similar profiles are obtained. Nevertheless, one notable difference is observed, namely, the absence of 2-methylbenzylamine, as depicted in Figure 12.13. It is hence illustrated that the hydrogenolysis pathway, which affords 2-methylbenzylamine, has been prevented in an acid rich environment. Therefore, as a consequence of the observed product distribution, the conditions presented in Figure 12.13 are found to be suitable for future studies relating

to the use of the 1,2-dicyanobenzene hydrogenation reaction as a probe of hydrogen supply.

Secondly, when the hydrogenation reaction of 2-cyanobenzylamine was considered, it was revealed that this process was kinetically favoured. The 2-cyanobenzylamine was fully converted by the time the first sample was taken (time = 3 minutes), and yielded xylene diamine with a selectivity of 56%. However, due to ongoing analytical difficulties at Syngenta, the remainder of mass was not accounted for. Further investigation into a more comprehensive analysis of the chromatographic output is underway. As the proposed reaction scheme (Scheme 12.4) suggests that, in addition to being a key intermediate in the formation of xylene diamine, 2-cyanobenzylamine is also an intermediate in the formation of isoindoline and 2-methylbenzylamine. It is thus likely that the production of isoindoline and 2-methylbenzylamine will account for the observed missing mass. It is additionally noted that only minor sample discolouration was observed for the samples collected from the Syngenta reactor. Whilst a number of factors may have contributed to this outcome, it is believed that acid concentration and perhaps dilution play the most significant roles. Further investigation into this is necessary.

12.11 Conclusions and Future Directions

A preliminary investigation into the liquid phase hydrogenation reaction of 1,2-dicyanobenzene over a carbon supported palladium catalyst has been conducted. For this reaction system, it was proposed that such a study would reveal whether this was a suitable substrate to be explored further by Syngenta and collaborators for use as a hydrogen supply probe. The following conclusions regarding such suitability have been drawn:

- The development of suitable analytical methodology, such that all reaction components can be identified, has been achieved. However, further work in this area is required to obtain accurate and reliable quantification.

- Under neutral reaction conditions, nitrile conversion was incomplete within a 240 minute time frame. At reaction termination, however, both the intramolecular cyclisation product (isoindoline) and the partial hydrogenation product (2-cyanobenzylamine) were obtained.
- Inclusion of an acid additive afforded a different reaction profile. In this instance full nitrile conversion was achieved within the 240 minute reaction time. Both isoindoline and 2-cyanobenzylamine were again formed, confirming the occurrence of intramolecular cyclisation and hydrogenation. Also, an additional hydrogenation product (xylene diamine) and, hydrogenolysis product 2-methylbenzylamine were afforded.
- Discolouration of the reaction samples was observed for reactions conducted in an acidic medium. It was proposed that the discolouration was linked to the production of isoindoline. Further investigation to determine a definitive source is, however, necessary.
- Alteration of the hydrogen availability within the reaction system, through modification of the reaction parameters was conducted. A reduction in hydrogen pressure and agitation speed was found to afford a comparable profile to that obtained under reference conditions. Consequently, more extreme parameter changes should be invoked as a more advanced method of altering the hydrogen availability.
- An elevation in reaction temperature from 40 °C to 60 °C resulted in further insight into the reaction mechanism. The elevation in reaction rate which accompanied the temperature increase revealed that the partial hydrogenation product (2-cyanobenzylamine) was in fact an intermediate of the reaction. As such, it would be judicious to extend the analysis time for the reaction conducted at the lower temperature to ascertain if the same trend is observed.
- Catalyst durability was tested by conducting a generic repeat batch study. It was found that catalyst activity was maintained for two reagent additions over the same catalyst. However, a slowing in the rate of nitrile consumption was observed.

- Analysis of the mass balances associated with each of the examined reaction conditions revealed the presence of currently unidentified chemistry. These undesirable side reactions were found to be accelerated by an enhanced hydrogen supply and mediated by an acid presence.
- Studies conducted at Syngenta identified that an increase in the acid concentration in the reaction system prevented the occurrence of hydrogenolysis.
- Collectively, each of the discussed experiments has allowed the development of a proposed reaction scheme for the hydrogenation reaction of 1,2-dicyanobenzene to be achieved.
- Finally, it is deduced that the 1,2-dicyanobenzene hydrogenation reaction system is suitable for future investigation. Such studies are, however, out with the scope of this thesis.

12.12 References

- [1] M. Chatterjee, M. Sato, H. Kawanami, T. Yokoyama, T. Suzuki, T. Ishizaka, *Adv. Synth. Catal.*, 2010, **352(14-15)**, 2394–2398.
- [2] P. Marion, M. Joucla, C. Taisne and J. Jenck, *Stud. Surf. Sci. Catal.*, 1993, **78**, 291–298.
- [3] C. de Bellefon and P. Fouilloux, *Catal. Rev-Sci Eng.*, 1994, **36(3)**, 459–506.
- [4] R.C. Weast (editor), *Handbook of Chemistry and Physics*, 60th Edition, Boca Raton CRC Press Inc. (Florida), 1979.
- [5] J. Clayden, N. Greeves and S. Warren, *Organic Chemistry*, 2nd Edition, Oxford University Press Inc. (New York), 2012.
- [6] R.K. Marella, K.S. Koppadi, Y. Jyothi, K.S.R. Rao and D.R. Burri, *New J. Chem.*, 2013, **37**, 3229–3235.
- [7] P.N. Rylander, *Catalytic Hydrogenation over Platinum Metals*, Academic Press (New York), 1967.
- [8] A.J. Yap, A.F. Masters and T. Maschmeyer, *ChemCatChem*, 2012, **4**, 4839–4849.
- [9] T.S.A. Heugebaert, B.I. Roman and C.V. Stevens, *Chem. Soc. Rev.*, 2012, **41**, 5626–5640.
- [10] R.L. Augustine, *Heterogeneous Catalysis for the Synthetic Chemist*, Marcell Dekker Inc. (New York), 1996.
- [11] J. Volf and J. Pašek, *Stud. Surf. Sci. Catal.*, 1986, **27**, 105–144.